Aspects of chlorhexidine degradation

Purdy, K. R.

Award date:
1987

Awarding institution:
University of Bath

A S P E C T S O F

C H L O R H E X I D I N E D E G R A D A T I O N

THESIS

Submitted by K.R. Purdy, B.Sc., M.P.S.

for the degree of Doctor of Phil osophy

of the University of Bath

1987

This research has been carried out in the School of Pharmacy of the University of Bath under the supervision of B.J. Meakin, B.Pharm., F.P.S.

Keith Purdy

ProQuest LLC
789 East Eisenhower Parkway
P.O. Box 1346
Ann Arbor, MI 48106-1346

SUMMARY

This thesis examines the factors affecting the stability of chlorhexidine salts (principally gluconate) in dilute aqueous solution (0.001 to 0.05%w/v). Such studies are pertinent to the use of chlorhexidine as a preservative in aqueous pharmaceutical products.

The introduction details the factors affecting the stability of pharmaceuticals in solution. Published work on the physico-chemical properties of chlorhexidine and structurally related compounds is then reviewed together with methods available for the quantitative analysis of chlorhexidine.

The experimental section describes the evaluation of a HPLC stability indicating method for the quantitative determination of chlorhexidine in terms of sensitivity, precision, reproducibility and selectivity. Comparison is made between this method and the more conventional colorimetric methods based on the Holbrook technique and 4-chloroaniline determination. The degradation kinetics of dilute aqueous solutions of chlorhexidine gluconate have been examined by a pH-stating technique. Over the range pH 2 to 10, 0.002% w/v chlorhexidine gluconate showed a pH of maximum stability around pH 5 (at 90°C) with regions of specific acid/base catalysis present. Modifications attributable to a water catalysed reaction (pH 3.5 to 6.5) and presence of unionised chlorhexidine base (pH > 8.5) were also apparent. Concentration dependency was noted at both alkaline and neutral pH. Linear Arrhenius relationships were observed producing apparent activation energies varying from 69.5 to 96.1 $kJ.mol^{-1}$.

Degradation rate dependence upon ionic strength was consistent with a negative salt effect in alkaline solution. Variable effects on rate were observed in the presence of buffers and with different types of surfactant. Limited studies indicated chlorhexidine solutions are photochemically stable at netural pH but are not amenable to γ-irradiation sterilisation. Quantitative analysis of 4-chloroaniline has shown that this compound is not, as previous literature might suggest, the major degradation product of chlorhexidine. HPLC analysis indicates that up to six degradation products may occur.

In the discussion an interpretation of kinetic data is presented. Qualitative information from chromatographic studies is used to support a proposed degradation pathway for chlorhexidine. Finally the kinetic data has been used to assess the stability of chlorhexidine to heat sterilisation processes and on long term storage.

TO JACQUELINE

ACKNOWLEDGEMENTS

Sincere thanks are due to Mr. Brian Meakin for his guidance, advice and helpful discussion throughout this study. I am also grateful to Mr. John Fernie and Mr. Fred Bailey of ICI Pharmaceuticals Division for their advice. I would like to thank the Science and Engineering Research Council for the Grant Award which made this research possible and ICI Pharmaceuticals Division for fincancial assistance.

I would also like to acknowledge the assistance of Dr. Alan Casey (chlorhexidine chemistry), Professor David Games (HPLC-mass spectroscopy), Miss Maggie Gill (multiple linear regression analysis) and Mr. Graham Bird (linear regression analysis). I am indebted to the staff of the Pharmaceutics Department for their help and to many colleagues, both past and present, for their encouragement. Special thanks are due to Mrs. Belinda Tomlinson and Mrs. Carol Rollings for the speed and care with which they typed this thesis.

Finally, I would like to thank my wife for her continual support, understanding and encouragement during all stages of this work.

CONTENTS

APPENDICES

INTRODUCTION

CHAPTER 1

PHARMACEUTICAL STABILITY

1.1 INTRODUCTION

The generation of stability data is essential to ensure the quality, strength, purity and identity of a pharmaceutical product throughout its life. Stability investigations are performed at all stages of pharmaceutical development including fundamental studies on rates and mechanisms of reaction, influence of formulation variables, role of containers and effect of storage conditons. The information generated ultimately leads to the establishment of shelf-life and optimum storage conditions for a pharmaceutical product. Improvements in sensitivity and selectivity of analytical methodology have enabled the determination of reaction rates from complex degradation mechanisms.

The mechanisms of pharmaceutical instability may be grouped into three categories:

Chemical

Degradative reactions such as oxidation, reduction and hydrolysis are the major causes of instability. These reactions may be further influenced by the effects of, for example, pH, temperature and ionic strength. Interactions or incompatibilities may also exist in the solid-state between active components and excipients.

Light and ionising radiation may also play a role in chemical degradation and will be discussed in section 1.6.3 and 1.6.4.

Physical

Unlike chemical degradation, physical instability does not necessarily involve the production of distinctly different chemical

compounds. Physical instability manifests itself as a gross change of physical or chemical properties, for example, crystal growth, emulsion cracking, viscosity changes and suspension sedimentation. These effects may be a consequence of exposure to heat, moisture or shock effects (i.e. milling). Sorption and container interactions are also examples of physical instability.

Biochemical

Microbial contamination may promote drug degradation due to enzyme catalysis.

General pharmaceutical stability has been reviewed by Connors et al (1979), Garrett (1962), Mollica et al (1978) and Parrott (1966).

1.2 CHEMICAL REACTION KINETICS

Whilst thermodynamic parameters predict the feasibility of a chemical reaction, kinetics indicate the rate or velocity at which the reaction takes place. Reaction kinetics is, therefore, the study of rate of chemical change and the factors on which it depends. Knowledge of the mechanisms of pharmaceutical degradation is important and such information is often derived from the study of reaction kinetics.

Rates of reaction are studied by determination of product or reactant concentration as a function of time. Therefore the validity of any information generated is dependent on the accuracy of quantitative assay methods used to determine product or reactant concentrations.

1.2.1 Rates and Orders of Reaction

The rate, or velocity, of a reaction is given by (1):

$$\frac{-dC}{dt} \qquad \ldots.(1)$$

where the decrease (indicated by the negative sign) in concentration, C, is measured as a function of time, t. According to the law of mass action, the rate of reaction is proportional to the molar concentration of reactants each raised to a power equal to the number of molecules undergoing reaction. For a reaction such as :

$$aA + bB \longrightarrow \text{products}$$

where a moles of compound A react with b moles of compound B, then the rate of reaction will be given by equation 2 :

$$-\frac{1}{a} \cdot \frac{d[A]}{dt} = -\frac{1}{b} \cdot \frac{d[B]}{dt} \qquad \ldots.(2)$$

which according to the law of mass action becomes equation 3 :

$$\text{rate} = k[A]^a[B]^b \qquad \ldots.(3)$$

where k is the rate constant and [A] and [B] are the concentrations of compounds A and B respectively.

Rates of reaction are therefore influenced by the concentration of reactant or reactants with the order of reaction describing the overall relationship. From equation (3) the overall order of reaction, n, would be given by the sum of the individual orders (equation 4) :

$$n = a + b \qquad \ldots.(4)$$

Reaction kinetics are usually described by zero-, first-, pseudo first- or second-order rate equations. The derivation of rate equations and half-lives for each order of reaction are summarised in Table 1.1. Pharmaceutical compounds often degrade by complex mechanisms involving multistep or parallel reactions (e.g. steroids, antibiotics and barbiturates), with fractional reaction orders being derived from experimental analysis. Nevertheless, kinetic data for such reactions are invariably generated according to the appropriate equation of Table 1.1.

Order	Integrated Rate Equation	Linear Graphical Solution: x	y	rate constant (k)	Half-life Equation	Units of rate constant
0	$k = \frac{[x]}{t}$	time	$[x]$	= slope	$t_{\frac{1}{2}} = \frac{[A_o]}{2k}$	mol dm^{-3} s^{-1}
1	$k = \frac{1}{t} \log_e \frac{[A_o]}{[A_o]-[x]}$	time	$\log \frac{[A_o]}{[A_o]-[x]}$	= 2.303 x slope	$t_{\frac{1}{2}} = \frac{0.693}{k}$	s^{-1}
2	$k = \frac{1}{t([A_o]-[B_o])} \log_e \frac{[B_o]([A_o]-[x])}{[A_o]([B_o]-[x])}$	time	$\log \frac{[B_o]([A_o]-[x])}{[A_o]([B_o]-[x])}$	$= \frac{2.303}{([A_o]-[B_o])}$ x slope	$t_{\frac{1}{2}} = \frac{1}{[A_o]k}$ (when $[A_o]=[B_o]$)	dm^3 mol^{-1} s^{-1}

TABLE 1.1 : Kinetic equations for zero-, first- and second-order reactions.

Where [x] is the concentration of reactant utilised after time t

$[A_o]$ and $[B_o]$ are the initial concentrations of reactants A and B respectively

Determination of the order of reaction is most conveniently performed by the fitting of kinetic data to theoretical graphical plots. The order providing the best linear graphical solution is then adopted as the apparent order of reaction. Other methods of determining the order of reaction include the Differential (van't Hoff) Method, Isolation Method, Half-life and graphical (Powell Plots) methods (Frost and Pearson, 1961; Laidler, 1965). A useful graphical application of a half-life method is derived from equation 5 :

$$\log t_{\frac{1}{2}} = \log f - (1-n) \log C_o \qquad \ldots.(5)$$

where $t_{\frac{1}{2}}$ is the half-life, f is a function of the order of reaction (n) and rate constant (k), and remains constant for a reaction at a given temperature. A plot of log $t_{\frac{1}{2}}$ vs log C_o should be linear with a slope of (1-n) provided the order does not change with initial concentration, C_o, of reactant. Meakin et al (1978) have successfully used such a plot in the description of concentration dependent degradation kinetics for promethazine hydrochloride in aqueous solution.

It must be remembered that the apparent order of reaction is an experimentally derived value and is only valid under defined conditions.

1.2.2 Pseudo first-order Reactions

A pseudo first-order reaction is essentially a second-order or bimolecular reaction behaving as first-order since one reactant is present in excess. Hydrolysis reactions are usually described by pseudo first-order kinetics since water is present in

large excess. The rate of reaction is dependent only on the reactant undergoing a change in concentration. The rate equation (6) for a pseudo first-order reaction is given by :

$$\frac{-d[A]}{dt} = k_{obs}[A] \qquad ....(6)$$

where k_{obs} is the observed or apparent rate constant.

1.2.3 Complex Reactions

Although kinetic data are calculated from simple reactions of zero-, first- or second-order it is often found that chemical reactions consist of a combination of reactions. Each reaction will have its own rate constant and reaction order. Complex reaction mechanisms may involve simultaneous, consecutive and opposing reactions.

1.2.3.1 Simultaneous (Parallel) Reactions

A reactant, A, is simultaneously converted to products B and C, each at finite rates with rate constants k_1 and k_2 :

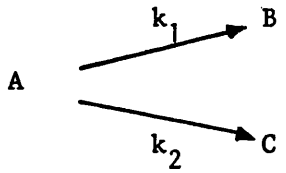

If the equation (7) for the decrease in A is first-order :

$$\frac{-d[A]}{dt} = k_1[A] + k_2[A] = (k_1+k_2)[A] \qquad ....(7)$$

which on integration and exponential arrangement yields equation 8 :

$$[A] = [A_o]\exp^{-(k_1+k_2)t} \qquad ....(8)$$

where $[A_o]$ is the initial concentration and [A] is the concentration after time t. Similarly, it has been shown (equations 9 and 10) by Kostenbauder and Bogardus (1985) that :

$$[B] = \frac{k_1[A_o]}{(k_1+k_2)}\left[1 - \exp^{-(k_1+k_2)t}\right] \qquad ....(9)$$

and $$[C] = \frac{k_2[A_o]}{(k_1+k_2)}\left[1 - \exp^{-(k_1+k_2)t}\right] \quad \ldots.(10)$$

Equations (9) and (10) show that the fraction of A converted to B is $\frac{k_1}{(k_1+k_2)}$ and the fraction converted to C is $\frac{k_2}{(k_1+k_2)}$, both at infinite time.

The rate of each parallel reaction may be dependent on similar or totally independent factors thus changes in reaction conditions may appear to be unpredictable or anomalous unless parallel processes have been previously described. The base catalysed degradation of prednisolone has been reported by Guttman and Meister (1958) to proceed through at least three parallel first-order reactions with one being oxygen dependent. The antibiotics cefotaxime (Berge et al, 1983), cephalothin (Yamana and Tsuji, 1976) and clindamycin (Oesterling, 1970) have also been shown to degrade by parallel reaction mechanisms.

1.2.3.2 Consecutive Reactions

Two first-order reactions may occur consecutively :

$$A \xrightarrow{k_1} B \xrightarrow{k_2} C$$

where k_1 and k_2 are again finite rates. The rate equations (11-13) for each reaction are :

$$\frac{-d[A]}{dt} = k_1[A] \quad \ldots.(11)$$

$$\frac{-d[B]}{dt} = -k_1[A] + k_2[B] \quad \ldots.(12)$$

$$\frac{d[C]}{dt} = k_2[B] \quad \ldots.(13)$$

Again Kostenbauder and Bogardus (1985) have shown integration and exponential rearrangement to produce equations 14 to 16 :

$$[A] = [A_o]\exp^{-k_1 t} \qquad \ldots.(14)$$

$$[B] = \frac{k_1[A_o]}{(k_1+k_2)}\left[\exp^{-k_1 t} - \exp^{-k_2 t}\right] \qquad \ldots.(15)$$

$$[C] = [A_o]\left[1 + \frac{1}{(k_1+k_2)}\left(k_2\exp^{-k_1 t} - k_1\exp^{-k_2 t}\right)\right] \ldots.(16)$$

Where the rates of reaction are vastly different, the overall rate of reaction will be dependent on the slowest or rate-determining step.

Pharmaceuticals degrading via consecutive reaction mechanisms generally also exhibit parallel and/or reversible degradative mechanisms with the overall kinetics being very complex. Examples include : barbituric acid derivatives - consecutive and parallel (Garrett et al, 1971; Khan and Khan, 1976), hydrocortisone - consecutive and parallel (Allen and Gupta, 1974; Mauger et al, 1969) and benzylpenicillin which exhibits consecutive, parallel and reversible reactions (Blaha et al, 1976).

1.2.3.3 Opposing (Reversible) Reactions

The rate equation (17) for a first-order reversible reaction :

$$A \underset{k_2}{\overset{k_1}{\rightleftharpoons}} B$$

is given by :

$$\frac{d[A]}{dt} = -k_1[A] + k_2[B] \qquad \ldots.(17)$$

At equilibrium, the velocity of the forward and reverse reactions are equal and the equilibrium constant, K, may be obtained from

equation 18 :

$$\frac{[B_e]}{[A_e]} = \frac{[A_o] - [A_e]}{[A_e]} = \frac{k_1}{k_2} = K \qquad \ldots.(18)$$

where $[A_e]$ and $[B_e]$ are the concentrations of A and B at equilibrium respectively. Reversible reactions will result in degradation down to the equilibrium state when no further net loss of drug occurs.

McCormick et al (1957) provide a pharmaceutical example in the reversible acid-catalysed epimerization of tetracyclines to 4-epitetracyclines which have reduced potency. Hydrochlorthiazide (Rehm and Smith, 1960), pilocarpine (Chung et al, 1970) and warfarin (Lippold and Garrett, 1971) also exhibit reversible degradative reactions.

1.3 TEMPERATURE AND REACTION RATE

A chemical reaction will proceed at different rates depending on the temperature. The Arrhenius equation (19) provides an empirical relationship between the rate constant, k and absolute temperature, T :

$$k = A \exp^{-Ea/RT} \qquad \ldots.(19)$$

where A is the "pre-exponental factor" (see 1.3.1 and 1.3.2), R is the gas constant and Ea is the experimental activation energy. Equation (19) may be expressed logarithmically as equation 20 :

$$\log_e k = \log_e A - \frac{Ea}{RT} \qquad \ldots.(20)$$

The activation energy may be determined from a linear plot of $\log_e k$ vs 1/T where the slope is Ea/R and intercept is $\log_e A$. Alternatively, knowledge of the rate constant at two significantly

different temperatures may yield the activation energy according to equation (21) :

$$Ea = \frac{2.303\ R\ (T_1 T_2)\ (\log k_2 - \log k_1)}{T_2 - T_1} \qquad ....(21)$$

Both determinations assume that the activation energy remains independent of temperature.

The Arrhenius equation has been rationalised by two theories - the Collision Theory and the Transition State Theory.

1.3.1 Collision Theory

For two molecules to undergo reaction the collision theory requires that they collide or interact. Although collision is a prerequisite for reaction only those colliding molecules with an energy above the activation energy, Ea, will undergo chemical reaction. A high activation energy results in a slower reaction rate since the proportion of colliding molecules having the necessary energy will be small. Therefore, in the Arrhenius equation, the pre-exponential factor is related to the frequency of collisions with $\exp^{-Ea/RT}$ being the probability of a reaction between molecules of energy > Ea at a temperature T.

1.3.2 Transition State Theory

The study of reaction mechanisms has been assisted by the development of the transition state theory, which assumes :

(i) the transformation from reactant state to product state proceeds through an intermediate (transition) state of higher energy than either the reactants or products.

(ii) the molecules existing in the transition state are in equilibrium with the reactant molecules.

(iii) the rate of reaction is proportional to the concentration of molecules in the transition state.

Considering a bimolecular reaction :

$$A + B \rightleftharpoons AB^{\dagger} \longrightarrow \text{Products}$$

where $AB^{\dagger}$ represents the transition state (indicated by $\dagger$). Assuming that an equilibrium exists between the initial and transition states an equilibrium constant $K^{\dagger}$ may be derived (equation 22) :

$$K^{\dagger} = \frac{[AB^{\dagger}]}{[A][B]} \qquad \ldots.(22)$$

Applying standard thermodynamic relationships gives equations 23 and 24 :

$$\Delta G^{o\dagger} = -RT \log_e K^{\dagger} \qquad \ldots.(23)$$

$$\Delta G^{o\dagger} = \Delta H^{o\dagger} - T\Delta S^{o\dagger} \qquad \ldots.(24)$$

where $\Delta G^{o\dagger}$, $\Delta H^{o\dagger}$ and $\Delta S^{o\dagger}$ are the standard free energy, enthalpy and entropy of activation respectively.

The relationship between the rate constant, k, and the equilibrium constant, $K^{\dagger}$, is given by equation 25 :

$$k = \frac{RT}{Nh} K^{\dagger} \qquad \ldots.(25)$$

where N and h are Avogadro's number and Plank's constant respectively.

Experimental rate data may be used to calculate standard free energy and entropy of activation from the derived equations 26 to 28 (Connors, 1981 and Connors et al, 1979) :

$$\Delta H^{o\dagger} = Ea - RT \qquad \ldots.(26)$$

$$\Delta S^{o\dagger} = \frac{\Delta H^{o\dagger}}{T} - R \log_e \left(\frac{T}{k}\right) - R \log_e \left(\frac{R}{Nh}\right) \qquad \ldots.(27)$$

$$k = \frac{RT}{Nh} \exp\left(\frac{-\Delta G^{o\dagger}}{RT}\right) \quad \ldots.(28)$$

Consequently, a large value of $\Delta G^{o\dagger}$ leads to a smaller rate constant. Therefore, the higher the energy barrier to the transition state ($\Delta G^{o\dagger}$) the slower the reaction.

The transition state theory relates the pre-exponential factor to the entropy of activation of the transition state and the activation energy to the enthalpy of activation of the transition state.

1.3.3 Deviations from the Arrhenius Relationship

Observation of the rate data often disclose a slight but significant departure from a straight line when $\log_e k$ is plotted against 1/T. This deviation may be due to two effects :

1.3.3.1 Variation of pre-exponential factor and activation energy with temperature

Although the Arrhenius equation (19) often successfully describes the relationship between the rate of reaction and temperature it is a simplification and not exactly correct. This is because the pre-exponential factor, A, is temperature dependent and the activation energy, Ea, is not necessarily temperature independent (Rogers, 1970). However, in most practical situations variation of Ea with temperature cannot be measured.

A more accurate relationship would be equation 29 (expressed logarithmically as equation 30) which accounts for the variation of A with temperature :

$$k = AT^c \exp^{-Ea/RT} \quad \ldots.(29)$$

where c has a value depending upon the nature of the reaction considered. If equation 29 is correct, with c not zero, then a plot of $\log_e k$ against 1/T will show slight curvature. Equations 24 and 28 may be combined to produce an Absolute rate equation (equation 30, or expressed

logarithmically as equation 30a):

$$k = \frac{RT}{Nh} \exp\left(\frac{\Delta S^{o\dagger}}{R} - \frac{\Delta H^{o\dagger}}{RT}\right) \quad \ldots.(30)$$

$$\log_e k = \frac{RT}{Nh} + \left(\frac{\Delta S^{o\dagger}}{R} - \frac{\Delta H^{o\dagger}}{RT}\right) \quad \ldots.(30a)$$

A plot of $\log_e \frac{k}{T}$ against 1/T should be linear with the activation energy obtained from equation 26. Arrhenius (equation 19) therefore gives an apparent activation energy which may differ from the real value (from equation 30) by 0.5 to 10 kJ. mol^{-1} (Laidler, 1965).

1.3.3.2 Complex reactions

Gross curvature in $\log_e k$ against 1/T plots usually indicates the existence of complex reaction mechanisms.

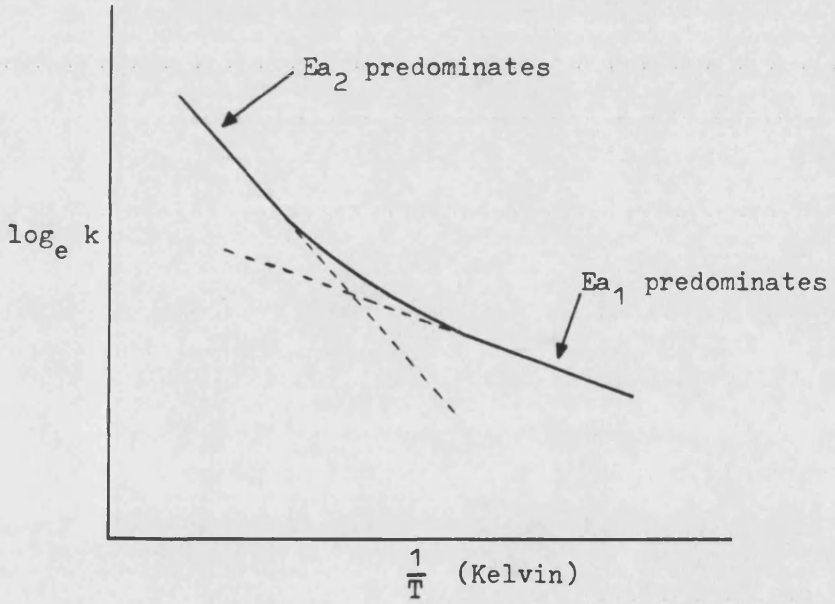

Figure 1.1 Plot of $\log_e k$ against 1/T showing a non-linear Arrhenius relationship due to reaction pathways of widely different activation energies

Figure 1.1 illustrates such a plot where two competing reactions occur with grossly different activation energies. The curve may

sometimes be resolved into two parts, each of which approaches linearity and the activation energy of each reaction may be determined from the individual slopes. However, in practice the observed rate constant at any one temperature is usually a complicated function of many rate constants (i.e. simultaneous, consecutive or opposing reactions).

Reactions possessing an apparent critical temperature are often implicated in deviations from $\log_e$ k against 1/T plots. However, it is more probable that the observed deviation is due to the rates at lower temperatures being so slow that they cannot be measured.

Knowledge of the effects of temperature on the rates and mechanisms of reaction is important since many stability tests are carried out under accelerated conditions. The theory of accelerated stability testing is discussed in section 1.7.

1.4 CATALYSIS

The degradation of a drug in solution is usually potentiated by some catalytic effect. Several types of catalysis may occur, either alone or as a combination of effects.

1.4.1 Specific Acid-Base Catalysis

Specific acid-base catalysis exists when the rate law for decomposition is found to contain either of the terms $[H^+]$ or $[OH^-]$ and is, therefore, directly dependent on the pH of solution. The overall rate constant may be expressed by equation 31 :

$$k_{obs} = k_o + k_{H^+}[H^+] + k_{OH^-}[OH^-] \quad \ldots\ldots(31)$$

where k_o, k_{H^+} and k_{OH^-} are the rate constants for the uncatalysed/water catalysed reaction, the hydroxonium ion catalysed reaction and the hydroxyl ion catalysed reaction respectively. At low pH, the term $k_{H^+}\ [H^+]$ is greater than k_o or $k_{OH^-}[OH^-]$ due to the greater hydrogen ion concentration. By ignoring activity considerations the rate of specific acid catalysis may be given by equation 32 :

$$k_{obs} = k_{H^+}\ [H^+] \qquad ....(32)$$

Similarly, at high pH the rate of specific base catalysis is given by equation 33 :

$$k_{obs} = k_{OH^-}\ [OH^-] \qquad ....(33)$$

When the hydroxonium ion and hydroxyl ion concentrations are low or the products of $k_{H^+}\ [H^+]$ and $k_{OH^-}\ [OH^-]$ are small, the value of k_o is important (equation 34) and the reaction is said to be solvent catalysed (unionised water is considered to be a reacting species) :

$$k_{obs} = k_o \qquad ....(34)$$

By similar arguments, in slightly acidic or alkaline conditions, either solvent and specific hydroxonium ion catalysis or solvent and specific hydroxyl ion catalysis can be observed.

The effects of specific acid-base catalysis can be neatly summarised in a pH-rate profile where the change in reaction rate is observed with pH. The various types of plot encountered are discussed in section 1.5.1. The observance of the pH at which the reaction rate is at a minimum is important as it determines the "pH of optimum stability."

1.4.2 General Acid-Base Catalysis

General acid catalysis is defined as catalysis by a proton donating acid other than the hydroxonium ion, whilst general

base catalysis is via a base, other than the hydroxyl ion, acting as a proton acceptor (sharing of an electron pair with a proton). General acid and base catalysts are classified as Brönsted acids and Brönsted bases respectively.

Many pharmaceutical solutions incorporate buffers to regulate pH. Since the buffer must comprise a conjugate acid-base pair, buffer components can act as general acid-base catalysts. In addition to this direct effect buffers may catalyse degradation as a result of impurities present in the salts.

Examples of catalysis by buffer salts include ampicillin (Hou and Poole, 1969), benzylpencillin (Finholt et al, 1965; Hou and Poole, 1971), chloramphenicol (Higuchi et al, 1954), methotrexate (Hansen et al, 1983) and nicotinamide (Finholt and Higuchi, 1962). Buffer concentration should therefore be kept at a minimum for drugs exhibiting general acid-base catalysis. The presence of trace metal contamination in commonly used buffer salts was found to be responsible for prednisolone degradation (Oesterling and Guttman, 1964).

The Brönsted Catalysis Law provides a relationship between the strength of an acid or base, determined by its ionisation constant, and its efficiency as a catalyst determined by the observed rate constant. The Brönsted relationship may be expressed simply by equations 35 and 36 :

$$k_A = B_A K_A^{\alpha} \qquad \ldots.(35)$$

$$k_B = B_B K_B^{\beta} \qquad \ldots.(36)$$

Where k_A and k_B are the rate constants for general acid and base catalysis respectively, K_A and K_B are the acidic and basic

ionisation constants and B_A, B_B, α and β are constants characteristic of the reaction, solvent and temperature. Catalytic constants of acidic species may be obtained by plotting the Brönsted relationship in the form of equation 37 :

$$\log k_A = \alpha \log K_A + \log B_A \quad \ldots.(37)$$

1.4.3 Electrophilic and Nucleophilic Catalysis

Catalysis may occur by mechanisms which do not involve proton transfer. An electrophilic catalyst acts as an electron pair acceptor (Lewis acid), the metal ion catalysis of ascorbic acid being an example (Finholt et al, 1966). A nucleophilic catalyst is a general base but acts by forming a bond (donating an electron pair) with an atom other than hydrogen (usually carbon). The imidazole catalysed hydrolysis of 4-nitrophenyl acetate is an example of nucleophilic catalysis (Connors et al, 1979).

1.5 REACTIONS IN SOLUTION

1.5.1 pH Effects

As a result of catalytic effects, the rates of reaction in aqueous solution are usually dependent on pH. A study of the pH dependence of reaction rates provides practical information about drug stability and catalytic mechanisms. Data are usually presented as a plot of log k_{obs} vs pH where characteristic features such as linear segments, maxima, minima and inflection points can be related to the rate equation. Analysis of the resultant pH-rate profile may reveal :

1.5.1.1 Linear relationships

A linear relationship between log k and pH usually indicates that simple specific acid or base catalysis occurs over a

particular pH range. If only a portion of the whole log k vs pH profile is considered it is possible to neglect the terms describing the rest of the plot. For example, in a system undergoing specific acid catalysis, the hydrogen ion concentration is large in the acid region. Equation 31 therefore reduces to equation 38 or 39 :

$$k_{obs} = k_{H^+} [H^+]$$

$$\left(\text{since } [OH^-] = \frac{K_w}{[H^+]}\right) \quad \ldots.(38)$$

or $$\log k_{obs} = \log k_{H^+} - pH \quad \ldots.(39)$$

Therefore, in the acidic region a plot of log k vs pH should give a straight line with slope -n, where n is the order with respect to the hydrogen ion. Similarly in basic solution a straight line will be produced if the reaction is specific-base catalysed.

If only specific acid-base catalysis occurs, both slopes will equal one and the resultant profile will be "V" shape. Practically, slopes of ± unity are infrequent and an absolute point minima is rarely observed since other terms in the overall rate equation are too significant to be neglected. Additionally at high and low pH values (< 3, > 11) activity effects become significant since pH is a function of the activity of the hydroxonium ion and not its concentration.

However, linear portions with very close similarities to the ideal "V" shape profile have been observed with atropine (Lund and Waaler, 1968; Zvirblis *et al*, 1956), benzylpenicillin (Finholt *et al*, 1965) and diazepam (Mayer *et al*, 1974).

1.5.1.2 Sigmoid portions

An inflection in a pH-rate profile is usually indicative of reactant ionisation with the two species exhibiting different

reaction rates. The overall rate of reaction will be dependent on the ionisation constant (pKa) and the individual reactivities of ionised and unionised species. Analysis of the kinetic data from a sigmoid pH-rate profile may provide estimates of pKa and the reaction rate constants of each reactant species (Connors, 1981).

The classic log k vs pH plot for aspirin shows a sigmoid portion superimposed on to a V-graph (Edwards, 1950). This profile identified the hydrolysis of the anion to be the major degradative mechanism in solution (see section 1.6.2.2).

Other examples of pH-rate profiles influenced by substrate ionisation include ampicillin (Hou and Poole, 1969), barbiturates (Garrett et al, 1971) and thiamime (Windheuser and Higuchi, 1962). Alternatively, sigmoid pH-rate profiles may be produced by pH dependent rates of parallel reactions. A change of pH will alter the predominance of parallel reactions resulting in variable overall rate constants. The degradation of clindamycin (Oesterling, 1970) is an example of this type of pH effect.

1.5.1.3 Bell-shaped curves

pH-rate profiles may exhibit a maxima or "bell-shaped" peak. This feature is essentially two sigmoid curves back to back and the two inflections indicate two ionisations of the reactant(s). For example, in a dibasic acid the monoanion may be the most reactive species, or in a reaction between an acid and base the two inflections represent their respective ionisations and subsequent reactivity.

Another mechanism which may be associated with a bell-shaped pH-rate profile is a pH dependent change in the rate determining step for a multi-step (consecutive) reaction. The pH dependent reversible hydrolysis of hydrochlorthiazide illustrates such an effect (Mollica et al, 1971). The pH was observed to exert a direct effect on reaction mechanisms rather than influence the kinetics by ionised-unionised species ratios. The catalysis of penicillin degradation by catechols provide other examples where catalysis by the catechol monoanion results in a bell-shaped plot and a pH of maximum instability (Schwartz, 1964).

1.5.1.4 Plateau portions

Certain regions in a pH-rate profile may be characterised as being independent of pH, i.e. an apparent plateau. The pH-rate profiles of cephalosporins exhibit large plateaus (Yamana and Tsuji, 1976) thought to be associated with the pH independent β-lactam ring cleavage. Other examples of pH independent water attack or intramolecular catalysis resulting in plateau pH-rate profiles include aspirin (Garrett, 1957), chlordiazepoxide (Maulding et al, 1975) and sulphacetamide (Meakin et al, 1971a).

1.5.2 Ionic Strength

The ionic strength, I, of a solution is given by equation 40 :

$$I = \frac{1}{2}\sum(C_i Z_i^2) \qquad \ldots.(40)$$

where C_i is the molar concentration of each ion and Z_i its charge.

A kinetic study should always take into account "salt effects". This is done by varying the ionic strength by addition of an inert electrolyte (usually potassium chloride) whilst keeping

other rate determinants constant. The observed rate constant will either increase, remain constant or decrease compared with the observed rate constant at "zero" ionic strength (infinite dilution). The effect is denoted positive, absent or negative salt effect respectively and is valuable in the identification of reaction mechanisms. Any quantitative relationship is only theoretically valid in low concentrations of ionic species but kinetic salt effects are usually extended outside these regions in pharmaceutical systems (Carstensen, 1970).

The Brönsted-Bjerrum equation (derived from the Debye-Hückel limiting law) relates the rate constant to ionic strength by equation 41 :

$$\log k = \log k_i + 2QZ_AZ_B \sqrt{I} \qquad ....(41)$$

where k_i is the rate constant at infinite dilution, Q is a constant related to temperature and Z_A and Z_B are the respective charges of the two reacting species A and B. Since the Debye-Hückel limiting law only holds for concentrations up to 0.01M ionic strength, a modified Debye-Hückel equation for ionic strengths up to 0.1M alters equation 41 to equation 42 :

$$\log k = \log k_i + 2QZ_AZ_B \frac{\sqrt{I}}{1+\beta\sqrt{I}} \qquad ....(42)$$

where β is a constant dependent on the ionic diameter of the reacting species. Since β is taken to be fairly close to unity, equation 42 may be rewritten as equation 43 :

$$\log k = \log k_i + 2QZ_AZ_B \frac{\sqrt{I}}{1+\sqrt{I}} \qquad ....(43)$$

This equation has been applied with reasonable accuracy to

pharmaceutical systems with an ionic strength up to 0.5M (Carstensen, 1970). From equation 43 a linear relationship is predicted if log $\frac{k}{k_i}$ is plotted against $\sqrt{I}$ with a slope proportional to the product of $Z_A Z_B$. The value of $Z_A Z_B$ may be positive, negative or zero indicating the presence or absence of a primary salt effect. No observed kinetic salt effect (zero slope) indicates that the degradative reaction does not involve a charged species since either Z_A or Z_B would have to be zero. No kinetic salt effects were observed in the degradation of carbuterol (Ravin et al, 1978), chloramphenicol (Higuchi et al, 1954), hydrochlorthiazide (Mollica et al, 1971) and moxalactam (Hashimoto et al, 1984).

At high ionic strength (> 0.5-1M), the reaction of neutral substrate molecules may sometimes exhibit a linear relationship between the rate constant and ionic strength. This is due to the effect of ionic strength on the activity coefficient of a neutral molecule. However, such high ionic strengths are rarely encountered in pharmaceutical solutions.

Ion-dipole reactions are generally insensitive to ionic strength effects but the importance of solvent polarity on such reactions is discussed later (see section 1.5.3).

Reactions between charged species of opposite or identical change are implicated where kinetic salt effects are observed. An increase in ionic strength is expected to decrease the rate of reaction between oppositely charged ions (negative salt effect) and increase the rate of reaction between similarly charged ions (positive salt effect); the numerical values of the slope will be integral numbers corresponding to the charges on the reacting species.

Finholt et al (1965) observed a positive primary salt effect (slope = 2) for the degradation of benzylpenicillin in neutral to slightly alkaline solution. These observations helped identify the reaction mechanisms involved. Felmeister et al (1965) also observed a kinetic salt effect (slope 1.6 to 2.3) and used this to support a proposed reaction mechanism for the oxidation of chlorpromazine. An integral negative salt effect (slope = 0.9) was observed by Hussain et al (1968) which was again used as supportive evidence in the proposed reaction mechanism for echothiophate iodide degradation.

Observed salt effects which deviate from the theoretical integer slope values indicate that parallel reactions of different ionic character may be occurring.

The degradation of ampicillin in acidic solution produced a non-integral value thought to be a consequence of the compexity of degradation in acid (Hou and Poole, 1969). The negative fractional kinetic salt effects (slope = 0.37 to 0.54) observed by Windheuser and Higuchi (1962) were used as supportive evidence for the proposed degradative mechanism of thiamine involving four separate reaction mechanisms. A secondary salt effect (discussed below) was also thought to be important in thiamine degradation. Other examples of fractional slopes include barbitone (Goyan et al, 1960) - parallel reactions, indomethacin (Hajratwala and Dawson, 1977) - complex reaction and nicotinamide (Finholt and Higuchi, 1962).

In performing kinetic studies it is important to establish any primary salt effect separately from any catalytic

effect of buffer species as both, either or none of these effects may influence the reaction kinetics.

A secondary salt effect may be observed when the ionic strength has a direct influence on the ionisation of a reactive species. For example, in buffer catalysed degradation the ionised species may be catalytic, but not the corresponding acid. The rate constant would therefore be influenced by the effect of ionic strength on the concentration of ionised catalytic species. Both primary and secondary salt effects were observed in the hydrolytic degradation of thiamine (Windheuser and Higuchi, 1962).

1.5.3 Solvent Polarity

The dielectric constant of a solvent is known to influence the rate of reaction between ionic species. Generally, an increase in dielectric constant increases the rate of reaction between ions of like sign and decreases it for reactions of opposite sign. Examples of both effects in pharmaceutical systems have been provided by Garrett (1962).

If the reaction involves an ion-dipole interaction, an increase in dielectric constant causes an increase in reaction rate for a negative ion reactant and decrease for a positive ion reactant. Experimental evidence of this type supported the postulation that the degradation of chloramphenicol (Marcus and Taraszka, 1959) and glucose (Heimlich and Martin, 1960) involved ion-dipole reactions. The rate constant for dipole-dipole reactions is usually increased by increasing the dielectric constant (Garrett, 1962).

Therefore, study of the effects of changing solvent polarity may provide indications of degradative reaction mechanisms. Knowledge of these mechanisms may then aid the stabilisation of a pharmaceutical through the use of mixed solvent systems.

1.6 DEGRADATIVE REACTION MECHANISMS

Hydrolysis and oxidation are the main degradative mechanisms for pharmaceuticals in solution. Other mechanisms such as isomerisation, epimerisation, addition, elimination, acylation and polymerisation are less important and have been reviewed by Mollica *et al* (1978).

Compounds containing carbon-nitrogen bonds (like chlorhexidine) generally degrade by hydrolytic mechanisms. Hydrolysis will, therefore, be discussed in detail. Oxidative mechanisms are also discussed since oxidation and hydrolysis often occur simultaneously, for example in chloramphenicol (Shih, 1971).

Photolytic degradative mechanisms and effects due to ionising radiation are discussed separately.

1.6.1 Oxidation

Oxidative reactions involve the removal of electrons from an atom or molecule and do not necessarily require molecular oxygen, to occur. However, in pharmaceuticals, oxidation is usually mediated through a reaction with atmospheric oxygen, this process being referred to as auto-oxidation.

Auto-oxidation involves free-radical (chain) reactions and in most practical cases the rate of reaction is independent of oxygen supply since little is needed once the chain reaction is

initiated. However, oxygen limitation can affect the rate of reaction (for example, stability studies performed in ampoules). The rate of auto-oxidative reactions may be influenced by temperature, pH, electromagnetic irradiation (photochemical oxidation) or the presence of catalysts (heavy metals, peroxides or buffers).

The products of oxidation are usually more electronically conjugated (i.e. more electronegative) than the reactants, producing highly coloured solutions indicative of oxidative degradation. Functional groups susceptible to oxidation include phenols, esters, carboxylic acids, nitrates and aldehydes. Pharmaceutical compounds such as vitamins, antibiotics and steroids undergo oxidative degradation. Individual examples have been listed by Connors et al (1979) and Mollica et al (1978).

1.6.2 Hydrolysis

In hydrolytic reactions water acts as a nucleophile by attacking an electropositive centre. The commonest hydrolytic reactions involve attack on "labile" carbonyl centres such as those in esters and amides. Pure solvent (i.e. water) alone has the capability to hydrolyse compounds but generally hydrolytic reactions proceed through protolytic mechanisms involving hydroxonium or hydroxyl ions.

1.6.2.1 Kinetics of Hydrolytic Degradation

The overall rate of hydrolysis is frequently the sum of a whole series of parallel reactions involving the drug in various

forms and a variety of attacking species as shown by equation 44 :

$$k_{obs} = k_o + k_{H^+}\ [H^+] + k_{OH^-}[OH^-] + k_N[N] + k_{GB}[GB] + k_{GA}[GA] \ldots . \quad (44)$$

where

k_o is the rate constant for the uncatalysed/water catalysed reaction,

k_{H^+} is the rate constant for the hydroxonium ion catalysed reaction,

k_{OH^-} is the rate constant for the hydroxyl ion catalysed reaction,

k_N is the rate constant for nucleophilic catalysis (Lewis base),

k_{GB} is the rate constant for general base catalysis (Brönsted base)

and k_{GA} is the rate constant for general acid catalysis (Brönsted acid)

The importance of species specific effects (such as ionisation constant) in relation to the overall rate constant can be illustrated by the hydrolysis of ester and amide functional groups.

1.6.2.2 Examples of Hyrolytic Degradative Mechanisms

Esters :

The hydrolysis of an ester involves the cleavage of a covalent bond between oxygen and carbon, invariably at an acyl-oxygen linkage. A generalised mechanism for either acid or alkaline hydrolysis of esters has been presented by Walters (1950) :

acid catalysed:

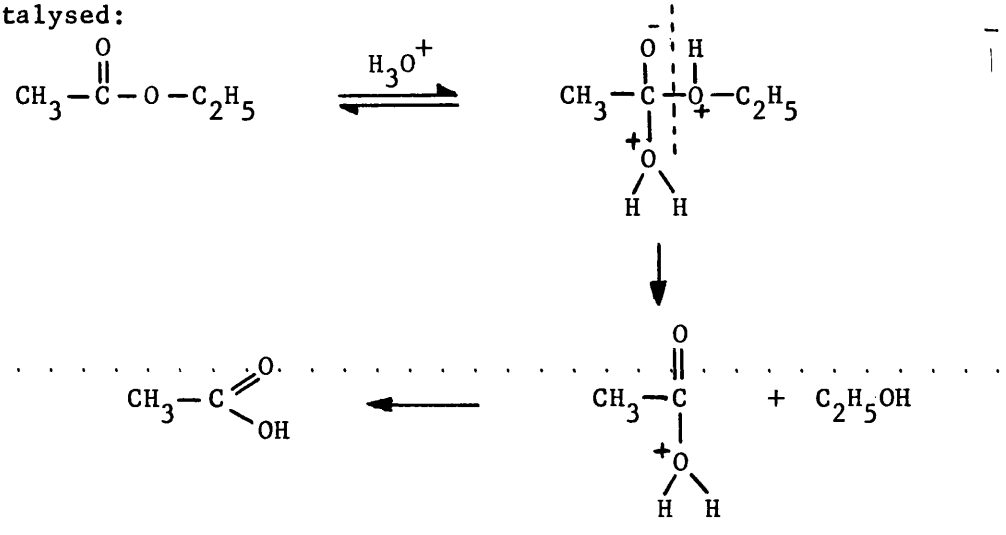

base catalysed:

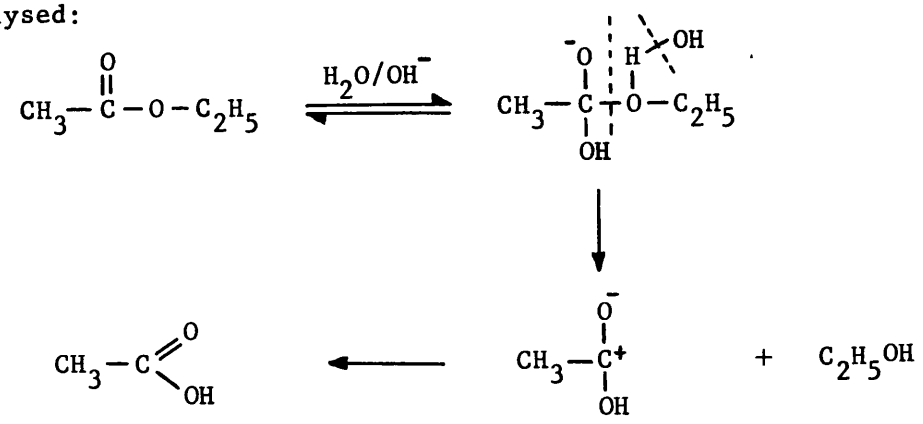

Study of aspirin hydrolysis has contributed much to the knowledge of ester degradative mechanisms. Edwards (1950 and 1952) identified the hydrolysis of aspirin to involve six degradative mechanisms occurring simultaneously - these being the reactions of unionised and ionised aspirin with the hydroxonium ion, hydroxide ion or molecular water. Garrett (1957) favoured a more complex mechanism which explained the previously observed pH-independent hydrolysis and dependence on ionic charge. Kelly (1970), after an extensive review of the literature, then proposed three mechanisms for the intramolecular catalytic hydrolysis of aspirin by the carboxyl group. Kinetic evidence favoured a general base catalysis of water attack by the carboxylate anion with intra- and inter-molecular catalysis being considered to occur by the same

mechanism. This example of aspirin illustrates the complexity of mechanisms which may be involved in the degradation of a relatively simple molecular structure.

Ester hydrolysis is also responsible for the degradation of other pharmaceuticals such as atropine (Lund and Waaler, 1968), benzocaine and procaine (Connors et al, 1979).

Amides :

The acid and basic hydrolysis of amides may be represented by $A_{ac}2$ and $B_{ac}2$ mechanisms respectively (Koshy, 1969) :

Acid hydrolysis :

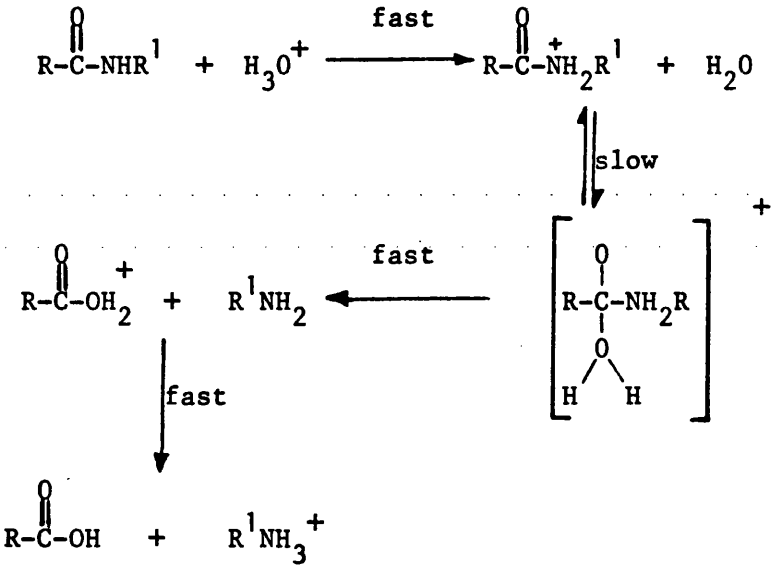

Base hydrolysis :

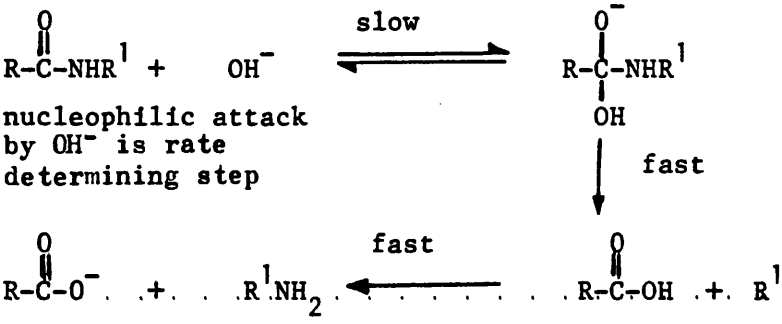

Because of the relative stability of the amide linkage other degradative mechanisms can occur in addition to amide hydrolysis. For example, chloramphenicol degrades via amide hydrolysis and by dehalogenation, the mechanism being dependent on the pH of solution (Higuchi and Bias, 1953; Higuchi et al, 1954). Where other functional groups are absent, i.e. nicotinamide (Finholt and Higuchi, 1962), the amide linkage shows great stability with hydrolysis only occurring on general acid and base catalysis. The stability of the amide group has been attributed to "amide resonance" involving the delocalisation of nitrogen lone pair electrons (Johnson et al, 1949).

Other Functional Groups :

The hydrolysis of other functional groups has been identified as being responsible for their instability in aqueous solution. Four groups are discussed here : imides, di-imides, lactams and lactones. Imides , such as glutethimide (Wesolowski et al, 1968), degrade by hydroxyl ion attack on the unhindered carbonyl followed by ring cleavage. Di-imides, such as the barbiturates, are prone to steric and ionic charge effects which influence the site of hydrolytic ring cleavage (Gardner and Goyan, 1973; Garrett et al, 1971). The hydrolysis of β-lactam antibiotics has been extensively studied and provides good examples of the effect of substituents on reactivity. The bicyclic β-lactam-thiazolidine structure (in penicillins) is much more sensitive to electrophiles and nucleophiles than the simple β-lactam structure (Hou and Poole, 1971). Initial β-lactam cleavage is responsible for many succeeding degradative reactions of penicillins. It has been proposed that the

instability of the β-lactam group is caused by the strain imposed by fusion on to the thiazolidine ring which inhibits any stabilising amide resonance effects. Lactones, such as pilocarpine and wafarin, generally degrade by mechanisms involving lactone ring opening (Chung et al, 1970; Connors et al, 1979).

Although reactivity may be predicted by the presence of certain functional groups within a drug molecule the degradative mechanism is likely to be influenced by structural effects. Consequently, structural analogy can only aid, and not replace, experimentally derived kinetic data as supportive evidence for proposed degradative mechanisms.

1.6.2.3. Application of the Arrhenius Relationship to Hydrolysis Reactions

The combined effects of specific and general acid-base catalysis has been discussed earlier (see section 1.4). Each contributory reaction will have its own activation parameters (section 1.3.3). Thus for the overall reaction rate equation (45) :

$$k_{obs} = k_{H^+}[H^+] + k_{OH^-}[OH^-] + k_w[H_2O] \quad ....(45)$$

the determination of an overall activation energy at a particular pH is easily performed by plotting log k_{obs} against 1/T, but in practice it represents a more complex situation (equation 46) :

$$k_{obs} = A \exp^{-E/RT} = A_{H^+}[H] \exp^{-E_{H^+}/RT} + ... \quad ....(46)$$

with each term having greater or less importance at particular pH values as explained earlier (section 1.5.1). Since a plot of log k_{obs} against 1/T is a function of all terms in equation (46) the value of the overall activation energy generated must be regarded as being apparent, as the values of Ea_{H^+}, Ea_{OH^-} and Ea_{H_2O} are rarely the same. The apparent activation energy obtained by an Arrhenius

plot will be controlled by the activation energy of the predominant reaction at that particular pH in the same way that k_{obs} is controlled by the predominant individual rate constant. The design and interpretation of kinetic studies must take into account the variable activation energies of each reaction, particularly when constructing an accelerated pH-temperature study.

Another special case involves the interpretation of accelerated studies where the rate of reaction is dependent upon hydroxyl ion concentration. If the rate is determined at several temperatures with constant pH then equations 47 to 49 may be written :

$$k_{OH^-}[OH^-] = k_{obs} = A \exp^{-(Ea_{OH^-}/RT)} \quad ....(47)$$

rearranging :

$$k_{OH^-} = \frac{k_{obs}}{[OH^-]} = A \exp^{-(Ea_{OH^-}/RT)} \quad ....(48)$$

$$k_{obs} = [OH^-] A \exp^{-(Ea_{OH^-}/RT)} \quad ....(49)$$

Since pK_w varies with temperature, $[OH^-]$ will vary whilst $[H^+]$ remains constant by definition. Therefore equations 50 to 52 apply :

$$[OH^-] = \frac{K_w}{[H^+]} \quad ....(50)$$

with $$k_{obs} = \frac{K_w}{[H^+]} A \exp^{-(Ea_{OH^-}/RT)} \quad ....(51)$$

or $$\log k_{obs} = \log \frac{A}{[H^+]} + \log K_w - \frac{Ea_{OH^-}}{2.303RT} \quad ....(52)$$

From the van't Hoff equation (in the form of equation 53) :

$$\log K_w = \frac{-\Delta H^o_w}{2.303RT} + \frac{\Delta S^o_w}{2.303R} \quad ....(53)$$

combination of equations (52) and (53) produces equation 54 to 56 :

$$\log k_{obs} = \log \frac{A}{[H^+]} + \frac{\Delta S^o_w}{2.303R} - \frac{Ea_{OH^-} + \Delta H^o_w}{2.303RT} \quad ....(54)$$

$$\text{or} \qquad k_{obs} = A^1 \exp^{-(Ea_{OH^-} + \Delta H^o_w)/RT} \quad ....(55)$$

$$\text{where} \qquad \log A^1 = \log \frac{A}{[H^+]} + \frac{\Delta S^o_w}{2.303R} \quad ....(56)$$

with equation (56) remaining constant with temperature. Therefore, a plot of log k_{obs} against 1/T would give a slope of $-\left(\frac{Ea_{OH^-} + \Delta H^o_w}{2.303R}\right)$ and the standard enthalpy for the ionisation of water (ΔH^o_w) must be subtracted from the overall activation energy obtained from the Arrhenius plot. In this way the true value for the activation energy of the specific hydroxyl ion catalysed reaction is obtained. A value for the enthalpy of ionisation of water is quoted by Matter-Müller and Strumm (1984) as 55.71 $kJ.mol^{-1}$.

1.6.3 Photochemical Decomposition

Investigation of photochemical effects on pharmaceutical compounds is becoming increasingly more important due to the complex chemical structure of many new drugs. Light may provide the necessary activation energy for a reaction to occur. However, the electromagnetic radiation must be of the correct frequency and possess sufficient energy to cause activation. The energy of electromagnetic radiation is proportional to the reciprocal of its wavelength so radiation of lower wavelength has a higher energy. Therefore the ultraviolet and violet regions are more active in initiating photochemical reactions. However, the ability of a molecule to absorb energy depends on the presence of an energy absorbing group.

Once absorbed, light induces molecular excitation of electrons from lower to higher energy orbitals. The excited molecule is unstable and may then return to the lower energy state in one of four ways :

(i) The absorbing molecule decomposes.

(ii) The energy is transferred to another molecule which may then decompose (photosensitisation).

(iii) The energy is converted to heat.

(iv) The absorbing molecule emits light of a different wavelength and no decomposition occurs (fluorescence or phosphorescence).

These events are classified primary photochemical reactions since they are a direct consequence of light absorption. Secondary photochemical reactions result from the production of free radicals and once initiated by light may continue in the dark.

Factors influencing the rate of photochemical decomposition include :

(i) Metal ion concentration.

(ii) Oxygen tension.

(iii) Presence of anti-oxidants.

(iv) pH - since this influences ionisation and photochemically initiated red-ox reactions.

(v) Solvent system.

(vi) Presence of micelles or macromolecules.

(vii) Temperature.

The generation of heat in photochemical reactions is an important practical consequence since decomposition may be due to

the combined effects of photolysis and raised temperature. Thermal effects may also influence subsequent chain reactions following a photochemical reaction. Consideration of these effects must be given in experimental design.

Since photodegradation is usually slow, accelerated light stability tests are used. However, traditional tests at a sunlit window are unable to differentiate between thermal and photochemical effects, whereas simulated daylight conditions can be controllable by the use of light sources with similar spectral composition to daylight.

The photodegradation of chlorpromazine has been found to involve hydroxylation and free radical mechanisms (Felmeister and Discher, 1964). A semiquinone free radical intermediate was formed on irradiation which then underwent disproportionation to yield a photolabile precursor of phenolic and unidentified degradation products.

1.6.4 Stability to Ionising Radiation

Radiation sterilisation is an alternative to the heat sterilisation of thermolabile pharmaceuticals (Jacobs and Melumad, 1976) or as a method of microbial control for a wider range of non-sterile formulations (e.g. creams and ointments). The British Pharmacopoeia (1980) recommends a dose requirement of 25 kGy (2.5 M rads) but this may be reduced for materials with a low initial microbial load (Trigger and Caldwell, 1968).

Pharmaceuticals in their dry solid state are, in general, considerably more stable to ionising radiation than in aqueous solution or suspension (Bor, 1981). However, the presence of water

of crystallisation in ampicillin makes the compound more sensitive than the anhydrous form (Dziegielewski, 1975).

The chemical interaction of molecules with γ-wave irradiation may be described simply by : (i) quantum energy absorption where a quantum causes the ejection of a reactive inner shell electron (similar to photochemical decomposition involving ultraviolet or visible light), (ii) Compton scattering results from absorption of high energy γ-rays producing a photon with low energy and of different wavelength, (iii) pair-production involving photon interaction with the nucleus of an atom producing an unstable electron-positron pair. Excited molecules return to their ground states by similar mechanisms to those described for photochemical decomposition (section 1.6.3).

In solution degradative effects are usually due to the excitation of the solvent. The effect of ionising irradiation on water itself is the production of molecular hydrogen and hydrogen peroxide. However, little decomposition of water is actually detected due to the recombination of free radicals to reform water. A simple summary of a radiation induced effect on water is expressed by equation 57 :

$$H_2O \longrightarrow H\cdot + e^-_{aq} + OH\cdot + H_3O^+ + H_2 + H_2O_2 \quad ....(57)$$

with each product having the capability of further reactivity. Pharmaceutical degradation in aqueous solution results from drug molecules entering the free radical mechanism.

The chemical effects of irradiation are described by the G-value (positive or negative) which indicates the number of molecules formed or destroyed per 100 eV energy absorbed. The

G-values are dependent on the type of radiation induced reactions involved, with pharmaceuticals typically having G±1 to 5. A G-value much less than one is indicative of some form of radiolytic protection.

1.6.5 Degradation in the Presence of Surfactants

1.6.5.1 Introduction

The presence of surfactant micelles is known to influence the rate of many chemical reactions and the extensive literature on micellar catalysis and inhibition has been reviewed by Fendler and Fendler (1975; 1980). The significance of micellar effects are such that reactions can be completely inhibited in the presence of a surfactant or acceleration can occur resulting in increases of up to 10^5 in observed rate constants (Martinek et al, 1977).

1.6.5.2 Micelle Structure

An understanding of ionic micelle structure has aided the interpretation of catalytic and inhibitory effects. A diagrammatic cross section of the conventionally accepted model of a typical ionic micelle (Stigter, 1974) is shown in Figure 1.2.

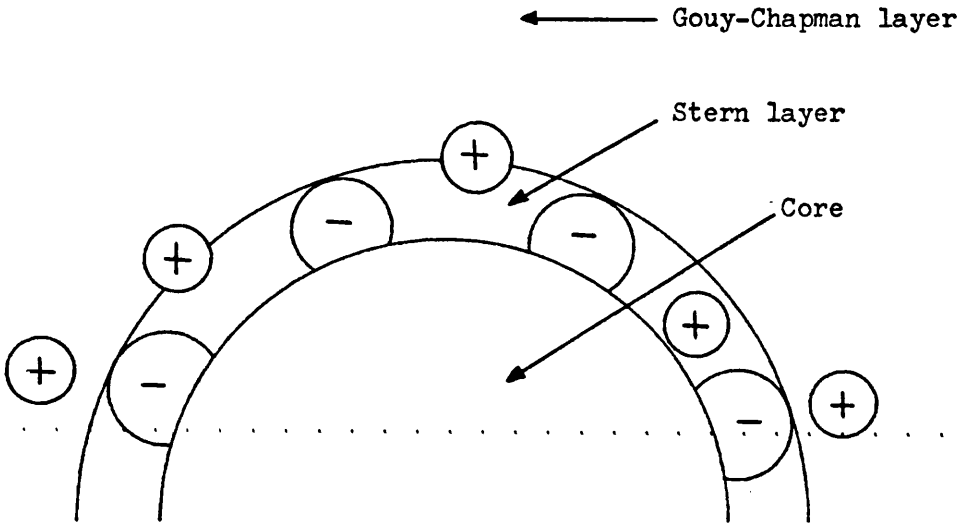

Figure 1.2 Partial cross section of an anionic micelle with hydrated cationic counterions (Stigter, 1974)

The core contains associated hydrophobic hydrocarbon chains with polar head groups projecting outwards towards the bulk aqueous phase. The Stern layer surrounds the core and contains both the ionised polar head groups and a large proportion (70-80%) of counterions. Surrounding the Stern layer is the Gouy - Chapman layer, which is much more diffuse and contains the remaining counterions (Bunton 1979 a).

The chemical properties of the Stern layer and Gouy - Chapman layer are of obvious importance in influencing micellar effects (Bunton, 1979 b). For example, since hydroxonium and hydroxyl ions act as counterions, the pH at the surface of an ionic micelle may vary by 1-2 pH units from that of the bulk aqueous solution (Chaimovich et al 1982). Hydroxonium-ion and hydroxide-ion catalysed reactions therefore depend on the concentration of micellar bound ion and not on the experimental pH. The solvent environment, and therefore subsequent reactivity, of ionic reactants or reactive ions may be affected by their incorporation into the micelle or close proximity to the Stern layer.

The polarity of the micellar environment, as assessed by dielectric constant, increases significantly from the core surface through the Stern layer and reaches that of water towards the exterior of the Gouy - Chapman layer (Kalyanasundaram and Thomas, 1977). This change in polarity across the micellar surface may influence reaction rates by a submicroscopic solvent effect (see also section 1.5.3).

Although the structure of non-ionic micelles is less well defined, it is known that considerable amounts of water can be hydrogen bonded, to polyoxyethylene chains for example, forming a palisade layer around the hydrophobic core (Attwood and Florence, 1983). Thus again marked polarity gradation will occur from the micelle core to the bulk aqueous phase. Reactant binding via non-ionic hydrogen bonding mechanisms will also occur within the palisade layer.

Micelles may therefore influence the type of reaction products generated, especially in functional micelles which contain reactive groups within the surfactant molecule (Bunton, 1979 a). The effect on reaction products is by the provision of a particular environment since micellar structures are too loose and mobile to have a direct mechanistic influence.

Reactants are not without their effects on surfactants. The critical micelle concentration (CMC) is often reduced in the presence of reactants due to induced micellisation or the formation of submicellar aggregates of surfactant and reactant (Bunton, 1979 a).

Salt effects on CMC and aggregation numbers for ionic surfactants and on cloud point for non-ionics are reviewed by Attwood and Florence (1983).

Temperature also influences the structure and properties of micelles. The size of ionic micelles has been reported to decrease with temperature whilst some non-ionic surfactant micelles show an increase in aggregation number and hydrocarbon chain hydration with temperature (Attwood, 1968). Temperature has a

significant effect on the solubility of non-ionic surfactants. Above the cloud point reversible phase separation occurs resulting in the separation of a surfactant rich co-acervate phase from an aqueous phase containing surfactant monomers. Therefore, knowledge of the likely effects of temperature on surfactant properties is important if reliable predictions of room temperature stability are to be made from accelerated stability studies involving micellar systems.

1.6.5.3 Kinetic Modelling of Micellar Reactivity

In order to explain the observed kinetic effects associated with micelle presence, a series of models have been conceived. Two such models (the electrostatic potential model and pseudophase model) have been widely applied. However, each model has required rationalisation as more and more complex kinetic effects have been observed in the presence of surfactants, reactants and other added species. Therefore it is probably more beneficial to consider each model not as a definitive theory but as merely an extension to its predecessors.

The electrostatic potential model, first proposed by Hartley (1934; 1948), explained micellar catalysis and inhibition in terms of proximity effects. For example, in a base catalysed reaction, hydroxide ions would be attracted to the surface of positively charged cationic micelles. Reactant molecules present in the surface layer of these cationic micelles would be exposed to a higher concentration of hydroxide ion than in the bulk aqueous solution and micellar catalysis would occur. The converse situation would pertain to base catalysed reactions in the presence of anionic

micelles which would repel the attacking ion. Similar arguments could be applied to the effects of anionic and cationic micelles on the rates of acid catalysed reactions.

In the presence of non-ionic micelles, proximity effects in terms of hydrophobic-hydrophilic interactions were thought to be important. Hyrophobic reactants would be taken into the micellar interior and reactivity would be dependent on the ability of hydrophilic ions to diffuse into this unfavourable region. This model was considered to function well since micellar catalysis of non-ionic reactants with non-ionic nucleophiles could also be explained by proximity effects with micellar charge being unimportant in these systems.

However, as more information on micellar structure became available, particularly that relating to ionic micelles, the electrostatic model failed to explain many observed effects. For instance rate constants were observed to go through a maxima with increasing surfactant concentration. For bimolecular reactions the distribution of the two species between micelle and bulk aqueous phase is an important consideration.

The pseudophase model (Romsted, 1977) therefore developed the electrostatic potential model by assuming that reactions could occur in either the bulk aqueous phase or in a micellar pseudophase. The variation in the rate constant for the overall reaction with surfactant concentration could then be analysed in terms of reactant concentrations and rate constants for simultaneous reactions in each pseudophase.

Several important assumptions have been made in the application of this model which include; (i) the solution consists of two phases, a bulk aqueous phase and a micellar phase, (ii) the rates in each pseudophase depend on the reactant concentrations and rate constants in each pseudophase, (iii) a distribution of reactant exists between the two phases, (iv) reactant-product combinations do not affect micellar properties, (v) partition between phases is unaltered by the chemical reaction with reactants being rapidly equilibrated between the phases and (vi) no reaction occurs across the pseudophase boundary between the micellar phase and aqueous phase.

The success of the pseudophase model has been its ability to interpret micellar effects for both unimolecular and bimolecular reactions. The observed maxima in rate-surfactant profiles for bimolecular reactions may be explained as follows. The micellar partition coefficient of reactant (K_m) is given by equation 58 :

$$K_m = \frac{C_m}{C_{aq}} \qquad \ldots.(58)$$

Where C_m and C_{aq} are the concentration of reactant in the micellar and bulk aqueous phases respectively. The rates of reaction in each phase are given by equations 59 and 60 :

$$\text{Rate}_{(m)} = -k_m C_m \qquad \ldots.(59)$$

$$\text{Rate}_{(aq)} = -k_{aq} C_{aq} \qquad \ldots.(60)$$

where k_m and k_{aq} are the apparent first-order rate constants in the micellar and aqueous phases. As surfactant concentration increases both C_m and C_{aq} fall to maintain K_m constant. If $k_m > k_{aq}$ the

overall rate increases. As surfactant concentration increases further, virtually all the reactant is partitioned into the micellar phase and C_{aq} will approach zero and the overall rate reaches a maximum. With a further increase in surfactant concentration a decrease in the micellar rate (and hence overall rate) is observed since the micellar reactant concentration (C_m) drops.

The pseudophase model also allows the use of micellar binding (or partition) constants to explain catalysis or inhibition. For example, micellar rate enhancement of ester hydrolysis was found to decrease with increasing alkyl chain length (Fendler and Fendler, 1980; Lippold et al, 1972). Since binding constants were found to increase with alkyl chain length (hence hydrophobicity), the observed kinetic effects were explained by the inability of the hydroxide ion to penetrate deep into the micellar core. Thus, the pseudophase model explains micellar effects in terms of the binding or partition of reactants into particular areas of the micelle (Stern layer or hydrophobic core).

However, some of the assumptions of the pseudophase model fail when applied to situations involving buffers or added neutral salts. Buffer equilibria are significantly affected by the presence of micelles which therefore induce pH changes. Buffer salts also act as micelle counterions. Typically, added salts decrease micellar rate enhancement effects by either (i) an electrostatic effect of reducing surface potential for charged micelles or (ii) competition between the reactive and inert counterions for the micellar surface. Salt effects may be specific by dependence on the hydrophobicity of species of opposite charge to the micelle. The

effects are greatest for large low charge density ions which are able to interact strongly with micelles (Bunton, 1973).

From studies with reactive counterion surfactants, i.e. the counterion is also the reactive ion, an ion-exchange model has been developed which essentially combines the fundamental principles of both electrostatic and pseudophase models (Bunton and Romsted, 1982). Micellar binding was considered by Chaimovich et al (1982) to be an ion-exchange process involving all counterionic species, this approach being theoretically applicable to situations involving buffers or added neutral salts. However, the Chaimovich concept requires a situation involving only two ionic species and a knowledge of their ion-exchange constants. Since the latter are not known the concept is presently theoretical rather than practical.

1.6.5.4. Micellar Catalysis and Inhibition of Hydrolysis Reactions

The mechanisms of base catalysed ester hydrolysis have been extensively studied (see 1.6.2.2) and these reactions have provided useful models for the investigation of micellar effects. Since the intermediate in a base catalysed hydrolysis reaction is negatively charged it has been assumed that the rate enhancement observed in cationic micellar systems is due to stabilisation of the intermediate as well as attraction of hydroxide ions (Attwood and Florence, 1983).

Observed maxima in micellar enhanced reactions, and in some cases inhibition, have been explained in terms of the site of interaction and counterion effects. For example, where an increase in ester hydrolysis with surfactant (cetyltrimethyl ammonium bromide - CTAB) concentration was observed it was concluded by

Meakin et al (1971b) that the ester linkage was located in a region of high hydroxide ion concentration (i.e. at the micellar surface). Micellar inhibition is likely to occur in situations where reactant molecules are drawn deep into the micelle core resulting in physical protection.

The alkaline hydrolysis of benzocaine (Funusaki and Murata, 1980) was inhibited by CTAB micelles at high concentrations of CTAB, ester and added electrolytes (including buffers). These effects were thought to be due to (i) displacement of micelle surface-bound hydroxide ions by bromide ions as CTAB concentration increased and catalytically inactive salt as salt concentration increased, (ii) increased penetration of ester molecules into micelles, causing a reduced change density, as ester concentration increased.

1.6.5.5 Surfactant Purity and Stability

Peroxide impurities are present in many non-ionic surfactants and the resultant auto-oxidation of the surfactant may accelerate decomposition of drugs such as benzocaine and chloramphenicol (Azaz et al, 1973; Hamburger et al, 1975). The hydrolysis of alkyl sulphate surfactants has been observed to be acid catalysed and base inhibited on micelle formation (Kurz, 1962).

Therefore, reaction kinetics in the presence of surfactants liable to decomposition or to contain catalytic impurities must be interpreted with care.

1.7 ACCELERATED STABILITY TESTING

1.7.1 Conventional Studies

Accelerated stress conditions are used to generate stability data enabling the prediction of shelf-life. The Arrhenius relationship between temperature and reaction rate is used in thermally accelerated studies to calculate the rate of reaction at room temperature. Estimation of photolytic decomposition under "use" conditions from stress testing have been generally unsuccessful (Lin and Lachman, 1969) but studies by Mendenhall (1984) have shown a linear correlation between the logarithm of the observed rate constant and reciprocal light intensity.

Accelerated stability studies usually involve the storage of samples at different elevated temperatures in order to obtain the rate constant for degradation at each temperature. A plot of log k vs 1/T (in Kelvin) will, according to the Arrhenius equation (equations 20 and 21), predict the rate constant at room temperature and consequently stability under normal storage conditions. A vast amount of stability data can be generated where stress conditions accelerate drug decomposition as well as the detection of toxic or unsuitable degradation products, all within a short time period. However, it must be recognised that the accelerated method has limitations and a distinction must be made between reliable data and rough indications produced by these studies.

It is important to establish the criteria under which accelerated stability testing can be successfully carried out :

(i) Activation energies in the order of 40-120 $kJ.mol^{-1}$ are required to yield useful information. No advantage is gained by accelerated studies for reactions with low activation energies such as photolysis (typically 8-12 $kJ.mol^{-1}$) and some oxidative degradations (approximately 20 $kJ.mol^{-1}$) since rate enhancement at elevated temperature is small. Pyrolytic reactions (200-300 $kJ.mol^{-1}$) will undergo insignificant degradation when extrapolated to normal storage temperatures. Hydrolytic degradative reactions usually have activation energies of approximately 60-80 $kJ.mol^{-1}$ and are ideal candidates for accelerated stability studies.

(ii) The order of reaction should remain constant with raised temperature.

(iii) Allowance should be made for sample heat-up and cool-down periods.

(iv) Temperature variation should be kept at a minimum during accelerated studies. A ± 0.1°C variation did not affect shelf-life predictions whilst larger errors of ± 2-4°C resulted in a non-linear Arrhenius regression (Davies and Budgett, 1980). A maximum practical temperature variation of ± 1°C has been allowed by Clark and Hudson (1968).

(v) Decomposition should be associated with only one accelerated challenge and not a combination of stress conditions.

(vi) At least four different temperatures spread over a wide temperature range should be used to generate rate constants for an Arrhenius plot. The lowest temperature of the study should not be too far away from the temperature at which predictions are required in order to minimise extrapolation errors.

(vii) Statistical analysis should be performed on the data generated to validate predictions made by extrapolation.

(viii) The acceptability of predictions is greatly improved by good reproducibility of stability data generated at higher temperatures.

(ix) Errors in the assay procedure must be minimised by sufficient replication of analyses.

Pharmaceutical stability studies by Garrett (1962) and Carstensen and Su (1971) have identified some of the errors produced by accelerated stability testing whilst McLeod et al (1958) have applied statistical procedures to establish confidence limits. Bentley (1970) showed an improvement in predictions made from weighted linear regression of Arrhenius plots compared with standard un-weighted regression.

Commonly, errors are associated with a deviation from the Arrhenius relationship which may not become apparent until stability studies are performed under conventional storage conditions (Lin, 1969). These errors may be due to the direct effect of temperature on the solvent medium, such as changes in viscosity, drug solubility or oxygen content, or mechanistic effects such as changes in degradation pathways with increased temperature. Simultaneous reactions, e.g. acid-base catalysis, with different activation energies can lead to curvature in Arrhenius plots and therefore extrapolation errors.

1.7.2 Non-isothermal studies

During the last 25 years the concept of non-isothermal stability testing has been advocated at many times by numerous

workers. As described in Section 1.7.1 traditional isothermal stability testing involves accelerated degradation at high temperatures and the determination of rate constants and activation energy to predict shelf-life under normal storage conditions. However, many disadvantages are associated with this method including :

(i) A large number of samples are required in order to determine all parameters.

(ii) Controlled storage is required at several temperatures.

(iii) Reproducibility and precision of assay techniques must be maintained over the prolonged period of storage.

(iv) A preliminary estimation of drug stability is usually required in order to design experimentation and determine sampling frequency.

(v) Even accelerated storage studies may require extended storage periods.

The non-isothermal approach utilizes a programmed temperature change during a stability trial so that analytical results generated can be computed to yield the activation energy directly. The rate constant at any temperature may then be determined from a second calculation.

Eriksen and Stelmach (1965) list the following advantages of non-isothermal methodology :

(i) Only one stability run is required to generate all the desired data.

(ii) A stability study may be completed within one day.

(iii) Repetition of experimentation is completely independent allowing alteration of reaction speed if necessary.

(iv) Sampling intervals are controlled by mathematical modelling thus eliminating the need for preliminary estimations of rate constants.

The first pharmaceutical application of non-isothermal kinetics was described by Rogers (1963) and was followed by Eriksen and Stelmach (1965) with an improved mathematical treatment. The literature has since carried numerous reports of non-isothermal methodology and mathematical computation of data generated. These methods may be classified by data treatment.

(1) Direct :

Kinetic parameters are obtained by direct calculation from the analytical results. The experimental methodology generally utilizes a logarithmic or reciprocal relationship between temperature and time and rely on initial and infinite-time assay values (Eriksen and Stelmach, 1965; Rogers, 1963). The methods of Tucker (1981), Tucker and Owen (1982) and Yang (1982) eliminate bias estimates by the use of regression analyses which give equal weight to all data points.

(2) Curve Fitting :

Many authors have used the simpler approach of fitting an experimentally obtained non-isothermal degradation plot to theoretical plots derived by mathematical computation using linear, polynomial or non-linear temperature-time relationships (Maulding and Zoglio, 1970; Waltersson and Lundgen, 1983 and Zoglio et al, 1968). These methods require prior knowledge of the order of reaction. Zoglio et al (1975) calculated all parameters, including order of reaction, by a combination of both non-isothermal and isothermal kinetics.

The disadvantages of non-isothermal stability assessment may be listed :

(i) The experimental accuracy of the method is determined by the non-isothermal temperature programability of a water bath or oven - this requires advanced heating and monitoring circuits.

(ii) The non-isothermal temperature change has to be fitted to either a mathematical or graphical model, necessitating sophisticated on-line computer facilities.

(iii) Assay precision is of great importance in non-isothermal studies since degradation may be minimal during the initial periods of the study.

(iv) A change in reaction order or overall activation energy cannot be detected by this method.

(v) Extensive degradation (> 80%) is required for the calculation of necessary parameters in non-isothermal studies.

(vi) Degradative reactions involving equilibria or those influenced by pH or a kinetic salt effect are difficult to study by non-isothermal kinetics.

(vii) The data from non-isothermal degradative studies are not yet recognised by Licensing and Regulatory Authorities.

However, more fundamental problems are associated with the non-isothermal approach. At present, the method has only been validated for simple kinetic models, such as ester hydrolysis, where a wealth of information already exists. Technology is not available for the application of non-isothermal kinetics to solid dosage

forms, therefore this method is confined to solution dosage forms and preliminary kinetic studies. Until more information is available it is extremely unlikely that the non-isothermal approach will succeed conventional accelerated stability testing.

CHAPTER 2

C H L O R H E X I D I N E

2.1 INTRODUCTION

2.1.1 Background

Chlorhexidine is a bisbiguanide derivative commonly known by its tradename "Hibitane" (I.C.I. Pharmaceuticals). Since its discovery in the early 1950s , chlorhexidine has been widely used and still remains one of the most potent bactericidal compounds in use.

It is not absorbed from the gastro-intestinal tract or the skin, therefore its use is limited to that of a general antiseptic for topical use on skin and mucous membranes. After high dilution, chlorhexidine remains potent against a broad spectrum of microorganisms and is presented in a varity of formulations as a disinfectant/antiseptic, usually in combination with other antibacterial compounds (see section 2.1.5).

Its other major use is as an antimicrobial preservative in pharmaceutical products, particularly ophthalmic preparations due to its low ocular irritancy (Browne et al, 1975) at the concentrations commonly used.

Recently, the use of chlorhexidine as an antiplaque agent (Leach, 1977) and as a vaginal contraceptive (Pearson, 1985) have been reported.

2.1.2 Description

Chlorhexidine is N,N"-bis(4-chlorophenyl)-3,12-diimino-2,4,-

11,13-tetraazetetra decanediimidamide. Its structure is given in Figure 2.1, compound V (see section 2.2).

2.1.3 Mode of Action

Chlorhexidine inhibits the growth of a wide range of vegetative Gram-positive and Gram-negative bacteria, even after high dilution (Davies et al, 1954). It shows greater activity against Gram-positive bacteria whilst some species of Pseudomonas and Proteus are less susceptible (Martindale, 1982). Acid fast bacilli, heat resistant spores and animal viruses remain unaffected even in strong concentrations (Longworth, 1971) with mesophilic spores being destroyed at higher temperatures. Pathogenic fungi are also susceptible to inhibitory action (Lawrence, 1960). Hall (1967) has shown in vitro activity to be in the order : vegetative bacteria > fungi and yeasts > fungal spores > bacterial spores. The development of resistant strains has been minimal in clinical use (Longworth, 1971).

A reduction in antimicrobial activity has been observed by Lawrence (1960) and Lowbury (1957) in the presence of organic matter, e.g. blood, serum, milk and pus, due to precipitation and complexation of free chlorhexidine. However, Calman and Murray (1956) concluded that chlorhexidine was the best antibacterial agent in obstetric use for reasons of high activity and safety.

Structure-activity relationships indicate the microbial toxicity of chlorhexidine is due to its favourable hydrophilic-lipophilic balance (HLB). In a series of bisbiguanides, antimicrobial activity was retained after changing the terminal groups and hydrocarbon bridge length provided a similar HLB was maintained (Cutler et al, 1966).

At physiological pH bacteria carry net negative charges on their surfaces and therefore interact with the cationic chlorhexidine

molecule. Surface ionisation of bacteria is reduced in acid conditions, correspondingly chlorhexidine is less effective due to decreased adsorption (Davies, 1973). Hugo and Longworth (1964) have shown that chlorhexidine exhibits its maximum activity in alkaline conditions (pH 8 to 9) due to increased adsorption on the cellular surface. However, since these studies were performed in phosphate or phosphate-citrate buffers, an equally valid argument for increased activity may be pH dependent chlorhexidine-buffer interactions.

Leach (1977) has commented that the ionisation characteristics of chlorhexidine in the micro-environment present at the cell surface may differ from those in the bulk aqueous environment. Therefore bulk phase pH may only provide an indication of chlorhexidine and bacterial ionic charge.

Adsorption on to the bacterial cell is dependent on cell density, chlorhexidine concentration and composition of suspending medium. At neutral pH this process is usually rapid (Longworth, 1971) and initially causes disorganization of the lipoprotein membrane. Subsequent lethal activity is dependent on the concentration and extent of adsorption of chlorhexidine. At low concentrations (0.01% w/v) the permeability barriers are lowered allowing leakage and irreversible loss of cytoplasmic constituents (Hugo and Longworth, 1964; Rye and Wiseman, 1964 and 1965). Here chlorhexidine is acting as a cytoplasmic membrane poison and is bacteriostatic. Increasing the concentration produces an increase in adsorption but decrease in loss of cytoplasmic constituents, until at 0.05% w/v no loss can be detected, however, bactericidal activity is increased. Here chlorhexidine exerts a more rapid and profound lethal action by precipitating proteinaceous and pentose

containing components of the bacterial cytoplasm, this being bactericidal (Hugo and Longworth, 1965 and 1966; Davies and Field, 1969).

Differences between species are due to the varying capacities to adsorb chlorhexidine or resist lysis and coagulation. Certain antimicrobial properties of chlorhexidine are similar to those of many quaternary ammonium compounds (Weinburg, 1968).

From mode of action studies it has been concluded that chlorhexidine derives its activity from two main physico-chemical properties. Firstly, its dicationic nature allows an initial interaction with the negatively charged bacterial cell surface. Activity is aided by the fact that chlorhexidine is dicationic over a wide pH range. Secondly, the hydrophilic-lipophilic properties of the dication enable entry to the bacterial cytoplasm where a wide range of lethal reactions occur with the cytoplasmic components.

The mode of action of chlorhexidine against dental plaque has also been extensively studied, with reviews by Leach (1977) and Quintana (1973). Adsorption of chlorhexidine on to the tooth surface inhibits plaque formation by modification of the surface structure of the tooth (Quintana, 1973). Bound chlorhexidine is also gradually released from the tooth surface and, by a pH dependent process, precipitates salivary glycoproteins which are important in plaque colonization (Leach, 1977). Disruption of existing plaque may also occur due to the alteration in structure caused by chlorhexidine adsorption (Tanzer et al, 1972). The structural requirements for antiplaque activity have been identified by Tanzer et al (1977) and Warner et al (1976 and 1979).

2.1.4 Toxicity

At recommended concentrations the incidence of irritation or sensitization from topical administration to the skin, mucous membranes or eye has remained small (Browne *et al*, 1975; Calman and Murray, 1956). Hypersensitivity reactions have been discussed by van Ketel and Melzer-van-Riemsdijk (1980). When used in association with contact lens wear the incidence of chlorhexidine irritancy appears to be greater than when used in eye drops (Richardson *et al*, 1980; Ruben, 1980). Systemic toxicity is also minimal, presumably due to low systemic adsorption (Senior, 1973). Almost all data from formal toxicity studies by Butler and Iswaran (1979) were found to be negative.

However, *in vitro* studies by Ansel (1967) showed chlorhexidine to be destructive to erythrocytes at concentrations similar to those required for antimicrobial activity - total haemolysis and bacteriolysis occurring at similar concentrations. These results indicate chlorhexidine exerts a similar effect against erythrocytes and microorganisms by disruption of the structure and function of the cellular membrane. It is this non-selectivity of action that has limited the use of chlorhexidine to preparations for application to the skin and mucous membranes.

2.1.5 Pharmaceutical Uses

The medicinal and pharmaceutical usage of chlorhexidine may be broadly divided into two main categories: as an antiseptic and as a preservative although research into many new applications is in progress.

Table 2.1 provides an indication of the multitude of presentations available and their clinical usage.

Pharmaceutical form	Concentration (% w/v)	Salt form	Other actives	Usage	Examples
Solutions	20	gluconate		General antiseptic (for dilution)	"Hibitane 20%"
	5	gluconate	non-ionic surfactant	General antiseptic	"Hibitane concentrate"
	4	gluconate		Antiseptic hand and face wash, pre-operative skin preparation, instrument disinfection	"Hibiscrub" and "pHiso-Med"
	1.5	gluconate	cetrimide	General antiseptic	"Savlon Hosp. Conc."
	0.5	gluconate	isopropyl alcohol	Disinfection of intact skin	"Hibisol"
	0.2	gluconate		Antibacterial mouthwash	"Corsodyl"
	0.1	gluconate	chlorbutol	Mouth and throat infections	"Eludril"
	0.1	gluconate	hexamidine,chlorocresol	Infected skin and wounds, vaginal douche, pre-operative skin preparation	"Cyteal"
	0.1	acetate	amethocaine,ephedrine	Otitis media and externa	"Norgotin Ear Drops"
	0.05	gluconate	cetrimide	Burn and wound antiseptic	"Savloclens"
	0.015-0.05	gluconate		General antiseptic, burns, wounds, obstetric use and instrument storage	"Hibidil"
	0.05 (in glycerin)	gluconate/acetate		Urethral disinfection and catheter lubrication	
	0.02	gluconate/acetate		Bladder, pleural or peritoneal irrigation. Maintenance of indwelling catheter	"Uro-Tainer Chlorhexidine"
	0.015	gluconate	cetrimide	General antiseptic for swabbing, obstetrics	"Savlodil"
As a solution in other preparations	0.002-0.01	gluconate		Antimicrobial preservative for eye drops	
	0.002-0.006	gluconate		Preservative and disinfecting agent in contact lens solutions	
Sprays	0.5	gluconate	alcohol	Skin disinfection	"Dispray Quick-Prep"
	0.2	gluconate		Puerperal mastitis	"Rotersept"
	0.05	gluconate	amethocaine	Throat and mouth infections, mouth ulcers	"Eludril spray"

Pharmaceutical form	Concentration (% w/v)	Salt form	Other actives	Usage	Examples
Creams, Ointments and Gels	1.0	gluconate		General antiseptic for wounds and burns	"Hibitane Cream"
	1.0	gluconate		Obstetric use	"Hibitane Obstetric Cream"
	1.0	gluconate		Plaque inhibition	"Corsodyl Dental Gel"
	1.0	acetate	nystatin	Bacterial and fungal skin infections	"Nystaform Cream, Oint"
	0.5	acetate	nystatin, hydrocortisone	Bacterial and fungal dermatoses	"Nystaform HC Cream, Oint"
	0.2	hydrochloride		Burn and nasal cream	
	0.1	hydrochloride	neomycin	Nasal stapylococcal infections	"Naseptin"
	0.05	gluconate	lignocaine	Urethral and vaginal anaesthesia	"Xylocaine antiseptic Gel"
Others	0.5	acetate		Antiseptic dressing	"Bactigras"
	1.0	hydrochloride		Antiseptic Dusting Powder	Chlorhexidine Dusting Powder B.P.
	5 mg/lozenge	hydrochloride		Antiseptic adjuvant in throat and mouth infections	"Hibitane Lozenges"
Uses under Research	0.1 upwards	gluconate		Vaginal spermicide	
	0.02 to 2 (usually 0.2)	gluconate		Plaque inhibitor (in a variety of presentations)	

Table 2.1 Clinical and pharmaceutical uses of chlorhexidine together with examples of commercial products

2.2 SYNTHETIC ROUTE

Research in the mid-1940s by I.C.I. into the antimalarial properties of biguanide derivatives led to the discovery of proguanil ("Paludrine") by Curd and Rose (1946). This encouraged an interest in biguanide derivatives having wider ranging applications, particularly as antibacterial agents. During microbiological investigations of poly-biguanides by Davies *et al* (1954) it was found that bisbiguanides exhibited marked antibacterial properties *in vitro*. Out of many structural variants, chlorhexidine in particular had outstanding bacteriostatic properties and its monograph was incorporated into the British Pharmaceutical Codex (1959) as a potent topical antiseptic. The whole series of compounds were protected by British and United States Patents in 1954.

Rose and Swain (1956) published the synthetic route and structure-activity relationships for chlorhexidine and other bisbiguanides. This revealed a need for a penta-, hexa-, or hepta-methylene chain separating the biguanide groups and alkyl, aryl or heterocyclic terminal structures.

Although the exact details remain confidential, Figure 2.1 outlines the synthetic reaction sequence of chlorhexidine.

Some knowledge of the synthetic route is important in stability studies since one obvious degradative pathway is back along this route. The identification of impurities and intermediates along the synthetic chain is also useful in order to complete a degradative mechanism scheme.

2.3 CHEMICAL STRUCTURE

Information on allied chemical structure is useful in explaining or predicting degradative reactions of drug molecules. The

Stage 1 : preparation of a bicyanoguanidine

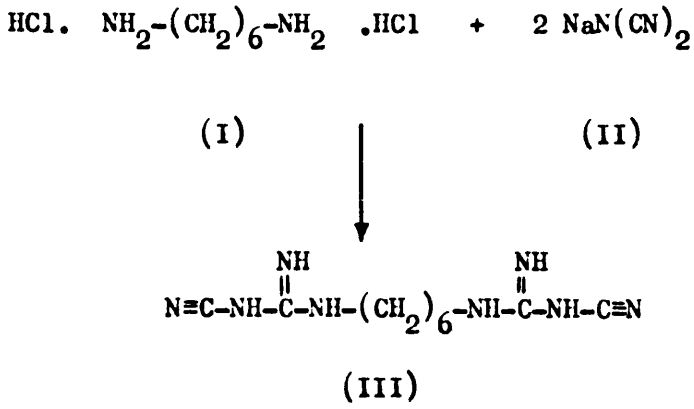

Stage 2 : preparation of chlorhexidine

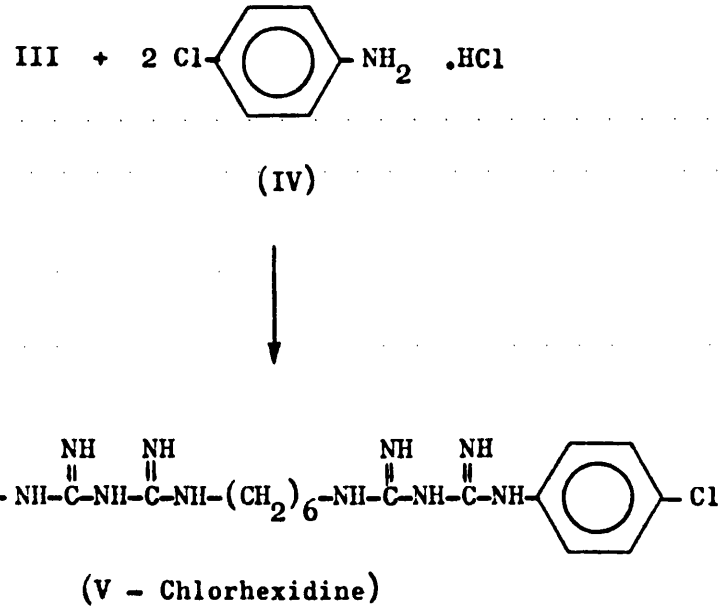

Figure 2.1 Synthetic reaction sequence for chlorhexidine

structure of the amidine and biguanide groups together with the structural effects of substitution and protonation are therefore pertinent to chlorhexidine.

2.3.1 Amidines

Amidines combine the properties of an azomethine-like C=N bond with an amidine-like C-N bond (Hafelinger, 1975). However, partial double bond characteristics are apparent in both the amino and imino groups with a mesomeric form being more representative of the true structure.

Structural determinations on substituted amidines indicate π-electron resonance with alteration of bond lengths by conjugation indicated by the mesomeric structures VI and VII (Hafelinger, 1975).

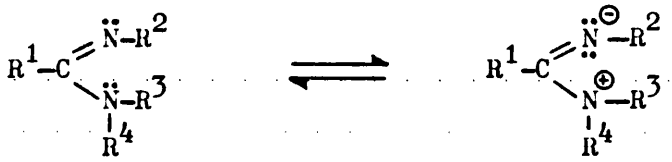

(VI) (VII)

Protonation occurs on the imino nitrogen (Kiro et al, 1972; Kotera et al, 1961) producing a symmetrical amidinium ion stabilized by resonance. For example, guanidine (VIII) becomes symmetrical with three equivalent amino groups having π-electron delocalization, as shown by IX (Haas et al, 1965). The strongly basic character of guanidine is mainly due to the resonance energy gained by protonation.

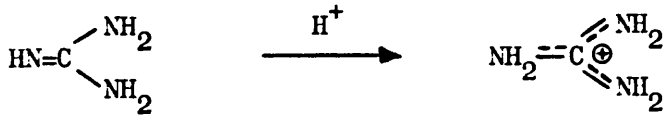

(VIII) (IX)

2.3.2 Biguanide

Biguanide is conventionally given the structure X

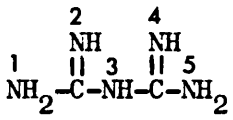

(X)

having well localized C=NH double bonds. Spectrophotometric experimentation (Nandi, 1972) indicates that biguanide possesses a conjugated C=N-C=N chromophore, with the nitrogen lone pair electrons capable of π-electron delocalization. This evidence supports the existence of the tautomer structure (Xa) for biguanide.

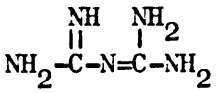

(Xa)

However, Elpbern (1968) and Kurzer and Pitchfork (1968) prefer the structure of biguanide to be explained in terms of resonance and not defined by a single structural formula. The π-electrons associated with the amine group may be partially delocalized to form a resonance hybrid of mesomers (XI) or completely delocalized to form the symmetrical structure XII.

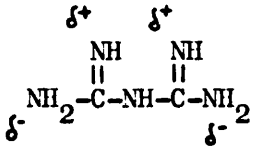

(XI)

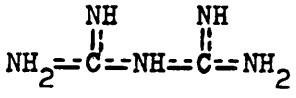

(XII)

Protonation of biguanide results in several resonance forms (Gage, 1949) some of which may be stabilized by hydrogen bond resonance. Assuming protonation occurs on the imino nitrogen, inducing proton migration from the bridging nitrogen, then the structure XIII will be formed, for which several resonance forms may be written (Fabbrizzi et al, 1977). All C-N bonds have double bond character and the four terminal amine groups are equivalent with the cationic charge distributed amongst them. The monocation is therefore stabilized by a high resonance energy.

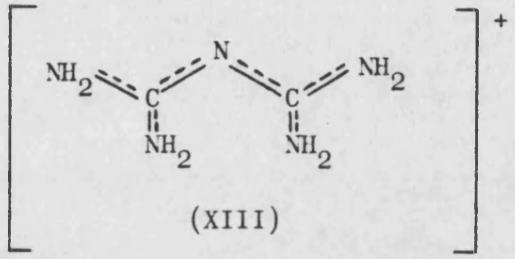

(XIII)

Protonation to the dication occurs in acidic media with the second proton bound by the bridging nitrogen leaving symmetry unchanged, as indicated by XIV (Fabbrizzi et al, 1977). A negative entropy change accompanies the second protonation which indicates there is no loss of associated resonance energy by formation of the dication.

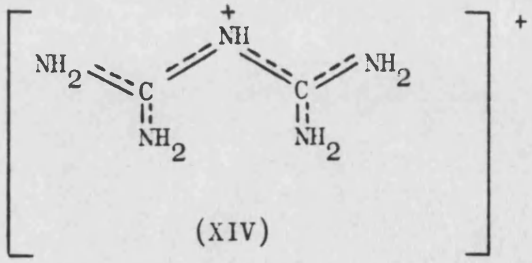

(XIV)

2.3.3 Substituted Biguanides

Studies by Fanshawe et al (1964) and Nandi (1972) on the non-protonated form suggest that both alkyl and aryl substituents exert hyperconjugative and electron donating inducing effects which extend the conjugated system. The extension of delocalized π-bonding results in the increased stability of a substituted biguanide compared with biguanide itself. Any energy difference generated by shifting resonance is likely to be small according to Fanshawe et al (1964).

In clinical use, substituted biguanides exist predominantly in the mono-protonated form (Kurzer and Pitchfork, 1968). The structural effects of substitution on to the protonated biguanide form are dependent on the electron donating or withdrawing properties of substituents. Any substituent which alters the energy difference between resonance forms will decrease the resonance energy favouring the formation of a particular tautomeric form.

Gage (1949) suggested several structures for alkyl and aryl, mono- and di-substituted biguanides for which spectrophotometric and potentiometric evidence remained unresolved. Shapiro et al (1959a) favour conjugated structures for phenylbiguanide and phenylethylbiguanide which could be converted into cyclic forms by intramolecular hydrogen bonding (XV). The cyclic form allows protonation to the dication by formation of a structure (XVI) which permits the widest possible charge separation between protons.

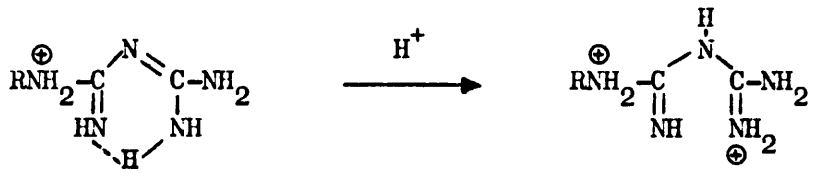

(XV) (XVI)

However, Fanshawe et al (1964) present conflicting evidence and favour protonation of the imino nitrogen resulting in a conjugated chromophore which permits proton delocalization over all four terminal nitrogen atoms (XVII). The conjugated system is destroyed by protonation on the central nitrogen atom to form the dication (XVIII).

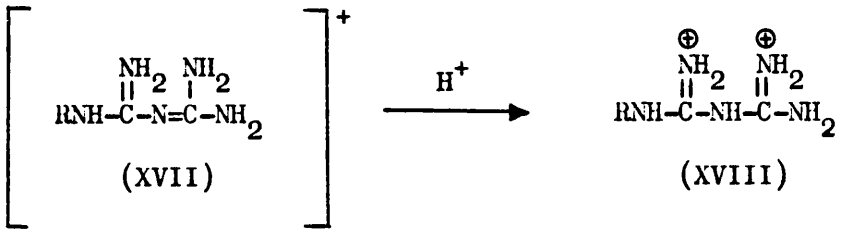

(XVII) (XVIII)

Nuclear Magnetic Resonance (NMR) evidence (Wellmann et al, 1967) from mono- and di-protonated substituted biguanides support the formation of highly symmetrical delocalized resonance hybrids. The bonding electrons are delocalized by resonance with no distinction being shown between double and single bonds, as illustrated by structures XIX and XX.

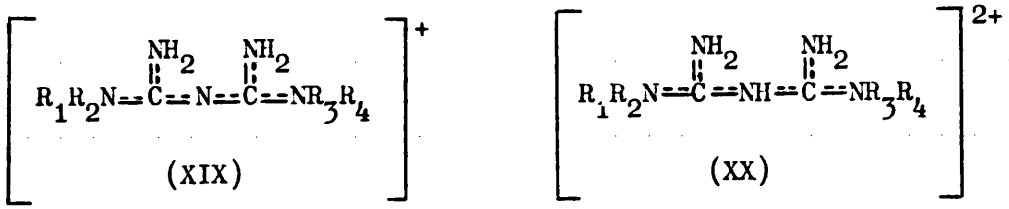

(XIX) (XX)

X-ray crystallographic studies by Brown (1967) provide an accurate structural description of 1-(4-chlorophenyl)-5-isopropylbiguanide hydrochloride (proguanil - "Paludrine"). All C-N bond lengths were shown to be similar, indicating that the positive charge is delocalized by π-bonding electrons.

The studies of Brown (1967) and Wellmann et al (1967) indicate resonance hybridization is an important feature of protonated substituted biguanides. This view is supported by Kurzer and Pitchfork (1968).

2.3.4 Bisbiguanides

A bisbiguanide (e.g. chlorhexidine) contains two biguanide groups linked by an alkyl or aryl bridge. Detailed structural determinations have not been carried out on bisbiguanides but, since they may be regarded as substituted biguanide derivatives, their structure may be inferred from sections 2.3.2 and 2.3.3.

In chlorhexidine, the π-electrons of both aryl rings would be expected to be delocalized with resonance behaviour also expected in the biguanide groups. The degree of delocalization will be dependent on the relative planes of π-bonding electrons in 4-chlorophenyl and biguanide groups.

However, from studies on proguanil (Brown, 1967), the structure of chlorhexidine is likely to be more correctly represented by resonance hybridization, as indicated in XXI.

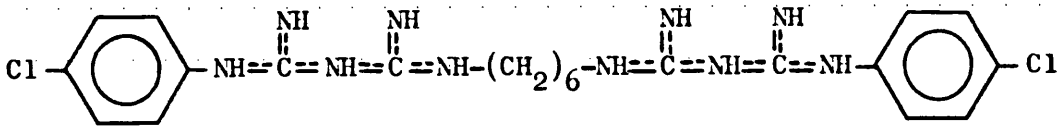

(XXI)

Protonation with resultant delocalization occurs in bisbiguanides and is similar to that observed in substituted biguanides. However, because two biguanide units are present, the molecule assumes an overall dicationic state with each biguanide group being mono-protonated and behaving independently due to separation by the hexamethylene chain. The biguanide groups may be further protonated to their dication state giving an overall tetra-cationic form. The various salt forms of chlorhexidine arising from its ionised states are discussed in section 2.4.2.

2.4 PHYSICO-CHEMICAL PROPERTIES

2.4.1 Appearance

Chlorhexidine base is a white, odourless, crystalline solid with a melting point of 132°C. Chlorhexidine hydrochloride and acetate have a similar appearance to the base with melting points of 255°C (with decomposition) and 154°C respectively. The gluconate salt is available commercially as a 20% w/v aqueous solution and has a pale straw colouration.

2.4.2 Solubility and Salt Formation

Chlorhexidine base is sparingly soluble in water although some salts have better solubility. Salts are formed readily, either by dissolution of the base in the appropriate aqueous acidic solution or by double decomposition of chlorhexidine acetate. Senior (1973) lists the aqueous solubilities of many chlorhexidine salts.

Table 2.2 gives the solubilities of chlorhexidine base and the three most commonly used salts (hydrochloride, acetate and gluconate). Although these salts are dibasic the prefix di- is commonly dropped.

Chlorhexidine	Aqueous solubility at 20°C (% w/v)
base	0.008
hydrochloride	0.06
acetate	1.8
gluconate	>70

Table 2.2 Aqueous solubilities of chlorhexidine base and salts at 20°C

2.4.3 Surface-active properties

Chlorhexidine has been shown to be weakly surface-active (Heard and Ashworth, 1968) although it does not show the classical amphipathic structure of traditional colloidal surface-active agents. Surface-active agents are characterized by the possession of both polar and non-polar regions in the same molecule, for example, a polar head group and a non-polar hydrocarbon chain. Chlorhexidine possesses both polar (biguanide) and non-polar (4-chlorophenyl and hexamethylene bridge) groups but it cannot be considered to be truly amphipathic since the structural arrangement is non-polar/polar/non-polar/polar/non-polar.

Heard and Ashworth (1968) illustrate the ability of chlorhexidine salts to produce a concentration dependent reduction in surface tension and increase in specific conductance, these phenomena being indicative of surface-active properties. However, plots by these workers of surface tension or specific conductance against concentration did not show the "classical" break or discontinuity at the critical micelle concentration (CMC) observed with traditional surface-active agents. For example, Figure 2.2 shows a plot of surface tension against log molar concentration taken from Heard and Ashworth (1968). Therefore the determination of CMC from inflection points by these workers questions the reliability of CMC values of 0.01 M (0.626% w/v) for the acetate salt and 0.0066 M (0.593% w/v) for the gluconate salt.

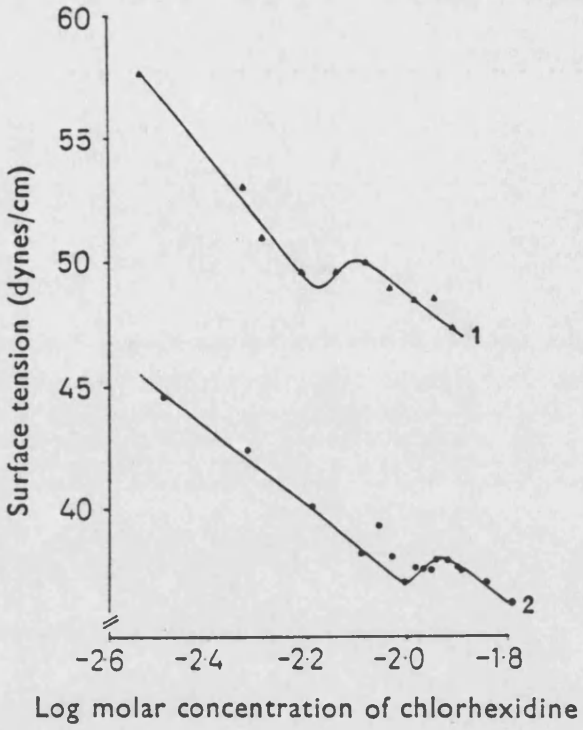

Figure 2.2 Determination of the CMC values of chlorhexidine gluconate (1) and acetate (2) by surface tension measurements [from Heard and Ashworth (1968)]

Perrin and Witzke (1971) report a CMC of 0.0044 M (0.395% w/v) for chlorhexidine gluconate by specific conductance and optical rotatory dispersion measurements. However, their interpretation of experimental data was equally tenuous. Although chlorhexidine acetate reduced surface tension, no association of molecules could be detected up to the solubility limit by Attwood and Natarajan (1979) using light scattering, surface tension or conductivity techniques.

Heard and Ashworth (1968) argue that micellar associations are most likely formed by hydrogen bonding between adjacent biguanide groups with counterion presence being an important determinant of CMC. Such associations would preclude the formation of structured micelles in favour of less ordered associations between a few chlorhexidine molecules.

Heard and Ashworth (1968) quote similar CMC values for the acetate and gluconate salts. From solubility considerations this behaviour would appear to be anomalous. Solubility is a result of appreciable attractive forces existing between the solute and solvent, therefore, aggregate or micelle formation must be accompanied by a compensating loss of entropy. Because of the widely different solubilities of gluconate and acetate salts it would be expected that they should exhibit a similar disparity between CMC values. Recent unpublished studies using conductivity and total intensity light scattering have demonstrated that chlorhexidine gluconate forms small aggregates (association number <10) at 0.039 molal concentration (~3.4% w/v, Attwood, 1985, personal communication).

The partitioning behaviour of chlorhexidine into decaoxyethylene oleic ether (Brij 96) and polyoxyethylene sorbitan monooleate (Tween 80) micelles has been reported by Wesoluch et al (1979). These workers suggest that solubilization of the relatively hydrophobic chlorhexidine base from solutions of the salts would be accompanied by an increase in pH since free acid form would be left in solution. As no significant change in pH was observed Wesoluch et al (1979) conclude that solubilization of the salt (ion-pair) form occurs.

These workers present further proof from calculations of chlorhexidine solubility with respect to the hydrocarbon or polyoxyethylene content of each surfactant. Better correlation was observed between chlorhexidine salt solubility and the $C_{17}H_{33}$ hydrocarbon segment, leading the workers to conclude that the site of solubilization was the hydrocarbon core of the micelle. However, more plausible explanations of the species and site involved in solubilization, defined in terms of energetics and steric hinderance, were not examined.

The surface-active and surface-chemical properties of chlorhexidine have been associated with its efficacy against dental plaque (Fisher et al, 1975a and b; Quintana et al, 1972). These studies have shown the ability of chlorhexidine to adsorb reversibly on to the tooth enamel (hydroxyapatite) where it impairs the structural integrity of plaque leading to its disruption and eventual elimination.

2.4.4 Incompatibilities

Since chlorhexidine salts are cationic in solution they are incompatible with many anionic compounds including surfactants. The incompatibility or insolubility of chlorhexidine with many pharmaceutical compounds has greatly limited its use as a preservative.

In order to avoid the formation of insoluble chlorhexidine salts, distilled or de-ionised water should be used in the preparation or dilution of solutions. In order to solubilize insoluble salts formed by dilution, many proprietary concentrated chlorhexidine solutions are formulated with a cationic or non-ionic surfactant.

2.4.5 Ionisation Properties

The ionisation constants (pKa values) for chlorhexidine are frequently quoted in the literature as being 2.2 and 10.3. However, all publications quoting these values cite Hugo and Longworth (1964) who in turn rely on a personal communication with I.C.I. Pharmaceuticals. No reference has ever been made to the methodology used to generate this data and attempts to gain this information have been unsuccessful.*

Much confusion has arisen amongst workers considering the ionic nature of chlorhexidine at particular pH values. Some workers (Hugo and Longworth, 1964; Yang and Banker, 1981) have misinterpreted the two constants, assuming them to be associated with single

* See Appendix 5

protonations to conclude that a dication exists below pH 2 and a monocation between pH 3-9. It is very important not to confuse the potential dicationic nature of each biguanide group with the dicationic form of a bisbiguanide where each biguanide group is mono-protonated. The biguanide groups in bisbiguanides therefore exhibit independent ionisation properties and the values previously quoted correspond to the formation of a tetracation below pH 2 and a dication between pH 3-9. Evidence for this conclusion comes from the following considerations;

(i) Biguanide and substituted biguanides

Examination of the ionisation properties of biguanide and substituted biguanides is useful to establish a theoretical basis for the prediction of chlorhexidine ionisation. Ultraviolet spectrophotometric and potentiometric evidence from Kurzer and Pitchfork (1968) and Ray (1961) show protonations of biguanide giving pKa values of 2.93 and 11.51. The high basic strength of biguanide (pKa 11.51) has been attributed to the formation of a monocation having a very large resonance energy (Fabbrizzi et al, 1977). The monocation is itself a weak base and will protonate to yield the dication in moderately acidic conditions (pKa 2.93).

Alkyl substitution of biguanide has a slight base weakening effect, reducing the observed pKa values by approximately 0.1 unit (Kurzer and Pitchfork, 1968). The effect of substituents on the protonation to the dication are variable, but never greater than ±0.2 units (Kurzer and Pitchfork, 1968). Dialkyl substitution has a slight effect on the ionisation constants, with Ray (1961) observing an increase in pKa values with increasing alkyl chain length.

Aryl substitution does however, have a much more pronounced effect, e.g. phenylbiguanide with pKa values of 2.16 and 10.72 (Kurzer and Pitchfork, 1968) and 4-chlorophenylbiguanide with pKa values of 2.2 and

10.4 (Ray, 1961). Subsequent alkyl substitution on to the other end of the biguanide molecule does not significantly alter these values, e.g. N^1-(4-chlorophenyl)-N^5-isopropyl biguanide, pKa 2.3 and 10.4 (Ray, 1961). These observations may be explained by the electron withdrawing properties of the phenyl and, to a greater extent, the 4-chlorophenyl groups exerting a base weakening effect on biguanide, reducing the basic ionisation from pKa 11.51 to 10.72 or 10.4 respectively. The effect of aryl substitution on to the protonated form also appears to be base weakening since a shift from pKa 2.9 to 2.2 is observed.

(ii) Bisbiguanides

Due to the separation of biguanide groups by the hexamethylene chain in chlorhexidine, it is expected that each biguanide group should behave similarly but almost independently. However, studies by Leach (1977) have shown the ionisation of one biguanide group to affect the ionisation of its opposite by a small but significant amount. He noted a minimum difference of 0.6 pKa between similar groups in chlorhexidine analogues. Therefore, under optimal experimental conditions it may be possible to determine four ionisation constants for a bisbiguanide.

Four pKa values for ethylenebisbiguanide have been reported by Sarma (1952), being 1.7, 2.9, 11.3 and 11.8. From studies by Dutta and Gupta (1961) it would appear that the difference in pKa between similar groups becomes greater as the central alkyl bridge length increases since hexamethylenebisbiguanide has observed pKa values of 2.31, 3.50, 10.75 and 11.52. It will, however, be noted that whilst hexamethylene appears to be base weakening with respect to the basic ionisations, it has a base strengthening effect on the second protonation of each biguanide group.

(iii) Predicted ionisation constants for chlorhexidine

Prediction of ionisation constants may be made by reference to Hammett or Taft equations, or by molecular structure and electron density considerations (Perrin et al, 1981). As discussed earlier (section 2.3.4), chlorhexidine exists as a resonance hybrid of mesomeric structures, making ionisation predictions difficult. The application of Hammett or Taft equations to bisbiguanides would require many theoretical approximations, making values produced approximate and difficult to justify.

However, a consideration of the likely effects of 4-chlorophenyl substitution on to hexamethylenebisbiguanide could give an indication of the expected ionisation constants for chlorhexidine.

4-Chlorophenyl is electron withdrawing and its base weakening effect has already been observed (biguanide pKa 2.93, 11.51; 4-chlorophenylbiguanide pKa 2.2, 10.4). The base-weakening (for the basic protonations) and base-strengthening (for the acidic protonations) effects of the hexamethylene chain have also been noted (hexamethylenebisbiguanide pKa 2.53, 3.50, 10.75 and 11.73). It is extremely unlikely that the two base weakening effects would be additive since the stronger electron withdrawing group (4-chlorophenyl) is likely to be dominant. Therefore, the basic ionisation constants for each biguanide group would probably be reduced by approximately 1 pKa unit.

Since the effect of the hexamethylene group is considered minimal for the basic protonations it would be better to use the pKa values of ethylenebisbiguanide as a reference. The $-CH_2-CH_2-$ group provides reasonable independence to each biguanide group without significant inductive or withdrawing effects being exerted by the bridging group itself. Therefore, values of pKa ~10.3 and ~10.8 are estimated for the basic ionisations of chlorhexidine.

Since hexamethylene exerted a base-strengthening effect on the acidic protonation which was of similar proportion to the base-weakening effect of 4-chlorophenyl substitution a large change in the acidic ionisation values should not be expected. Again, the values of ethylenebisbiguanide provide a useful starting point giving estimated values of pKa ~1.7 and ~2.9 for the acidic ionisations of chlorhexidine. If these values are compared with those quoted by Hugo and Longworth (1964) of pKa 2.2 and 10.3 then reasonable correlation exists, assuming that these values are the experimental means of overlapping ionisation processes. Even so, it is somewhat surprising that such large predicted differences in the ionisation constants of similar groups exist (1.2 pKa unit for the acidic ionisations and 0.5 pKa unit difference for the basic ionisations). In order to exert an effect on its opposite group the electron withdrawal or induction has to be transferred along the hexamethylene chain. The size of this electronic effect along such a group is considered minimal by Perrin et al (1981).

2.5 STABILITY OF CHLORHEXIDINE AND DEGRADATIVE REACTIONS

2.5.1 Chlorhexidine Stability

The introduction of chlorhexidine as a preservative in ophthalmic products led to the first doubts about its stability to the heat sterilization process. Both Foster (1965) and Polack (1967) suspected possible hydrolysis of the terminal 4-chlorophenyl groups yielding 4-chloroaniline. The first published stability study (Goodall et al, 1968) showed that chlorhexidine in solution could degrade to 4-chloroaniline when autoclaved. However, the authors concluded that the apparent loss of active ingredient was minimal and that 4-chloroaniline content was well below a toxicity limit of 500 ppm suggested by Scott and Eccleston (1966).

Further stability studies by Jaminet et al (1970) and Dolby et al (1972) revealed that raising the temperature beyond 110°C during autoclaving caused a significant increase in 4-chloroaniline content. Dolby et al (1972) proposed a pH of maximum stability between pH 5-6 and suggested that the gluconate salt was less stable than the acetate since it yielded more 4-chloroaniline per mole of chlorhexidine. Sterilization at lower temperatures (100°C for 60 minutes) had little degradative effect according to Jaminet et al (1970) although degradation was observed to increase with pH in the region 4.7 to 9. Both sets of workers used buffered systems with 4-chloroaniline being assayed by procedures according to Goodall et al (1968).

However, the previous workers assumed chlorhexidine stability could be assessed by 4-chloroaniline formation alone. The first published work recognising other degradation products was by Powelczyk and Plotkowiak (1976) using paper chromatographic techniques. Two degradation products were found in commercial solutions, another after slight thermal stress and two more after prolonged heating. 4-Chloroaniline was identified as being one of the decomposition products already present in commercial solutions. The rate of degradation was observed to increase with ionic strength of formate buffer in the acid region (pH 3.27) indicating a buffer and/or salt effect. In an unbuffered study, decomposition increased with decreasing pH below pH 6. This evidence, together with that of Jaminet et al (1970) for the alkaline region, indicates that degradation is both acid and base catalysed. Chlorhexidine was assayed spectrophotometrically by Powelczyk and Plotkowiak (1976) after separation from the degradation products since they were also found to absorb in the ultra-violet region.

After investigating the surface-active properties of chlorhexidine, Heard and Ashworth (1968) examined 4-chloroaniline formation above and below their proposed CMC values. No significant differences were detected and these workers conclude that no protection of hydrolysable groups could be afforded by micellization. Qualitative stability studies have been reported by Fiomaro et al (1983) and Grimm (1973) which add little to our knowledge.

From the limited research data available it may be concluded that far too much emphasis has been placed on interest in 4-chloroaniline content rather than loss of chlorhexidine in degradation studies. The reason for this is undoubtably due to the existence of successive British Pharmacopoeial monographs for chlorhexidine salts limiting 4-chloroaniline content to 500 ppm. This allowable limit is set for two reasons. Firstly, any decomposition of chlorhexidine must not produce toxic levels of 4-chloroaniline greater than those suggested by Scott and Eccleston (1966). Secondly, since 4-chloroaniline is involved in the synthesis of chlorhexidine, the limit is set as a manufacturing control.

In recognition of the existence of other degradation products, the monograph for Chlorhexidine Gluconate Solution in the 1983 Addendum to the British Pharmacopoeia 1980 includes a high performance liquid chromatographic method for the identification of related substances (section 2.6.3).

The stability of chlorhexidine to daylight and γ-irradiation has been the subject of limited studies. Whilst Madsen (1967) observed a 12% loss in chlorhexidne content after storage in daylight for one year, Dolby et al (1972) report no significant decrease in chlorhexidine concentration after similar storage. McCarthy (1978) reports chlorhexidine in solution to be unstable to the effects of γ-irradiation at standard sterilization doses.

2.5.2 Degradative Reactions of the Amidine Group

The amidine group can be hydrolysed under mild conditions which occurs in two steps, the first being faster with the rate being dependent on conditions and substituents, as shown in Figure 2.3 (De Wolfe, 1975). Substituents were shown to affect the reaction rate by steric and inductive effects but a general reduction in the rate was observed from mono- to di-substitution. De Wolfe (1975) noted that amidines generally hydrolyse more rapidly in alkaline rather than acidic solutions with the reactions being independent of ionic strength and essentially irreversible. One study of relevance to chlorhexidine degradation shows 4-chlorophenyl substituted amidines to hydrolyse more rapidly than other substituted amidines with the rate of hydrolysis increasing with hydroxide ion concentration (De Wolfe, 1975).

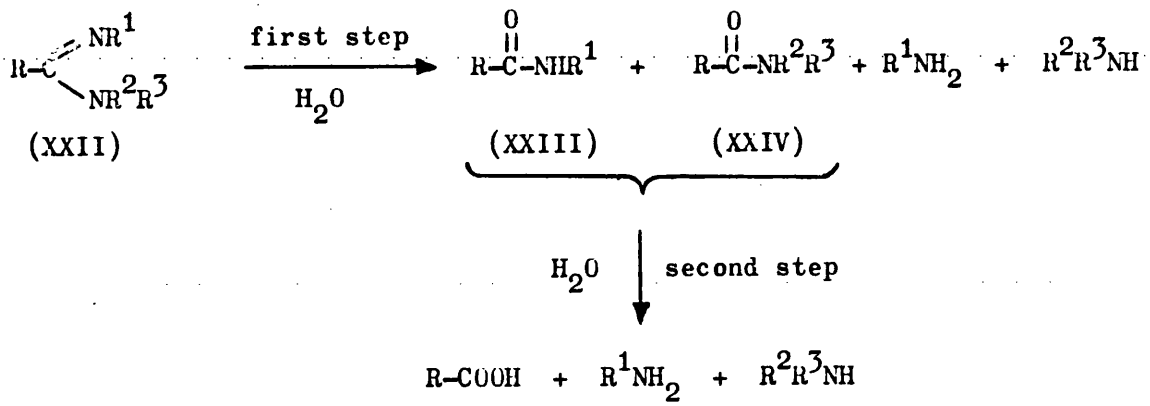

Figure 2.3 The hydrolysis of a substituted amidine

Kinetic experiments on diarylamidines support the mechanism of general base catalysis of the conjugate acid as shown in Figure 2.4. De Wolfe (1975) observed the rate of hydrolysis to be independent of pH below pH 5. This is in good agreement with the Bronsted Catalysis Law (see Chapter 1.4.2) for substituted amidines which demand that the water catalysed reaction be faster than the hydroxide-ion catalysed reaction below pH 6. This mechanism accounts for the observed buffer catalysis and independence of hydrolysis rate on the hydrogen-ion concentration in dilute acid since water acts as the base catalyst in the slowest step of the reaction. Water is therefore involved in the rate limiting transition state.

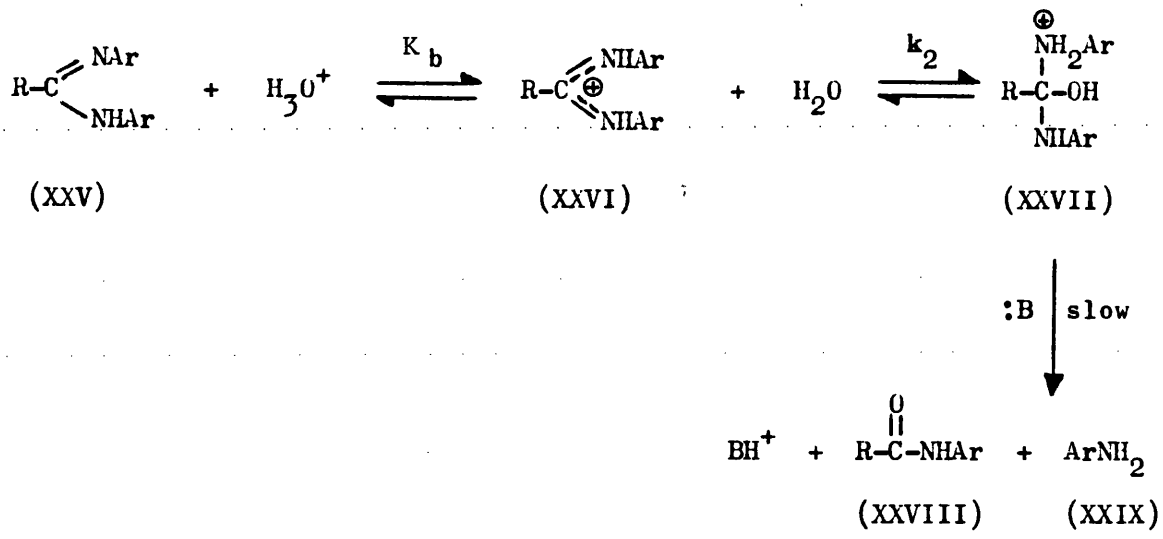

Figure 2.4 Hydrolytic breakdown of a diarylamidine illustrating general base catalysis

2.5.3 Degradative Reactions of Biguanides

Studies on biguanides are mainly limited to N^1-(4-chlorophenyl)-N^5-isopropyl biguanide (proguanil, XXX "Paludrine") or its analogues. Curd et al (1949) observed the precipitation of N^1-(4-chlorophenyl)-N^5-isopropylamidinourea (XXXI) from acidified solutions of proguanil (Figure 2.5). That the degradation product was XXXI and not its isomer N^1-isopropyl-N^5-(4-chlorophenyl)amidinourea (XXXII) was verified by unequivocal synthesis.

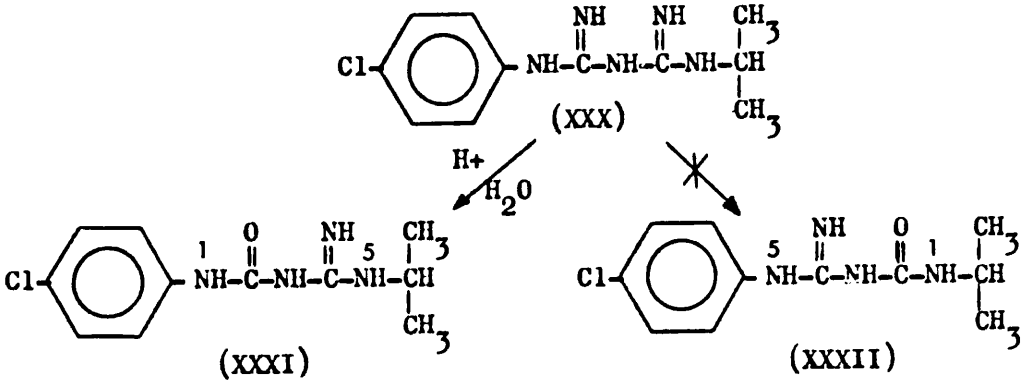

Figure 2.5 Reaction of proguanil in acidified solution yielding the amidinourea compound with deamination occurring adjacent to the phenyl ring

The amidinourea compound may also result from the synthetic pathway if too much acid is present in the condensation reaction between aniline and cyanoguanidine. Proguanil has also been shown to produce isopropylamine (XXXIII), 4-chloroaniline (XXXIV), methylamine (XXXV) and ammonia after extended alkaline hydrolysis (Figure 2.6) (Crounse, 1951).

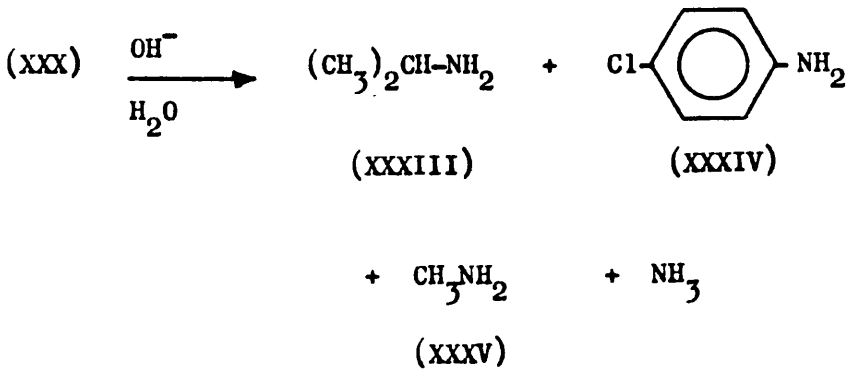

Figure 2.6 Alkaline hydrolysis of proguanil

Other studies on biguanides have shown that deamination followed by formation of the corresponding amidinourea compound invariably occurs on the carbon atom nearest to phenyl or sulphamidinophenyl substituents (Kundu and Ray, 1952; Ray, 1961). Substituents on the N^1-nitrogen appear to have an important influence on the rate of hydrolysis (Kundu, 1953) with an increase in stability to hydrolysis being observed by alkyl substitution on to the N^5-nitrogen, presumably due to hyper-conjugative effects (Ray, 1955).

Quantitative studies (Kurzer and Pitchfork, 1968) have shown that the rate of acid hydrolysis of proguanil and related biguanides decreases with an increasing degree of substitution in the biguanide structure. This evidence was substantiated by Shapiro (1959a) who demonstrated phenylethylbiguanide (XXXVI) to be more stable to acid and alkaline hydrolysis than phenylbiguanide (XXXVII). However, the degradation products from the two compounds were similar : phenylethylguanidine (XXXVIII), phenylethylurea (XXXIX) and phenylethylamine (XL), from phenylethylbiguanide (Figure 2.7) with phenylguanidine (XLI), phenylurea (XLII) and aniline (XLIII) from phenylbiguanide (Figure 2.8).

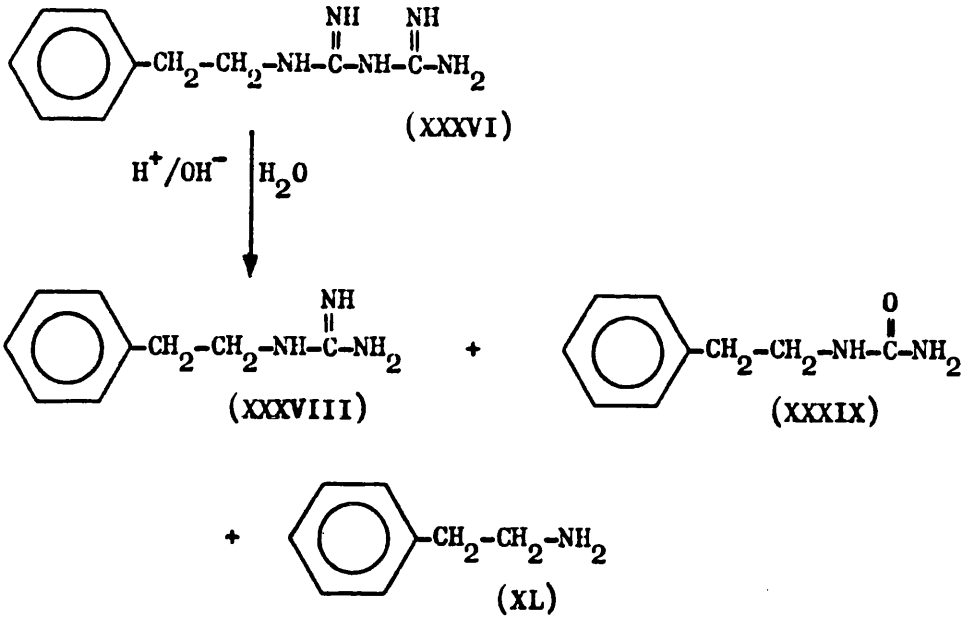

Figure 2.7 Degradation of phenylethylbiguanide

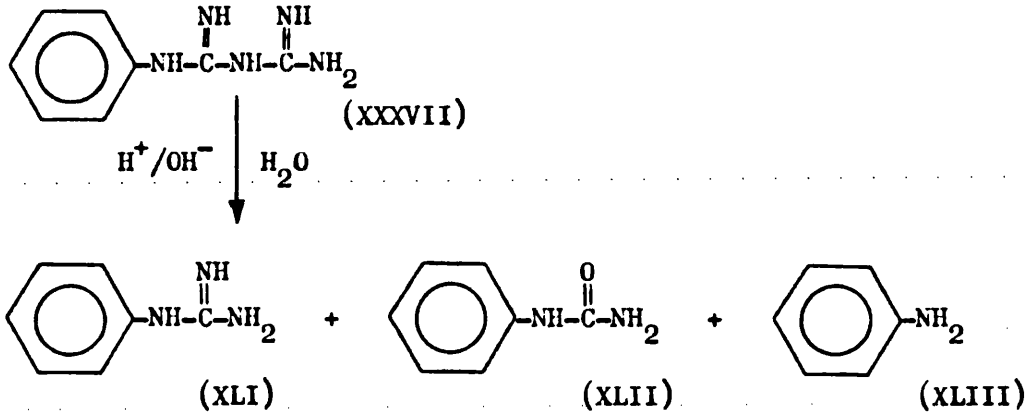

Figure 2.8 Degradation of phenylbiguanide

Considerable intramolecular hydrogen bonding is present in arylbiguanides providing the capability to form cyclic structures (Shapiro, 1959b). A known metabolite of proguanil possesses a heterocyclic ring structure (Crounse, 1951) and acylation of biguanides is well documented (Kurzer and Pitchfork, 1968).

Different degradation products are produced when biguanides are heated in the solid state. For example, the thermal decomposition

of phenylbiguanide (XXXVII) yields a mixture of phenylbiguanide, phenylguanidine (XLI), cyanamide (XLIV), guanidine (VIII) and phenylcyanamide (XLV), (Bell et al, 1977).

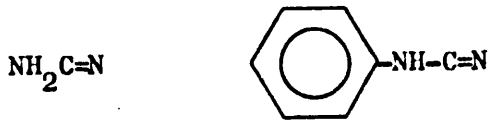

(XLIV) (XLV)

Biguanides are resistant to oxidation and reduction (Kurzer and Pitchfork, 1968). The same authors review the chemical reactivity of biguanides with the functional groups of other compounds.

In summary, the chemical properties of amidines and biguanides suggest that they are particularly susceptible to hydrolysis in acid or alkaline solution. Whilst the degree and type of substitution can modify these effects, the main degradative pathways remain similar. Amidines progress via the corresponding amidinourea to mixture of substituted carboxylic acids and primary and secondary amines. Biguanides also degrade initially to the corresponding amidinourea with further degradative pathways being dependent on the conditions of hydrolysis.

Given the information for amidines and biguanides it is feasible that chlorhexidine will also degrade to the corresponding amidinourea which may in turn be the mediator of further degradative pathways (see Chapter 8).

2.6 ANALYTICAL METHODS FOR THE DETERMINATION OF CHLORHEXIDINE

Many quantitative and qualitative methods have been employed in the estimation of chlorhexidine in various formulations. Generally they are required for routine quality control procedures and are,

therefore, not necessarily stability indicating. There are three main categories of chlorhexidine analysis, volumetric and gravimetric analysis, spectroscopy and chromatography, which illustrate the gradual change in analytical methodology towards highly sensitive and specific assay techniques. Other techniques such as polarography have been advocated from time to time (Jacobsen and Glyseth, 1975).

2.6.1 Volumetric and Gravimetric Analysis

The British Pharmacopoeia 1980 retains a non-aqueous titration with perchloric acid in glacial acetic acid for the pure material (chlorhexidine acetate and hydrochloride) and commercially available solution (20% w/v chlorhexidine gluconate). This method is used to generate precise assay values for primary standards used in other analytical methods and for the raw material used in product manufacture. For routine analysis in pharmaceutical preparations Pinzauti et al (1981a and b) describe potentiometric methods for 0.006% w/v chlorhexidine gluconate solutions with ±1.0% precision. Gravimetric analysis has also provided good correlation between label claim and generated assay values but without evidence of specificity (Pinzauti et al, 1976).

2.6.2 Spectroscopic Methods

Spectroscopic methods were favoured before HPLC methods became available due to their speed and relative specificity. The method of Holbrook (1958) has been adopted by many workers in numerous research fields as their "method of choice" (see Chapter 5.2.1 and 5.2.2). Assay is by colour complex formation between alkaline hypobromite solution and the biguanide groups of chlorhexidine. Precipitation of chlorhexidine base in this alkaline media is prevented

by the inclusion of cetrimide which solubilizes insoluble salts as well as the base. The assay is therefore of "total" chlorhexidine content and not "freely soluble" chlorhexidine alone. Holbrook (1958) demonstrated it to be a robust method for a wide variety of formulations but concluded that it was too time consuming for routine analysis.

However, closer examination of the method reveals an inherent insensitivity and several sources of potential inaccuracies. The colour-complex formation is time and temperature dependent requiring extremely reproducible experimentation. Errors may be further exacerbated by the necessary repetition of a reference calibration plot to obtain assay values. More importantly the only prerequisite for colour-complex formation is an intact biguanide group which leads to serious over-estimates as degraded material retaining a biguanide group can still take part in colour-complex formation and assay as chlorhexidine. The use of this method in previous stability studies can only cast doubt on results and conclusions because of the likely over-estimation of chlorhexidine.

Cropper et al (1975) recognised the problems associated with colour-complex formation and presented an elaborate series of experiments utilizing the Holbrook method, assay of 4-chloroaniline and derivatization of chlorhexidine in a final gas-liquid chromatographic (GLC) assay. Other workers (Jensen and Christensen, 1971; Lowry, 1979) have developed methods involving simple ultra-violet absorbance or dye-complexation, however both were limited by poor sensitivity. Andermann et al (1980) described an alternative colorimetric method to that of Holbrook and demonstrated sensitivity and precision although solvent extraction of a dye complex with bromocresol green was

involved. Interference by non-biguanide cationic drugs and excipients was not studied although such materials should respond to what is essentially an ion-pair extraction method.

2.6.3 Chromatography

Chromatography has been widely used to separate drugs from their degradation products and provides an advantageous alternative method to those methods described above. 4-Chloroaniline, at its proposed safety limit of 500 ppm, could be separated from chlorhexidine in pharmaceutical preparations and detected using the thin-layer chromatographic (TLC) system of Ciarlone *et al* (1976).

The most comprehensive stability study to date uses a paper chromatographic technique allowing both qualitative and quantitative evaluation (Pawelczyk and Plotkowiak, 1976). After separation from its degradation products by chromatography, chlorhexidine was eluted from the paper and quantified by ultra-violet absorbance. Assay by u.v. absorbance of the total solution prior to separation resulted in a two-fold error in the decomposition rate constant compared with the eluted extract containing chlorhexidine alone. This indicated that the degradation products also absorb in the same u.v. region as chlorhexidine and that the use of u.v. absorbance alone is likely to lead to erroneous assay values. Due to the many stages involved it is envisaged that lack of speed may be a disadvantage of this method in a formal stability study.

Gas chromatographic methods (Cropper *et al*, 1975; Siefert *et al*, 1975) are of little use since they rely on the hydrolysis of chlorhexidine to 4-chloroaniline which is then derivatized and detected by electron capture. This "sledgehammer" approach can at best merely measure an extractable proportion of 4-chloroaniline resultant from the

forced degradation of chlorhexidine under extremely variable conditions. The resultant recovery of chlorhexidine is low and variable. Miribel et al (1983) recognised the problems in derivatizing a fragment of the degraded chlorhexidine molecule and proposed a much improved stability indicating method involving the quantitative derivatization of the whole molecule to the disilyl extract. The method was admirably supported by mass spectra and NMR experimentation.

HPLC is the obvious choice for stability indicating assay methods due to its favourable combination of sensitivity, selectivity, precision and speed. Many workers have developed assays capable of the rapid analysis of chlorhexidine from a range of formulations (Bachner et al, 1981; Perez, 1980; Stuber and Muller, 1981).

Separation of chlorhexidine from synthesis precursors and degradation products was claimed, but not demonstrated, by Bailey et al (1975) in an automated technique. The method was based on normal phase chromatography although separation was likely to be an ion-exchange process under the conditions employed. Good precision was demonstrated with values similar to those obtained from the Holbrook colorimetric method. Collins et al (1979) and Perez (1981) recognise the need to distinguish between chlorhexidine and 4-chloroaniline by liquid chromatography but detection and quantitation of the latter was poor by the methods of these workers. The detection of chlorhexidine in blood and urine was outlined by Huston et al (1982) who used a reversed-phase method with good sensitivity but scattered results possibly due to their extraction procedure. This method has been updated Gaffney et al (1984) with quantitation by reference to an internal standard.

The 1983 Addendum to the British Pharmacopoeia 1980 now uses a HPLC method rather than TLC for the related substances limit test in its Chlorhexidine Gluconate Solution monograph. A reverse-phase ion-pair system is used with an acidified methanol : water mobile phase. A limiting peak area is imposed on peaks other than chlorhexidine and the solvent front. No mention is made in the method to the possible number of additional peaks due to degradation. The original TLC methods of the B.P. 1980 are retained for the Chlorhexidine Acetate and Hydrochloride (solids) monographs together with the 4-chloroaniline limit test on all three official preparations.

CHAPTER 3

HIGH PERFORMANCE LIQUID CHROMATOGRAPHY

3.1 INTRODUCTION

HPLC is now a routine method of analysis and there are numerous texts ranging from simple to advanced which detail the relevant theory to its application and use. Schram (1980) offers a laboratory guide, Parris (1976) and Pride and Gilbert (1979) are good general texts with Synder and Kirkland (1979) being one of the classical texts. A major bibliography on HPLC has been compiled by Colin et al (1985).

The main advantages of HPLC analysis of pharmaceuticals are speed, sensitivity, selectivity and reliability. The detection and quantitation of decomposition in stability studies is an important application of HPLC since specificity and selectivity can still be achieved at very low concentration.

3.2 MECHANISMS OF SEPARATION

Retention of individual components on to a stationary phase (chromatographic column) is necessary in order to obtain separation. Selective retention in a given system is due to specific interactions between the stationary phase and components of a mixture flowing down the column in the mobile phase. By examination of the surface chemistry of stationary phases it is possible to classify the mechanisms of interaction into four groups:

3.2.1 Partition

The distribution of solutes between the stationary and mobile phase depends on the relative phase solubility of individual components. These differences may be exploited by altering the polarity of each phase, allowing separation and differential elution. The partition mechanism is further classified according to relative polarities:

(i) normal phase chromatography consists of a polar stationary phase and non-polar mobile phase, typically used for fairly polar solutes;

(ii) reverse phase chromatography where the opposite criteria apply.

Separation of solutes may be further manipulated by gradient elution methods which involve a change in mobile phase polarity during chromatographic separation.

3.2.2 Adsorption

This mechanism involves competition between solute molecules and mobile phase for adsorbent sites on the stationary phase. Separation is therefore dependent on the magnitude of affinities between mobile phase-stationary phase, solute-stationary phase and mobile phase-solute. For separation to occur an equilibrium distribution must exist between adsorbed solute and solute solvated by mobile phase.

Selectivity may also be a function of the surface-chemical characteristics of the stationary phase. For example, silica support materials contain hydroxyl functional groups (silanol - SiOH), therefore basic components tend to interact to a greater extent than acidic or neutral solutes.

3.2.3 Ion Exchange

The stationary phase is either a cationic or anionic ion-exchange resin. Separation is achieved by an ion-exchange process with elution controlled by ionic strength and pH of the mobile phase. Because of its greater efficiency, ion-pair chromatography is now preferred to this method.

3.2.4 Ion-pairing

Ion-pair chromatography utilizes a counterion present in the mobile phase which forms a hydrophobic ion-pair with ionic solutes. The ion-pair complex subsequently interacts with the stationary phase allowing separation. Reverse phase ion-pair chromatography involves a chemically bonded silica stationary phase (i.e. hydrocarbon chains bonded to the silica surface) and an organic/aqueous mobile phase containing counterions. Selectivity may also be achieved by using more polar bonded phases (ie. amino or phenyl groups) offering specific chemical interactions.

3.2.5 Size Exclusion

Components are separated by a physical "sieving" effect dependent on the relative molecular sizes and shapes of the solute and porous stationary phase. Size exclusion chromatography is generally used for the separation of biological macromolecules or polymers.

However, many chromatographic separations are difficult to classify into particular mechanisms since theoretical considerations predict simultaneous adsorption/partition or ion-pair/partition processes.

3.3 CHROMATOGRAPHIC PARAMETERS

In order to evaluate chromatographic performance and determine the suitability of a particular method, several parameters are optimised. Solute retention is indicated by the column capacity factor, k^1, and is calculated by equation 61:

$$k^1 = \frac{tr-to}{to} \qquad ....(61)$$

where tr and to are the retention times of a solute peak and unretained (or solvent) peak respectively, as illustrated by Figure 3.1. Optimum values of k^1 are between 1.5 and 4 (Schram, 1980). Values less than 1.5 indicate little retention whilst those above 4 indicate excessive retention leading to long analysis time. The selectivity, α (always expressed as a number greater than 1), of a particular separation is given by equation 62:

$$\alpha = \frac{k^1_b}{k^1_a} \qquad ....(62)$$

where k^1_a and k^1_b are the capacity factors of compounds a and b respectively. For separation to occur, α must have a value other than unity.

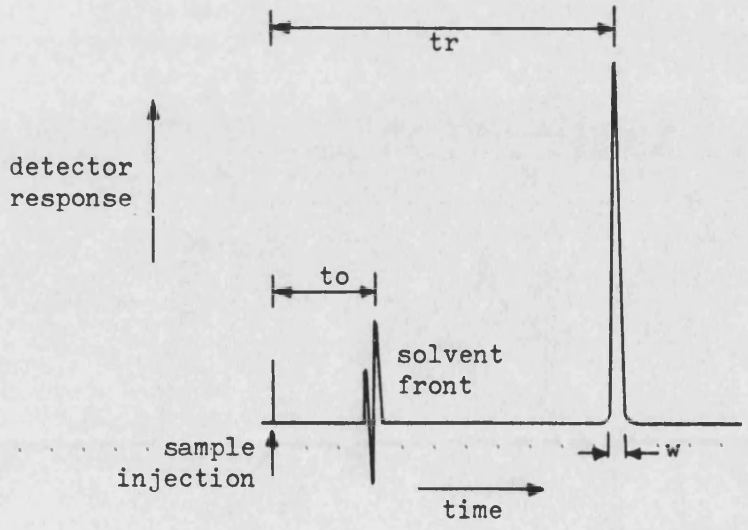

Figure 3.1 A typical chromatogram which allows calculation of column capacity factor and efficiency

In addition to showing selectivity, a chromatographic method must illustrate resolution between separated peaks. Resolution, R, of a particular separation can be calculated from equation 63:

$$R = 2\left(\frac{tr_a - tr_b}{w_a + w_b}\right) \qquad ....(63)$$

where tr_a, tr_b, w_a and w_b are the retention times and base widths (in time units) of peaks for compounds a and b respectively, as illustrated in Figure 3.2. Ideally resolution should be around 1.5 (Parris, 1976), values larger than this again lead to long analysis time.

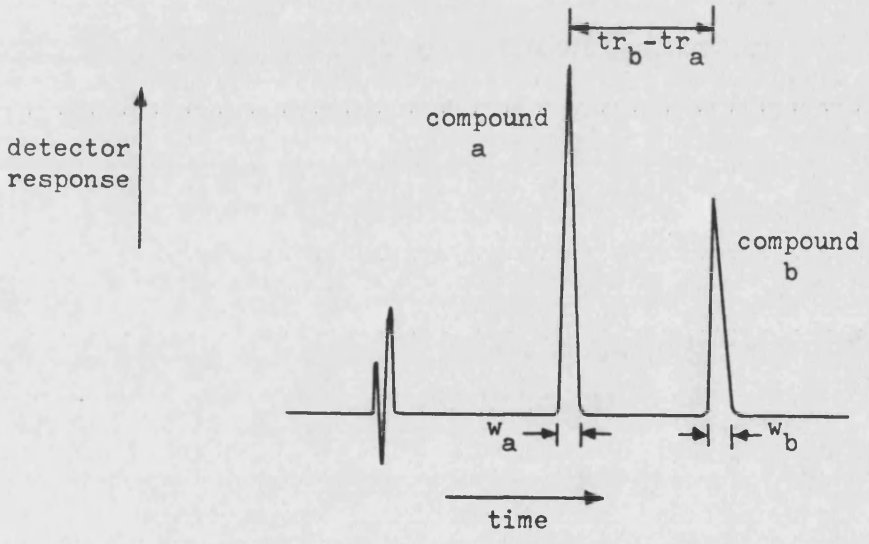

Figure 3.2 A typical chromatogram which allows the calculation of resolution between two compounds

The efficiency of a chromatographic separation is described in terms of the number of theoretical plates, N, which are often

visualised as the number of separation stages. The simplest way to calculate N is given by equation 64:

$$N = 16\left(\frac{tr}{w}\right)^2 \qquad \ldots.(64)$$

where w is the base width (in time units). Figure 3.1 provides an illustration of a typical chromatogram which allows calculation of column efficiency. Modern HPLC columns and stationary phase materials typically have values exceeding 4×10^5 plates m^{-1} for test mixtures (Schram, 1980). To compare the efficiences of different length columns the height of each theoretical plate, HETP, is calculated by dividing the column length by N.

A general expression (equation 65) has been derived by Parris (1976) which describes resolution in terms of column efficiency, selectivity and capacity factors:

$$R = \frac{1}{4}\sqrt{N}\cdot\left(\frac{\alpha-1}{\alpha}\right)\cdot\left(\frac{k^1}{k^1+1}\right) \qquad \ldots.(65)$$

Equation 65 illustrates that resolution is directly dependent on selectivity and capacity factor and is a function of the square root of column efficiency. Consequently a considerable increase in column efficiency is required to improve the resolution between two peaks.

3.4 COLUMN TESTING AND PERFORMANCE

Column performance and stability during use are usually checked by running a test mixture with a simple mobile phase. Column parameters are then compared with previous values. Test mixtures should contain at least two components, one with a low capacity factor ($k^1 \sim 1$) which provides an indication of HETP and another with a large capacity factor ($k^1 \sim 4$) indicating column efficiency.

In instances where the use of test mixtures is impractical it may be acceptable to perform testing in use by assessing shape characteristics and parameters associated with a single peak (usually the compound of interest in the usual mobile phase).

In order to maintain performance, care of the chromatographic column should be taken. For example, the use of mobile phases known to cause deterioration should be avoided if possible and a pre-column may, in certain cases, protect the analytical column from solvent or sample impurity contamination.

Practical Aspects:

Certain practical procedures are "good chromatographic practice":

(i) Composition of the mobile phase is important. It should be of high purity (HPLC Grade), filtered (or used with in-line filters) and degassed. Chromatographic separations involving an adsorption mechanism are often dependent on the water content of the mobile phase, therefore it is important to maintain a column equilbrium with water which is not affected by sample injection. If necessary aqueous samples should be diluted with mobile phase before injection.

(ii) For increased efficiency band broadening should be reduced. Band broadening may be due to settling of packing material at the column top - this may be reduced by regular replacement of PTFE inserts. Zero dead volume fittings are also required to reduce band broadening.

(iii) Fronting and tailing of peaks should be reduced. Tailing is sometimes due to inefficient flushing of the injector. Some fronting and tailing may be due to the mechanism of interaction between solute and stationary phase and is therefore unavoidable.

EXPERIMENTAL

CHAPTER 4

MATERIALS AND GENERAL METHODS

4.1 EQUIPMENT

The instrumentation/equipment used are listed in the following sections. Details of specific methods used are found in the relevant sections of Chapters 5 and 6.

4.1.1 Analytical Techniques

HPLC : Constametric IIIG dual-piston reciprocating pump (LDC)
Spectromonitor III variable wavelength u.v. detector (LDC)
LC-UV variable wavelength detector (Pye-Unicam)
CR650A chart recorder (JJ Instruments)
7010 loop injector valve (Rheodyne)
Autosampler (with 7010 Rheodyne valve, Applied Chromatography Systems)

All fittings were of the "zero dead volume" type with microbore (0.15 mm) tubing used between the column and low dead volume detector cell.

Other : SP1800 variable wavelength spectrophotometer (Pye Unicam)
Lambda 3 variable wavelength spectrophotometer (Perkin Elmer)
Hand-held u.v. (254 nm) TLC viewer
Single-pan Oertling R41 analytical balance
Buchi rotary evaporator (Fisons Scientific)

4.1.2 pH Determination

Electrodes (combinded glass - Ag/AgCl)
: Pye-Ingold 401 (general pH measurement)
Pye-Ingold 405-M5 (narrow diameter shaft, for pH measurement inside ampoules)
Pye-Ingold 465-90 (high temperature electrode, for kinetic experiments)

pH Meters : PHM 64 Research pH Meter (Radiometer) digital readout to 3 decimal places used with 401 and 405-M5 electrodes.
PHM 61 Laboratory pH Meter (Radiometer) scale reading to 0.02 units used with 465-90 high temperature electrodes

4.1.3 Kinetic Experiments

TTT60 Titrators (Radiometer)
ABU12 Autoburettes (Radiometer)
Underwater magnetic stirrers (Rank Brothers, Cambridge)
SU6 and UE2 Thermostatic control units, ±0.1°C (Grant Instruments)
Citenco Varilab stirrers (Fisons Scientific)
Northlight colour matching fluorescent tubes (Atlas)
3.5 cm Gravatom fixed ^{60}Cobalt source

4.1.4 Glassware

Grade A volumetric glassware was used throughout this study. All glassware was initially cleaned by immersion in "chromic acid" for one hour followed by three rinses with tap water and six rinses with distilled water. Sorption of chlorhexidine on to plastics has been well documented (McCarthy, 1970; Richardson *et al*, 1977 and 1979). Interactions between glass and chlorhexidine, resulting in a 25% decrease in chlorhexidine concentration in solution, have also been reported by McTaggart *et al*, 1979. Sorption on to glass was found to continue until all binding sites were saturated. Therefore all glassware, after cleaning, was immersed in appropriate concentrations of chlorhexidine gluconate for 24 hours and then rinsed thoroughly with distilled water and dried before use. The process of "chromic acid" cleaning and chlorhexidine "aging" was repeated when the glassware became too greasy for further use.

The ampoules used in stability studies were of the neutral glass type (FBG Trident Limited). All ampoules were chlorhexidine aged before use.

4.2 MATERIALS

Specific materials are listed in the following sections. All other chemicals or solvents were at least GPR grade (BDH); AnalaR quality materials were used whenever these were available.

4.2.1 Chlorhexidine

All chlorhexidine samples (base, acetate and hydrochloride salts and gluconate solution) were gifts from ICI Pharmaceuticals and used as received. Sample purity is discussed in Chapter 5.1.1.1.

4.2.2 Analytical Experimentation

Partisil 5 μm HPLC stationary phase (Whatman)
Acetonitrile, HPLC grade (Rathburn Chemicals)
Orthophosphoric acid, AnalaR (BDH)
Helium, Nitrogen and Compressed Air (Air Products Ltd.)
GF_{254} TLC plates (Whatman)
No. 3 Chromatographic Paper (Whatman)
Cetrimide BP (ICI Pharmaceuticals)

4.2.3 Buffers and pH-electrode Maintenance

All buffer salts used for pH-electrode standardisation (see section 4.3.1.1) were AnalaR quality. Viscolyte B solution (Pye-Unicam) was used when it became necessary to replace the electrolyte of the 465-90 high temperature pH-electrode. During the routine maintenance of these electrodes (see section 4.3.1.3), Glass Membrane Cleaner, Liquid Junction Diaphragm Cleaner and Regeneration Solution (all Radiometer) were used according to the manufacturer's instructions. After maintenance cleaning electrode response was checked against specification using the Pye-Unicam test procedure.

4.2.4 Kinetic Experimentation

All materials AnalaR except:

D-Gluconic acid, 50% w/w solution in water (Sigma Chemical Co.)
Sodium dodecyl sulphate, specially pure (BDH)
Cetomacrogol 1000 (Croda Chemicals)
Polysorbate (Tween) 80, pharmaceutical grade (Honeywill-Atlas)
Polyethylene glycols (Carbowaxes), pharmaceutical grades (Union Carbide)
White Soft Paraffin BP (Evans)

4.2.5 Distilled water

All water used was freshly double distilled from an all glass still.

4.3 GENERAL METHODS

4.3.1 Temperature Control

4.3.1.1 Thermometers

Thermometers were calibrated against primary mercury-in-glass reference thermometers graduated at intervals of 0.1°C, held within the department. These primary reference thermometers had been calibrated against a NPL certificated Platinum Resistance Thermometer which was sensitive to ±0.001°C.

4.3.1.2 Water Baths

All kinetic studies were carried out in thermostatically controlled water baths. Grant Instruments heater/stirrer units (model SU6) were used to control water bath temperature. The manufacturer's claimed sensitivity was ±0.05°C, but practically, measured temperature fluctuation was ±0.1°C. Water evaporation from the baths was reduced by a double blanket of polypropylene spheres with water level maintained by a constant head device.

Due to the lengthy storage periods involved in ampoule stability studies, water baths were replaced by oil baths containing Shell Voluta 75 Oil. Temperature control was by Grant Instruments heater/stirrer units (model UE2, manufacturers claimed sensitivity ±0.05°C). However, the stirrer units on these models were inefficient when used with oil (resultant temperature variation ±1°C) and consequently additional independent stirrers (Citenco) were added to give a temperature variation within ±0.2°C.

4.3.2 pH-Electrode Standardisation

4.3.2.1 Standard Buffer Solutions

Standard buffer solutions were prepared according to Perrin and Dempsey (1974). Since the data on temperature -pH relationships in this text relate to molal concentrations in some cases and molar concentrations in others, the following buffer solutions were used as standards for pH-electrode standardisation:

	pH at 25°C
0.1 molal Potassium tetroxalate	1.482
0.05 M Potassium hydrogen phthalate*	4.005
0.025 M Potassium dihydrogen orthophosphate and 0.025 M disodium hydrogen orthophosphate	6.865
0.01 molal Sodium tetraborate*	9.180
0.025 molal Sodium hydrogen carbonate and 0.025 molal sodium carbonate	10.012

*Primary standard solutions

After preparation all buffer solutions were stored in a refrigerator and discarded after one month.

4.3.2.2 General Standardisation

Pye-Ingold 401 and 405-M5 electrodes were standardised using the primary standard buffer solutions (phthalate and borate) at 25°C.

Electrode standardisation for the measurement of HPLC mobile phase pH (apparent) was by 0.1 molal potassium tetroxalate and phthalate primary standard at 25°C.

4.3.2.3 High Temperature Electrode Standardisation

High temperature electrodes were standardised by using standard buffers at the nearest pH either side of the kinetic experiment pH (i.e. for pH 5.0, phthalate and phosphate buffers were used). For pKa determinations, standard buffers above and below the experimental pH were used (i.e. borate and carbonate buffers for the basic ionisations, see also Appendix 5). All calibrations were performed at the temperature of the kinetic or pKa experimentation using the relevant standard buffer pH values from Perrin and Dempsey (1974).

Additional checks on the high temperature electrodes were made since they were required to remain in the reaction vessel for the duration of each kinetic experiment. Firstly, the calibration was checked at the end of each kinetic run. Secondly, at regular intervals (usually monthly) electrode response was checked according to the manufacturers' instructions. If it was outside specification the electrode was cleaned with electrode cleaner, liquid junction cleaner and reactivating solution (see section 4.2.3). Replacement of the reference electrolyte solution was also necessary in some instances. The electrode was then recalibrated and used for kinetic experiments or discarded if re-calibration was not possible. A high temperature electrode had a typical useful lifetime of 6-12 months.

4.3.3 Dilution of 20% w/v Chlorhexidine Gluconate Solutions

The commercial 20% w/v chlorhexidine gluconate solution is slightly viscous with a density of 1.06-1.07 $g.ml^{-1}$ (British Pharmacopoeia, 1980). It was noted during the preparation of dilutions from the commercial solution that pipettes took some time to drain. Inaccuracies may result from such methods due to variable volume delivery outside the pipette tolerance. Dilutions of the commercial solution were therefore made by weight transfer directly into analytical glassware.

The densities of the two commercial samples of 20% w/v chlorhexidine gluconate solution used throughout the study were determined by the British Pharmacopoeia (1980) method at 20°C. Each container of solution was shaken thoroughly prior to each density determination since phase separation may occur on storage (Fernie, ICI Pharmaceuticals, 1983, personal communication). The density data are shown in Table 4.1.

	Density ($g.ml^{-1}$) at 20°C			
Sample	1	2	3	Mean (SD)
20% w/v Solution 1				
determination 1	1.0634	1.0619	1.0614	1.0622 (0.0010)
2	1.0641	1.0637	1.0626	1.0635 (0.0008)
3	1.0631	1.0630	1.0627	1.0629 (0.0002)
20% w/v Solution 2				
determination 1	1.0670	1.0684	1.0681	1.0678 (0.0007)
2	1.0685	1.0689	1.0683	1.0686 (0.0003)

Table 4.1 Density data for commercial solutions of 20% w/v chlorhexidine gluconate

By reference to the most recent experimentally determined density value, the exact amount of chlorhexidine gluconate transferred was calculated. A 1.0% w/v solution was regularly prepared by the weight transfer method, all subsequent dilutions from this solution being made by pipette (volume transfer).

CHAPTER 5

ANALYTICAL METHODS

5.1 CHLORHEXIDINE

5.1.1 HPLC - Validation of Assay Method

Several HPLC methods were available at the initiation of this work (see Chapter 2.6.3). Most of these methods were intended for the quality control of chlorhexidine formulations and are not stability indicating. Although the method of Bailey *et al* (1975) claimed separation of chlorhexidine from its degradation products and impurities, the only illustrative evidence was resolution between chlorhexidine and 4-chloroaniline. This method was modified by the above workers in the Quality Control Department of ICI Pharmaceuticals and the new method validated as stability indicating. Therefore the latter, unpublished, method was used for all HPLC assays of chlorhexidine, details of which are listed below.

Hardware	: Constametric IIIG dual-piston reciprocating pump (LDC) Spectromonitor III variable wavelength u.v. detector (LDC) LC-UV variable wavelength detector (Pye-Unicam) CR650A chart recorder (JJ Instruments) 7010 loop injector valve (Rheodyne) Autosampler (with 7010 Rheodyne valve, Applied Chromatography Systems)
Analytical column	: 100 x 5 mm (i.d.) stainless steel packed with Partisil 5 µm (Whatman). Packed by a high pressure slurry method at 8000 psi.
Precolumn	: 150 x 5 mm stainless steel column packed with 37-52 µm silica.
Mobile phase	: 87 parts acetonitrile 13 parts 8% v/v orthophosphoric acid in double distilled water. Degassed daily by a helium purge.

Flow rate	: 1.5 ml.min^{-1} (providing a typical operating pressure of 600-800 psi).
Detector wavelength	: 254 nm
Detector sensitivity	: typically 0.005-0.08 AUFS
Sample volume	: 10 µl via Rheodyne loop valve
Sample preparation	: at least 1 in 5 dilution with mobile phase (see 5.1.1.2)
Temperature	: ambient
Quantitation	: by peak height ratio against external chlorhexidine acetate standards

In order to establish the specific and quantitative nature of the analysis for chlorhexidine the methodology was examined as follows:

5.1.1.1 Standardisation

The choice of external standardisation was made for two reasons. Firstly, an internal standard may interfere with, or mask, the peaks of degradation products. As the number and position of potential degradation product peaks was uncertain it was considered unwise to search for a suitable internal standard. Secondly, a pure reference standard material was readily available.

All quantitative determinations were therefore made against an external reference standard material of chlorhexidine acetate. This material was supplied by ICI Pharmaceuticals (Batch Ref. 950/46) with a quoted purity value of 97.4% w/w generated by a non-aqueous titration method (British Pharmacopoeia, 1980). No impurities were detected and the residual 2.6% w/w was attributed to be moisture. The reference standards were stored in a cool, dark cupboard in double sealed airtight containers.

External standardisation was validated as follows:

5.1.1.1.1 Equivalence Between Salts

Since only chlorhexidine acetate was available as a reference standard material it was necessary to demonstrate its chromatographic equivalence to the gluconate and hydrochloride salts and to chlorhexidine base. In order to establish whether the various

forms elute with the same or different retention times, aqueous solutions of 0.002% w/v of each salt and chlorhexidine base were prepared. After a final 1 in 5 dilution with mobile phase each material was injected in duplicate and the chromatograms produced are illustrated in Figure 5.1. In all cases peak shape and retention times (listed in Table 5.2) were identical.

Quantitative equivalence between the various forms was examined according to the following experimentation. Aqueous solutions of chlorhexidine base and the gluconate and hydrochloride salts were accurately prepared at known concentrations. The samples of chlorhexidine base, hydrochloride and gluconate salts (the latter as a 20% w/v solution) were provided by ICI Pharmaceuticals. Assay values were available for the two salt forms; 100% w/w with reference to the dried material for the hydrochloride and 19.34% w/v for the gluconate solution, both determined by the British Pharmacopoeia (1980) non-aqueous titration method. No assay value was available for chlorhexidine base although the material supplied had been recrystallised seven times and was therefore assumed to be 100% w/w with reference to the dried material (Fernie, ICI Pharmaceuticals, 1982, Personal Communication).

After a final 1 in 5 dilution with mobile phase these solutions were then assayed against chlorhexidine acetate reference standard. Assay values for chlorhexidine base and the gluconate and hydrochloride salts were calculated from molecular weight considerations (Table 5.1).

Salt	Molecular Weight	1 $mg.ml^{-1}$ chlorhexidine acetate standard therefore equivalent to
Base	505.5	0.808 $mg.ml^{-1}$
Hydrochloride	578.4	0.925 $mg.ml^{-1}$
Acetate	625.6	1.000 $mg.ml^{-1}$
Gluconate	897.8	1.435 $mg.ml^{-1}$

Table 5.1 Equivalencies of chlorhexidine base and salt forms

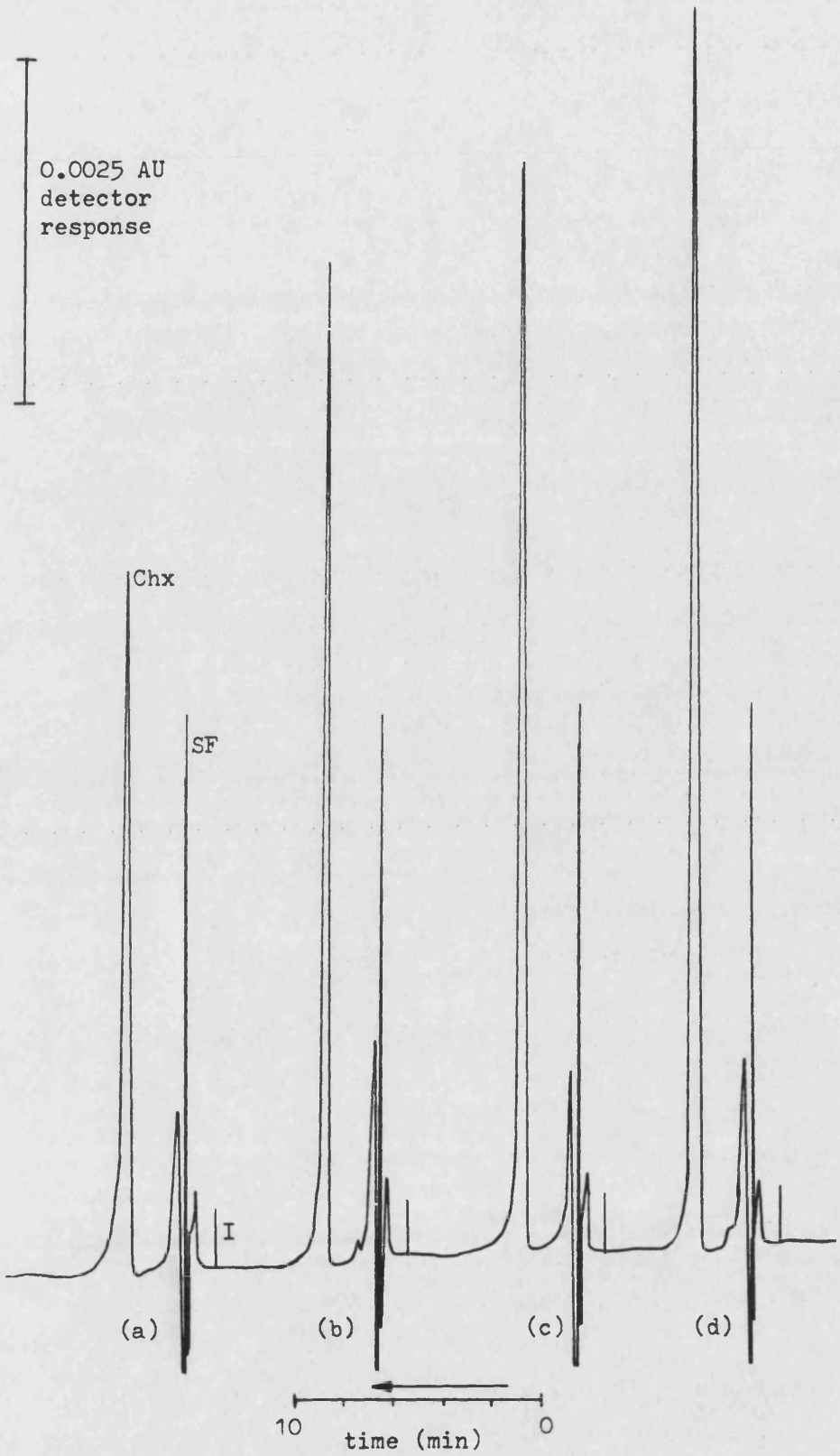

Figure 5.1 (a) 0.002% w/v chlorhexidine gluconate
(b) 0.002% w/v chlorhexidine acetate
(c) 0.002% w/v chlorhexidine hydrochloride
(d) 0.002% w/v chlorhexidine base

All concentrations before 1 in 5 dilution with mobile phase

I = injection SF = solvent front Chx = chlorhexidine peak

The data generated (mean of triplicate injections) are shown in Table 5.2 with percentage w/w (or w/v for gluconate solution) return calculated by reference to ICI assay values. The hydrochloride salt gave a return of 97.38% w/w compared with an ICI value of 100% for the dried material. However, dehydration of the sample in a vacuum at 60°C to constant weight revealed the presence of 2.7% w/w moisture. Therefore, the material "as received" was 97.3% w/w pure which compares well with the experimentally generated value of 97.38% w/w. The gluconate sample gave similar consistency between quoted (19.34% w/v) and assayed (19.41% w/v) values.

Salt	Retention time (minutes)	Concentration (% w/v x 10^2)		% Return	ICI assay data
		Theoretical (ICI data)	Actual assay against acetate standard		
Base	3.18	0.120	0.118	98.33% w/w	-
Hydrochloride	3.20	1.069	1.041	97.38% w/w	97.3 % w/w
Acetate	3.20	-	-	-	97.4 % w/w
Gluconate	3.18	1.934	1.941	19.41% w/v	19.34% w/v

Table 5.2 Quantitative equivalence of chlorhexidine base and salt forms

Chlorhexidine base gave a 98.33% w/w return with no moisture loss being detected on drying. Impurities may account for the observed reduced purity, although no additional peaks were detected on examination of its chromatogram.

Therefore, by use of appropriate multiplication factors it was possible to accurately assay the various forms of chlorhexidine against the reference standard chlorhexidine acetate material. The equivalence between the forms may be explained by reference to the chromatographic conditions. The mobile phase contains phosphate anions which are in excess compared to any anions derived from the chlorhexidine

salt (provided a 1 in 5 dilution at least is maintained, see 5.1.1.2.2). Since the apparent pH of such dilutions were measured as ~1.4 to 1.6 (see 5.1.1.2.3), chlorhexidine will be ionised and exist as di-, tri- or tetra-cations and phosphoric acid should partially exist as the dihydrogen phosphate ($H_2PO_4^-$). The chromatographically active species is therefore likely to be an association between positively charged chlorhexidine and phosphate anions. Provided this equilibrium is not disturbed the assay of chlorhexidine will be independent of the original form used.

5.1.1.1.2 Linearity of Response

Linearity of response was initially checked over the concentration range 10-500 $\mu g.ml^{-1}$ chlorhexidine acetate injected*, using detector settings 0.04-1.28 AUFS, in order to confirm a linear Beer-Lambert relationship and also linear detector response. Duplicate injections of aqueous solutions diluted 1 in 10 with mobile phase were made with peak height response normalised to 1.0 AUFS.** Figure 5.2 illustrates observed non-linearity above ~150 $\mu g.ml^{-1}$ chlorhexidine acetate injected. The curvature of the plot indicates a deviation from the Beer-Lambert Law rather than error in detector response which would be suspected if several linear regions of different slope were present.

*Footnote 1: Unless stated otherwise, the concentration values quoted are after final dilution and represent the solution concentration injected on to the analytical column

**Footnote 2: Normalisation involved calculating what the peak height would be at another detector setting, e.g. peak height of 171 mm at 0.16 AUFS = $171 \times \frac{0.16}{1.0} = 27.36$ mm at 1.0 AUFS

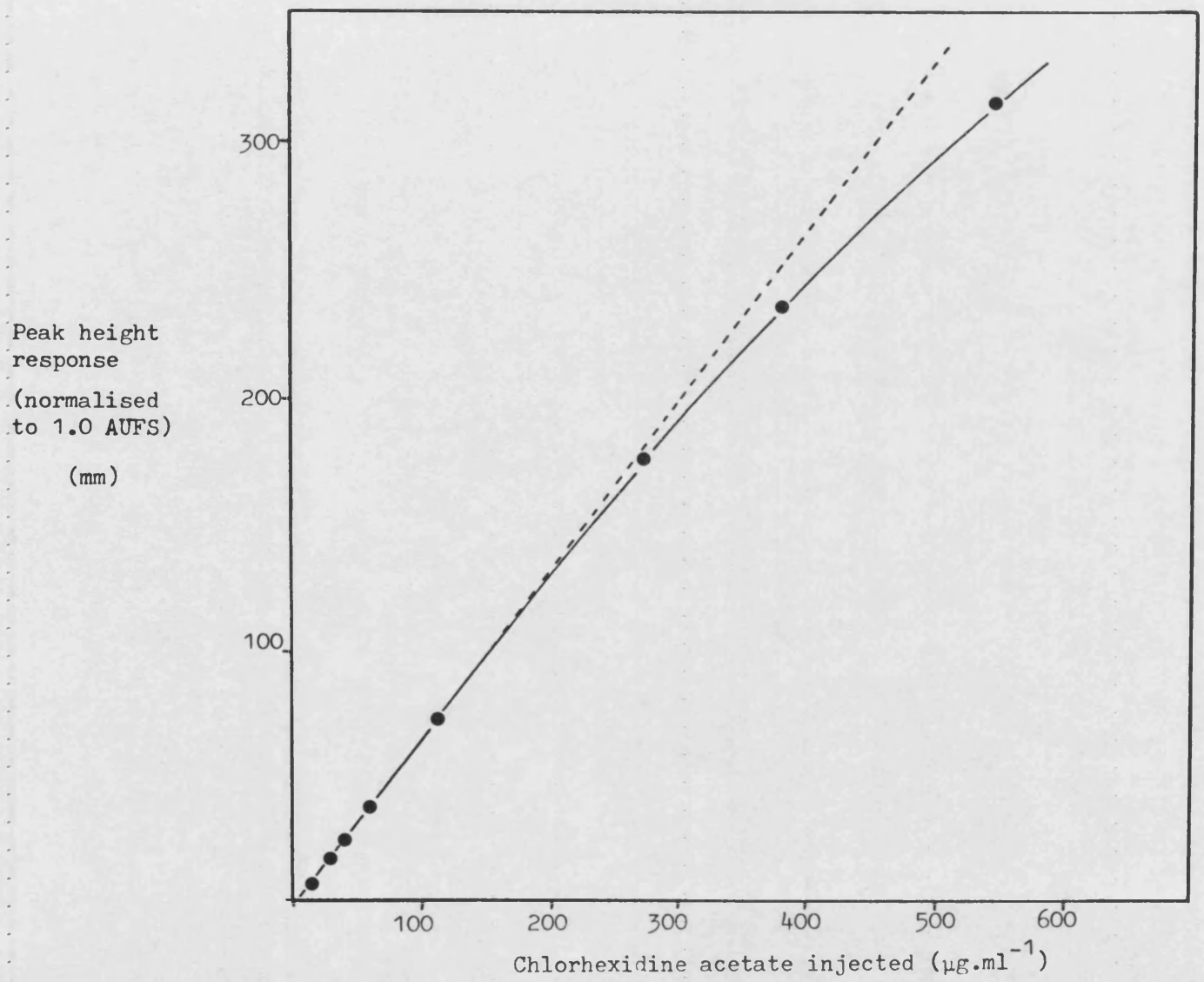

Figure 5.2 Beer-Lambert plot showing deviation from linearity at ~150µg.ml^{-1} chlorhexidine acetate injected

To accurately determine the linear region, the concentration range 2-140 $\mu g.ml^{-1}$ chlorhexidine acetate was examined. Triplicate injections of a serially diluted standard solution were made; the last dilution was always made with mobile phase to maintain a 1 in 10 dilution of aqueous standard in mobile phase. The mean peak height response for each dilution was normalised to 1.0 AUFS (all data presented in Table 5.3) and a plot of mean normalised peak height against injected chlorhexidine acetate concentration constructed (Figure 5.3). This plot clearly illustrates a deviation from linearity above injected chlorhexidine acetate concentrations of ~90 $\mu g.ml^{-1}$.

Concentration of chlorhexidine acetate $\mu g.ml^{-1}$	Mean peak height response mm	Detector sensitivity AUFS	Mean normalised peak height (1.0 AUFS) mm
2.338	157.0	0.01	1.57
4.676	176.5	0.02	3.53
9.352	170.33	0.04	6.81
23.38	215.5	0.08	17.24
46.76	215.0	0.16	34.40
70.14	162.67	0.32	52.05
93.52	215.0	0.32	68.80
116.90	133.0	0.64	85.12
140.28	156.67	0.64	100.27

Table 5.3 Experimental data for the determination of linearity of response

Further quantitative evidence for the deviation from linearity was obtained from separate linear regression (Appendix 1) of the above data in the concentration ranges 2-70 $\mu g.ml^{-1}$ and 90-140 $\mu g.ml^{-1}$ of chlorhexidine acetate injected. Examination of the regression data (Table 5.4) shows that a significant intercept (>±2SD) exists in the regressed slope for 90-140 $\mu g.ml^{-1}$ whereas the intercept was not significant for the 2-70 $\mu g.ml^{-1}$ data. Additionally, from a 't' test (Appendix 2), the higher concentration range gave a significantly

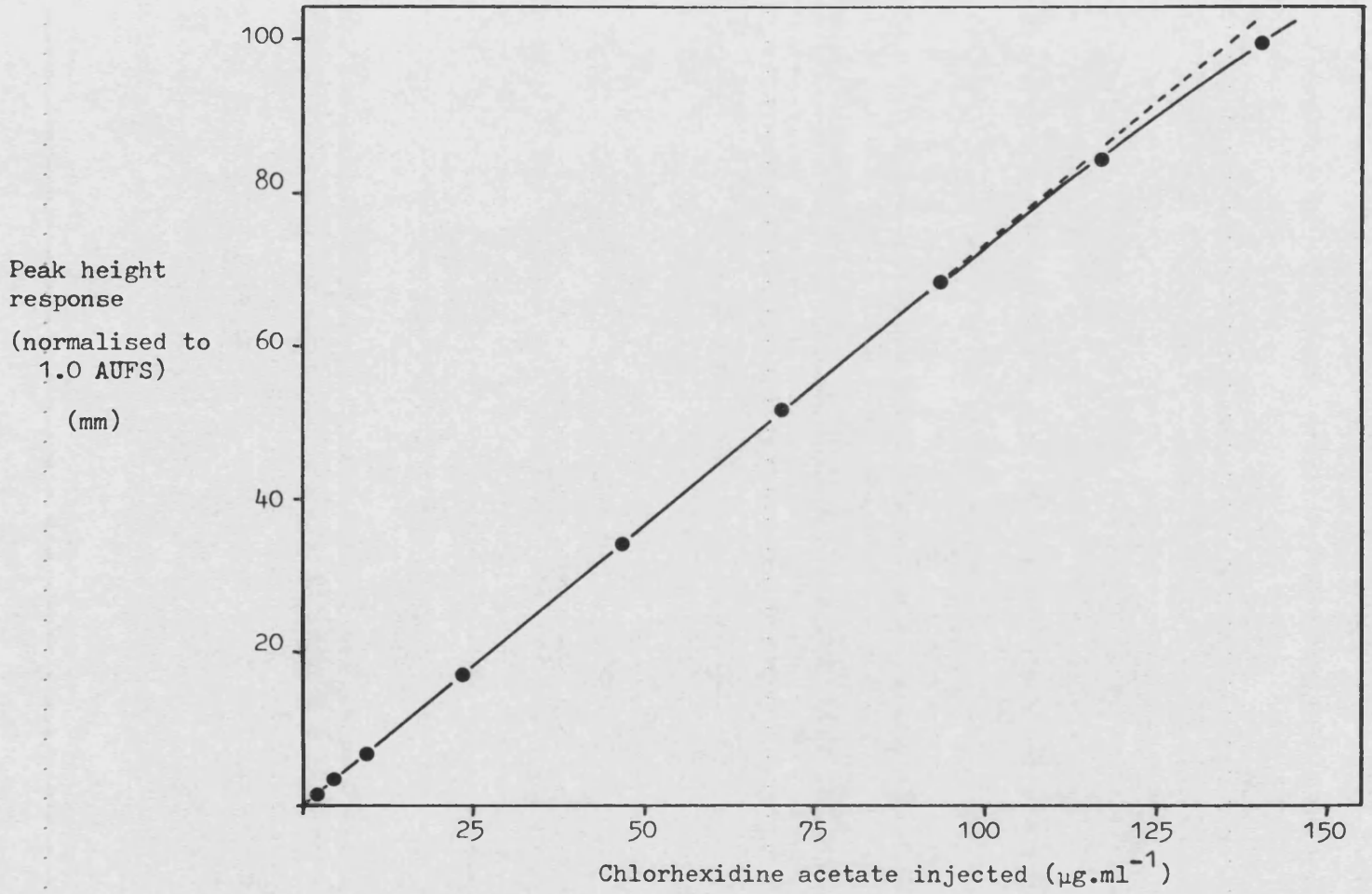

Figure 5.3 Observed linearity of response for injected chlorhexidine acetate concentrations up to 70µg.ml^{-1}

shallower slope (t_{slope} = 4.72, t_{tab} = 2.02, p = 0.05). Both these factors indicate a deviation from linearity in this range. Regression data for the range 2-70 $\mu g.ml^{-1}$ was good, therefore assays were limited to injected solutions <70 $\mu g.ml^{-1}$ chlorhexidine acetate and detector sensitivity <0.32 AUFS. The maximum concentration assayed during the study was 0.05% w/v chlorhexidine gluconate which, after a 1 in 10 dilution in mobile phase, remains inside the limit of linearity.

Concentration range (chlorhexidine acetate) $\mu g.ml^{-1}$	Regression Analysis	
2-70	Correlation coefficient	0.9999
	Slope (SD)	0.7418 (0.0023)
	Intercept (SD)	-0.100 (0.084)
	Relative standard deviation of slope	0.31%
90-140	Correlation coefficient	0.9998
	Slope (SD)	0.6730 (0.0144)
	Intercept (SD)	6.055 (1.711)
	Relative standard deviation of slope	2.15%
't' test on slopes	t_{slope} = 4.72, t_{tab} = 2.02, p = 0.05	

Table 5.4 Linear regression analysis of experimental data used in the determination of linearity of response

A second check of linearity was performed across a narrow concentration range using one detector setting (0.01 AUFS). Since most assays were to be performed on 0.002% w/v chlorhexidine gluconate (equivalent to 14 $\mu g.ml^{-1}$ chlorhexidine acetate) a series of chlorhexidine acetate standard solutions were prepared to give a range of 5.6-17.5 $\mu g.ml^{-1}$ before a 1 in 5 dilution with mobile phase. This concentration range was equivalent to 0.0008-0.0025% w/v chlorhexidine gluconate before mobile phase dilution. Triplicate injections were made and a plot of mean peak height response against chlorhexidine acetate concentration injected is shown in Figure 5.4 (slope drawn from linear regression analysis).

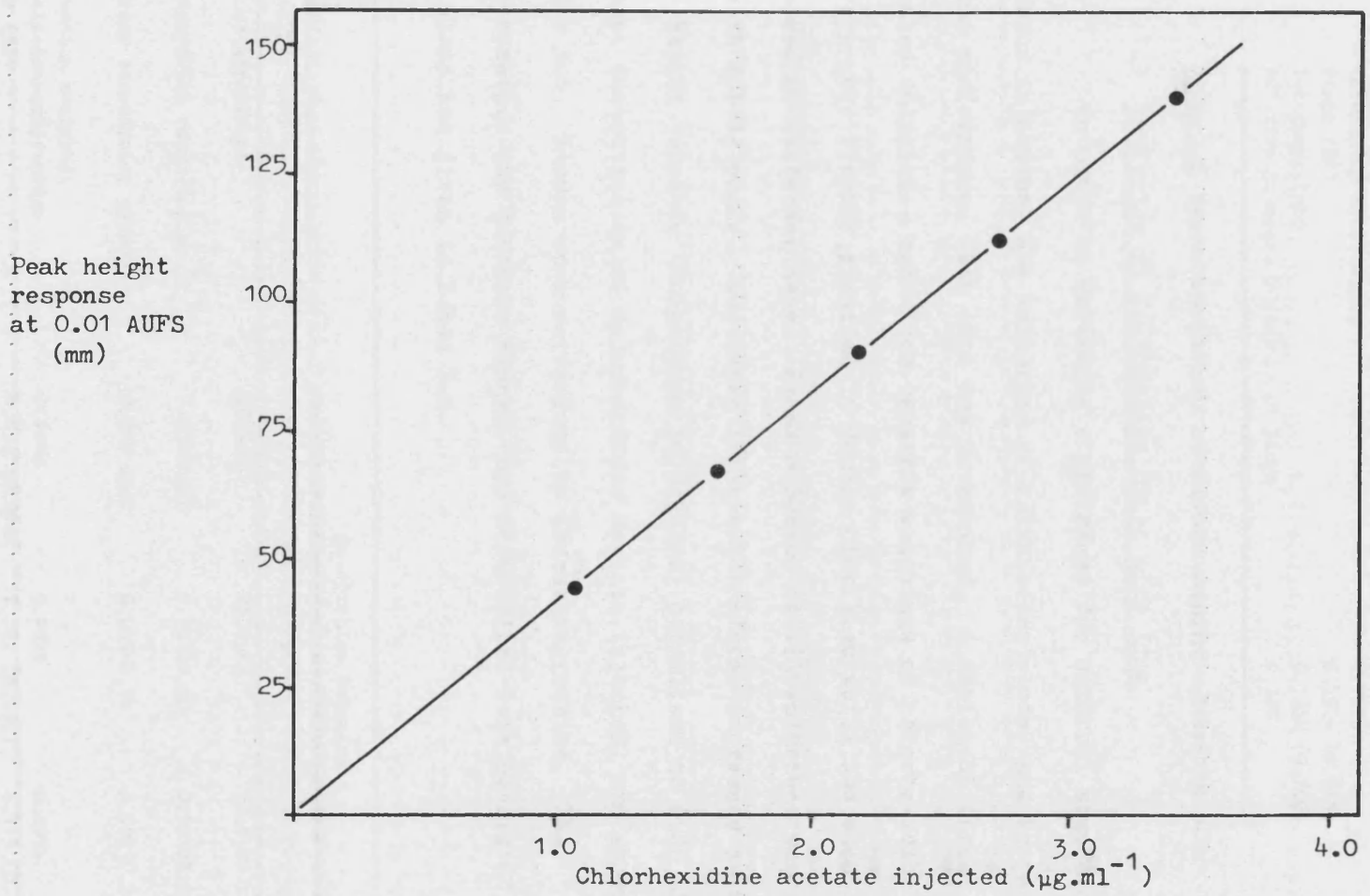

Figure 5.4 Linearity of response over the lowest working concentration range (equivalent to assays of 0.002%w/v chlorhexidine gluconate)

Linear regression data are given in Table 5.5 indicating the assay precision by external standardisation provided interpolation and not extrapolation is performed.

Corelation coefficient	0.9999
Slope (SD)	8.2524 (0.065)
Intercept (SD)	-0.1059 (0.760)
Relative Standard Deviation of Slope	0.78%

Table 5.5 Regression analysis of external standard calibration plot

5.1.1.1.3 Variation of Calibration Plots with Time

In order to determine a procedure for external standard solution injection, the variation of calibration plots, and hence column performance, with time was determined. A series of three standard solutions, each from separate weighings of chlorhexidine acetate were freshly prepared in double distilled water and each series injected on different days. Final dilution of all solutions was 1 in 10 with mobile phase. The three calibration plots, expressed as mean peak height response (triplicate injections) normalised to 0.08 AUFS against concentration of chlorhexidine acetate injected, are shown in Figure 5.5. Slopes were determined by linear regression. The concentration and detector ranges, and statistical data generated from the plots are given in Table 5.6.

	Calibration Solution		
	A	B	C
Date of experiment	27.4.82	29.4.82	26.5.82
Concentration range ($\mu g.ml^{-1}$)	1.13-56.40	0.78-39.00	0.55-55.20
Detector sensitivity (AUFS)	0.005-0.32	0.005-0.16	0.005-0.16
Regression analysis:			
Correlation coefficient	0.9996	0.9999	0.9994
Slope (SD)	8.478 (0.095)	7.752 (0.035)	8.119 (0.102)
Intercept (SD)	1.252 (2.546)	1.399 (0.637)	3.340 (2.262)
Relative standard deviation of slope	1.12%	0.45%	1.26%

Table 5.6 Variation in chlorhexidine acetate calibration plot data with time

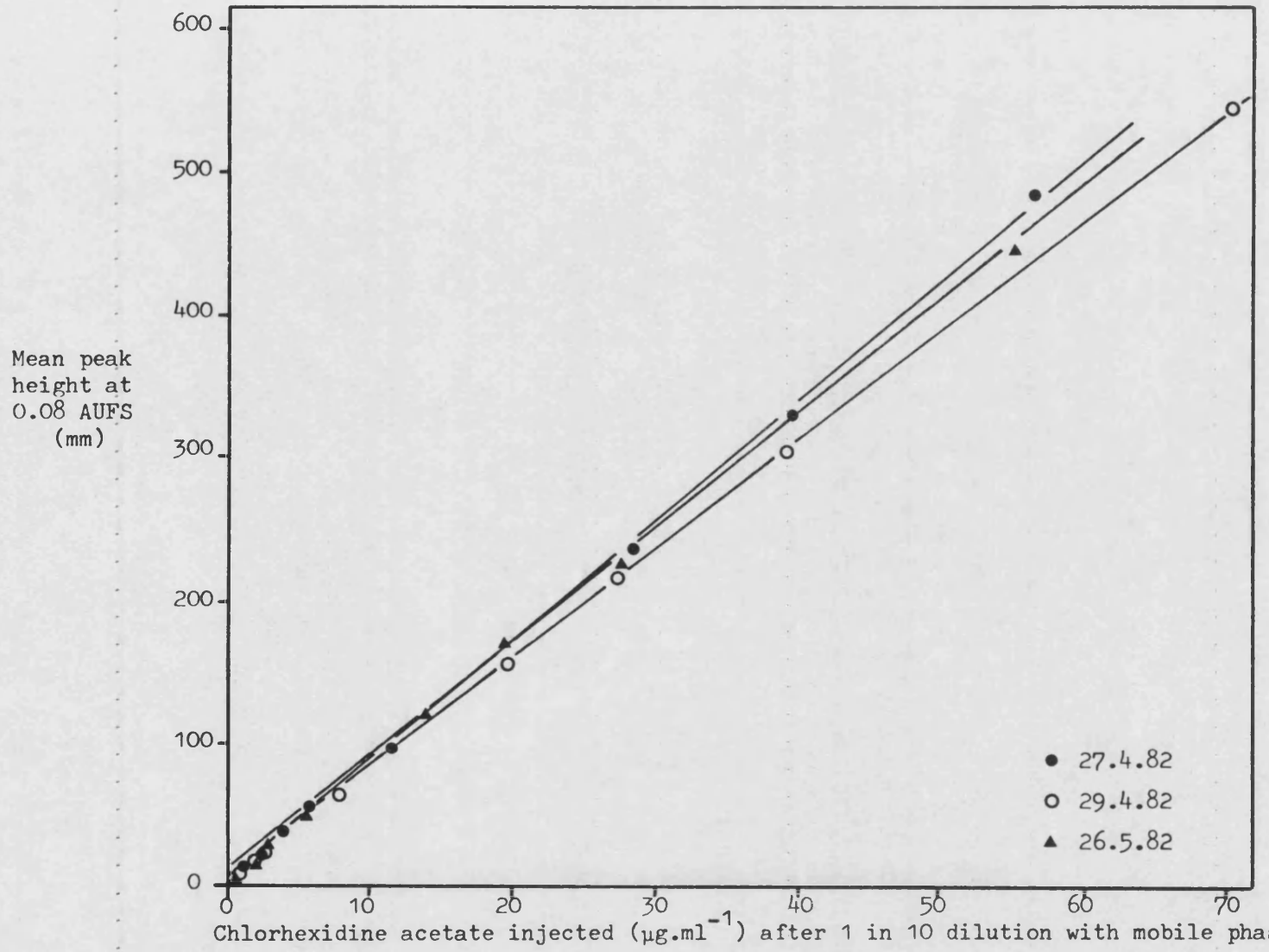

Figure 5.5 Calibration plots for chlorhexidine acetate solutions, prepared, serially diluted and injected on three different days

Multiple linear regression (Appendix 3) of the data indicated that the regressed slopes were all significantly different (F_{ratio} 27.77, F_{tab} 2.87, p = 0.05). Also examination of the statistical data for the intercepts of the three plots reveals the regressed slopes of solutions A and C pass through the origin (±2SD). However, the plot from solution B did not quite meet this criterion. Consequently calibration was performed daily (using three standard solutions) and a calibration plot constructed by regression analysis for that day's assays alone. The use of calibration plots for stability sample assay is discussed further when an example of a typical method of analysis is presented (see section 5.1.1.6). The same column was used throughout the study and although the slopes of calibration plots varied, column parameters (resolution, capacity factor) remained constant (see section 5.1.1.3.1).

5.1.1.2 Sample Preparation

It was considered important to develop a procedure for the preparation of standard and sample solutions which combined speed and ease of preparation without loss of reproducibility or precision. Because a range of concentrations were to be assayed it was considered advantageous to routinely prepare an aqueous stock standard solution which could be diluted appropriately before injection and assay. It was, therefore, necessary to investigate the effect of dilution on chromatographic response.

5.1.1.2.1 Effect of Dilution by Water

Injection of aqueous solutions of chlorhexidine resulted in an unresolved peak (Figure 5.6) mainly due to the large solvent response (solvent front) produced. This is a commonly observed phenomenon when using silica columns since small amounts of injected water easily disrupt the equilibria between mobile and stationary phases. Therefore the effects of dilution with mobile phase were examined.

5.1.1.2.2 Effect of Dilution by Mobile Phase

Initial experimentation showed that the maximum ratio of aqueous sample to mobile phase was 1 part made up to 5 parts ("a 1 in 5 dilution") respectively. The solvent front produced, although large, did not interfere with the chlorhexidine peak or any of its degradation products (Figure 5.7). A larger ratio of aqueous to mobile phase resulted in a significant loss in accuracy. Figure 5.8 illustrates the resultant chromatograms from 1 in 2, 1 in 3 and 1 in 4 dilutions, the amount of chlorhexidine injected on to the column being the same in each case.

Three calibration plots were generated by injection of (i) chlorhexidine acetate in mobile phase, (ii) after 1 in 10 dilution of aqueous standard solutions by mobile phase and (iii) after 1 in 5 dilution of aqueous standard solutions by mobile phase. This experiment was performed in order to determine whether the slopes produced by linear regression analysis were significantly different. Triplicate injections were made with the solutions randomised into a 4 x 4 Latin Square in order to make effective comparisons. The data generated, with mean peak height normalised to 0.08 AUFS, are given in Table 5.7.

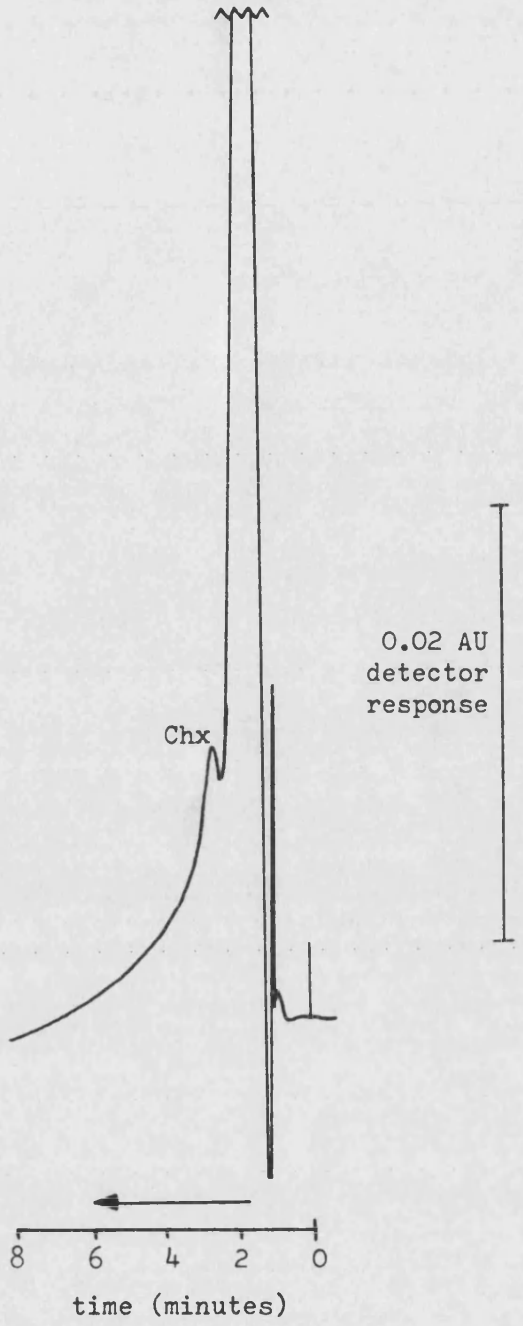

Figure 5.6 Injection of an aqueous solution of chlorhexidine gluconate (0.01% w/v) without prior dilution with mobile phase

Chx = chlorhexidine peak

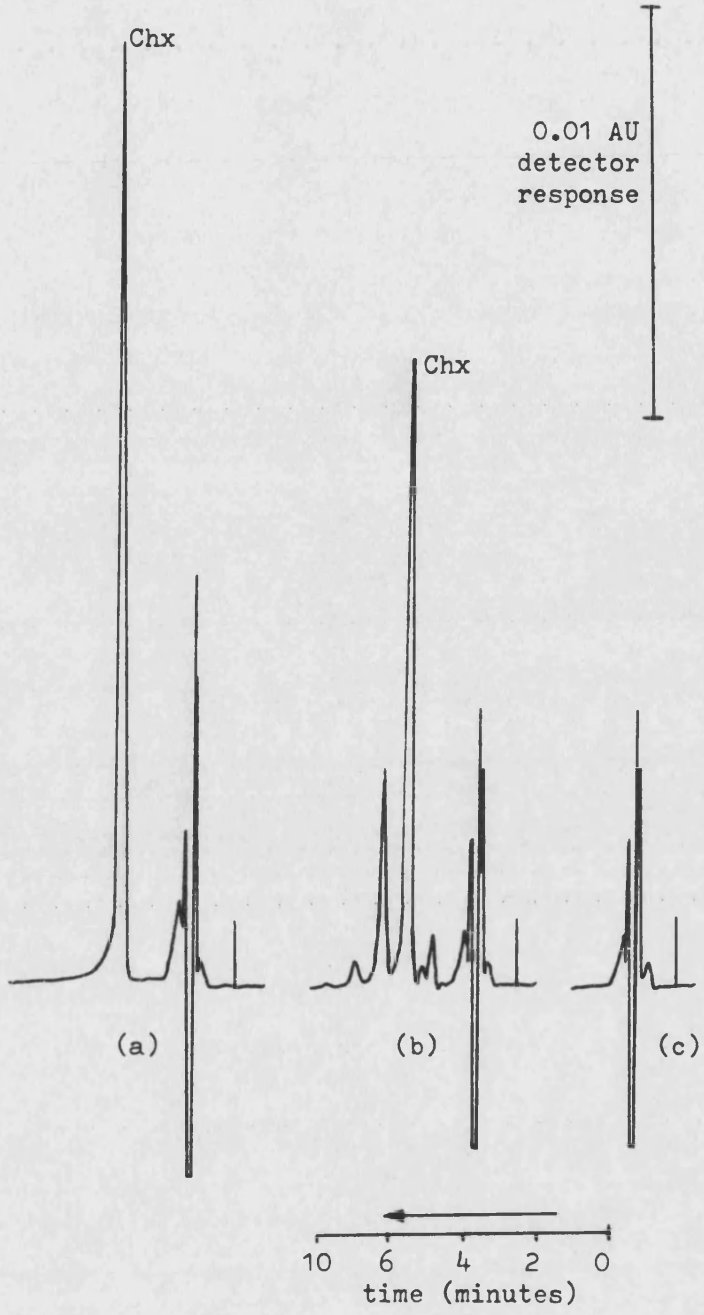

Figure 5.7 Chromatograms of 1 in 5 dilutions with mobile phase

(a) 1 part 0.002% w/v chlorhexidine gluconate to 5 parts with mobile phase
(b) 1 part degraded 0.002% w/v chlorhexidine gluconate to 5 parts with mobile phase
(c) 1 part water to 5 parts with mobile phase (producing typical solvent front)

Chx = chlorhexidine peak

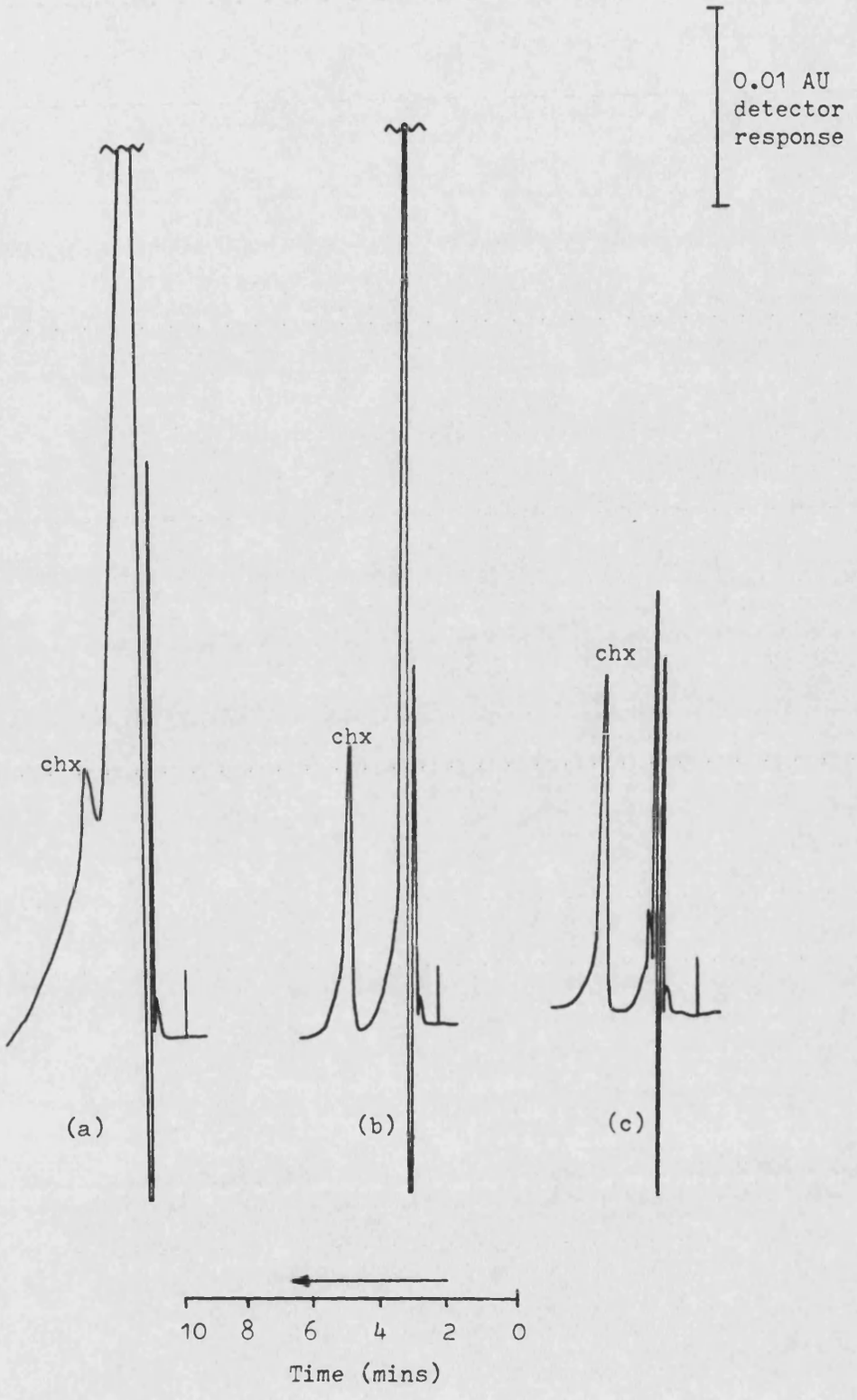

Figure 5.8 Injection of various mobile phase dilutions of 0.01% w/v chlorhexidine gluconate

(a) 1 in 2 dilution

(b) 1 in 3 dilution

(c) 1 in 4 dilution

	Chlorhexidine acetate dilution		
	Mobile phase	1 in 10	1 in 5
Concentration range ($\mu g.ml^{-1}$)	2.2-73	1.5-49	1.5-49
Regression analysis:			
Correlation coefficient	0.9999	0.9999	0.9999
Slope (SD)	7.908 (0.074)	7.962 (0.026)	7.752 (0.053)
Intercept (SD)	1.403 (2.669)	-0.548 (0.623)	-2.534 (1.259)
Relative standard deviation of slope	0.94%	0.33%	0.68%

Table 5.7 Effect of sample dilution on calibration plot data

Multiple linear regression of the data indicated that the regressed slopes are all significantly different (F_{ratio} 5.07, F_{tab} 3.63, $p = 0.05$). This meant that both standard and sample preparation had to be identical (i.e. either 1 in 10 or 1 in 5 but not mixed) in order to minimise the errors of external standardisation.

5.1.1.2.3 Effect of Stability Sample pH

Peak height response can often be dependent on the pH of an injected sample. Because samples of widely different pH were to be assayed it was important to determine the effect of sample pH differences in the establishment of a standard procedure.

The apparent pH of the neat mobile phase was determined as being approximately 0.8 (see Chapter 4.3.2). The effect of diluting aqueous chlorhexidine gluconate samples of identical concentration but different pH (by adjustment with 0.1 M HCl or 0.1 M NaOH) with mobile phase is listed in Table 5.8. Mean peak height response and retention times are also listed.

Initial aqueous sample pH (0.002% chlorhexidine gluconate)	1 in 10 dilution with mobile phase			1 in 5 dilution with mobile phase		
	pH	Peak height (mean in mm)	Retention time (minutes)	pH	Peak height (mean in mm)	Retention time (minutes)
4.00	1.44	137.0	3.15	1.56	137.0	3.17
5.00	1.44	138.0	3.17	1.57	137.0	3.17
6.00	1.44	138.0	3.15	1.58	137.0	3.17
7.00	1.45	137.5	3.15	1.60	137.5	3.18
8.00	1.47	138.5	3.17	1.61	137.0	3.17
9.00	1.47	138.0	3.17	1.61	138.0	3.15
10.00	1.48	138.0	3.17	1.63	137.5	3.18
Mean peak height (SD)		137.9 (0.5)			137.3 (0.4)	

Table 5.8 Effect of sample pH on chromatographic response

The variation in mean peak height response noted in Table 5.8 for identical concentrations at 1 in 5 and 1 in 10 dilution levels was expected and has been discussed in section 5.1.1.2.2. However it was apparent that the initial pH of the samples did not significantly influence the pH after dilution. The apparent pH of 1 in 5 and 1 in 10 dilutions were higher than that of neat mobile phase, this effect being simply due to the dilution of mobile phase acid strength rather than a direct influence of chlorhexidine on pH. Chromatographic analysis provided identical retention times and similar peak height response for each dilution level. Therefore the samples could be diluted by mobile phase without any preliminary adjustment to a particular pH.

5.1.1.2.4 Effect of Ionic Strength and Presence of Buffers or Surfactants

Problems were encountered in the assay of buffered chlorhexidine gluconate solutions, particularly when buffer

concentration was >0.05 Molar. Peak splitting was observed in all buffer systems used (see Chapter 6.6.7) but on an equimolar basis the peak splitting problems decreased in the order phosphate > acetate >> borate. Peak splitting observed in pH 4.0 acetate and pH 7.0 phosphate buffers is illustrated in Figures 5.9a and 5.10a respectively. Peak splitting was also observed when assaying chlorhexidine solutions at high ionic strength (>0.1 M) of counter ion (gluconate, acetate or chloride ions).

Preliminary dilution by double distilled water before dilution with mobile phase overcame the peak splitting problems and provided a resolved chlorhexidine peak with the usual retention characteristics. Figures 5.9b and 5.10b illustrate the effect of preliminary aqueous dilution to eliminate peak splitting in acetate and phosphate buffers. Typically, the preliminary dilution was 1 part buffered sample made up to 5 parts with double distilled water. However, this preliminary dilution required that the assays be performed on an increased detector sensitivity (0.002 AUFS). Baseline noise on this detector setting meant that the accuracy of peak height measurement was reduced to ±1 mm resulting in a ±1% error (maximum) in generated assay values. This was deemed acceptable considering the amount injected on to the column was only 8 ng chlorhexidine gluconate.

Surfactants were also present in some stability samples. At the concentrations used, CTAB 2×10^{-5} M to 2×10^{-2} M, Cetomacrogol 1000 1×10^{-6} M to 2×10^{-3} M and polysorbate 80 2×10^{-5} to 2×10^{-3} M, no disruption of retention characteristics were observed (Figure 5.11). Also the presence of surfactants did not affect generated assay data for chlorhexidine, peak height response being identical, with or without the presence of a surfactant (see Chapter 6.6.8).

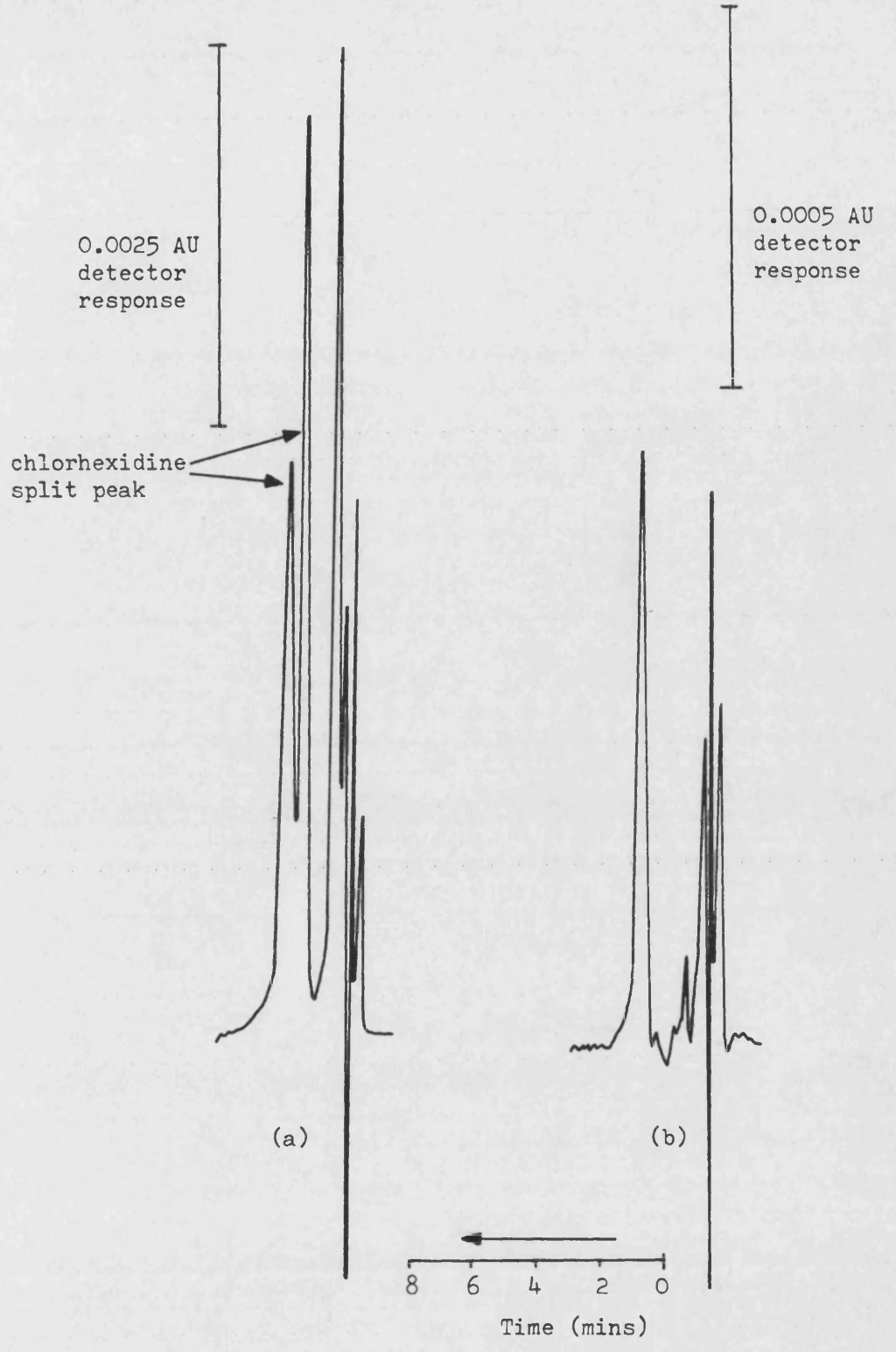

Figure 5.9 Chromatograms of 0.002% w/v chlorhexidine gluconate in pH 4.0 acetate buffer after:

(a) 2 in 10 dilution with mobile phase (showing split peak)

(b) preliminary 2 in 10 dilution with distilled water followed by 2 in 10 dilution with mobile phase

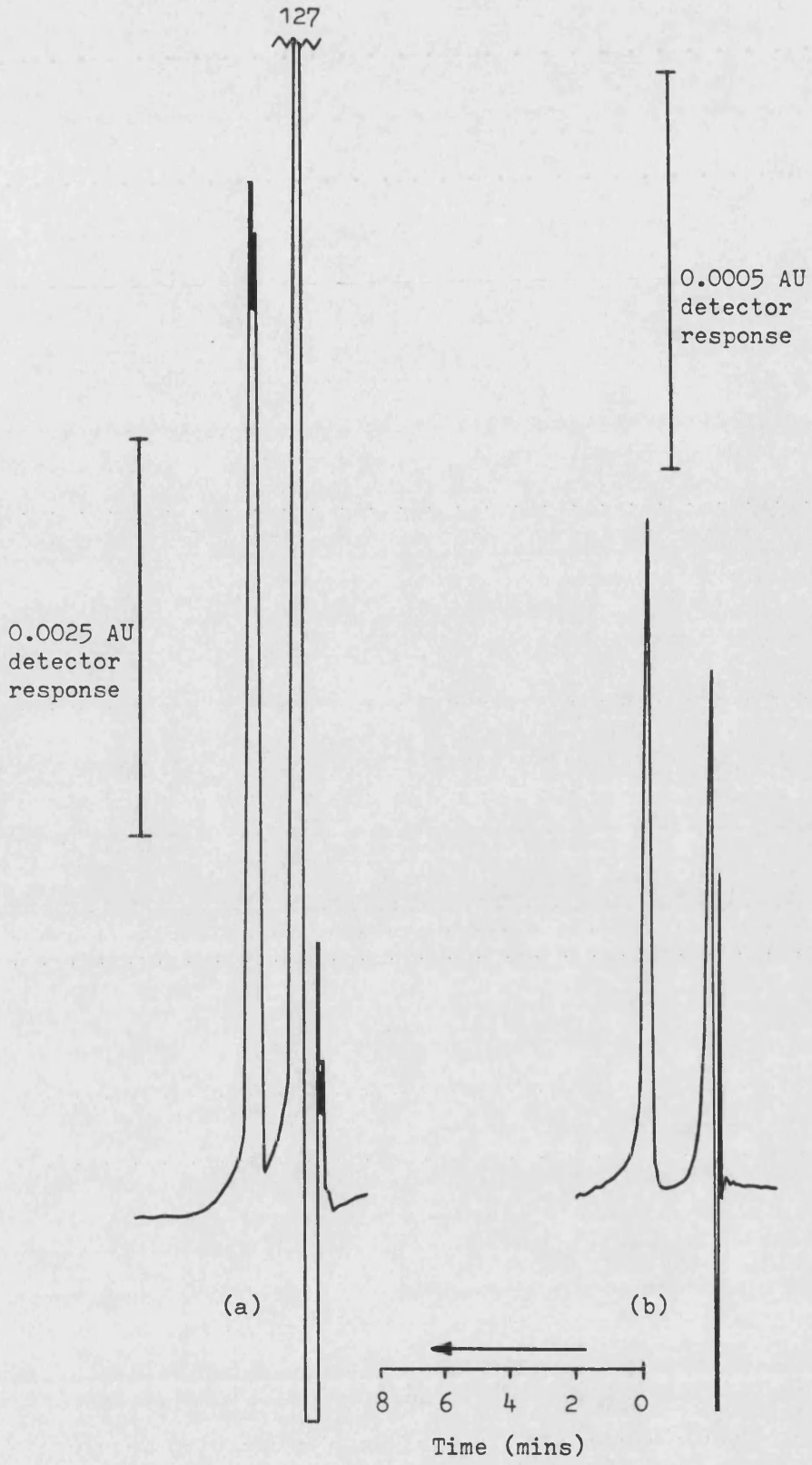

Figure 5.10 Chromatograms of 0.002% w/v chlorhexidine gluconate in pH 7.0 phosphate buffer after:

(a) 2 in 10 dilution with mobile phase (showing split peak)

(b) preliminary 2 in 10 dilution with distilled water followed by 2 in 10 dilution with mobile phase

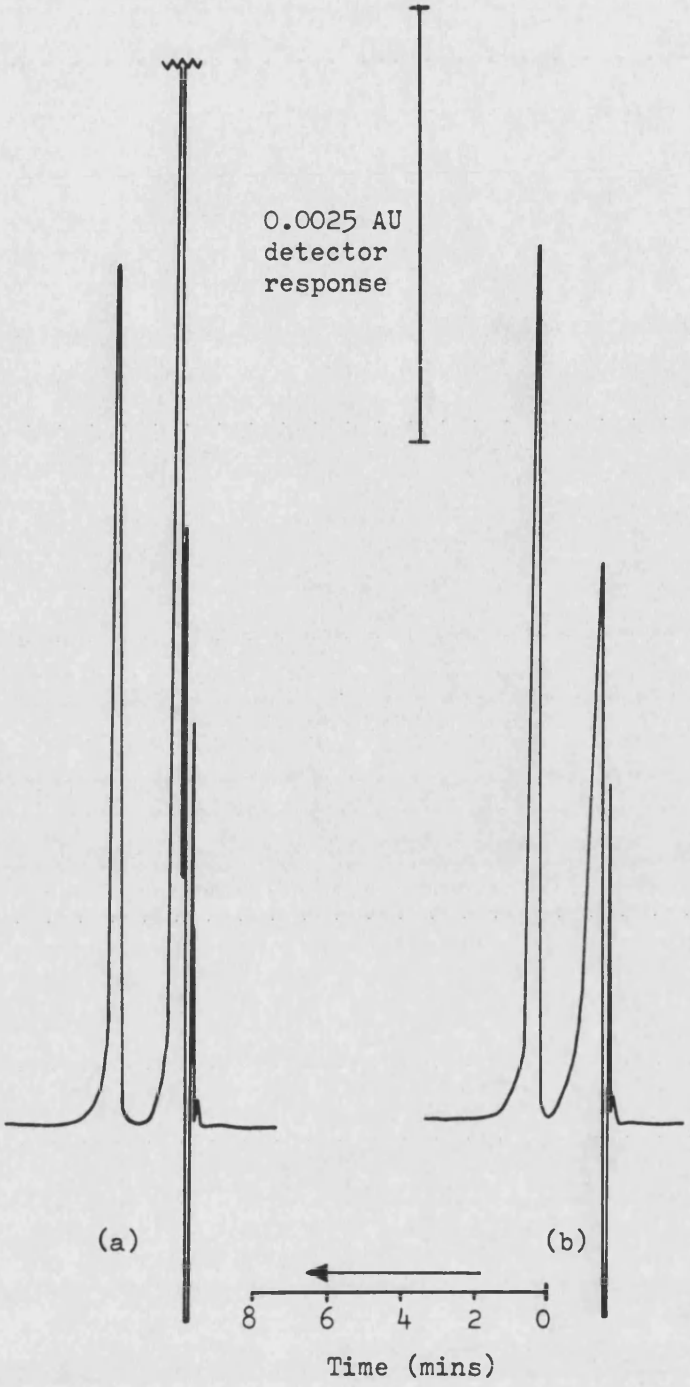

Figure 5.11 Effect of surfactants on chromatographic response. Injections made as 2 in 10 dilutions with mobile phase of 0.002% w/v chlorhexidine gluconate in:

(a) 2×10^{-2}M CTAB

(b) 2×10^{-3}M cetomacrogol 1000

5.1.1.3 Specificity for Chlorhexidine and its Degradation Products

5.1.1.3.1 Chlorhexidine

Figure 5.12 illustrates the resolution obtained between chlorhexidine and the solvent front. The shape of the solvent front obtained was dependent on the aqueous : organic ratio present in the injected sample (as previously discussed in section 5.1.1.2.2).

The resolution of chlorhexidine from its degradation products is shown in Figure 5.13 where the chromatograms from a typical stability run are presented (0.002% chlorhexidine gluconate degraded at pH 9 and 80°C). The chlorhexidine peaks remained sharp with no more tailing than that present in the initial sample. The resolution (equation 63) between chlorhexidine and its chromatographically nearest (and major) degradation product (D) was also calculated from the stability run illustrated in Figure 5.13. Resolution values obtained (Table 5.9) indicate adequate separation between the peaks of chlorhexidine and degradation product (D) (ideally $R > 1.5$). The tailing of the chlorhexidine peak did not allow accurate calculation of resolution above 95% residual chlorhexidine. From Figure 5.12, the column capacity factor, k^1, (equation 61) for chlorhexidine was calculated as 1.8 (optimum 1.5 to 4).

% Residual chlorhexidine gluconate (initial = 0.002% w/v)	Resolution value (R)
81.81	2.1
60.98	2.1
42.69	2.2
28.25	2.3

Table 5.9 Resolution values calculated for chlorhexidine and its nearest degradation product

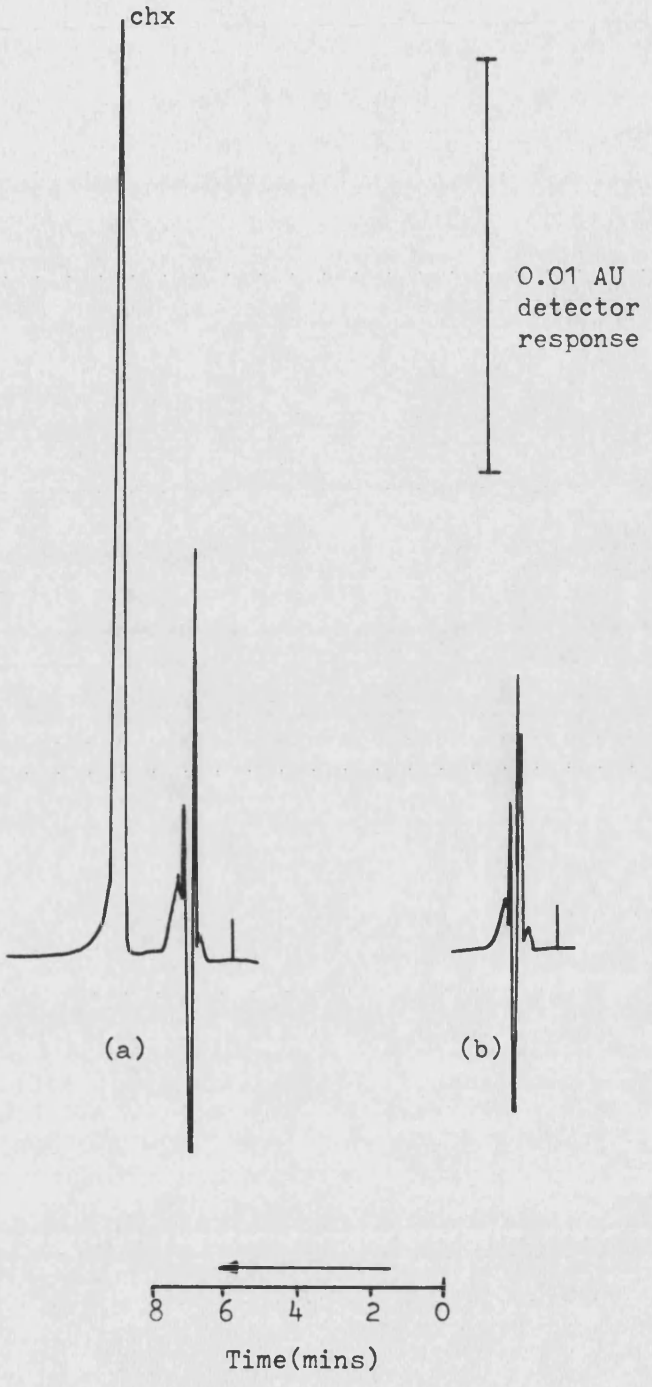

Figure 5.12 Chromatograms illustrating the normal solvent response and the resolution of chlorhexidine from the normal solvent response

(a) 0.002% w/v chlorhexidine gluconate

(b) distilled water

Both injections made as 2 in 10 dilutions with mobile phase

Figure 5.13 Chromatograms of initial (a) and degraded (b-e) chlorhexidine gluconate solutions after 2 in 10 dilution with mobile phase

(a) 100% residual (initial)

(b) 82% residual

(c) 61% residual

(d) 43% residual

(e) 28% residual

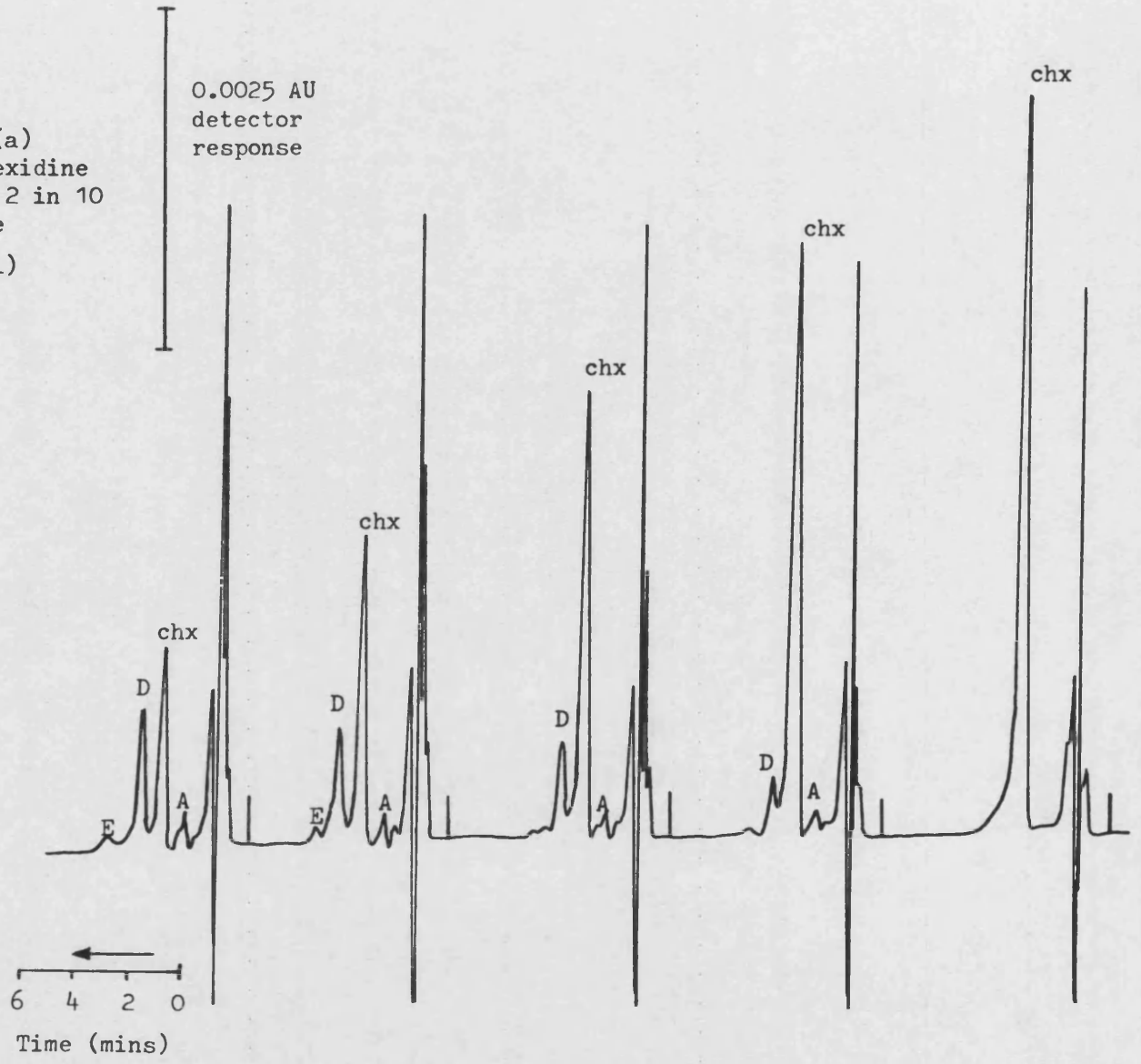

5.1.1.3.2 Degradation Products

Figure 5.13 also illustrates that the peaks of degradation products were well resolved but baseline separation was not apparent.

Studies with degraded chlorhexidine solutions were also undertaken in the Quality Control Department at ICI to establish the number and position of degradation products or impurities. Seven degradation products/impurities have been identified by ICI, all of which were resolved by the stability indicating HPLC method. The degradation products/impurities have been given an alphabetic nomenclature in order of retention time (listed in Table 5.10). The proposed structures of the degradation products are shown in Figure 8.5 with discussion in Chapter 8.

Degradation product/impurity	Retention time (minutes)
Alpha	2.20
A	2.82
Chlorhexidine	3.73
D	4.83
E	5.37
F	6.63
G	~7
H	~16

Table 5.10 Retention time and nomenclature of degradation products/impurities

Figure 5.14 illustrates a degraded chlorhexidine system (ICI source, degradation conditions unknown) with six degradation products apparent. Injection was made in mobile phase thus eliminating the usually large aqueous solvent front produced. Degradation studies presented in this thesis have regularly produced five degradation products α, A, D, E and G as illustrated in Figure 5.15 which also illustrates the normal solvent front.

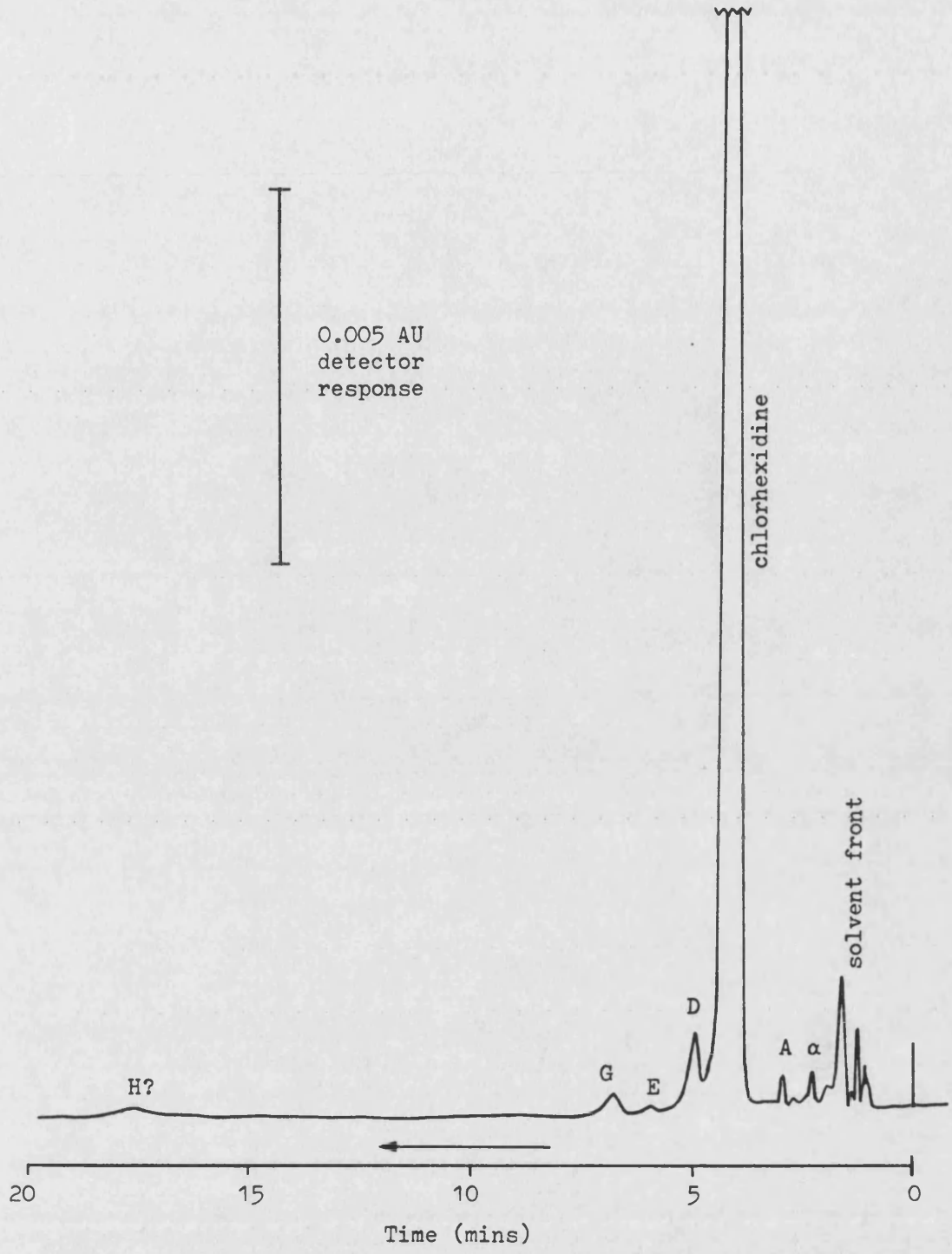

Figure 5.14 Injection made in mobile phase of a degraded chlorhexidine solution illustrating six degradation products/impurities (α, A, D, E, G and H). HPLC analysis was performed at ICI Pharmaceuticals (degradation conditions unknown)

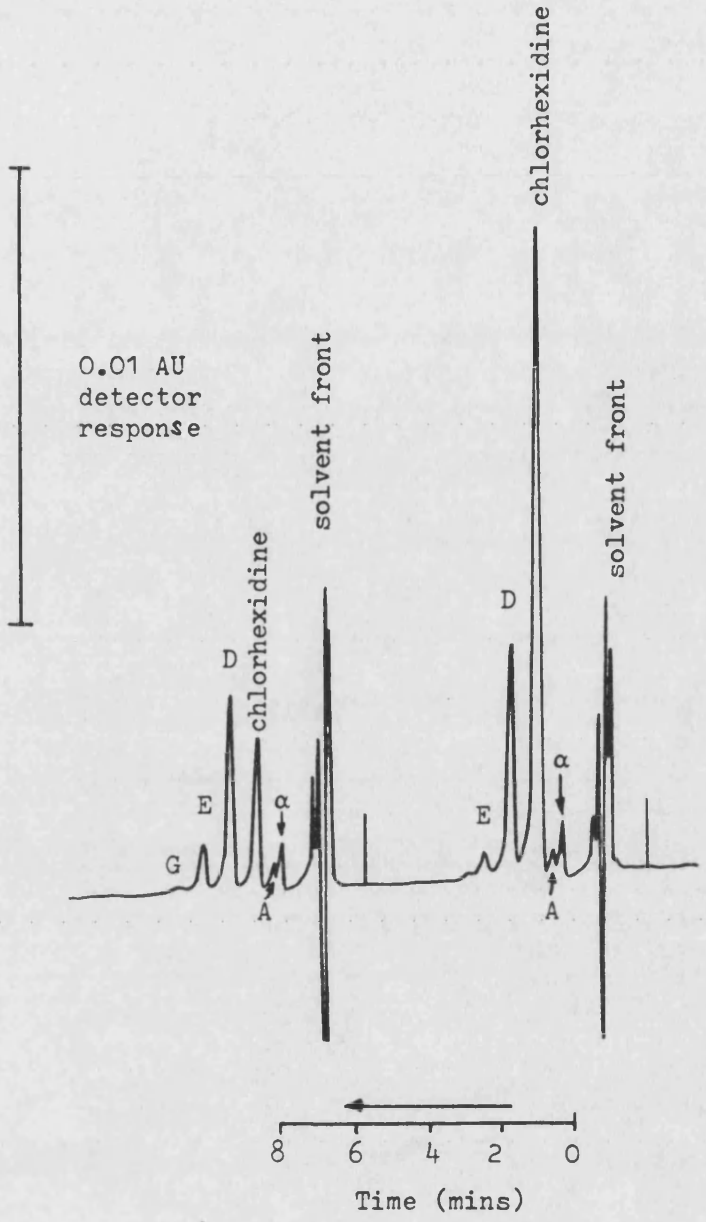

Figure 5.15 Chromatograms of typically degraded chlorhexidine gluconate solutions illustrating five degradation products (0.01%, 90°C at pH 9.0)

Chromatograms were also examined at wavelengths other than 254 nm. This experimentation was performed in order to determine whether the degradation products had a λ_{max} significantly different to 254 nm and to identify whether any degradation products were undetected at this wavelength.

A degraded chlorhexidine gluconate solution showing three degradation products (A, D and E) by assay at 254 nm was examined at wavelengths between 220-290 nm. The chromatograms produced are shown in Figures 5.16 and 5.17. No change in the ratio of chlorhexidine peak height to its major degradation product (D) peak height was observed. Apart from intensity differences, the similarity of each chromatogram indicated that other degradation products were not present.

5.1.1.4 Reproducibility

5.1.1.4.1 Injection

The reproducibility of manual injection was determined by making repeated injections of chlorhexidine acetate standard solutions. Four different concentrations were used with the final dilution being 1 in 10 with mobile phase (except the 1.621 $\mu g.ml^{-1}$ solution which was produced by a 1 in 5 dilution). Figures 5.18 and 5.19 illustrate the chromatograms obtained for the 1.621 $\mu g.ml^{-1}$ and 5.904 $\mu g.ml^{-1}$ standard solutions respectively. The results from statistical treatment of all data are presented in Table 5.11.

	Injected chlorhexidine acetate concentration ($\mu g.ml^{-1}$)			
	1.621	5.904	13.47	34.61
Detector sensitivity (AUFS)	0.01	0.04	0.08	0.16
Number of injections	8	8	14	8
Mean peak height (mm) (SD)	125.25 (1.91)	104.75 (1.07)	113.36 (0.91)	149.25 (0.60)
Coefficient of variation	1.52%	1.02%	0.90%	0.40%

Table 5.11 Statistical data for reproducibility of sample injection

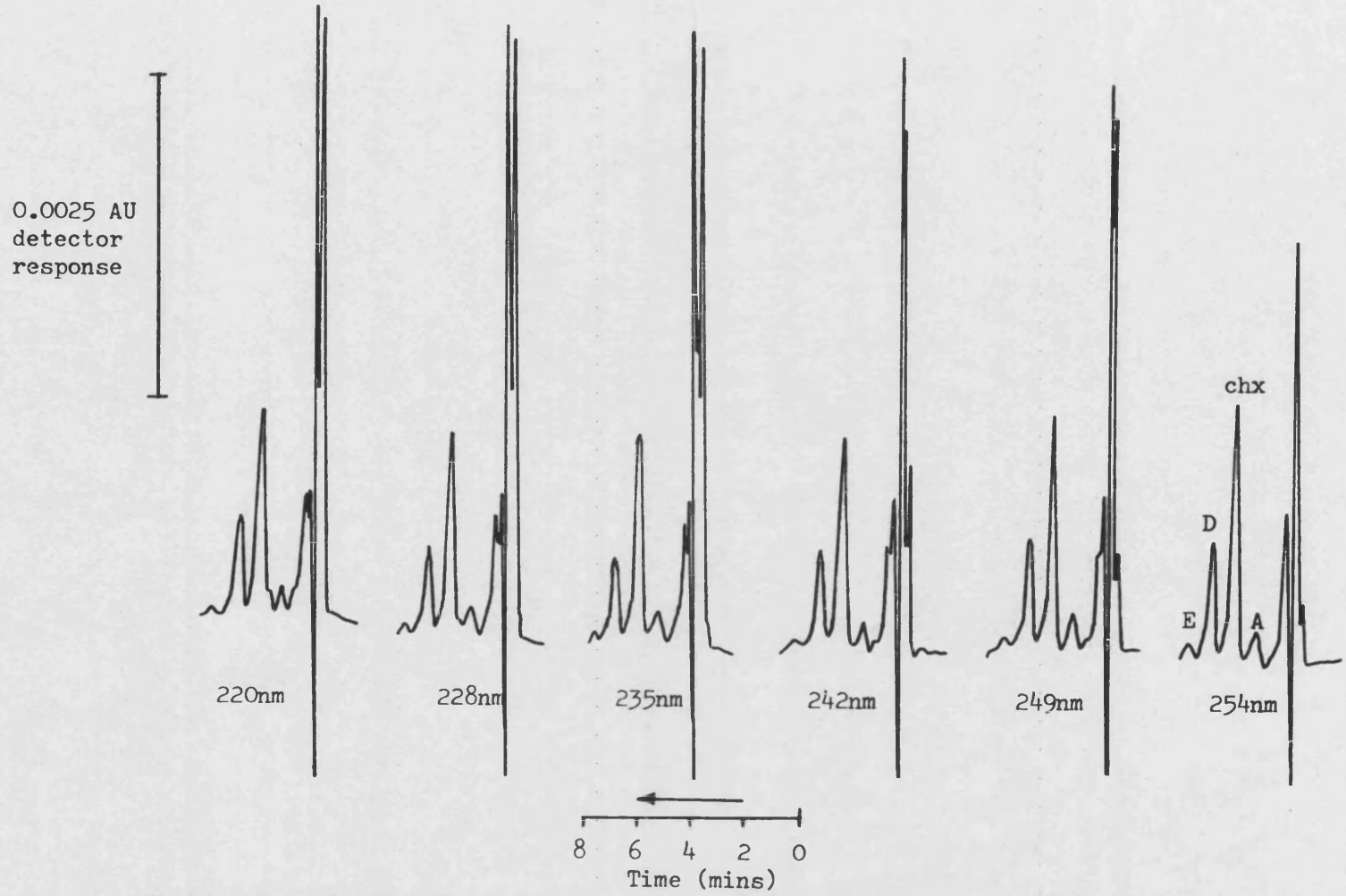

Figure 5.16 Chromatograms of a degraded chlorhexidine gluconate solution analysed at various detector wavelengths below 254nm

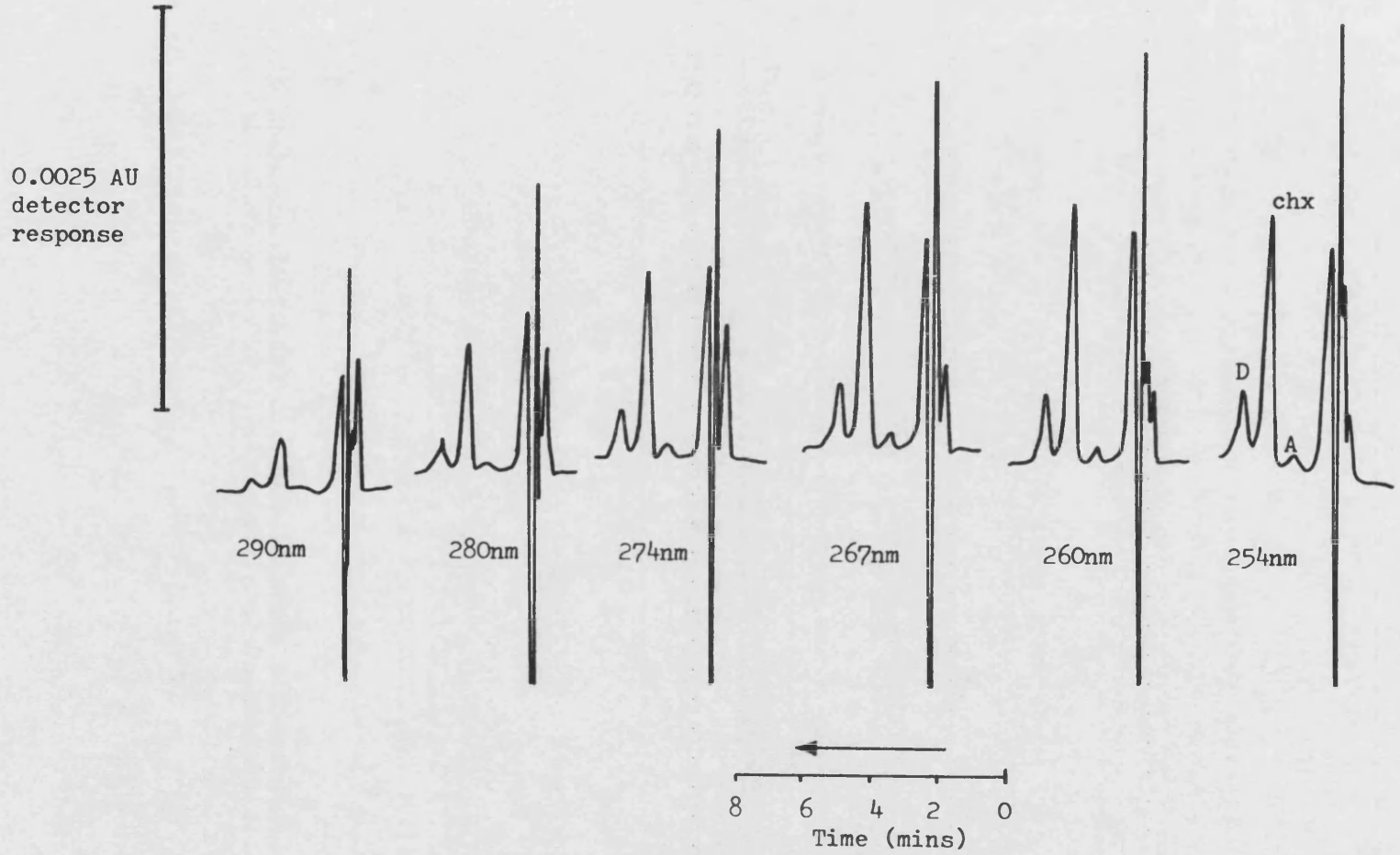

Figure 5.17 Chromatograms of a degraded chlorhexidine gluconate solution analysed at various detector wavelengths above 254nm

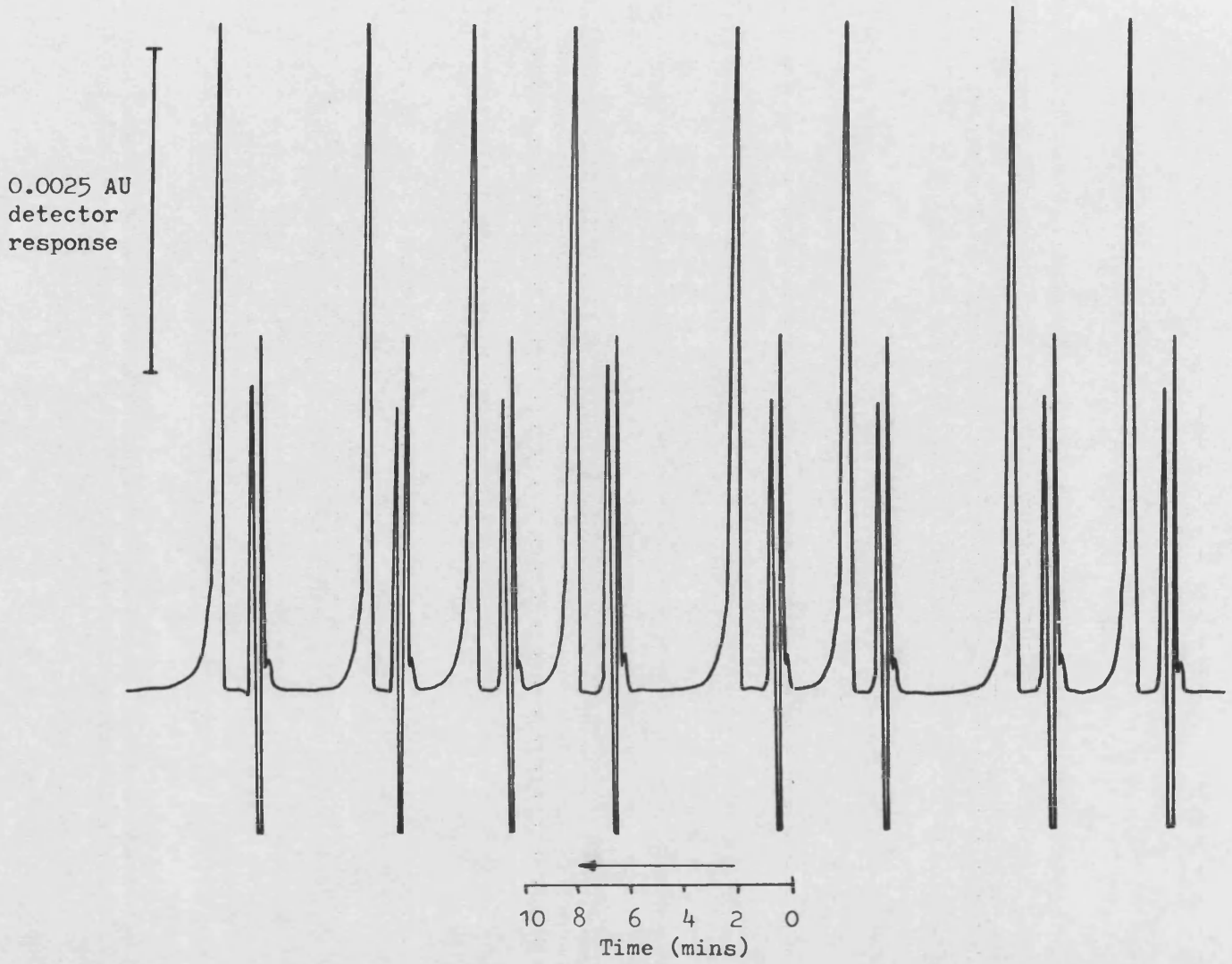

Figure 5.18 Chromatogram showing reproducibility of sample injection using a 1.621μg.ml^{-1} chlorhexidine acetate standard solution (after 2 in 10 dilution with mobile phase)

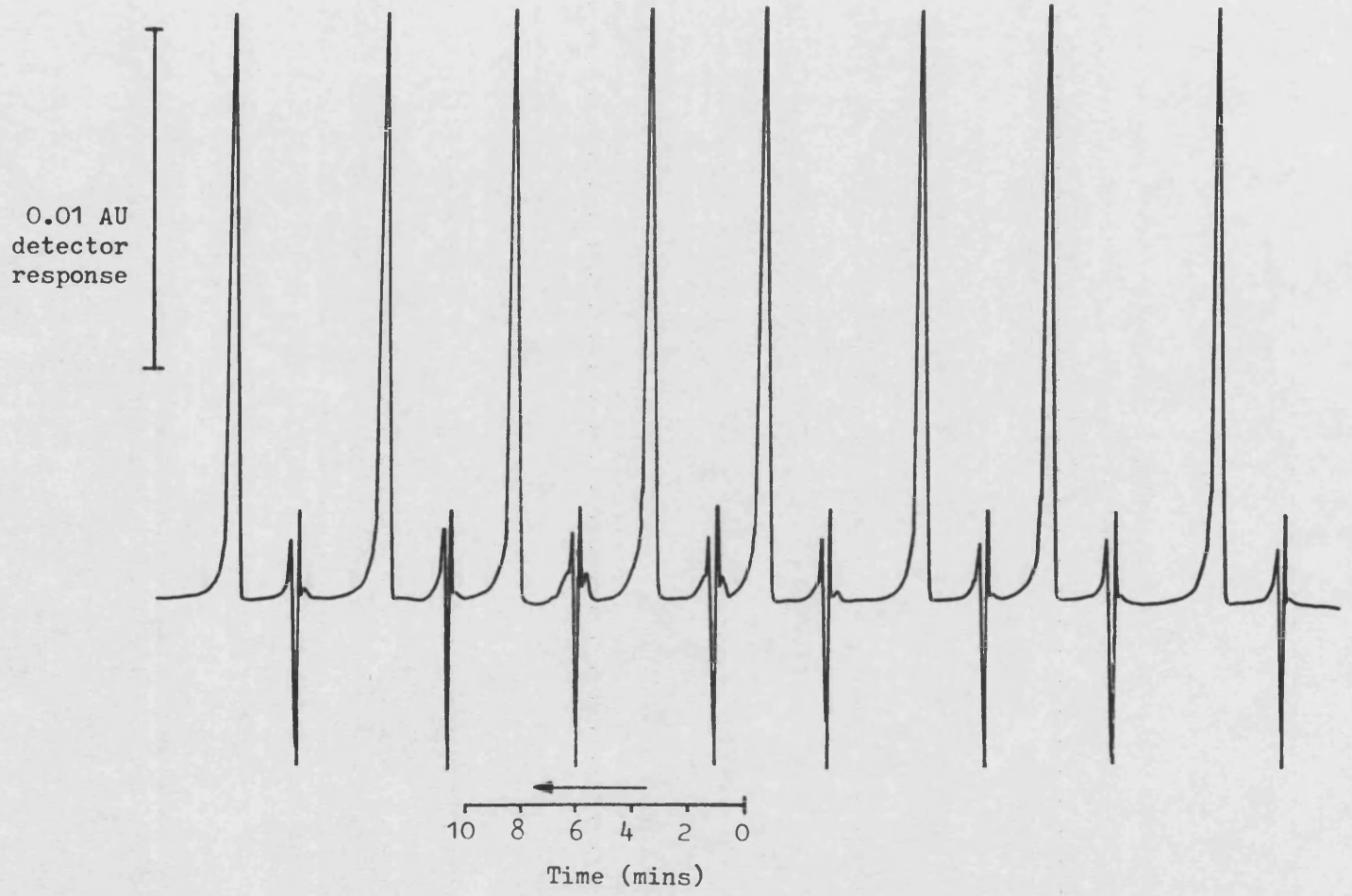

Figure 5.19 Chromatogram showing reproducibility of sample injection using a 5.904μg.ml^{-1} chlorhexidine acetate standard solution (after 1 in 10 dilution with mobile phase)

Although the coefficient of variation increases with decreasing chlorhexidine acetate concentration reproducibility was considered very good. It must also be noted that peak height measurements were made manually by a ruler, therefore the accuracy of determination was always ±0.25 mm. Given this constraint the data presented in Table 5.10 illustrates excellent reproducibility of manual injection.

The reproducibility of automated injection by the ACS Autosampler (air actuated Rheodyne valve) was also determined. Two standard solutions were prepared at the concentrations 1.732 $\mu g.ml^{-1}$ (after a 1 in 5 final dilution with mobile phase) and 8.66 $\mu g.ml^{-1}$ (after a 1 in 10 final dilution with mobile phase). The statistical data for autosampler injection reproducibility are presented in Table 5.12. Slight improvement in reproducibility was observed compared with manual injection.

	Injected chlorhexidine acetate concentration ($\mu g.ml^{-1}$)	
	1.732	8.66
Detector sensitivity (AUFS)	0.01	0.04
Number of injections	10	10
Mean peak height (mm) (SD)	146.85 (1.29)	164.15 (0.85)
Coefficient of variation	0.88%	0.52%

Table 5.12 Statistical data for reproducibility of autosampler injection

5.1.1.4.2 Sample Preparation

The reproducibility of sample preparation was determined at two concentrations of chlorhexidine acetate injected : 1.706 $\mu g.ml^{-1}$ (detector sensitivity 0.01 AUFS) and 9.359 $\mu g.ml^{-1}$ (0.04 AUFS). At the lower concentration two equivalent standard solutions (samples 1 and 2)

were prepared by a 2 in 10 dilution of the same stock solution. At the higher concentration two equivalent standard solutions (samples 3 and 4) were prepared by a 1 in 10 dilution of a different stock solution. Each standard solution was then assayed in quadruplicate and the data generated is presented in Table 5.13.

Standard solution concentration ($\mu g.ml^{-1}$)	Individual peak height response (mm)				Statistical data		
	1	2	3	4	Mean	Standard deviation	Coefficient of variation
1.706 (sample 1)	141.0	142.0	142.0	142.5	141.9	0.63	0.44%
1.706 (sample 2)	139.0	138.0	138.0	139.0	138.5	0.58	0.42%
9.359 (sample 3)	176.0	176.0	175.0	177.0	176.0	0.82	0.46%
9.359 (sample 4)	177.0	177.0	178.0	178.0	177.5	0.58	0.33%

Table 5.13 Experimental data for the reproducibility of sample preparation

A 't' test was applied to the low concentration data giving a t value of 7.94 (t_{tab} = 2.45, p = 0.05). This shows that the mean peak height response of sample 1 is significantly different from that of sample 2. However, it is pertinent to examine the tolerance or delivery error of the analytical glassware used. For example, the tolerance of a Grade A 10 ml volumetric flask is ±0.02 ml and the delivery error of Grade A 1 and 2 ml pipettes is ±0.01 ml (Beckett and Stenlake, 1962). Therefore the quoted nominal concentration obtained by a 1 in 10 or 2 in 10 dilution may vary between 98.8 and 101.2% (i.e. ±1.2% error). Adjustment of sample 1 and 2 peak height data, assuming the flasks were at their maximum tolerance, would result in a t value of 0.066 (t_{tab} 2.45, p = 0.05). This illustrated that within the limits of the glassware used no significant difference existed between the peak height response of samples 1 and 2. A 't' test was also

applied to the higher concentration data (samlpes 3 and 4) giving a t value of 2.99 (t_{tab} 2.45, p = 0.05). Similar tolerance arguments produce a t value of 1.21 which shows no significant difference between the peak height responses of samples 3 and 4.

5.1.1.4.3 Overall Error

The overall error of the assay method was a combination of three factors already discussed (peak height measurement, glassware, reproducibility) and calibration plot error. However to add these errors together seriously overestimates the likely overall error. A more statistically valid method (Saunders and Fleming, 1971) is to use the formula (equation 66):

$$\text{Overall error} = \sqrt{X^2 + Y^2 + Z^2} \qquad \ldots\ (66)$$

where X, Y, and Z are the individual errors of a particular method or experiment.

Table 5.14 provides an illustration of the overall error for the assay of a 0.002% w/v chlorhexidine gluconate solution (typical peak height at 0.01 AUFS = 150 mm). Injection errors were calculated from confidence limits (p = 0.99, see Appendix 4) and the two extreme values for manual and automatic injection used (from Tables 5.11 and 5.12 respectively). The confidence limit (p = 0.99) for calibration plot error was taken from the data in Table 5.15.

Error source		Value
Measurement (±0.25 mm)		± 0.2%
Glassware		± 1.2%
Injection reproducibility	- manual	± 1.7%
	- automatic	± 0.8%
Calibration plot		± 2.2%
Overall error	- manual	± 3.0%
	- automatic	± 2.6%

Table 5.14 Individual and overall errors of HPLC assay method

The calculated overall errors assume that all data were accepted. In practice, erroneous data (i.e. anomalous peak heights) were detected and the assay repeated. The practical overall error may be taken from initial assay values for chlorhexidine degradation experiments (Chapter 6). Comparison of the theoretical initial concentration with the assayed initial concentration was always <±2% (this data also contains an additional glassware tolerance error).

5.1.1.5 Sensitivity

The limit of reliable, qualitative detection of chlorhexidine was considered to be a peak height of 10 mm at 0.001 AUFS. This corresponds to an injected chlorhexidine gluconate concentration of approximately 4×10^{-6} % w/v or to 0.45 ng chlorhexidine gluconate.

For accurate quantitation a value of ten times the above was considered as the limit of quantitative detection, i.e. 4×10^{-5}% w/v or 4.5 ng chlorhexidine gluconate. At this limit baseline noise could produce a 2 mm error in peak height measurement equivalent to a 4% error in generated assay values. However, this sensitivity was never required since the lowest assayed concentration in degradation studies was 8×10^{-5}% w/v chlorhexidine gluconate, double the quantitative detection limit.

5.1.1.6 Typical Method of Analysis

An example of standard preparation, calibration and stability sample assay for a 0.002 % w/v chlorhexidine gluconate solution degraded at pH 9.0 and 90°C follows. This procedure was identical for higher concentrations, except for different concentration calculations and a final 1 in 10 dilution with mobile phase.

5.1.1.6.1 Standard Preparation

Aqueous solutions of approximately 1 $mg.ml^{-1}$ chlorhexidine acetate reference standard were accurately prepared each week. Stock solutions were stored in a refrigerator and used for one week only. Subsequent aqueous dilutions were made until a 1 in 5 dilution with mobile phase achieved three standard solutions of approximately 3, 2 and 0.8 $\mu g.ml^{-1}$. These solutions were calculated to be approximately equivalent to 1 in 5 dilutions of 0.0022, 0.0014 and 0.0006% w/v chlorhexidine gluconate respectively and therefore provide a calibration plot between 30-110% initial concentration of a nominal 0.002% w/v solution.

5.1.1.6.2 Calibration

The three standard solutions prepared were injected in duplicate at the start and end of each day's HPLC assays. Duplicate injections of the standard solutions were also interspersed with the stability samples throughout the day. The peak height data generated were used to construct a calibration plot for that day's assays, as illustrated in Table 5.15.

The data were examined to detect differences between column response at the start and end of each day's assays. A significant difference was considered to be a ±1.0% change in slope value. If no significant difference occurred all data were regressed and slope and intercept data used to calculate stability sample concentrations from peak height measurement. If the individual slope values showed a greater than ±1.0% change then the day's stability sample assays were repeated against a fresh set of standard solutions and the "not greater than ±1.0%" criterion applied to the new data.

Standard concentration ($\mu g.ml^{-1}$)		Mean peak height (mm)	Regression analysis	
Start of day	0.772	44.5	Correlation coefficient	0.9985
	2.059	112.75	Slope (SD)	57.844 (3.206)
	3.089	179.0	Intercept (SD)	-2.062 (7.018)
			Relative SD of slope	5.54%
Interspersed throughout day	0.772	45.0	Correlation coefficient	0.9981
	2.059	113.0	Slope (SD)	58.250 (3.606)
	3.089	180.5	Intercept (SD)	-2.113 (7.893)
			Relative SD of slope	6.19%
End of day	0.772	44.0	Correlation coefficient	0.9987
	2.059	113.0	Slope (SD)	58.075 (2.972)
	3.089	179.0	Intercept (SD)	-2.601 (6.505)
			Relative SD of slope	5.12%
All data			Correlation coefficient	0.9984
			Slope (SD)	58.056 (1.247)
			Intercept (SD)	-2.259 (2.730)
			Relative SD of slope	2.15%

Table 5.15 Calibration plot data for a typical day's analysis

Multiple linear regression analysis of the data presented in Table 5.15 indicated that the regressed slopes were not significantly different (F_{ratio} 0.013, F_{tab} 9.12, $p = 0.05$). This evidence provides some validation of the "not greater than ± 1%" criterion.

5.1.1.6.3 Stability Sample Assays

After 1 in 5 dilution with mobile phase the samples from degradation runs were assayed in duplicate. From the regressed slope of all data in Table 5.15 the mean peak height obtained was converted to chlorhexidine acetate concentration. Multiplication by 1.435 converts the acetate concentration into gluconate concentration (%w/v). Table 5.16 shows a typical set of data.

Sample (time in hours)	Mean peak height (mm)	Equivalent to chx acetate ($\mu g.ml^{-1}$)	Equivalent to chx gluconate (x 1.435 x 5 (dilution factor) (%w/v x 10^3)	% Residual
0 (initial)	165.75	2.894	2.076	100
0.5	149.0	2.605	1.869	90.03
1.75	125.5	2.201	1.579	76.06
2.5	110.5	1.942	1.394	67.15
3	103.25	1.817	1.304	62.81
4	88.75	1.568	1.125	54.19
4.5	81.0	1.434	1.029	49.57
5	75.25	1.335	0.958	46.15
5.5	68.0	1.210	0.868	41.81

Table 5.16 Example of calculations involved to produce a typical set of stability data

5.1.2 COLORIMETRIC

5.1.2.1 Introduction

A colorimetric assay method for chlorhexidine previously described by Holbrook (1958) has subsequently been used by many other workers as a general assay method for chlorhexidine (Heard and Ashworth, 1968; MacKeen and Green, 1978; Plaut *et al*, 1980 and Richardson *et al*, 1977; 1980).

The method relies on the formation of a colour complex between chlorhexidine and sodium hypobromite. The exact mechanism is not properly understood but probably involves ring compound formation. Subsequent conjugation to the benzene ring of the 4-chlorophenyl group results in absorption at 480 nm (Bailey, ICI Pharmaceuticals, 1986, Personal Communication).

5.1.2.2 Method

5 to 15 ml (depending upon the extent of degradation) of a 0.002% w/v chlorhexidine gluconate solution were placed in a 25 ml volumetric flask and 5 ml of a 20% w/v cetrimide solution added together with 1 ml of isopropanol to suppress frothing. 2 ml of alkaline sodium hypobromite, prepared according to the method of Holbrook (1958) which had previously been assayed and accurately diluted to give 1.0% available bromine, was then added and the solution made up to 25 ml. The solution was placed in a water bath at 25°C and left for exactly 25 minutes when its absorbance was determined in a 4 cm cell at 480 nm against a blank solution prepared as above but omitting chlorhexidine.

Chlorhexidine gluconate content was determined by reference to a calibration plot (absorbance at 480 mm against molar chlorhexidine concentration) prepared as described above with known amounts of chlorhexidine acetate reference standard.

5.1.2.3 Validity of Assay Method

Preliminary investigations of the method indicated calibration plots to be linear and reproducible. Experimental and linear regression analysis data from two typical calibration plots are presented in Table 5.17. Plots of molar chlorhexidine acetate against absorbance at 480 nm (4 cm cells) for each calibration are shown in Figure 5.20, the slopes being drawn from linear regression analysis. Different stock solutions of alkaline sodium hypobromite (1.0% available bromine) were used for the above two calibration plots leading to the observed difference (3.3%) between the slopes. However a 't' test showed this difference was not significant. To minimise errors, calibration plots were always performed at the same time as stability sample assay.

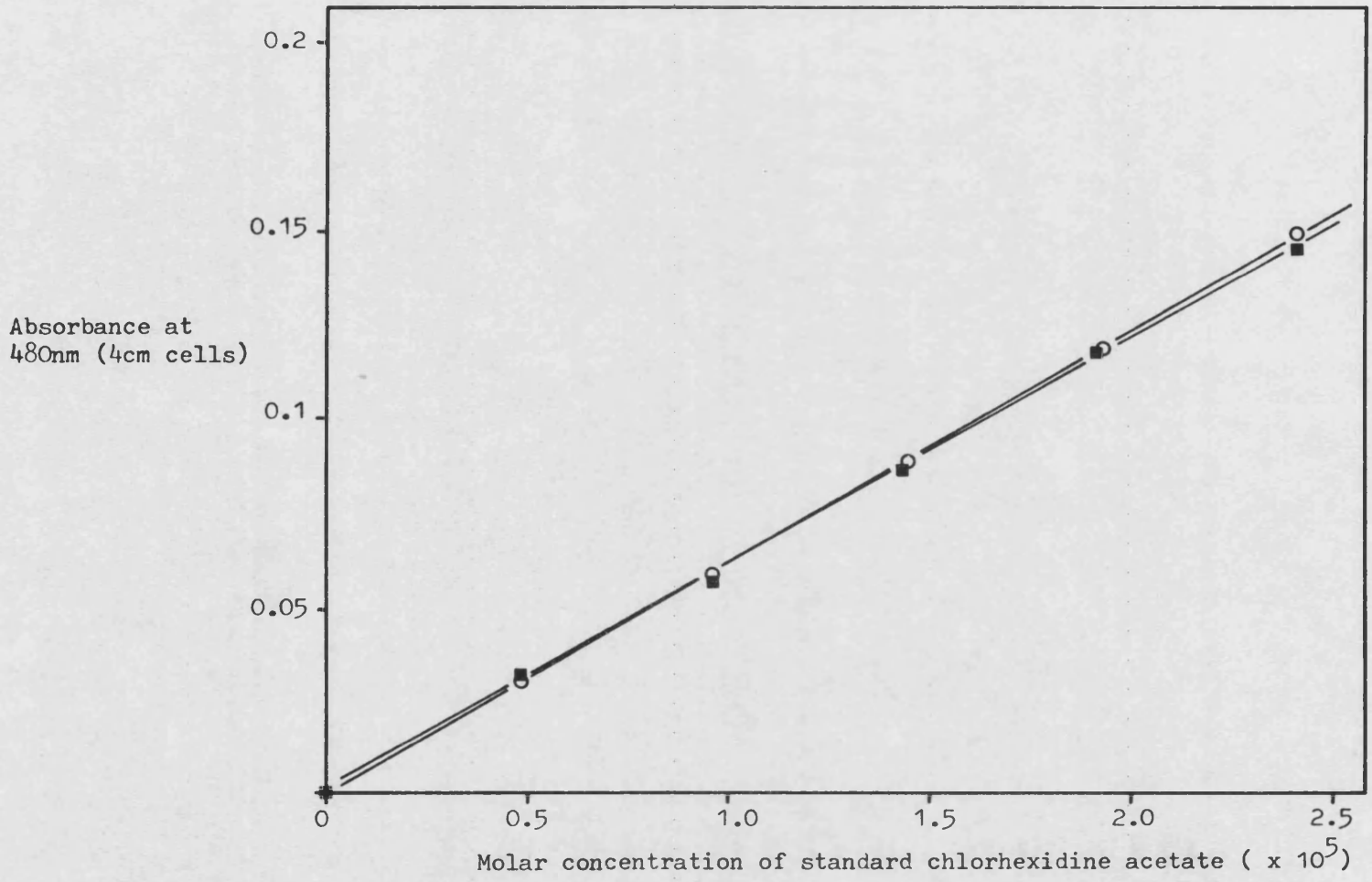

Figure 5.20 Two calibration plots of absorbance against standard chlorhexidine acetate concentration (Holbrook assay method)

Chlorhexidine acetate standard concentration (molarity x 10^3)	Absorbance at 480 mm (4 cm cells)	
	Calibration 1	Calibration 2
0.482	0.030	0.031
0.964	0.058	0.056
1.446	0.088	0.087
1.928	0.119	0.119
2.410	0.150	0.145
Regression analysis: Correlation coefficient	0.9998	0.9991
Slope (SD)	6244.8 (74.8)	6037.3 (147.2)
Intercept (SD)	-0.0013 (0.0012)	0.0003 (0.0024)
Relative SD of slope	1.2%	2.4%
't' test on slopes	$t_{slope} = 1.26$, $t_{tab} = 2.45$, $p = 0.05$	

Table 5.17 Experimental data for linearity and reproducibility of chlorhexidine colorimetric assay

The specificity of the assay method for chlorhexidine was more thoroughly examined with reference to the HPLC method. In order to form a colour complex hypobromite reacts with part or whole of the biguanide moiety in the chlorhexidine molecule. Therefore, degradation products which also contain the same reactive groups will also form a colour complex and assay as chlorhexidine thus underestimating the extent of degradation.

Samples were taken from a stability run of 0.002% w/v chlorhexidine gluconate at pH 9.0 and 80°C and assayed by the stability indicating HPLC method and by the colorimetric method. The results are listed in Table 5.18 and clearly indicate that the colorimetric method overestimates the residual chlorhexidine.

Sample (hrs)	HPLC Assay			Colorimetric Assay		
	Chlorhexidine gluconate ($\%w/v \times 10^3$)	% residual	% degraded	Chlorhexidine gluconate ($\%w/v \times 10^3$)	% residual	% degraded
0 (initial)	2.020	100	0	2.058	100	0
3	1.858	91.96	8.04	1.969	95.69	4.31
5	1.678	83.08	16.92	1.913	92.96	7.04
7.5	1.501	74.33	25.67	1.790	86.96	13.04
22	0.782	38.70	61.30	1.258	61.12	38.88
30	0.575	28.49	71.51	1.136	55.20	44.80
45.5	0.407	20.17	79.83	0.966	46.92	53.08

Table 5.18 Comparison of assay data generated by HPLC and colorimetric methods

It is interesting to compare the data expressed as percent degraded by each assay method. The extent of degradation detected by the colorimetric method was approximately half that observed by the HPLC method. This evidence supports the theory that one half of the chlorhexidine molecule may remain intact during the degradation cascade of reactions. Whilst the HPLC assay separates degradation products, the colorimetric assay responds to an undegraded biguanide group and assays this as half a chlorhexidine molecule. Therefore the extent of degradation is likely to be half that observed by the HPLC method. Pawelczyk and Plotkowiak (1976) have also concluded that the colorimetric assay method should not be used as a quantitative stability indicating method for chlorhexidine.

The degradative reaction mechanism is discussed further in Chapter 8.

5.1.3 THIN-LAYER AND PAPER CHROMATOGRAPHY

In order to provide supportive evidence that the HPLC method was stability indicating (i.e. its ability to resolve chlorhexidine

from all its degradation products) additional chromatographic techniques were employed. Solutions investigated were:

(i) 0.05% w/v chlorhexidine gluconate

(ii) 0.001% w/v 4-chloroaniline

(iii) 0.002% w/v chlorhexidine gluconate degraded at pH 9.0, 80°C to approximately 60% residual

(iv) as (iii) to approximately 30% residual

Because of the trace amounts of degradation products present in solutions (iii) and (iv) the solutions were concentrated by use of a rotary evaporator to an equivalent chlorhexidine gluconate concentration of 0.1 - 0.05% w/v.

Initially a thin-layer chromatographic (TLC) method for nitrogenous bases was performed according to Clarke (1975):

plates : silica gel GF_{254} (Whatman)
samples : acidified by addition of glacial acetic acid
solvent : strong ammonia solution : methanol (1.5:100)
development: ascending, run time 30 minutes
location : u.v. light (254 nm)
Dragendorff reagent spray
iodine-carbon tetrachloride spray.

However, poor resolution between chlorhexidine and its degradation products was obtained.

The British Pharmacopoeia (1980) TLC method for the detection of related substances (chlorhexidine acetate monograph) was therefore used in order to detect degradation products:

plates : silica gel GF_{254} (Whatman)
samples : acidified by glacial acetic acid
solvent : chloroform : ethanol : formic acid (50:50:7)
development: ascending, run time 30 minutes
location : u.v. light (254 nm)
Dragendorff reagent spray

The resultant chromatogram is illustrated in Figure 5.21, 4-chloroaniline responding to Dragendorff's reagent whilst chlorhexidine and its degradation products were visible under u.v. light. Although

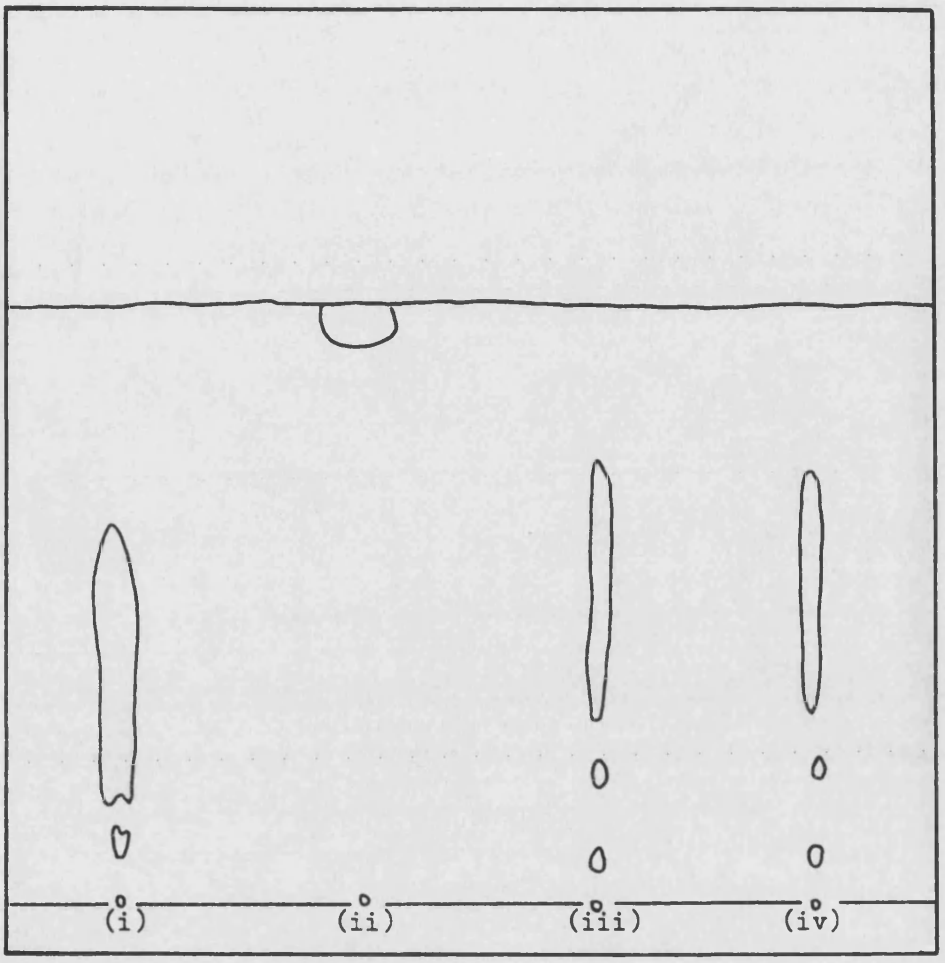

Figure 5.21 Thin-layer chromatogram of:

(i) 0.05% w/v chlorhexidine gluconate

(ii) 0.001% w/v 4-chloroaniline

(iii) 0.002% w/v chlorhexidine gluconate degraded to ~60% residual

(iv) 0.002% w/v chlorhexidine gluconate degraded to ~30% residual

Spots (iii) and (iv) applied as x50 concentrates

the chromatogram illustrated differences between the degraded samples (iii and iv) and chlorhexidine gluconate alone (i) it was difficult to determine the number of degradation products resolved. Also chlorhexidine itself was not resolved into a single band but produced a streak.

Attention was then given to the paper chromatographic system of Pawelczyk and Plotkowiak (1976) since these workers reported detection of five degradation products/impurities by their method:

paper : Whatman Number 3
samples : acidified by glacial acetic acid, or applied without prior treatment
solvent : isopropanol : glacial acetic acid : water : chloroform : acetone (10:1:3:5:2)
development: ascending, run time 20 hours
location : u.v. light (254 nm)
Dragendorff reagent spray

After developing, viewing under u.v. light and spraying with Dragendorff's reagent produced the chromatogram illustrated in Figure 5.22. Calculation of Rf values allows a comparison to be made with Pawelczyk and Plotkowiak's observations (Table 5.19).

	Rf values	
	Observed	Pawelczyk and Plotkowiak (1976)
chlorhexidine	0.66, 0.70, 0.62	0.70
4-chloroaniline	1.0	1.0
degradation product (DP1)	0.21, 0.22	0.20
degradation product		0.25
degradation product (DP2)	0.51, 0.53	0.55
degradation product		0.60

Table 5.19 Paper chromatographic retention (Rf) values for chlorhexidine and resolved degradation products

Without direct reference to the chromatograms obtained by Pawelczyk and Plotkowiak it was difficult to compare the two sets of data comprehensively. However, one major difference was due to the use

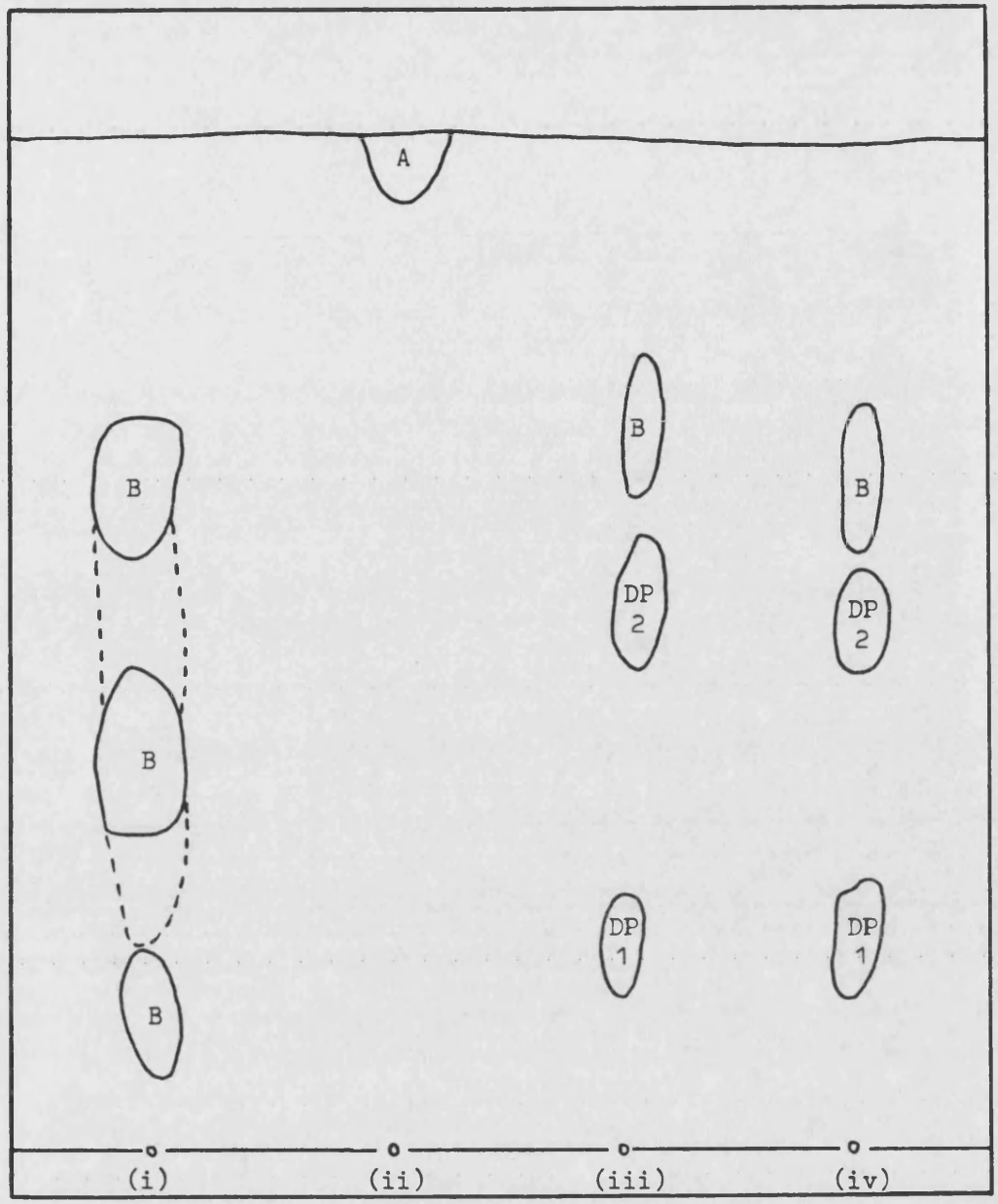

Figure 5.22 Paper chromatogram of:

(i) 0.05% w/v chlorhexidine gluconate

(ii) 0.001% w/v 4-chloroaniline

(iii) 0.002% w/v chlorhexidine gluconate degraded to ~60% residual

(iv) 0.002% w/v chlorhexidine gluconate degraded to ~30% residual

Spots (iii) and (iv) applied as x50 concentrates

A - 4-chloroaniline, R_f 1.0

B - chlorhexidine streak although three areas of greater concentration apparent

DP1 - degradation product R_f 0.21-0.22

DP2 - degradation product R_f 0.51-0.53

of a 0.27% w/v chlorhexidine gluconate solution by the Polish workers in their degradation and paper chromatography studies. Consequently, degradation products were present at higher concentrations than those produced in these studies, even after concentration by rotary evaporation. These workers also state that their degradation products with Rf values 0.20 and 0.25 were only produced after prolonged heating of chlorhexidine gluconate solutions.

The paper chromatogram illustrated in Figure 5.22 shows a streaked chlorhexidine spot (in common with previous TLC observations). The degraded solutions (iii and iv) clearly show three separate spots, one corresponding to residual chlorhexidine (Rf 0.62 to 0.70). The other two spots correspond to degradation products (DP1 and DP2) with Rf values of 0.21 - 0.22 and 0.51 - 0.53 respectively. These values are very similar to Pawelczyk and Plotkowiak's two sets of two spots (0.20 and 0.25; 0.55 and 0.60). Whether the latter are separately resolved spots or streaks of the same compounds remains unclear without additional chromatographic evidence.

The paper chromatograms of chlorhexidine gluconate and degraded solutions did not show any detectable 4-chloroaniline.

The paper chromatographic studies performed indicate that certainly two, or possibly four, degradation products were produced in heat stressed chlorhexidine gluconate solutions. The stability indicating HPLC method also identified the presence of four degradation products in the degraded sample containing 30% residual chlorhexidine (iv). However, the HPLC method is much more sensitive to degradation products, being able to detect them in only partially degraded dilute solution (i.e. 80-90% residual, 0.002% w/v chlorhexidine gluconate).

Further evidence of the validity of the HPLC method is its ability to resolve a total of seven degradation products (see section 5.1.1.3).

5.2 4-CHLOROANILINE

5.2.1 Introduction

4-Chloroaniline may be present in chlorhexidine preparations as a manufacturing impurity or it may result from chlorhexidine hydrolysis (Goodall et al, 1968). The British Pharmacopoeia (1980) imposes a "not greater than standard" of 500 ppm 4-chloroaniline in its chlorhexidine monographs (i.e. <500 µg 4-chloroaniline per gram of chlorhexidine acetate or hydrochloride and <500 µg 4-chloroaniline per 5 millilitres of chlorhexidine gluconate (20% w/v) solution). However, in aqueous solution the content of 4-chloroaniline has been shown to increase, particularly when heated (Dolby et al, 1972; Foster, 1965; Goodall et al, 1968; Jaminet et al, 1970 and Polack, 1967). For this reason it was considered important to validate an assay method for 4-chloroaniline in order to determine its presence in degraded chlorhexidine solutions.

5.2.2 HPLC

100 ml of 0.002% w/v chlorhexidine gluconate solution was "spiked" by the addition of 0.5 µg 4-chloroaniline and assayed by the stability indicating HPLC method. By comparison with an unspiked solution it was possible to determine an extra peak eluting shortly after the solvent front (Figure 5.23). Close inspection of the chromatograms of degraded chlorhexidine gluconate solutions (Figure 5.15) also reveals an extra solvent front peak which may be 4-chloroaniline. Although other HPLC assays for 4-chloroaniline were available in the literature (Perez, 1981 and Richard et al, 1984),

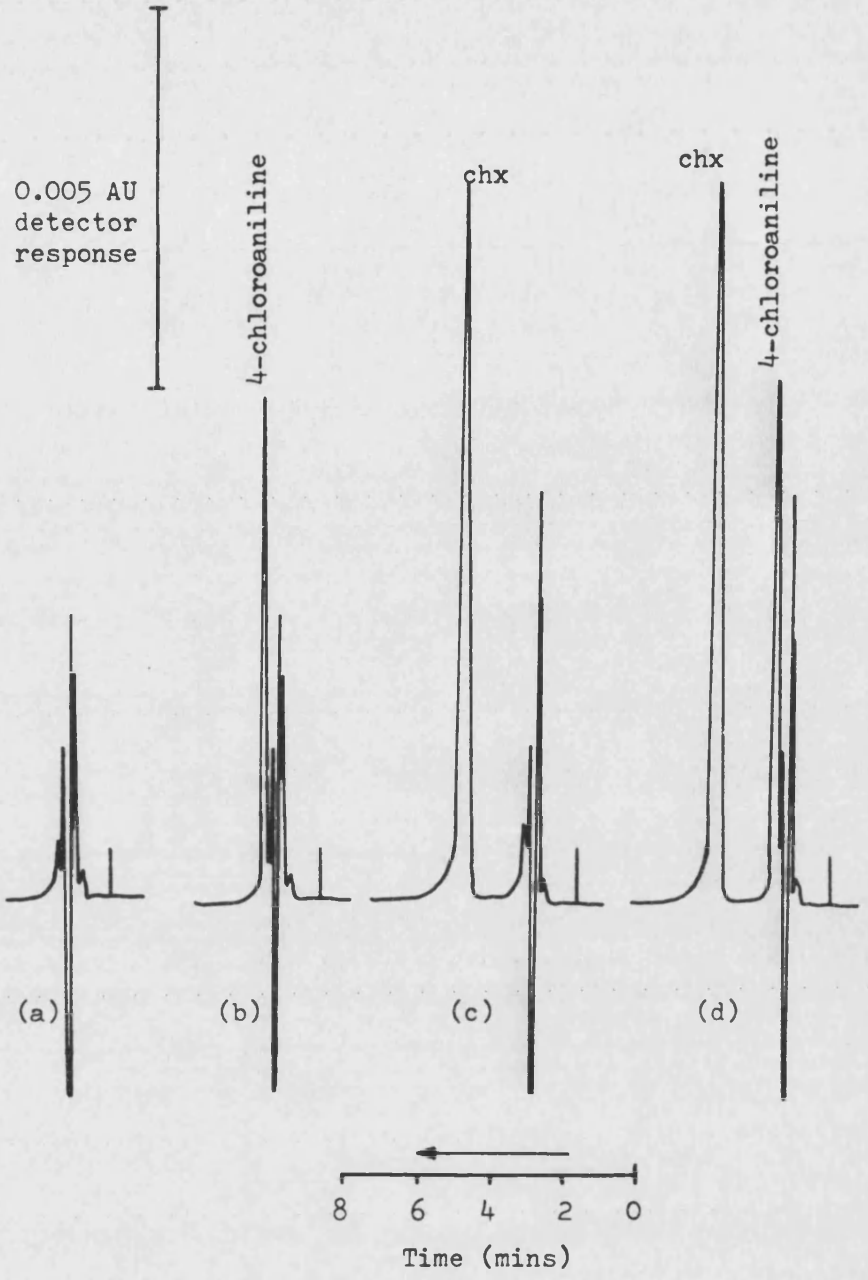

Figure 5.23 Chromatograms illustrating the presence of 4-chloroaniline

(a) distilled water

(b) 0.0005% w/v 4-chloroaniline

(c) 0.002% w/v chlorhexidine gluconate

(d) 0.002% w/v chlorhexidine gluconate and 0.0005% w/v 4-chloroaniline

All injections made as 2 in 10 dilutions with mobile phase

resources were not available to provide a second HPLC system for concomitant determination of 4-chloroaniline. A colorimetric method was therefore used.

5.2.3 Colorimetric

A colorimetric assay for 4-chloroaniline was performed by a method modified by Goodall et al (1968) from that of Bratton and Marshall (1939). This method involves the diazotisation of 4-chloroaniline by nitrous acid, the resultant diazonium salt is then coupled to produce a dye and assayed spectrophotometrically.

The reaction is as follows:

(i) Diazotisation

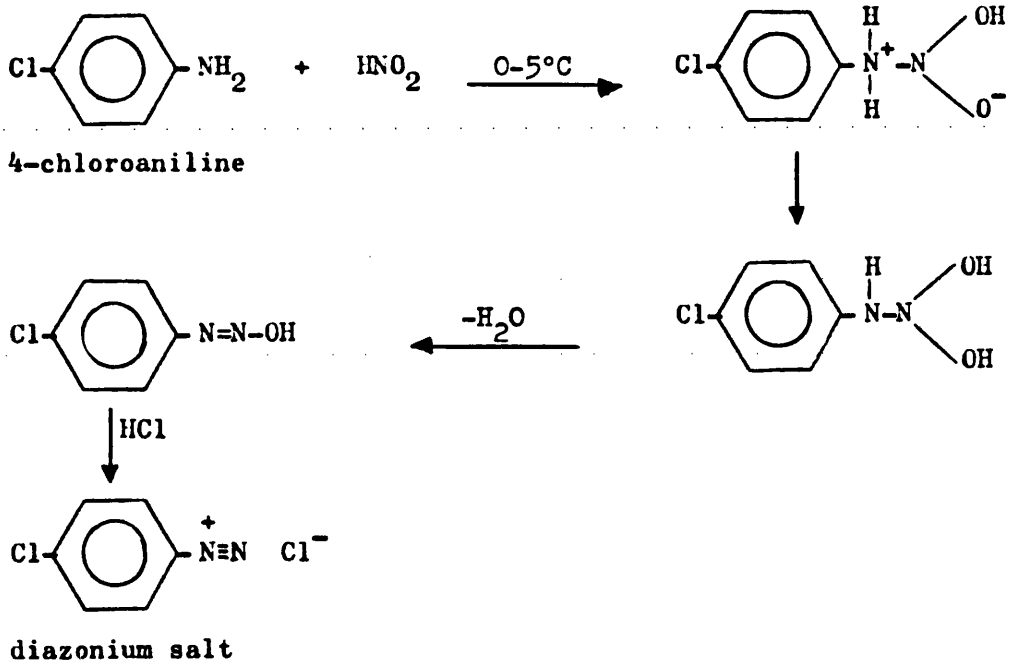

(ii) Dye coupling

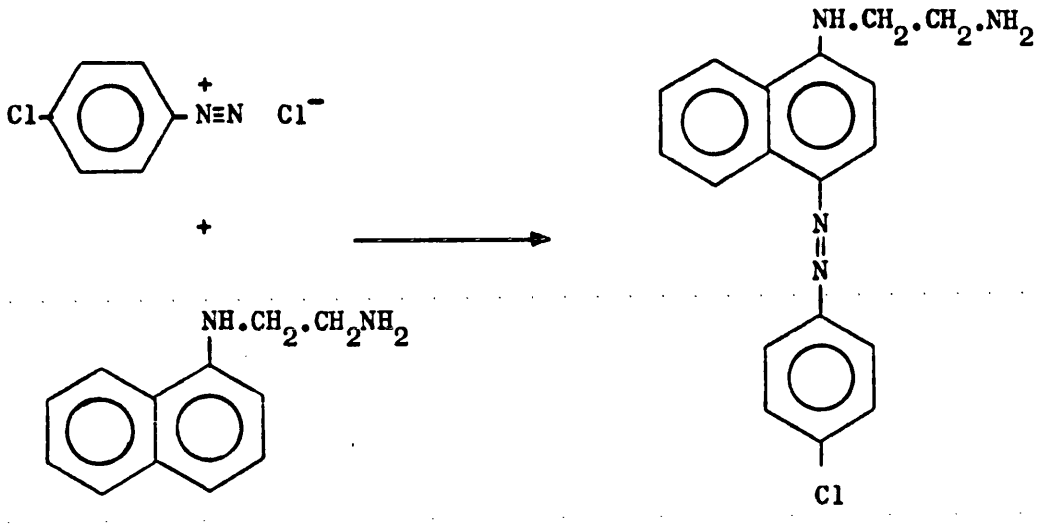

The method described by Goodall et al (1968) has been used by Dolby et al (1972) and Jaminet et al (1970) as a stability indicating method for chlorhexidine, i.e. residual chlorhexidine was calculated directly from increases in 4-chloroaniline content.

However, diazotisation reactions should always take place at low temperatures (0-5°C) due to the instability of the diazonium salt formed. Workers following the Goodall et al (1968) method all use ambient temperatures for diazotisation and may therefore underestimate 4-chloroaniline content in aqueous chlorhexidine solutions.

5.2.3.1 Method

The method of Goodall et al (1968) was performed but produced variable results due to very poor calibration plots. This was undoubtably due to the instability of the diazonium salt at ambient temperatures. Therefore the method was slightly modified as follows:

15 to 20 ml of sample were placed in a 25 ml volumetric flask and 1 ml of 1 M hydrochloric acid added. The flask was then placed in an ice bath at 0-5°C and the following procedure performed at this temperature. 0.5 ml of a 3.5% w/v sodium nitrite solution was added to diazotise the 4-chloroaniline. After one minute, 1 ml of 5% w/v ammonium sulphonate solution was added to neutralise any excess nitrous acid. After 5 minutes 2.5 ml of a 0.1% w/v solution of N-naphthyl ethylenediamine hydrochloride was added and the solution made up to 25 ml with distilled water. After exactly 30 minutes storage in the dark, the solution was removed from the ice bath and its absorbance was determined in 10 mm cells a 560 nm against a blank prepared as above with distilled water instead of test sample. If the coupled pink colour was faint, 4 cm cells were used and calculation made to produce a value equivalent to a 10 mm cell. Bubbles of nitrogen tended to form on the cell faces and had to be detached before absorbance measurement. Adhesion was minimised by prior cleaning of the cells in "chromic acid".

4-Chloroaniline content was determined by reference to a calibration plot (absorbance at 560 nm against molar 4-chloroaniline concentration) prepared as described above using different volumes of an appropriately diluted solution of 4-chloroaniline.

5.2.3.2 Calibration

The experimental and linear regression analysis data from four calibration plots, performed on the same day using the same batches of reagents, are shown in Table 5.20. The mean value of the four slopes had a coefficient of variation of 0.4%, this being considered sufficiently small enough to allow only one calibration

plot to be performed for each day's 4-chloroaniline assays. A plot of 4-chloroaniline concentration against mean absorbance (with error bars indicating the range) is shown in Figure 5.24 using the data listed in Table 5.20.

4-Chloroaniline concentration (Molar x 10^5)	Absorbance at 560 nm (10 mm cells)				
	Calibration				Mean
	1	2	3	4	
0.1568	0.082	0.083	0.082	0.083	0.0825
0.3136	0.167	0.168	0.167	0.166	0.167
0.6272	0.315	0.317	0.315	0.318	0.3163
0.9408	0.465	0.466	0.466	0.468	0.4663
1.254	0.609	0.611	0.612	0.613	0.6113
1.568	0.742	0.743	0.744	0.747	0.744
Regression analysis:					
Correlation coefficient	0.9996	0.9996	0.9996	0.9996	0.9996
Slope (SD)	46776(662)	46794(685)	46976(672)	47128(654)	46918(667)
Intercept (SD)	0.018(0.006)	0.019(0.007)	0.017(0.006)	0.017(0.006)	0.018(0.006)
Relative SD of slope	1.4%	1.5%	1.4%	1.4%	1.4%

Table 5.20 Experimental data for linearity and reproducibility of 4-chloroaniline assay

New batches of reagents were prepared daily (due to the discolouration of N-naphthyl ethylenediamine hydrochloride solution) and fresh calibration plots constructed.

5.2.3.3 Sensitivity

The detection limit of the assay method was 0.02 µg/ml (4-chloroaniline base). This concentration produced an absorbance of 0.03 in 4 cm cells. This limit is equivalent to the 4-chloroaniline concentration produced by 0.5% degradation of a 0.002% w/v chlorhexidine gluconate solution (assuming 4-chloroaniline was the only degradation product). Above the detection limit concentration changes of as little as 1.5 ng could be detected by this method.

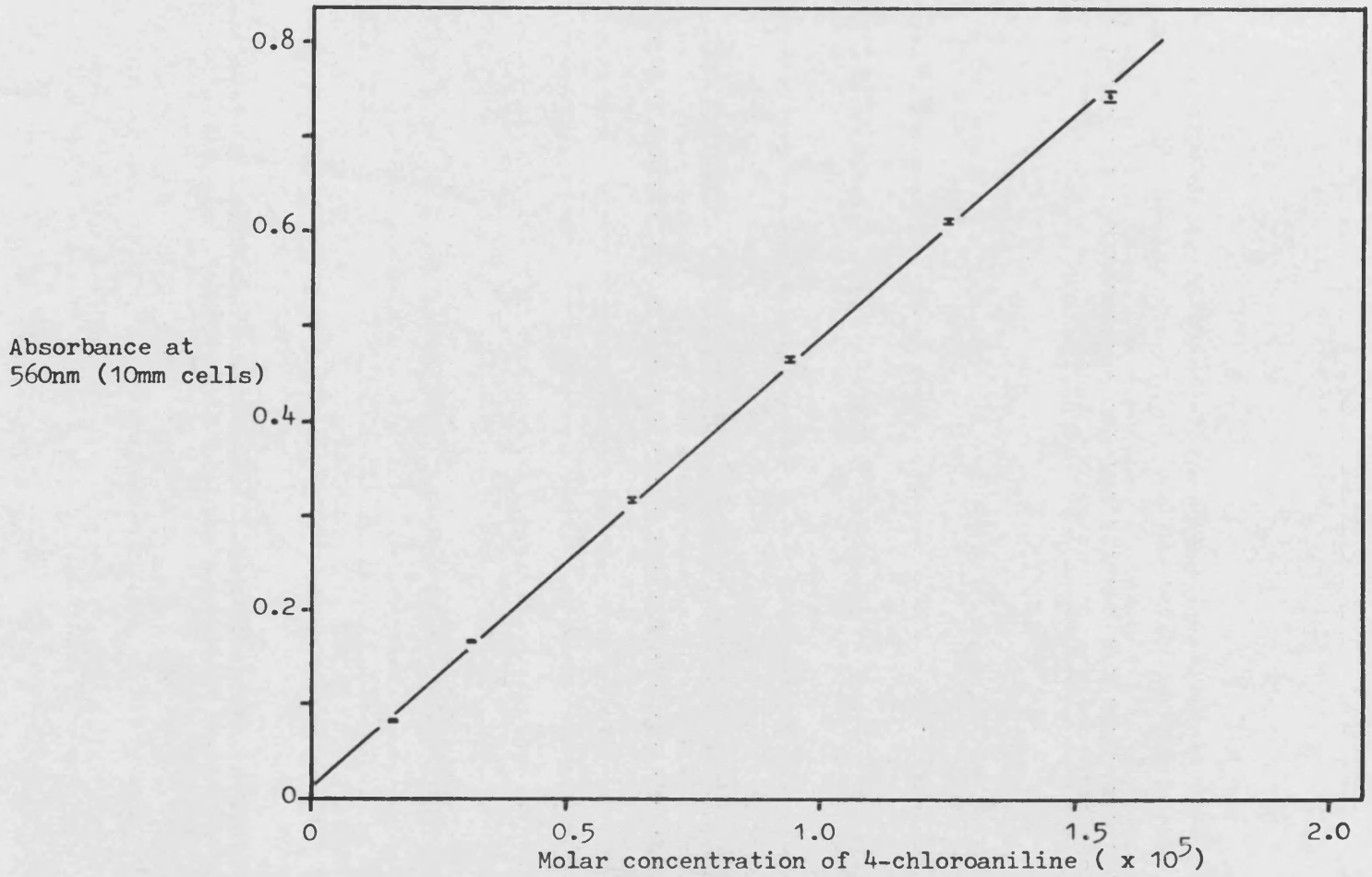

Figure 5.24 Calibration plot of mean absorbance against standard 4-chloroaniline concentration (error bars indicate range)

CHAPTER 6

DEGRADATION KINETICS

6.1 INTRODUCTION

The major aim of this study was to investigate the degradation kinetics of chlorhexidine in aqueous solution. Influences such as pH, temperature and chlorhexidine concentration were initially studied in order to establish basic kinetic behaviour. Effects due to the presence of buffers or surfactants were then noted. Such information was then applied to the prediction of shelf-life.

However, careful control of each separate variable was required to enable the measurement of rate constants under defined conditions. Before kinetic data are presented, experimental design and methods of control are discussed, together with the mathematical treatment and reproducibility of generated data.

Degradation rate constants were quantified by the assay of residual chlorhexidine using the HPLC stability indicating method (see Chapter 5.1.1). Quantitative (for 4-chloroaniline) and qualitative detection of degradation products is detailed in Chapter 7 and the proposed reaction mechanism presented in Chapter 8.

The effects of light (photochemical degradation) and ionising irradiation on chlorhexidine are described separately in sections 6.7

and 6.8 respectively. Since the experimental methods are specific to these studies they are detailed within the relevant sub-sections.

6.2 EXPERIMENTAL DESIGN

Kinetic data were generated by one of two experimental methods:

(i) pH-statting in a reaction flask,

(ii) sealed ampoules containing buffered or unbuffered solutions.

Each system was subjected to thermal stress in a water bath maintained at the appropriate temperature (±0.1°C).

The pH-stat system was used for the majority of experiments. Solutions in ampoules were used where the rate of degradation was very slow (i.e. in distilled water) or where a large number of stress conditions were required (i.e. buffered solutions). Each method is discussed in detail as follows.

6.2.1 Reaction Flask (pH-stat)

250 ml Quickfit round bottomed flasks with four necks for condenser, pH-electrode, acid or alkali titrant and sample withdrawal were used. To ensure that the vessel contents (200 ml) were maintained at the same temperature as the water bath it was immersed to the necks. The reaction solution was stirred by the use of an underwater stirrer and magnetic follower. A diagramatic representation of the system is shown in Figure 6.1. A description of the pH-stat technique is given in section 6.3.1.1.

Polypropylene stoppers were used to house the pH-electrode and acid/alkali titrant delivery tube with the aperture being made as narrow as possible to make a tight contact fit. All other fittings were ground

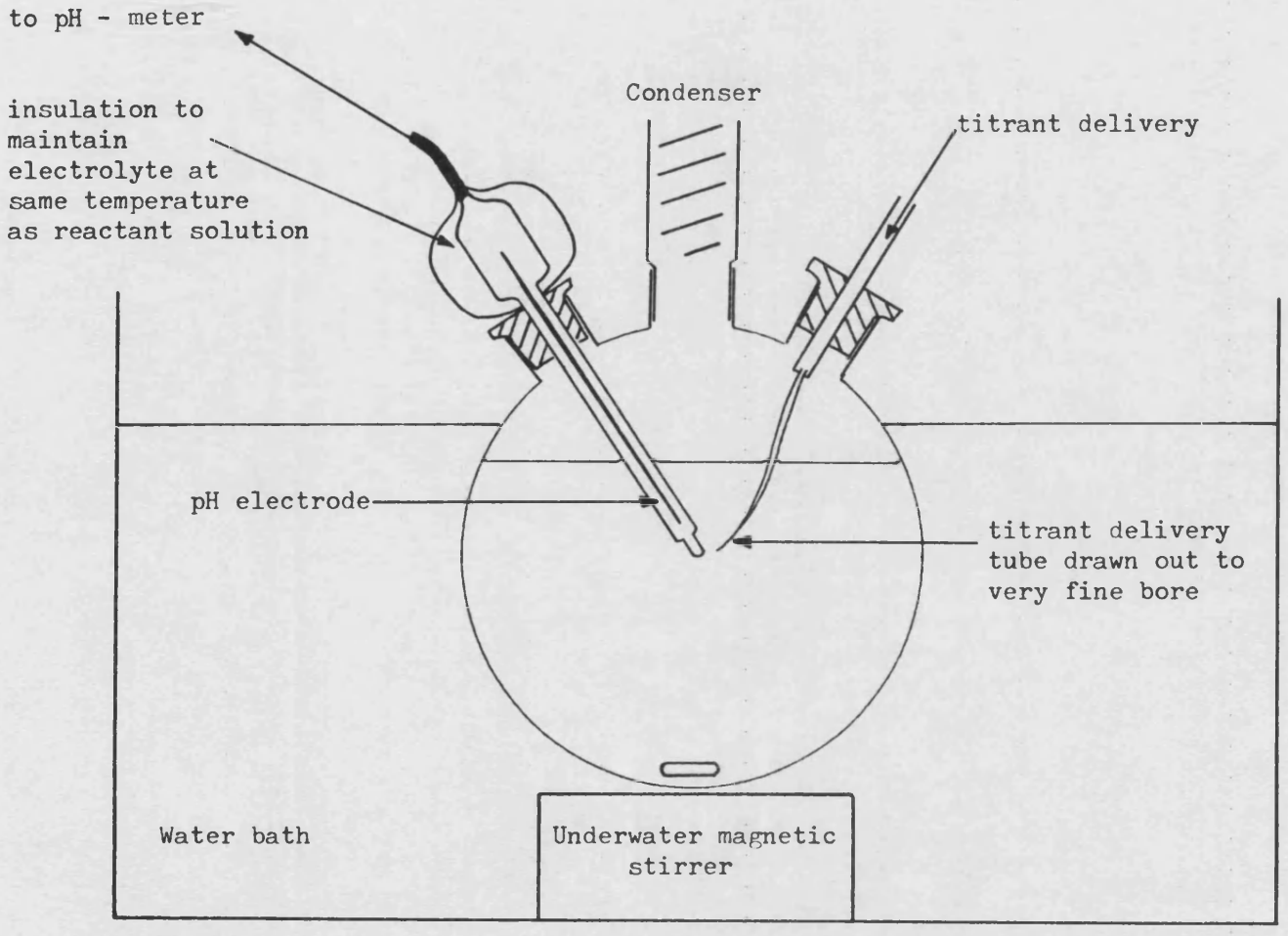

Figure 6.1 Diagramatic representation of reaction vessel set-up for pH-stat system

glass. Since the degradation of chlorhexidine is concentration dependent (section 6.6.3) any evaporation of water at the temperature of the stability studies (60-90°C) would result in an underestimation of the extent of chlorhexidine degradation. A high efficiency jacketed coil condenser was therefore fitted to the central neck of reaction flasks. However, the contact fittings between the pH-electrode/titrant delivery tube and polypropylene stoppers remained potential sites for water vapour leakage.

The efficiency of the condenser system and closures was therefore checked by measuring the concentration of a model compound in the reaction flask system at 90°C over a two week period. Benzoic acid was chosen because of its stability and ease of concentration measurements by u.v. spectroscopy (λ_{max} 273 nm). An aqueous solution of benzoic acid was prepared with an absorbance of approximately 0.5, (10 mm cells). This was held in the reaction flask under standard stirring conditions. Over a two week period at 90°C no significant change in absorbance was noted (Table 6.1), thus validating the condenser efficiency and contact fit seals.

Time (days)	Absorbance (in 10 mm cells at 273 nm)
0	0.511
1	0.510
2	0.509
4	0.510
7	0.509
10	0.510
14	0.510
Mean	0.510
Standard deviation	6.90×10^{-4}
Coefficient of variation	0.14%

Table 6.1 Data illustrating no significant change in the absorbance of a benzoic acid solution held in the reaction flask apparatus for two weeks at 90°C

The standard protocol to set up a stability run was as follows; 195 ml of distilled water was allowed to equilibrate to water bath temperature. The solution pH was then adjusted to near the required pH by dropwise addition of 1 M NaOH or HCl then finally adjusted to the required value using the pH-stat system (see section 6.3.1.1.2). 5 ml of an appropriate chlorhexidine solution was then added to produce the required initial concentration and after a few seconds a sample (~4 ml) withdrawn (zero time or initial sample). Other samples were taken at appropriate time intervals. All samples were immediately chilled (~4°C) to quench the reaction and stored at this temperature until HPLC assay. No significant assay differences were noted between samples (degraded at pH 9.0) assayed immediately and the same samples stored for up to four weeks at 4°C (Table 6.2).

Sample concentration (% w/v chlorhexidine gluconate x 10^3)		
Immediate HPLC assay	HPLC assay after storage at 4°C for	
	1 week	4 weeks
1.363	1.361	1.362
2.009	2.010	2.008
10.136	10.135	10.134

Table 6.2 HPLC assay data illustrating no change in chlorhexidine concentration after storage in a refrigerator

6.2.2 Ampoules

Certain stability studies were performed by filling solutions into 10 ml amber neutral glass ampoules, hermetically sealing and storing at the appropriate temperature by immersion in a water bath.

Approximately ten ampoules were used for each stability study with sampling by withdrawal of an ampoule after appropriate time intervals. The ampoules were then chilled and stored at 4°C until HPLC assay. The solution pH inside each ampoule was determined using a micro pH-electrode, both before sealing and after stress storage (prior to HPLC assay). Like all other glassware, the ampoules were chlorhexidine aged with the appropriate chlorhexidine study concentration (see Chapter 4.1.4).

6.3 CONTROL OF EXPERIMENTAL VARIABLES

6.3.1 pH Control

The pH of a solution may be maintained by the use of buffers or by a "pH-stat system". The presence of buffers has been shown to influence the degradation kinetics of many pharmaceuticals in solution (see Chapter 1.4.2), therefore the pH-stat system is preferred when performing basic kinetic studies.

6.3.1.1 pH-Stat

6.3.1.1.1 Basic Principle

The pH of a reactant solution is continuously measured by a pH-electrode and the millivolt output relayed via a pH-meter to a titration control unit which is pre-set to a required pH. As the reaction proceeds, pH changes are corrected by the addition of titrant (acid or alkali) from an autoburette as demanded by the titration control unit. Usually a drift towards either acidity or alkalinity is

noted, this being dependent upon the reactants used or products produced. Such a drift only requires one control unit and one corrective titrant.

The frequency of titrant addition is controlled by a proportionality band control which progressively reduces the frequency of additions as the reactant solution pH nears its pre-set value. Optimisation of this facility is important since a too frequent addition would result in overshooting the pre-set pH and titration control/autoburette shut-off. If titrant additions are too slow then the required pH may not be regained. Either situation would produce significant inaccuracies in pH dependent kinetic data and necessitate a repeat of that stability study.

6.3.1.1.2 Experimental

The following apparatus were used:

Pye-Ingold 465-90 High Temperature Electrodes
Radiometer PHM61 pH-Meters (sensitivity ±0.03 pH)
Radiometer TTT60 Titrators
Radiometer ABU12 Autoburettes

Two systems comprising the above apparatus were routinely available. A third system was occasionally available, identical to the above except a Radiometer PHM62 pH-meter (sensitivity ±0.02 pH) was used. The control specification for the pH-stat systems were ±0.05 pH units (±0.03 pH-meter sensitivity and ±0.02 pH-stat control) or ±0.04 pH units if the Radiometer PHM62 pH-meter was used. Figure 6.2 provides a diagramatic illustration of the pH-stat system.

Preliminary experiments showed the following conditions provided the best pH control during degradation studies:

Autoburette : titrant 0.04 M NaOH (between pH 6-10)
0.02 M HCl (between pH 3-5)
(the solution was self-buffering at pH2)
increment 2.5 to 5
burette volume 2.5 ml

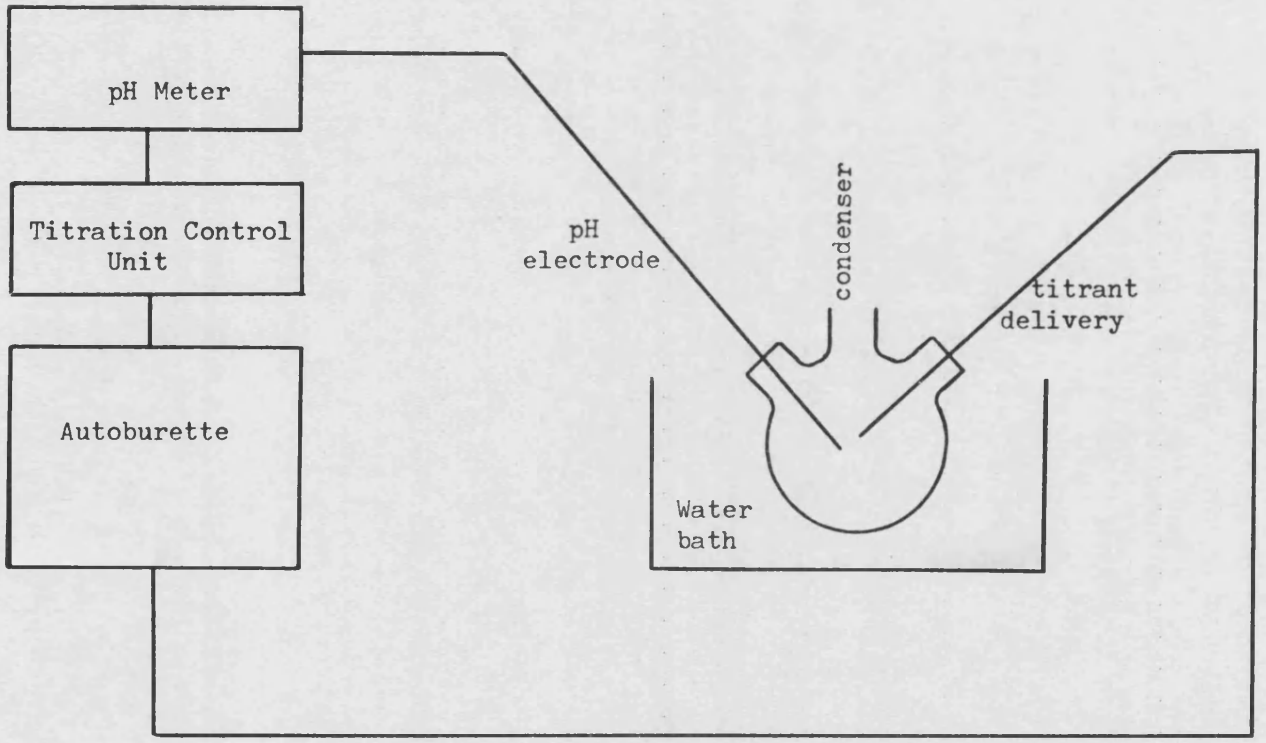

Figure 6.2 Diagramatic representation of a pH-stat system. Direct control of titrant delivery is via pH electrode - meter - titration control unit

Titrator : end point control - as required for the stability study
proportional band - usually 5 (if degradation fast [i.e. $t_{\frac{1}{2}} < 3$ hours] set at 2-3)
delay sec - ∞
up/down - up pH 6-10 (NaOH titrant)
- down pH 3-5 (HCl titrant)

Particular attention was given to match titrant strength with proportional band setting in order to maintain pH without overshooting and shut-off. The following practical points were also pertinent to the experimental procedure.

(i) The use of underwater electrical stirrers can sometimes influence pH-electrode response. Preliminary experiments showed no differences in response or drift when using the underwater stirrer and magnetic follower.

(ii) The tip of the titrant delivery tube was situated in close proximity to the glass membrane of the pH-electrode. Therefore, the relay between pH and titrant addition was as fast as practically possible so preventing pH overshoot.

(iii) The delivery tube tip was drawn out (by heat) to a very fine capillary. This also prevented pH overshoot by keeping the volume of titrant added between titrator signal and autoburette "shut off", very small.

6.3.1.1.3 pH Response over a Degradation Study

The use and calibration of the Pye-Ingold 465-90 high temperature electrode is described in Chapter 4.3.2. Because of the possibility of pH-electrode response drift over extended stability runs, the electrode was standardised immediately before a study and checked on completion of the investigation (using two appropriate standard buffer solutions at the relevant kinetic temperature). A drift of greater than ±0.03 pH units between the measured and standard

value in either buffer system falls outside the pH-meter sensitivity and therefore constitutes a detectable drift in electrode response. Because of the dependence of chlorhexidine degradation rate constants on pH (see section 6.6.1), repeat stability studies were performed in instances where such drifts occurred. However, such repeats were infrequent due to the regular pH-electrode cleaning and maintenance procedures employed.

6.3.1.2 Buffers

Kinetic experiments with pH control by buffers were performed in order to assess whether general (buffer) acid-base catalysis occurred in addition to specific acid-base catalysis. The stability studies using buffered solutions were carried out in ampoules. Experimental details of the buffers used are given in section 6.6.7.

6.3.2 Concentration

Stock solutions of chlorhexidine were prepared and their concentration determined by HPLC assay. By appropriate dilution, the initial concentration of each degradation reaction could be controlled to within the practical limit of the dilution error. This procedure was considered important in order to confirm that differences in observed rate constants obtained under various stress conditions were not influenced by unintended variation of initial concentration. The significance of initial concentration became apparent when the rate constant was observed to decrease with increasing initial chlorhexidine concentration, all other variables being constant (see section 6.6.3).

However, an initial (zero time) sample was always taken to provide a practical initial concentration for each degradation reaction. This sample was assayed by HPLC along with the degraded

samples after storage in a refrigerator and used as the initial (Co) concentration for calculation purposes. The difference between the experimental and theoretical initial chlorhexidine concentration was never greater than 2%.

6.4 TREATMENT OF GENERATED DATA

The determination of reaction order was necessary to evaluate rate constants from experimental degradation data. First-order rate plots (log percentage residual concentration against time) showed very good linearity down to approximately 30% residual with relative standard deviations of observed first-order rate constants being <3% (with one exception where it was 3.6%). Attempts to fit data to zero or second-order kinetics produced non-linear plots. Therefore all data were plotted according to first-order kinetics. Percentage residual concentration was calculated by reference to the zero-time (100% initial) sample. Figure 6.3 shows such a plot for 0.002% w/v chlorhexidine gluconate at pH 9.0 (pH-stat) and 90°C; the observed rate constant was derived from linear regression analysis of all data points including the zero-time sample.

However, studies at various initial chlorhexidine concentrations showed that the observed rate constant decreases with increasing chlorhexidine concentration (see section 6.6.3). This provided evidence that in spite of the linearity of the log concentration-time plots, the degradation mechanism is not a simple first- (or pseudo-first) order reaction. Attempts to establish an apparent order of reaction from a log-log plot of half-life against initial chlorhexidine concentration are discussed in section 6.6.3.

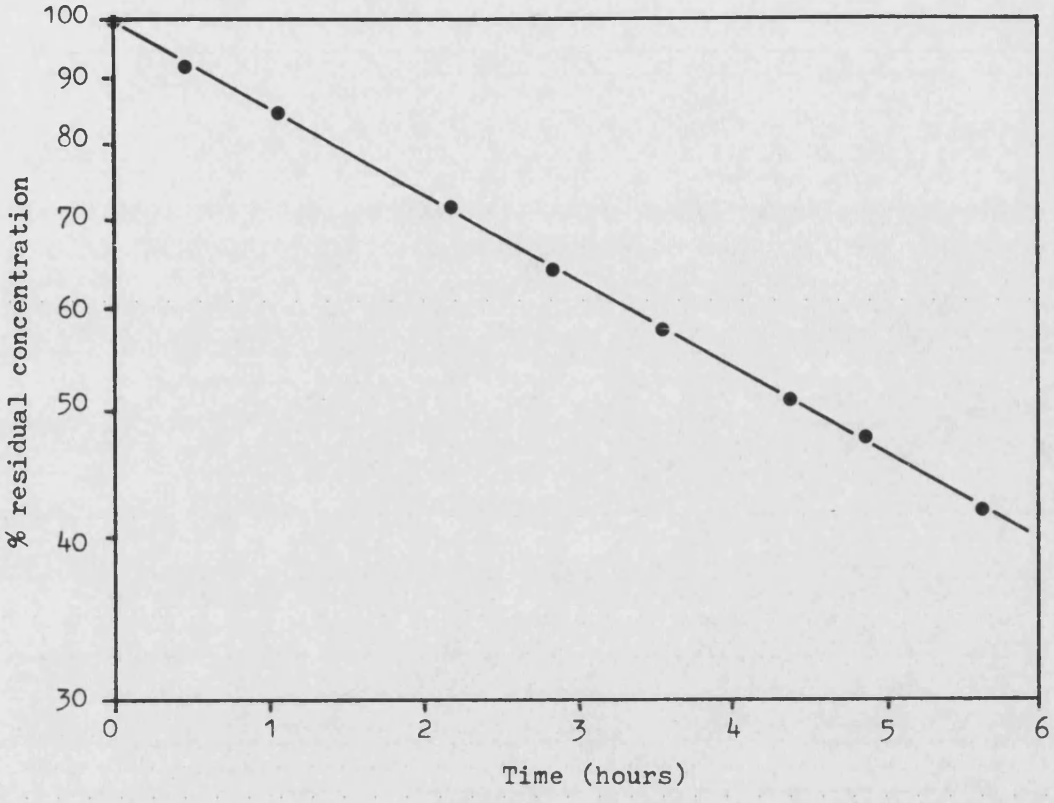

Figure 6.3 Typical log percent residual chlorhexidine concentration against time plot for 0.002% w/v chlorhexidine gluconate, pH 9.0 and 90°C

Linear regression analysis gives:

Slope 6.94×10^{-2}

RSD slope 2.2%

$k_{obs} = 2.303 \times 6.94 \times 10^{-2}$

$= 0.1598\ hr^{-1}$

$= 4.44 \times 10^{-5}\ sec^{-1}$

6.5 REPRODUCIBILITY OF KINETIC DATA

In order to investigate the maximum number of variables affecting chlorhexidine degradation kinetics, it was not possible to replicate all experiments. Only two sets of pH-statting equipment were routinely available and the relative stability of chlorhexidine at pH 4 to 7 (section 6.6.1) meant long kinetic runs of up to four weeks.

The potential experimental factors which might lead to incorrect rate constants from single determinations, or poor reproducibility of rate constants from replicate determinations were therefore examined. Criteria used for the rejection of suspect experimental data were established following experimental investigation into the repeatability of results where data were very sensitive to kinetic conditions.

6.5.1 Instrumental Variation

In order to assess the need for replication of experiments it was useful to consider likely sources of experimental error. The control of temperature (±0.1°C) and pH (±0.05 units) during kinetic experiments has been described (Chapter 4.3.1 and section 6.3.1 respectively). Variation within the limits of temperature control has little influence since a ±0.1°C shift results in a ±4% change in degradation rate constant at 25°C when calculated from Arrhenius constants (section 6.6.4). This value is comparable to the relative standard deviations (RSD) of the plots.

However, the potential for more significant errors due to the possible pH variation of 0.05 unit was apparent once the pH-rate profile (section 6.6.1) was constructed. The likely influence of pH-stat sensitivity was calculated in two regions: where specific base

catalysis occurs (pH 8 to 9) and where the water catalysed/specific base catalysed reaction takes place (pH 6 to 7).

Specific base catalysis

Figure 6.4 (section 6.6.1) shows a slope of approximately unity at ~pH 8, this indicates that the degradation reaction is specific base catalysed (see Chapter 1.5.1.1) and the overall rate constant may be described by equation 33:

$$k_{obs} = k_{OH^-} [OH^-] \quad \ldots (33)$$

At pH 8.0 and 90°C the observed degradation rate constant for 0.002% w/v chlorhexidine gluconate was 7.59×10^{-6} sec^{-1} (Table 6.6). The hydroxide-ion concentration may be calculated from the pK_w of water at 90°C, (= 12.45, Harned and Owen, 1958), using equation 67:

$$[OH^-] = 10^{(pH-pK_w)} \quad \ldots (67)$$

and k_{OH^-} at 90°C is then calculated as 0.214 $sec^{-1}l.mol^{-1}$.

The pH-stat sensitivity of ±0.05 pH units can now be applied to predict the maximum error in the observed rate constant due to instrument sensitivity. From equation 33, k_{obs} is 6.77×10^{-6} sec^{-1} and 8.52×10^{-6} at pH 7.95 and 8.05 respectively, equivalent to a spread of ±11% relative to the experimental value.

Water catalysed/specific base catalysis

At pH 6 the pH-rate profile illustrates that both water catalysed and specific base catalysed reactions occur simultaneously (see Chapter 1.5.1.4). The overall rate constant is therefore given by equation 68:

$$k_{obs} = k_o + k_{OH^-}[OH^-] \quad \ldots (68)$$

At pH 6.0 (90°C, 0.002% w/v chlorhexidine gluconate), the observed rate constant was determined as 4.65×10^{-7} sec^{-1}. The calculated

hydroxide-ion concentration is 3.55×10^{-7} M, k_{OH^-} is 0.214 $sec^{-1}/(l.mol^{-1})$ and k_o is therefore 3.89×10^{-7} sec^{-1}. Values for k_{obs} at pH 5.95 and 6.05 are therefore prediced as 4.57×10^{-7} and 4.74×10^{-7} sec^{-1} compared to the experimental value of 4.65×10^{-7} sec^{-1}.

These calculations illustrate that a maximum error, due to pH-stat sensitivity, of about ±1.9% in degradation rate constants would be expected at pH 6. This figure is within the data acceptance criterion of ±3% for rate constants discussed in section 6.5.2(b). However at pH 9, a potential error of ±11% is clearly not. The reproducibility and validity of data produced in this very sensitive region was therefore established experimentally (section 6.5.3).

6.5.2 Criteria for the Rejection of Experimental Data

Experimental data were rejected and a repeat experiment performed if any one of the following situations applied.

(a) Variation in Initial Chlorhexidine Concentration

If the HPLC assay of the initial sample from a degradation experiment was greater than ±2% of that theoretically present (see section 6.3.2) then the experiment was repeated. This control was required since small changes in the initial concentration were found to have a significant influence on generated rate constants (see section 6.6.3). These variations could mask the effect of the experimental variable under test.

(b) RSD in Rate Constant ⩾ 3%

Any degradation data exhibiting a RSD of the rate plot slope in excess of 5% usually resulted from experimentation where, for example, pH control was inadequate (i.e. pH-stat overshoot). Therefore a ⩾ 3% RSD in rate constant was imposed to provide a practical "safety margin". This goodness of fit to the first order rate plot was a good

measure of pH stability during the kinetic run, since pH drift would result in upward or downward curvature.

(c) Electrode Response Outside pH-meter Sensitivity

At the end of each pH-stat experiment electrode response to the standard buffers was checked and if outside the pH-meter sensitivity of ±0.03 pH units, the experiment was rejected. This strict procedure was required since significant errors in the rate constant could result from pH-electrode drift as evidenced by the calculations detailed in section 6.5.1.

6.5.3 Replicate Experimentation

6.5.3.1 pH-Stat

The degradation of 0.002% w/v chlorhexidine gluconate at pH 9.0 and 90°C was chosen to test the reproducibility of the pH-stat technique. The high temperature meant the reactions were fast ($t_{\frac{1}{2}}$ ~4.4 hours) whilst pH 9.0 was chosen since potentially large errors due to pH-stat sensitivity were possible (see section 6.5.1). Experimentation was repeated at regular intervals during the early degradation studies. As an additional check of experimental technique the degradation rate was redetermined approximately two years after the original replicate estimations. Initial chlorhexidine gluconate concentration was tightly controlled to eliminate concentration effects on the generated rate constants (see section 6.6.3).

The results of all replicate determinations of the observed rate constant at this degradation condition are listed in Table 6.3. Multiple linear regression analysis (Appendix 3) was performed on all sets of raw data to test whether any significant difference occurred. The result (F_{ratio} 1.05, F_{tab} 2.25, $p = 0.05$) indicated that the slopes (and therefore first-order rate constants) were not significantly

	Replicate degradation experiments on 0.002% w/v chlorhexidine gluconate at pH 9.0 (pH-stat) and 90°C					
	1	2	3	4	5	6
Date of experiment	28.5.82	7.6.82	9.6.82	11.6.82	22.6.82	8.8.84
Initial concentration (% w/v x 10^3)	2.036	2.030	2.021	1.998	2.011	2.010
Degradation rate constant (sec^{-1} x 10^5)	4.41	4.59	4.56	4.44	4.52	4.45
SD rate constant (sec^{-1} x 10^7)	7.4	8.6	6.1	9.7	10.0	12.9
RSD rate constant	1.7%	1.9%	1.4%	2.2%	2.2%	2.9%
Correlation coefficient	0.9994	0.9995	0.9997	0.9990	0.9985	0.9976
Intercept (log % residual conc.)	1.996	1.998	2.003	2.004	2.006	2.002
SD intercept (x 10^3)	3.7	4.7	3.2	7.0	6.6	7.8
Calculated % residual conc.(initial)	99.1	99.5	100.7	100.9	101.4	100.5
Multiple linear regression (all data) F_{ratio} 1.05, F_{tab} 2.25, p = 0.05						

Table 6.3 Reproducibility of degradation experiments on 0.002% w/v chlorhexidine gluconate at pH 9.0 (pH-stat) and 90°C

different. The coefficient of variation of the six determinations was 1.6%, with the full spread about the mean observed rate constant being ± 2.1%; this is good evidence that the reproducibility of experimental technique was very satisfactory. These results also provide confirmation that reproducibility could be maintained over the duration of the experimental studies since no significant difference was observed between the data generated during 1982 and that of August 1984.

The reproducibility of long duration degradation studies was tested by experimentation on 0.002% w/v chlorhexidine gluconate at pH 7.0 and 90°C (length of experiment = 17 days). The data generated are listed in Table 6.4 with multiple linear regression again showing no significant difference between the two sets of raw data (F_{ratio} 0.49, F_{tab} 3.81, p = 0.05). This observation is important since it justifies the use of the criterion applied to pH-electrode drift (i.e. must be within pH-meter sensitivity, see section 6.5.2(c).

	Duplicate degradation experiments on 0.002% chlorhexidine gluconate at pH 7.0 (pH-stat) and 90°C	
	1	2
Initial concentration (% w/v x 10^3)	2.037	2.022
Degradation rate constant (sec^{-1} x 10^6)	1.00	1.03
SD rate constant (sec^{-1} x 10^8)	2.8	1.7
RSD rate constant	2.8%	1.7%
Correlation coefficient	0.9976	0.9990
Intercept (log % residual conc.)	1.995	1.992
SD intercept (x 10^3)	5.1	4.7
Calculated % residual conc.(initial)	98.9	98.2
Multiple linear regression F_{ratio} 0.49, F_{tab} 3.81, p = 0.05		

Table 6.4 Reproducibility of degradation experiments where the rate constant is small (i.e. long duration experiments)

Since the replicate data generated by both short and long duration experiments show no significant difference at extreme stress (pH 9.0), the replication of individual degradation experiments was considered unnecessary for the pH-stat method. However, all experiments were scrutinised by the rejection criteria previously discussed.

6.5.3.2 Buffered Solutions

The reproducibility of rate constants generated in buffered solution by either the reaction flask technique (without pH-statting) or in ampoules was investigated by degrading 0.002% w/v chlorhexidine gluconate solutions in single strength sodium tetraborate/HCl buffer, pH 8.88, at 90°C. This experimentation was necessary to confirm that degradation rate constants produced by ampoule studies were not significantly different to those produced by the reaction flask technique. The results of individual determinations are given in Table 6.5. Multiple linear regression of the data showed that derived first-order rate constants were not significantly different (F_{ratio} 0.033, F_{tab} 4.46, $p = 0.05$). This result therefore allowed direct comparison of rate constants derived from buffered solutions (ampoules) with those from pH-stat experimentation to identify possible buffer effects.

	0.002% w/v Chlorhexidine gluconate in single strength sodium tetraborate buffer at 90°C, degraded in:	
	reaction flask	ampoule
Initial concentration (% w/v x 10^3)	2.001	2.008
Degradation rate constant (sec^{-1} x 10^6)	6.56	6.56
SD rate constant (sec^{-1} x 10^7)	1.8	1.0
RSD rate constant	2.7%	1.6%
Correlation coefficient	0.9956	0.9995
Intercept (log % residual conc.)	1.992	1.994
SD intercept (x 10^3)	13.6	4.2
Calculated % residual conc.(initial)	98.2	98.6
Multiple linear regresion	F_{ratio} 0.033, F_{tab} 4.46, p = 0.05	

Table 6.5 Reproducibility of a degradation experiment performed in the reaction flask apparatus and in ampoules

6.6 DEGRADATION KINETICS

6.6.1 Effect of pH

The rate of degradation of a 0.002% w/v chlorhexidine gluconate solution at 90°C was investigated over the range pH 2 to 10 using the pH-stat system. The generated first-order kinetic data are shown in Table 6.6; relative standard deviations were <3% in all cases.

The pH-rate profile (Figure 6.4) shows degradation to be both acid and base catalysed with a minimum around pH 5. Below pH 3 and between pH 7.5-8.5 the slopes of -1.07 and 1.01 respectively, suggest the reaction is specifically hydroxonium-ion and hydroxide -ion catalysed in these regions. These findings are consistent with a hydrolytic reaction mechanism (Chapter 1.4.1 and 1.5.1). Between pH 3 and 7 the observed rate constant is influenced by a combination of hydroxonium-ion, hydroxide-ion and water catalysed reactions.

pH (at 90°C)		Observed first-order degradation rate constant (sec^{-1})	standard deviation (sec^{-1})
2.0		1.08×10^{-5}	2.7×10^{-7}
3.0		9.23×10^{-7}	2.7×10^{-8}
4.0		3.44×10^{-7}	8.0×10^{-9}
5.0		2.73×10^{-7}	7.2×10^{-9}
6.0		4.65×10^{-7}	1.4×10^{-8}
7.0	replicate 1	1.00×10^{-6}	2.8×10^{-8}
7.0	replicate 2	1.03×10^{-6}	1.7×10^{-8}
7.5		2.32×10^{-6}	6.1×10^{-8}
8.0		7.59×10^{-6}	1.3×10^{-7}
8.5		2.37×10^{-5}	4.2×10^{-7}
9.0	replicate 1	4.41×10^{-5}	7.4×10^{-7}
9.0	replicate 2	4.59×10^{-5}	8.6×10^{-7}
9.0	replicate 3	4.56×10^{-5}	6.1×10^{-7}
9.0	replicate 4	4.44×10^{-5}	9.7×10^{-7}
9.0	replicate 5	4.52×10^{-5}	1.0×10^{-6}
9.0	replicate 6	4.45×10^{-5}	1.3×10^{-6}
10.0	replicate 1	8.66×10^{-5}	2.2×10^{-6}
10.0	replicate 2	9.19×10^{-5}	2.6×10^{-6}

Table 6.6 Effect of pH on the observed first-order degradation rate constants of 0.002% w/v chlorhexidine gluconate degraded at 90°C

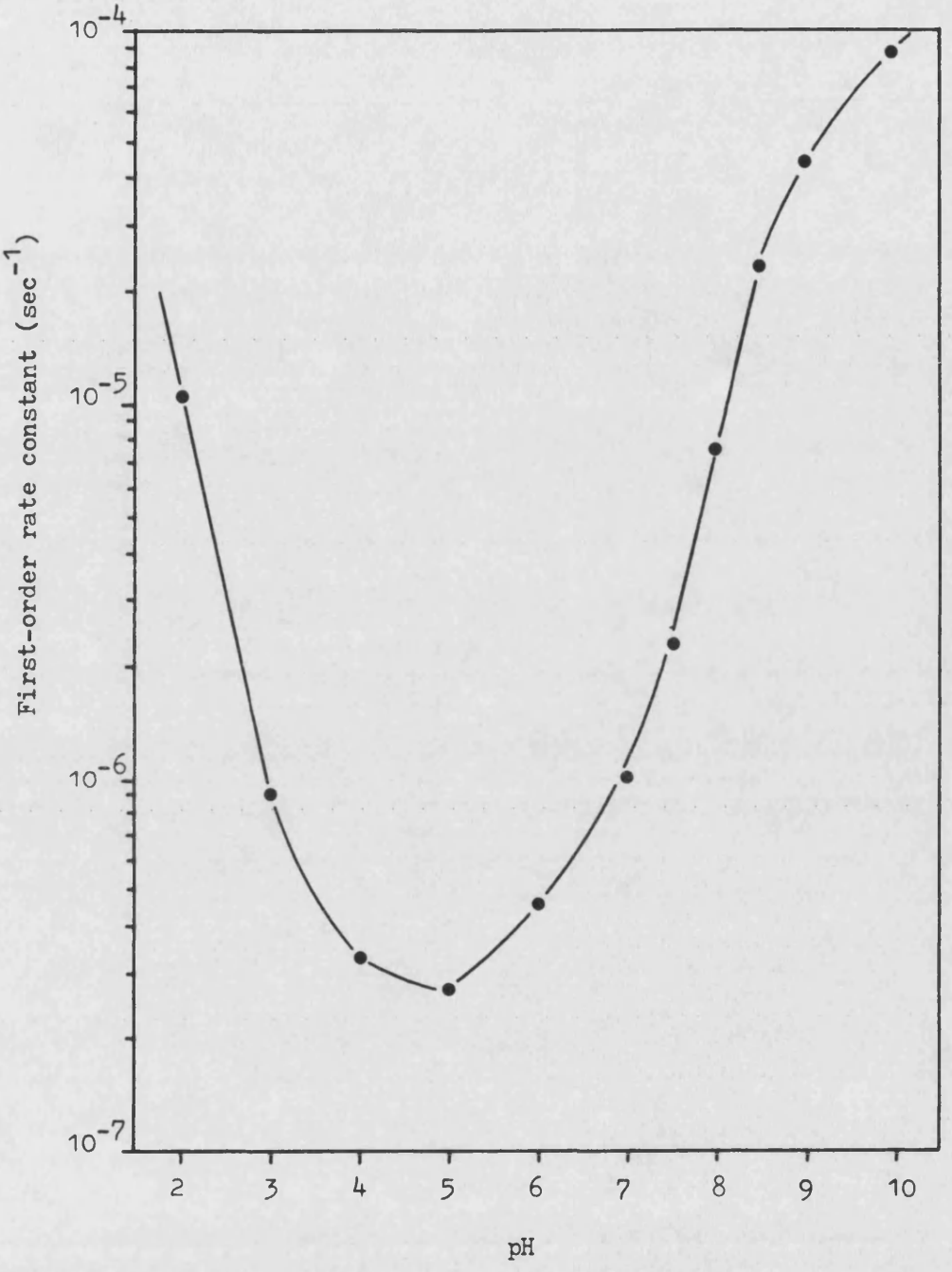

Figure 6.4 Effect of pH on the observed first-order degradation rate constant of 0.002% w/v chlorhexidine gluconate solutions at 90°C using a pH-stat system

Since specific acid catalysis only occurs in the region of pH 2 to 3 it was considered of little practical importance for stability determinations applied to pharmaceutical formulations; from the pH-rate profile it is apparent that the major influence is specific base catalysis which begins to occur at pH 5 to 6. The majority of the following studies were therefore performed at pH 9.0 where the rate constant is not prohibitively small for numerous experimental effects to be noted.

6.6.2 Effect of Salt Form

In order to determine whether salt form had any influence on degradation kinetics, experimentation was performed using equimolar concentrations of chlorhexidine base and the gluconate, acetate and hydrochloride salts. A concentration of 2.2×10^{-5} M was selected (equivalent to 0.002% w/v chlorhexidine gluconate) and solutions were degraded at pH 9.0 (pH-stat) and 90°C. Triplicate experiments were carried out using the base and the data is shown plotted in Figure 6.5. Figure 6.6 illustrates the results for the acetate, hydrochloride and gluconate salts. Comparison of the two plots indicates that salt form has no effect on degradation rate at pH 9.0 and 90°C. This is confirmed by multiple linear regression analyses of the derived rate constant data (given in Table 6.7) which showed no significant difference at the 5% level of probability. The triplicate determination of the rate constant for chlorhexidine base under these conditions provides further supportive evidence for the reproducibility of the pH-statting results (mean 4.53×10^{-5} sec^{-1}, coefficient of variation 2.5%).

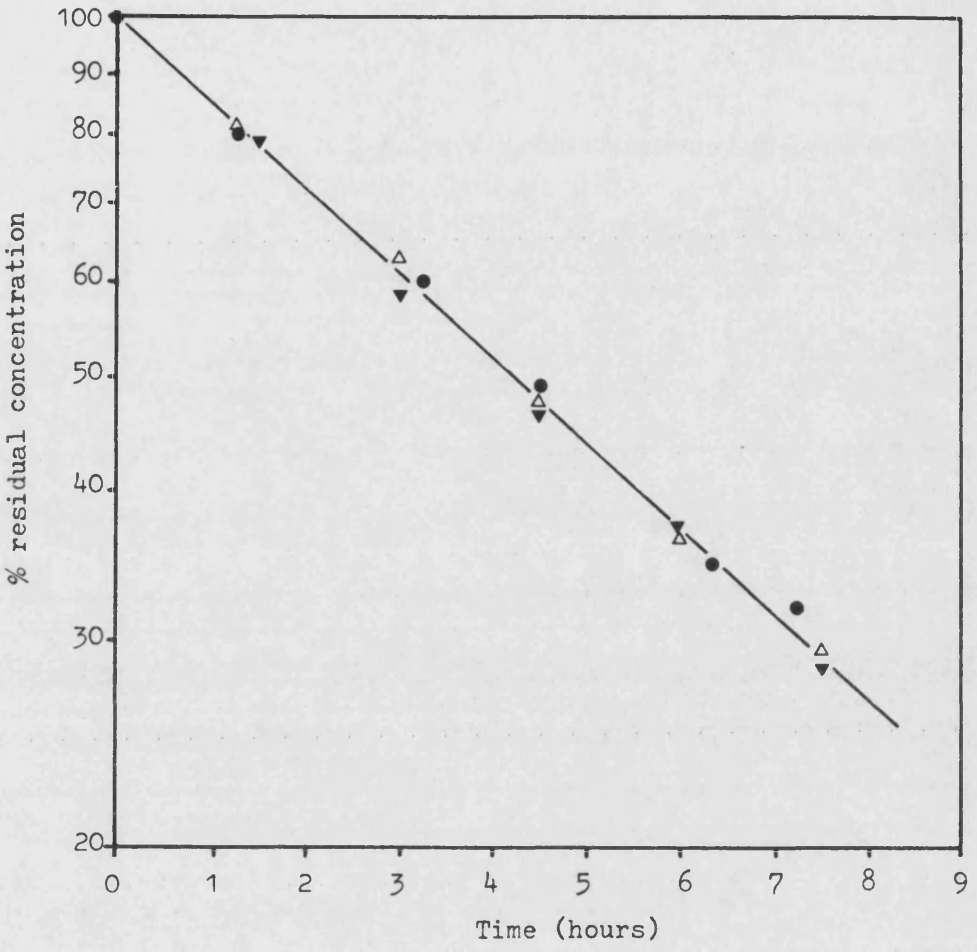

Figure 6.5 First-order degradation profiles of 2.2×10^{-5}M chlorhexidine base degraded at pH 9.0 and 90°C (performed in triplicate)

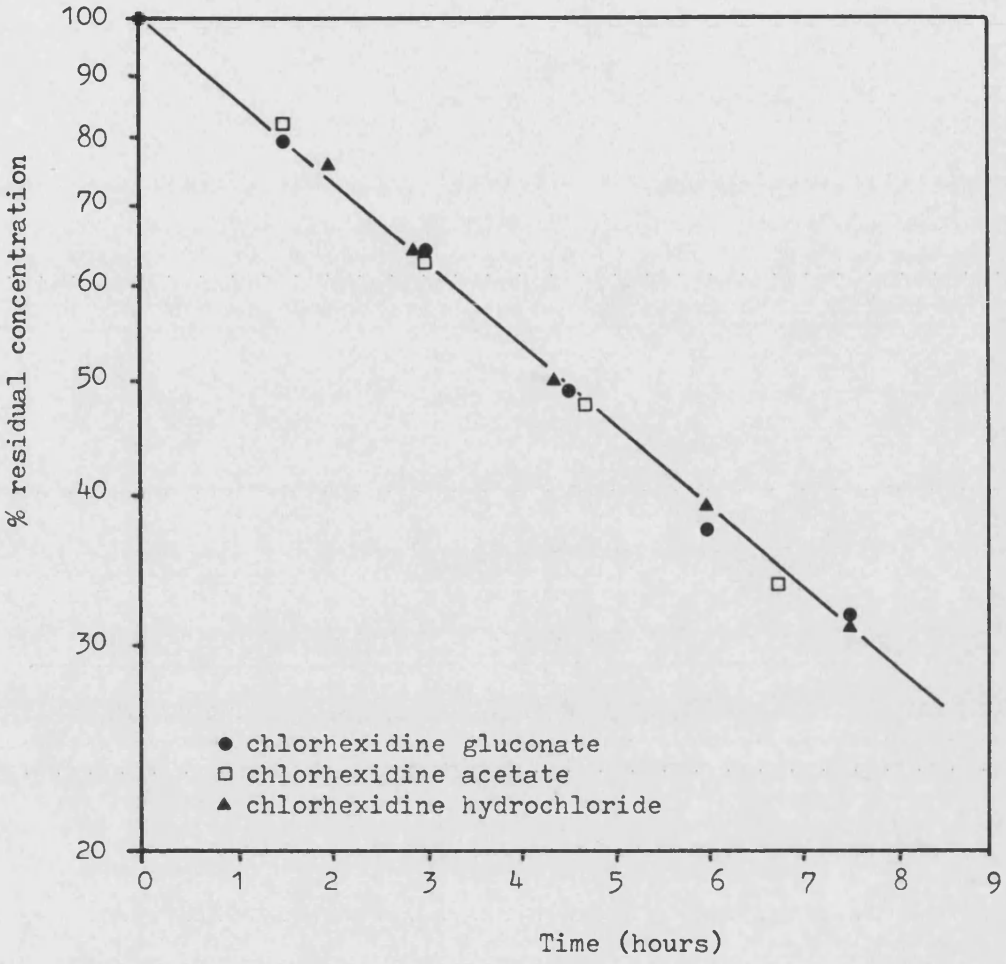

Figure 6.6 First-order degradation plot of 2.2×10^{-5}M solutions of chlorhexidine gluconate, acetate and hydrochloride salts degraded at pH 9.0 and 90°C. Linear regression line drawn using all data points

	Degradation experiments on 2.2×10^{-5} M chlorhexidine base, acetate and hydrochloride at pH 9.0 (pH-stat) and 90°C				
	Base			Acetate	Hydrochloride
	1	2	3		
Degradation rate constant ($sec^{-1} \times 10^{5}$)	4.56	4.40	4.62	4.51	4.34
SD rate constant ($sec^{-1} \times 10^{7}$)	8.1	12.3	10.2	10.6	8.7
RSD rate constant	1.8%	2.8%	2.2%	2.4%	2.0%
Correlation coefficient	0.9994	0.9985	0.9990	0.9992	0.9992
Intercept (log % residual conc.)	2.003	1.998	1.996	2.010	2.004
SD intercept ($\times 10^{3}$)	5.8	8.7	7.3	6.6	6.2
Calculated % residual conc. (initial)	100.7	99.5	99.1	102.3	100.9
Multiple linear regression:					
gluconate replicates (Table 6.3)	F_{ratio} 1.05 F_{tab} 2.25, $p = 0.05$				
base replicates	F_{ratio} 1.50, F_{tab} 3.26, $p = 0.05$				
acetate and hydrochloride	F_{ratio} 0.98, F_{tab} 4.74, $p = 0.05$				
all data	F_{ratio} 1.68, F_{tab} 1.82, $p = 0.05$				

Table 6.7 Effect of original form of chlorhexidine on generated first-order degradation data. 2.2×10^{-5} M solutions of chlorhexidine base, acetate, hydrochloride and gluconate salts were degraded at pH 9.0 and 90°C

6.6.3 Effect of Concentration

The effect of initial concentration on the rate of chlorhexidine gluconate degradation was determined at pH 2.0, ~6 and 9.0 since the pH-rate profile (Figure 6.4) indicated mechanistic changes. Derived rate constants are given in Tables 6.8 and 6.9.

The most comprehensive study was performed at pH 9.0 (pH-stat) and 80°C over the concentration range 0.001-0.055% w/v. The degradation profiles shown in Figure 6.7 clearly demonstrate that the degradation rate for chlorhexidine decreases with increasing concentration. It is also pertinent to examine the significance of small changes in initial concentration around 0.002% w/v chlorhexidine gluconate. Four nominally replicate experiments were performed with initial chlorhexidine gluconate concentration not as tightly controlled as in other studies (range 0.0018-0.00227% w/v). Multiple linear regression of these raw data showed a significant difference to exist between the data (F_{ratio} 23.34, F_{tab} 2.84, $p = 0.05$). This observation highlighted the possible significance of small initial concentration changes on degradation rate constants and resulted in the implementation of strict control of initial chlorhexidine concentration in degradation studies (section 6.5.2).

The effect of concentration was also studied at pH 2.0 and 80°C over the range 0.002-0.051% w/v chlorhexidine gluconate. It was noted that no titrant was added during the kinetic run and therefore the solutions were self-buffering at this pH. First-order rate plots from these experiments are shown in Figure 6.8 and suggest that, in contrast to the base catalysed process, there is no concentration dependency for the

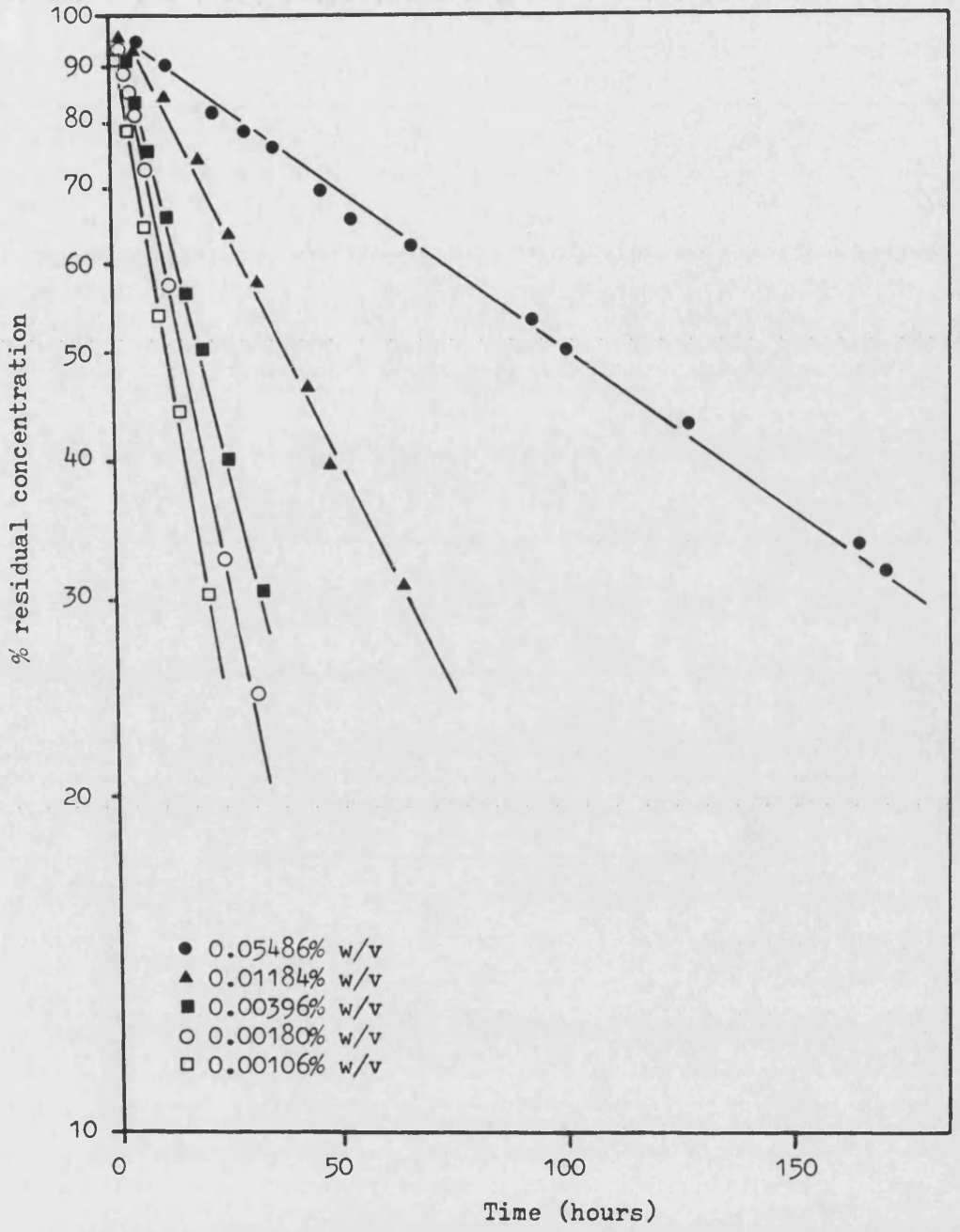

Figure 6.7 Effect of initial chlorhexidine gluconate concentration on first-order degradation plots. All systems degraded at pH 9.0 and 80°C

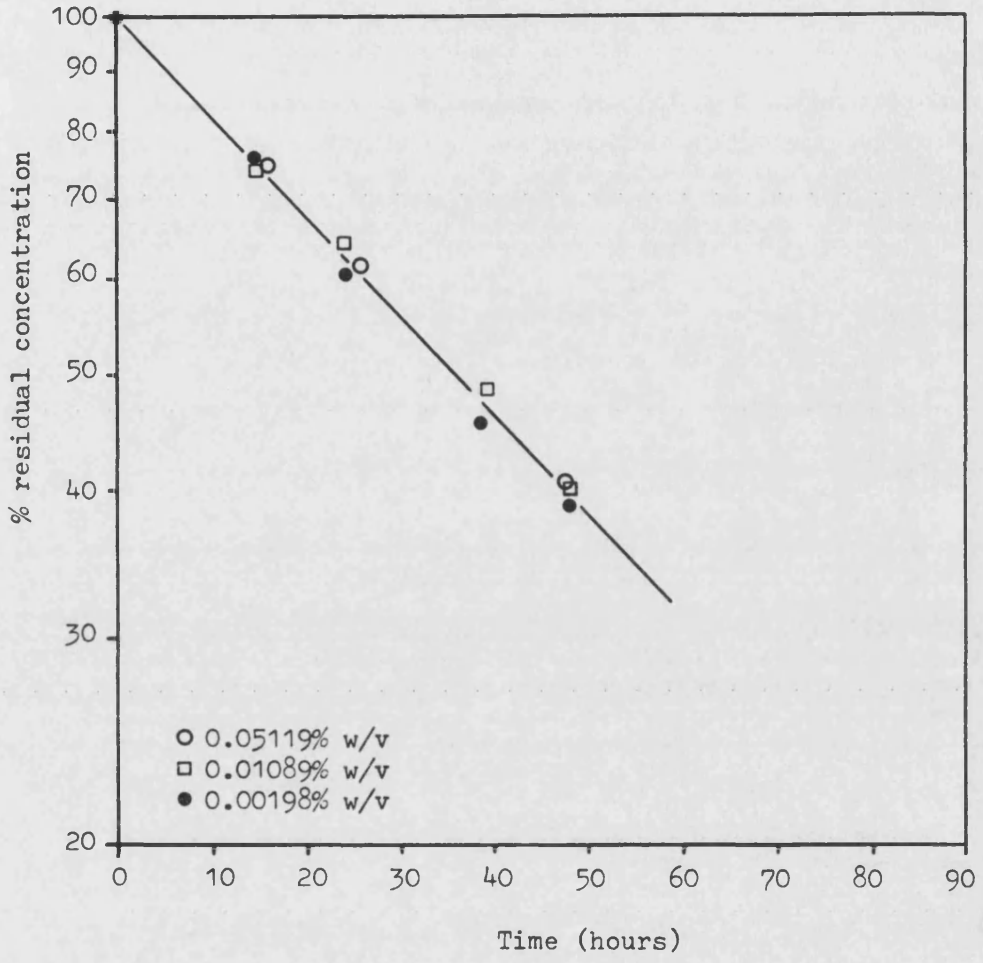

Figure 6.8 Effect of initial chlorhexidine gluconate concentration on first-order degradation plots at pH 2.0 and 80°C. Slope drawn from linear regression analysis

acid catalysed degradation of chlorhexidine. Multiple linear regression analysis (Table 6.8) confirmed this visual observation at the 5% level of probability.

Initial chlorhexidine gluconate concentration (% w/v x 10^3)	Observed first-order degradation rate constant (sec^{-1} x 10^5)	SD (sec^{-1} x 10^7)
pH 9.0 (pH-stat):		
1.06	1.32	3.3
*1.80	1.32	3.1
*2.05	1.43	2.6
*2.13	1.27	2.1
*2.27	2.20	2.2
3.96	1.00	2.6
11.84	0.522	2.7
54.86	0.181	0.44
*Multiple linear regression of these data: F_{ratio} 23.34, F_{tab} 2.84, p = 0.05		
pH 2.0 (self-buffering):		
1.98	0.536	1.6
10.89	0.524	1.1
51.19	0.526	0.48
Multiple linear regression: F_{ratio} 0.70, F_{tab} 3.84, p = 0.05		

Table 6.8 Effect of initial chlorhexidine gluconate concentration on generated first-order degradation rate constants. Experiments were performed at 80°C and either pH 9.0 or pH 2.0

The effect of concentration was also determined at ~pH 6 using chlorhexidine gluconate solutions in distilled water. Because the degradation rate was very slow in this region ($t_{\frac{1}{2}}$ 11-33 days) the dedicated use of pH-stat equipment was unjustified. Therefore, solutions were filled into 10 ml amber neutral glass ampoules (chlorhexidine aged) sealed and subjected to thermal stress at the

higher temperature of 90°C to accelerate decomposition. This procedure presented various practical difficulties since it was not possible to control or measure the pH inside each ampoule as degradation proceeded. Therefore the initial solution pH of each ampoule was determined at 25°C prior to sealing, and again after sampling (immediately prior to analysis). However, since the degradation was performed at 90°C, the pH of a separate sample of each initial concentration was determined at 90°C to identify the pH at which degradation took place. These various pH values and the rate constants for initial concentrations of 0.001-0.051% chlorhexidine gluconate are given in Table 6.9. Figure 6.9 illustrates the individual degradation profiles over this concentration range. The tabulated data shows that the maximum and minimum pH values at 25°C are covered by the range 5.39 to 5.66 for all concentrations. At 90°C, the initial pH of all concentrations increased by 0.5-0.6 pH unit relative to their initial values at 25°C. It is surmised that a similar rise would occur for the degraded solutions although it is recognised that the presence of degradation products may modify this effect. It may therefore be argued that the observed differences in the rate constants given in Table 6.9 are due to pH variation and not concentration effects. However, if we fit the observed rate constants generated at 90°C to the pH-degradation rate profile for 0.002% w/v chlorhexidine gluconate also at 90°C (section 6.6.1), then the spread of experimental pH required to eliminate any concentration effect may be noted (Figure 6.10). The four constants which could be fitted required the experimental pH range 5.6 to 6.7. Since the initial pH of each concentration (measured at 90°C) did not show such variation and those determined for the degraded samples

	Initial chlorhexidine gluconate concentration (% w/v x 10^3) in distilled water														
	1.00			2.03			5.07			10.88			50.90		
	Time (hrs)	% residual	pH (25°C)	Time (hrs)	% residual	pH (25°C)	Time (hrs)	% residual	pH (25°C)	Time (hrs)	% residual	pH (25°C)	Time (hrs)	% residual	pH (25°C)
	0	100	5.43	0	100	5.43	0	100	5.60	0	100	5.42	0	100	5.66
	6	97.1	5.51	6	98.6	5.56	8	97.4	5.60	8	97.5	5.58	72	94.3	5.59
Degradation	30	92.0	5.57	30	93.7	5.49	32	95.6	5.55	32	96.9	5.43	120	91.2	5.60
data	78	81.0	5.57	78	84.6	5.50	56	93.3	5.53	104	88.0	5.40	168	84.6	5.60
	198	58.6	5.63	193	64.7	5.61	104	88.4	5.60	197	76.8	5.39	336	73.6	5.60
	307	44.1	5.61	411	38.3	5.58	197	79.5	5.62	437	56.4	5.47	501	63.8	5.60
	411	32.9	5.59				251	73.7	5.57	680	40.1	5.42	744	52.8	5.64
pH (at 25°C):															
maximum		5.63			5.61			5.62			5.58			5.66	
minimum		5.43			5.43			5.53			5.39			5.60	
total scatter		0.20			0.18			0.09			0.19			0.06	
Initial pH (at 90°C)		6.01			5.95			6.14			5.99			6.18	
Rate constant (sec^{-1} x 10^7)		7.44			6.48			3.29			3.71			2.42	
SD rate constant (sec^{-1} x 10^9)		4.3			5.5			6.1			5.0			6.7	
RSD slope		0.6%			0.8%			1.9%			1.3%			2.8%	

Table 6.9 Effect of initial chlorhexidine gluconate concentration on generated first-order degradation rate constants. Experiments were performed in ampoules at 90°C, individual pH measurements at 25 and 90°C are also tabulated.

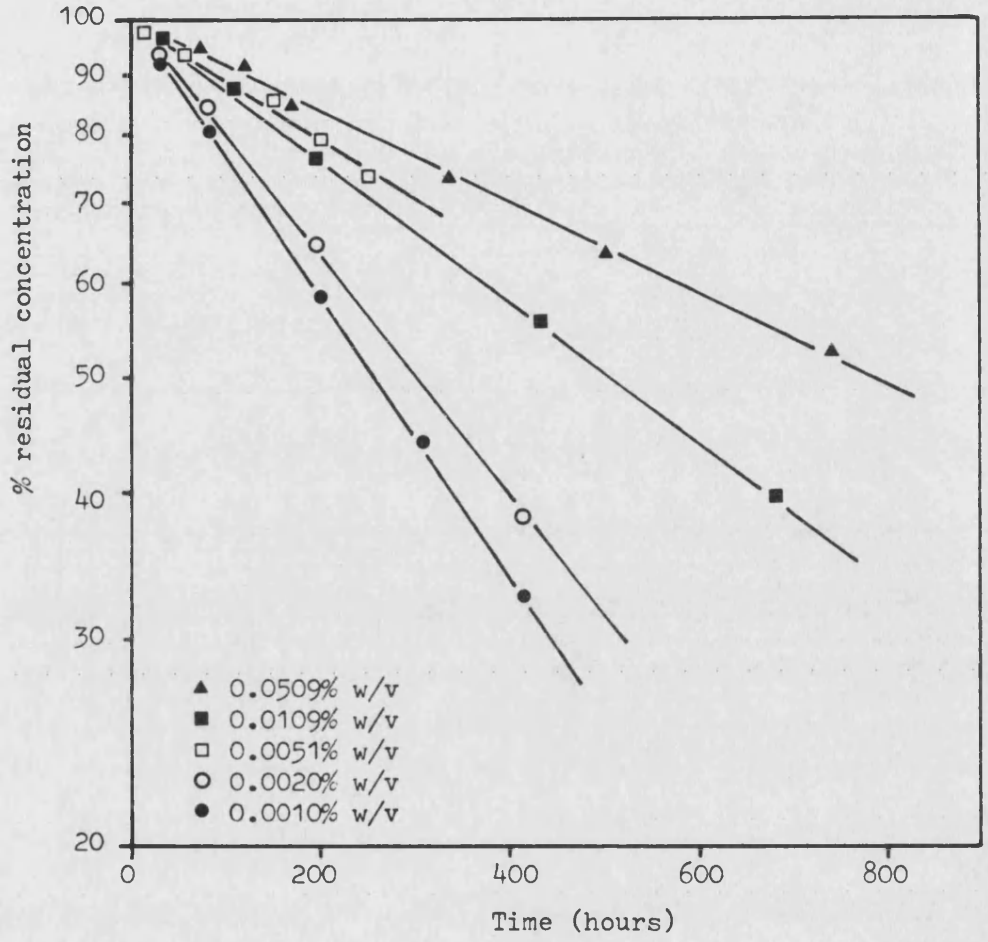

Figure 6.9 Effect of initial chlorhexidine gluconate concentration on first-order degradation plots at pH ~6 and 90°C

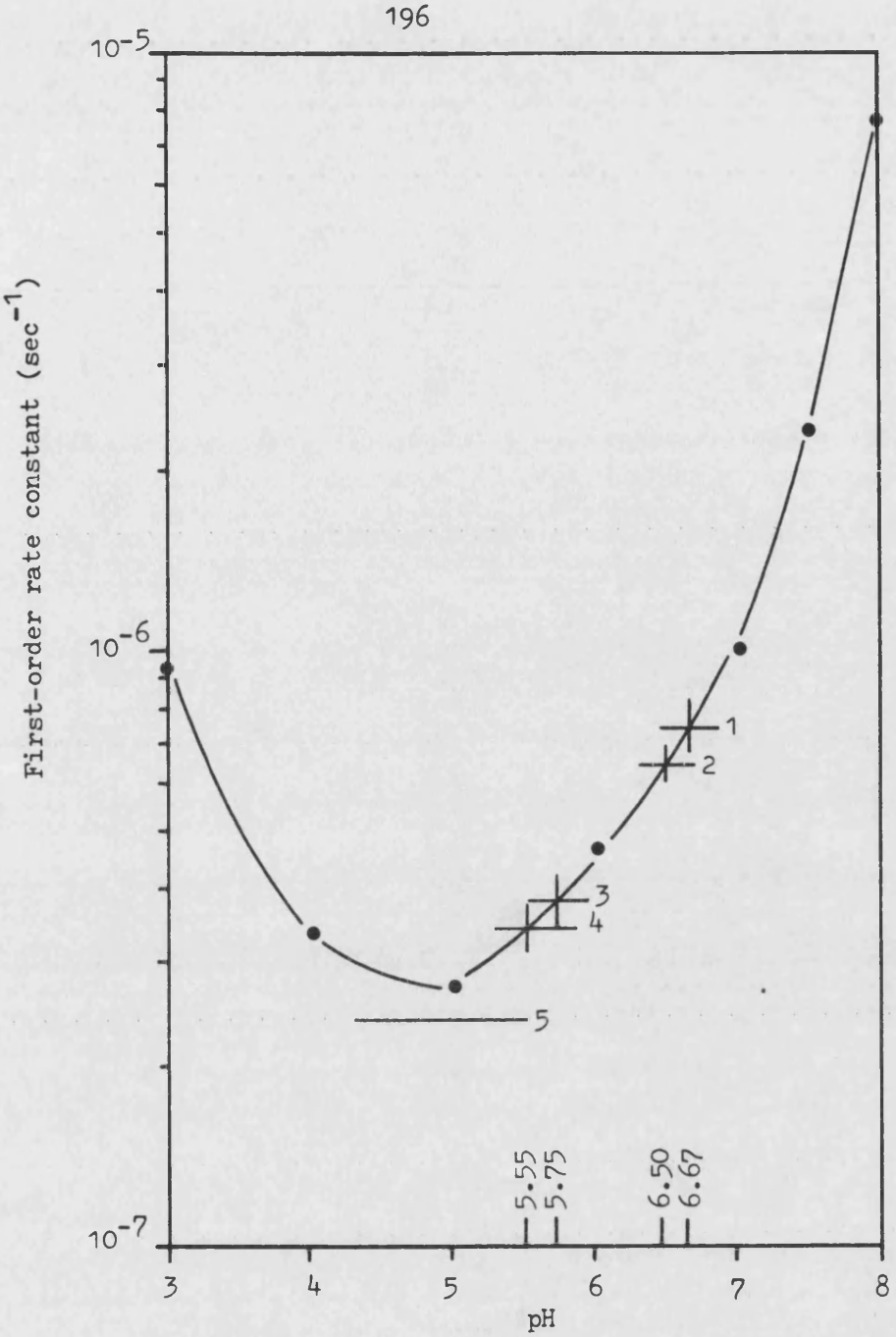

Figure 6.10 Generated rate constants for 0.001 to 0.051 % w/v initial chlorhexidine gluconate at 90°C (Table 6.9) are fitted to the pH-rate profile (also 90°C) in order to identify the pH range required to negate any concentration effect

1 0.001% : 7.44 x 10^{-7} sec^{-1} gives pH 6.67
2 0.002% : 6.48 x 10^{-7} sec^{-1} gives pH 6.50
3 0.011% : 3.71 x 10^{-7} sec^{-1} gives pH 5.75
4 0.005% : 3.29 x 10^{-7} sec^{-1} gives pH 5.55
5 0.051% : 2.42 x 10^{-7} sec^{-1} could not be fitted

(within a given concentration) had a total scatter of less than 0.2 pH unit at 25°C, it is apparent that the generated rate constants are due to a concentration effect. The fact that one rate constant (for 0.051% w/v chlorhexidine gluconate) could not be fitted to the pH-rate profile provides further evidence for this argument. It is also unlikely that the observed decrease in rate constant with increasing concentration would occur by chance.

The effect of concentration at pH values 2.0 (80°C), ~6 (90°C) and 9.0 (80°C) may be summarised by a plot of log $t_{\frac{1}{2}}$ against log initial concentration. Provided the order of reaction, n, does not change with initial concentration the slope of such a plot is (1-n), according to equation 5 (Chapter 1.2.1). Half lifes were determined from the relevant rate constant using the equation $t_{\frac{1}{2}} = 0.693/k$ and the data generated (Table 6.10) is plotted out in Figure 6.11. At pH 2.0, the derived slope was 0.006, which is close to the value (zero) consistent with a first-order rate process. At pH ~6.0 in distilled water the half life plot is linear giving a reaction order of ~0.7. The curved line for data at pH 9.0 may in part be associated with the presence of both di-protonated and non-protonated chlorhexidine species (Chapter 8). The plot also suggests a reaction order varying from 0.4-0.8. Fractional apparent orders, as found here, are usually associated with complex reaction mechanisms involving simultaneous, consecutive and/or reversible reactions (Chapter 1.2).

Initial chlorhexidine gluconate concentration (% w/v x 10^{3})	Log initial concentration	Half-life (hours)	Log half-life
pH 2.0 (self-buffering):			
1.98	-2.703	35.9	1.555
10.89	-1.963	36.7	1.565
51.19	-1.291	36.6	1.564
Linear regression analysis of log initial conc. vs log $t_{\frac{1}{2}}$:			
Correlation coefficient	0.8328		
Slope (SD)	0.0064 (0.004)		
RSD slope	66%		
Calculated reaction order	0.99		
pH ~6 (distilled water):			
1.00	-3.000	258.7	2.413
2.03	-2.693	297.1	2.473
5.07	-2.295	585.1	2.767
10.88	-1.963	518.3	2.715
50.90	-1.293	794.5	2.900
Linear regression analysis of log initial conc. vs log $t_{\frac{1}{2}}$:			
Correlation coefficient	0.9361		
Slope (SD)	0.289 (0.063)		
RSD slope	22%		
Calculated reaction order	0.71		
pH 9.0 (pH-stat):			
1.06	-2.975	14.0	1.146
1.80	-2.745	14.6	1.164
2.05	-2.688	13.5	1.130
2.13	-2.672	15.2	1.182
2.27	-2.644	16.0	1.204
3.96	-2.402	19.3	1.284
11.84	-1.927	36.9	1.567
54.86	-1.261	106.4	2.027
Linear regression of log initial conc. vs log $t_{\frac{1}{2}}$ not performed since Figure 6.11 indicates a non-linear relationship			

Table 6.10 Concentration effect data expressed as log initial concentration and log half-life. Linear regression analysis for Figure 6.11 is also given.

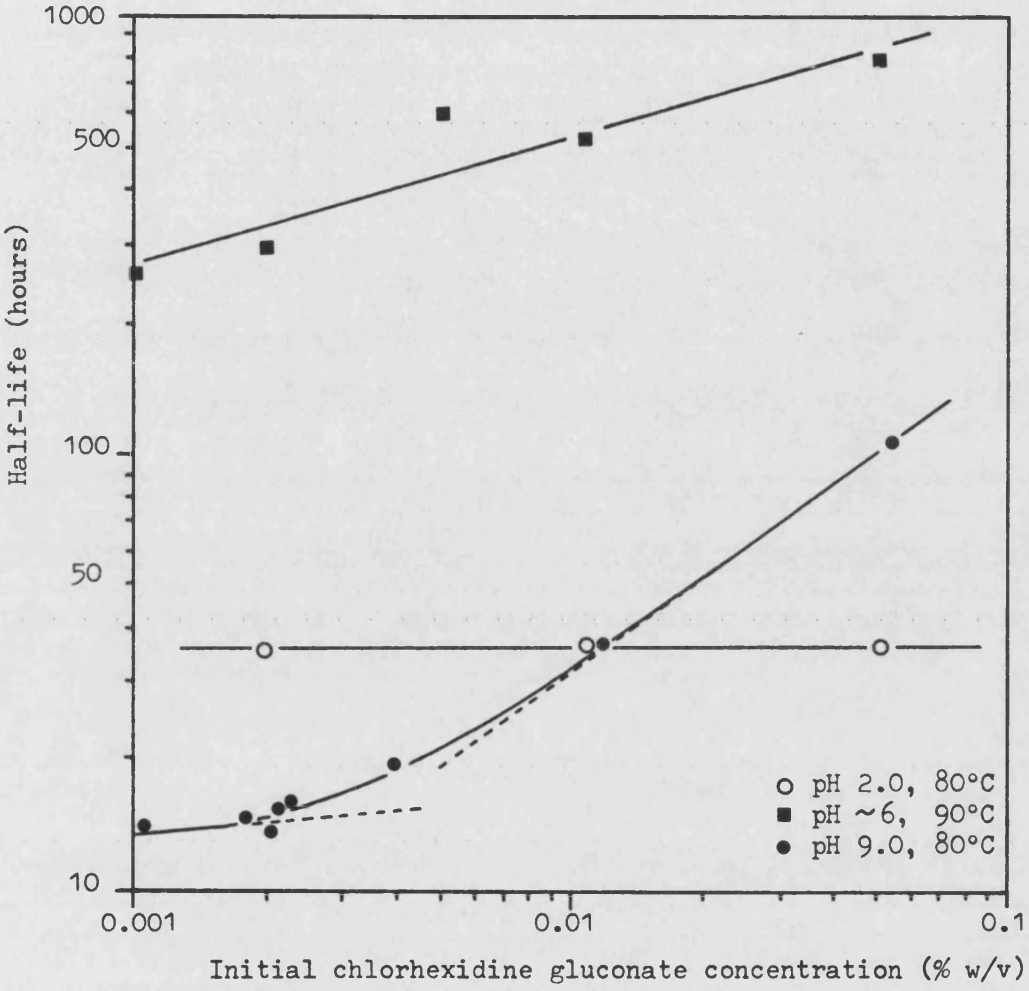

Figure 6.11 Log/log plot of initial chlorhexidine gluconate concentration against half-life (calculated from first-order kinetics) for degradation at pH 2.0 (80°C), ~6 (90°C) and 9.0 (80°C). Slopes are drawn from linear regression analysis of pH 2.0 and ~6 data. Tangents drawn to pH 9.0 data

6.6.4 Effect of Temperature

The relationship between temperature, over the range 60-90°C, and the rate of degradation of 0.002% w/v chlorhexidine gluconate solutions was examined at pH 2.0 (self-buffering), pH ~6 (ampoules) and pH 9.0 (pH-stat). Degradation profiles for each temperature are shown in Figures 6.12 (pH 2.0), 6.13 (pH ~6) and 6.14 (pH 9.0). First-order rate constants at each condition are listed in Table 6.11.

Arrhenius plots at the three pH values are shown in Figure 6.15. Activation energies and pre-exponential (frequency) factors, derived from the Arrhenius equation by linear regression analysis of the data (equation 20, Chapter 1.3), are also given in Table 6.11.

6.6.5 Effect of Ionic Strength

The presence of primary salt effects were tested in 2.2×10^{-5} M solutions of chlorhexidine salts (equivalent to 0.002% w/v chlorhexidine gluconate) at pH 9.0 (pH-stat) and 90°C. The study was also designed to investigate the influence of counter-ion strength on chlorhexidine degradation by adjusting ionic strength with potassium chloride for chlorhexidine hydrochloride, gluconic acid for chlorhexidine gluconate and acetic acid for chlorhexidine acetate solutions.

Assuming that chlorhexidine is only present as the dication at pH 9.0, at 90°C the combined ionic strength of chlorhexidine and hydroxyl ions, together with their associated counter-ions is 4.64×10^{-4} M. Therefore rate constants generated for chlorhexidine salts, at pH 9.0 and 90°C (Tables 6.3 and 6.7), were not produced at an "infinite dilution"; consequently these data are incorporated into the individual ionic strength effects. The addition of potassium chloride

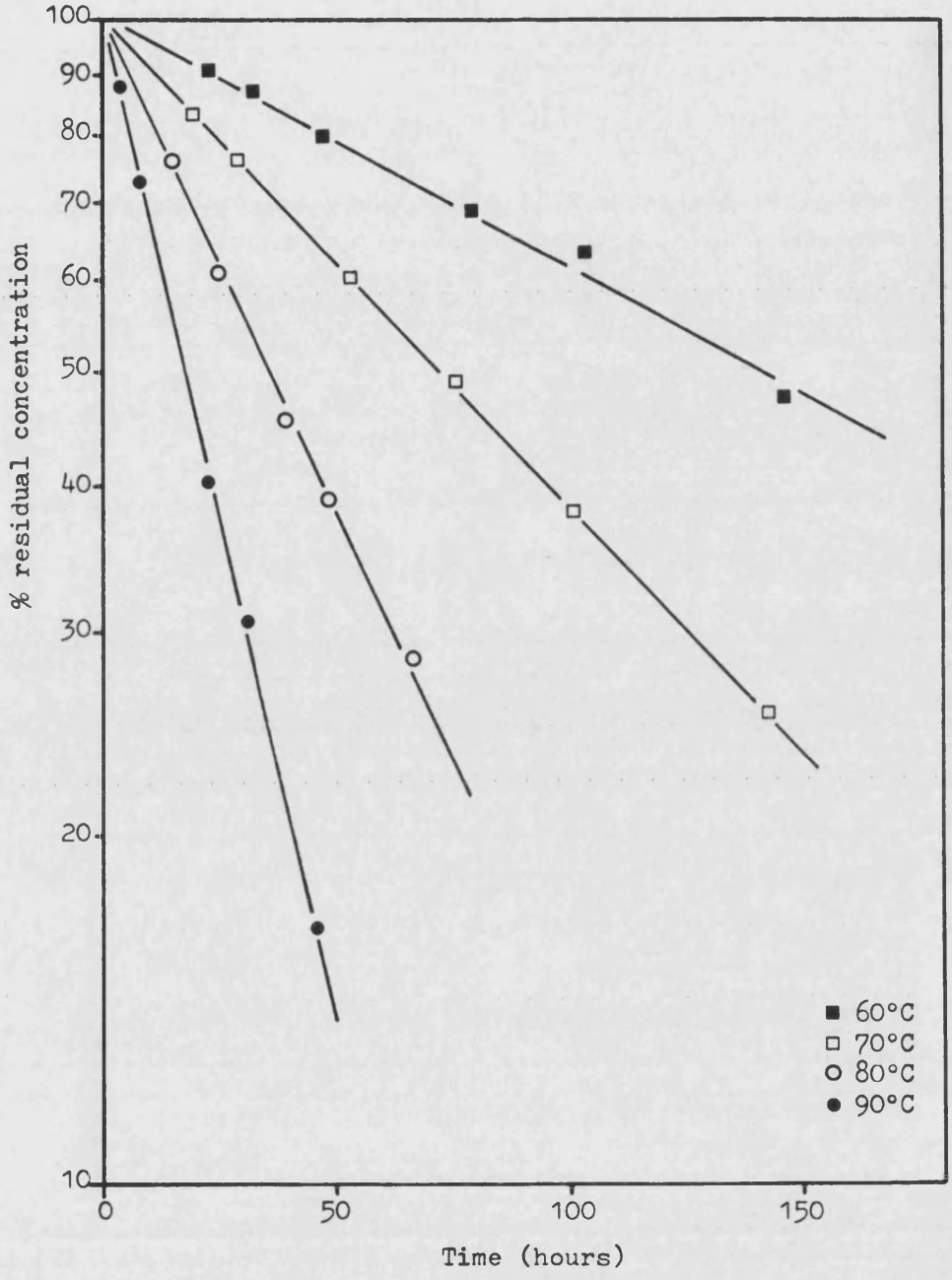

Figure 6.12 Effect of temperature on the first-order degradation plots of 0.002% w/v chlorhexidine gluconate at pH 2.0

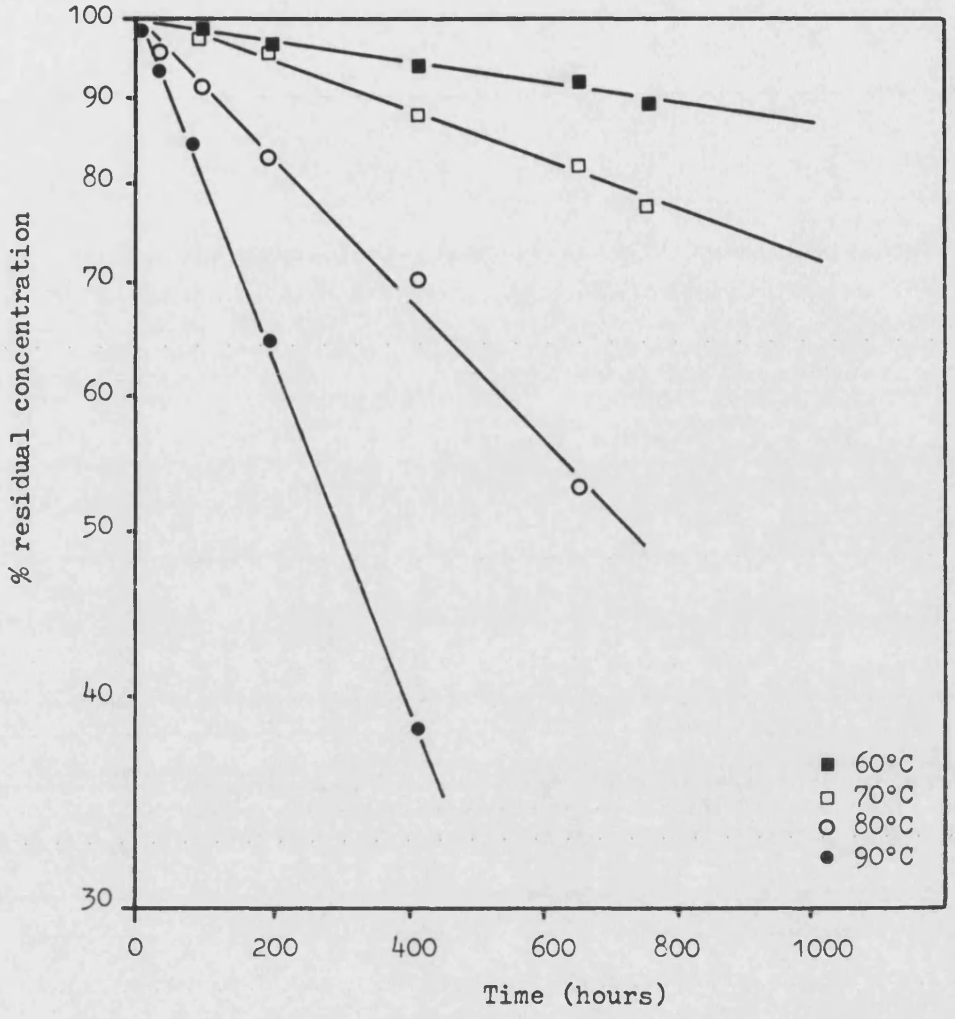

Figure 6.13 Effect of temperature on the first-order degradation plots of 0.002% w/v chlorhexidine gluconate at pH ~6

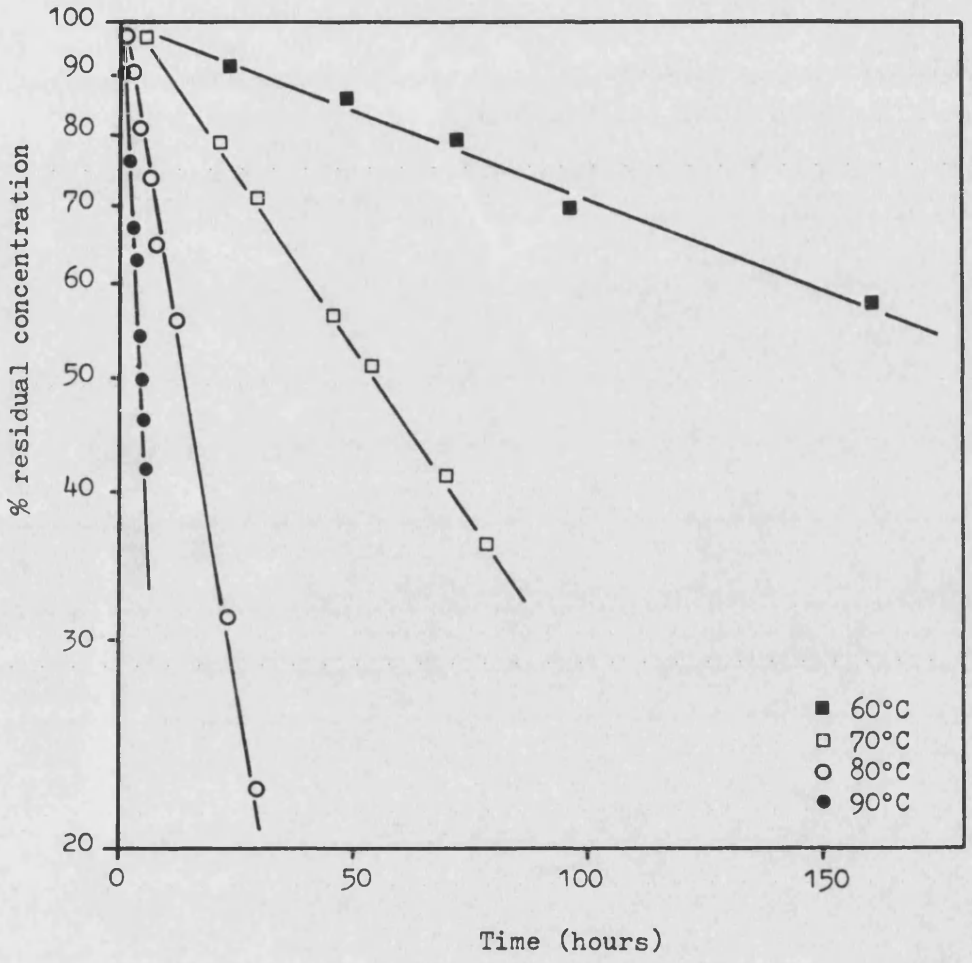

Figure 6.14 Effect of temperature on the first-order degradation plots of 0.002% w/v chlorhexidine gluconate at pH 9.0

		pH		
		2.0 (Self-buffering)	~6 (ampoules)	9.0 (pH-stat)
Degradation rate constant (sec^{-1}) (SD, sec^{-1})	60°C	1.38×10^{-6} (4.0×10^{-8})	3.77×10^{-8} (7.6×10^{-10})	9.71×10^{-7} (1.9×10^{-8})
	70°C	2.67×10^{-6} (1.7×10^{-8})	9.36×10^{-8} (1.7×10^{-9})	3.67×10^{-6} (6.7×10^{-8})
	80°C	5.53×10^{-6} (9.3×10^{-8})	2.59×10^{-7} (5.7×10^{-9})	1.43×10^{-5} (2.5×10^{-7})
	90°C	1.08×10^{-5} (2.7×10^{-7})	6.48×10^{-7} (5.5×10^{-9})	4.45×10^{-5} (5.3×10^{-7})
Linear regression analysis of Arrhenius plots:				
Correlation coefficient		0.9994	0.9993	0.9997
Slope (SD)		3630.1 (91.1)	5016.2 (135.2)	6744.4 (115.4)
RSD slope		2.5%	2.7%	1.7%
Intercept (SD)		5.027 (0.262)	7.623 (0.389)	14.239 (0.332)
From slope:				
Apparent Activation energy ($kJ\ mol^{-1}$ ± 95% confidence limit)		69.5 (±2.8)	96.1 (±4.1)	129.1 (±3.5)
From intercept:				
Frequency Factor (sec^{-1})		1.06×10^{5}	4.20×10^{7}	1.73×10^{14}

Table 6.11 Effect of temperature on first-order degradation rate constants at pH 2.0, ~6 and 9.0 using 0.002% chlorhexidine gluconate. Linear regression analysis was also performed on the data fitted to the Arrhenius relationship.

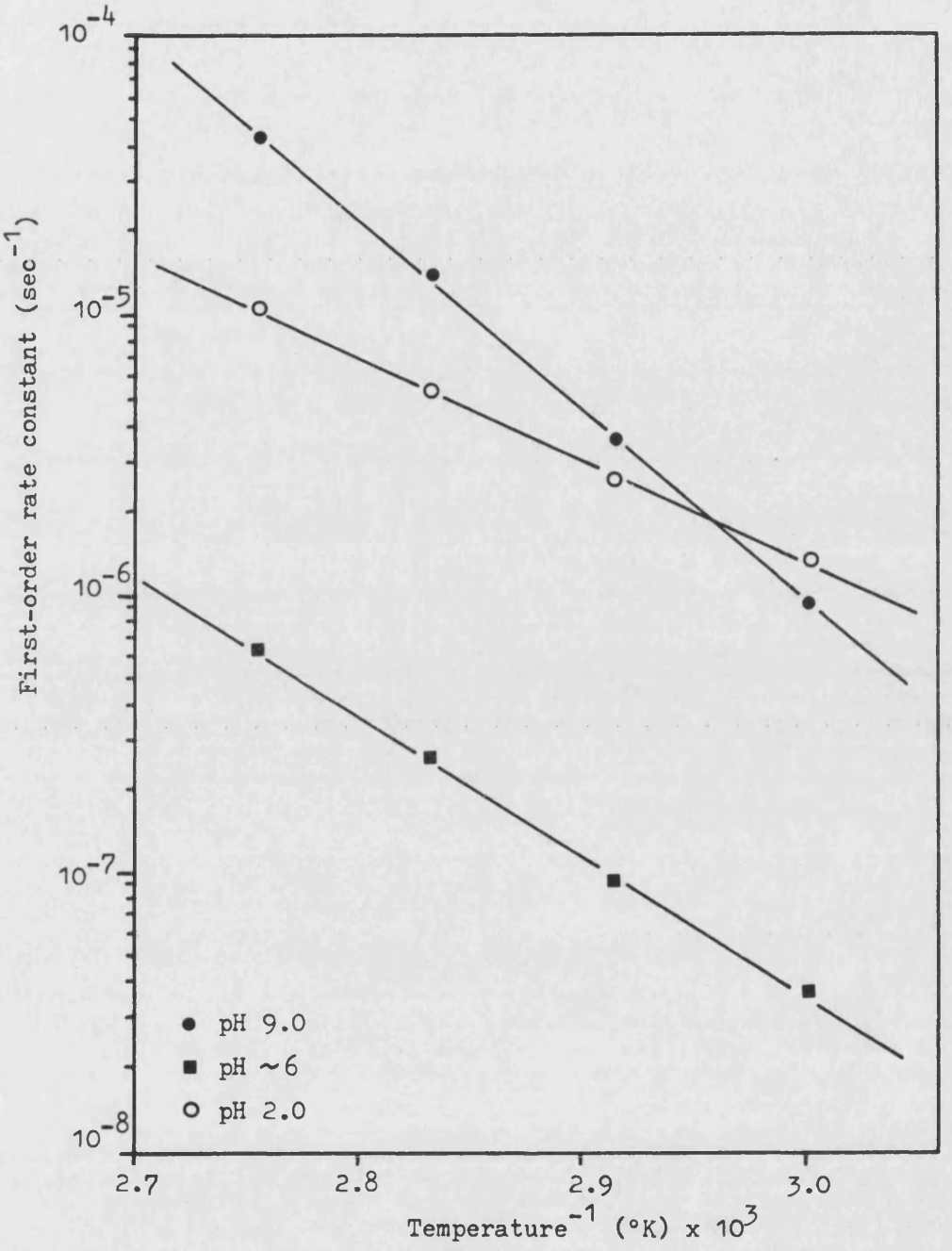

Figure 6.15 Arrhenius plot illustrating the effect of temperature on observed first-order degradation rate constants of 0.002% w/v chlorhexidine gluconate solutions at pH 2.0, ~6 and 9.0. The slopes yield apparent activation energies

or gluconic acid in concentrations ranging from 0.01 to 0.5 M, taking into account the "original" ionic strength, therefore resulted in total ionic strengths of 0.0105 to 0.501 M.

Because of problems with the HPLC assay at higher ionic strengths than 0.1 M, solutions were pre-diluted with distilled water prior to the 2 in 10 dilution with mobile phase. This was an attempt to "dilute-out" the counter-ion influence on chromatographic response (see Chapter 5.1.1.2.4). Pre-dilution required the detector sensitivity to be set at its maximum; practically this was 0.005 AUFS. At ionic strengths less than 0.1 M pre-dilution was not generally required for chlorhexidine hydrochloride and gluconate solutions. Whilst chlorhexidine hydrochloride solutions of up to 0.5 M ionic strength could be assayed, chlorhexidine gluconate solutions of >0.1 M ionic strength could not be assayed due to peak splitting even after dilution. The situation was even worse for chlorhexidine acetate solutions since solutions of >0.01 M ionic strength could not be assayed by HPLC due to counter-ion interference as the chlorhexidine peak remained unresolved from the solvent front. The colorimetric assay of Holbrook (1958) was not considered as an alternative method due to its lack of sensitivity (Chapter 5.1.2.3). Consequently no data on the effect of ionic strength adjustment by acetic acid on chlorhexidine acetate was obtained.

Degradation profiles for chlorhexidine hydrochloride at ionic strengths 0.01 to 0.5 M added potassium chloride are shown in Figure 6.16. Table 6.12 lists the observed rate constants from experimentation with chlorhexidine hydrochloride and gluconate at various ionic strengths. These data show that increasing ionic strength decreases the observed degradation rate constant. This

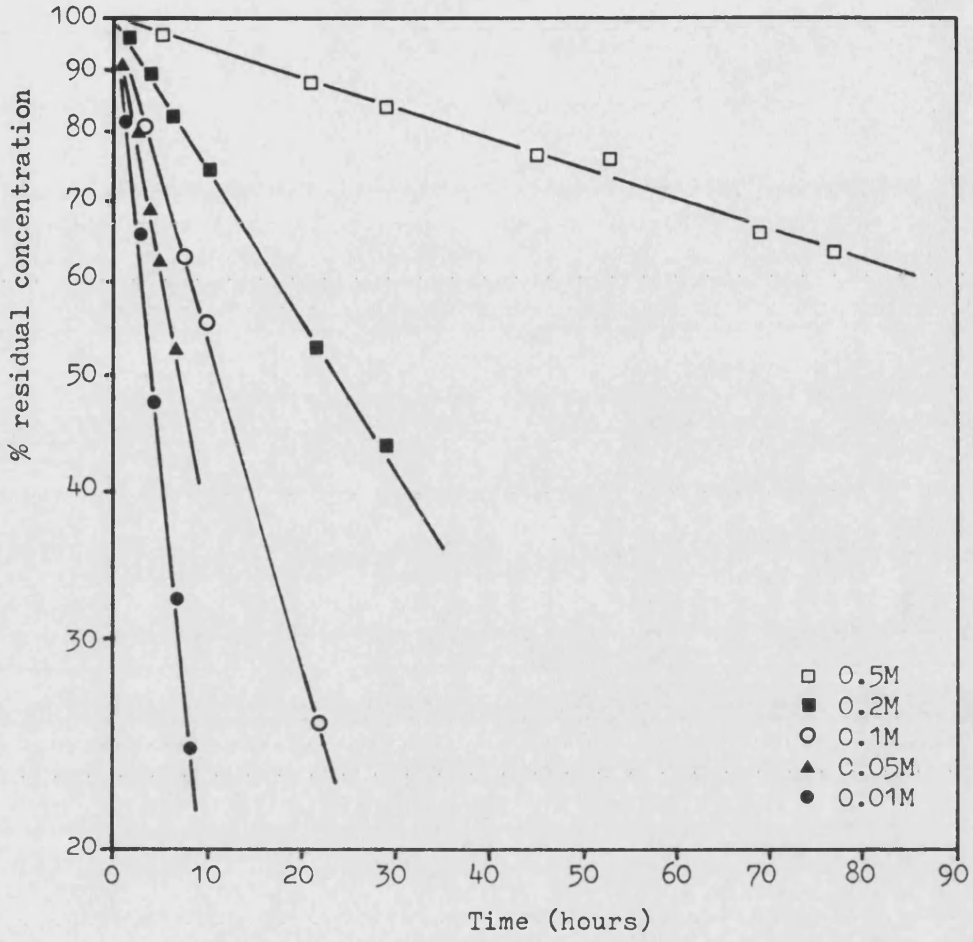

Figure 6.16 Effect of ionic strength $(KCl)_5$ on the first-order degradation plots of 2.2×10^{-5} M chlorhexidine hydrochloride solutions at pH 9.0 and 90°C

indicates the presence of a negative salt effect. In its various forms the Bronsted-Bjerrum equation (equations 41 to 43) predicts a linear relationship if the logarithm of the observed rate constant is plotted against the square root of ionic strength. The slope produced is proportional to the product of the respective charges ($Z_A Z_B$) of the two reacting species. Such plots were constructed for chlorhexidine hydrochloride and gluconate (Figure 6.17). Table 6.12 also shows the results from linear regression analysis of the data which gave slopes of -2.20 (±0.17) and -2.17 (±0.59) for the hydrochloride and gluconate solutions respectively.

Ionic strength (M)	Observed first-order degradation rate constant ($sec^{-1} \times 10^5$ (SD, $sec^{-1} \times 10^7$)	
	gluconate	hydrochloride
4.64×10^{-4}	4.45 (5.3)	4.34 (8.7)
1.05×10^{-2}	4.43 (13.0)	4.82 (14.0)
5.05×10^{-2}	2.32 (4.3)	2.75 (6.2)
0.101	1.05 (3.0)	1.71 (3.0)
0.201	-	0.80 (1.4)
0.501	-	0.16 (0.2)
Linear regression analysis of log k against $\sqrt{I}$:		
Correlation coefficient	0.9529	0.9831
Slope (±95% confidence limit)	-2.17 (±0.59)	-2.20 (±0.17)
RSD slope	23%	9.5%
Intercept	-4.221	-4.150
Rate constant at infinite dilution (from intercept)	6.02×10^{-5} sec^{-1}	7.08×10^{-5} sec^{-1}

Table 6.12 Effect of ionic strength on first-order degradation rate constants of 2.2×10^{-5} M chlorhexidine gluconate or hydrochloride at pH 9.0 and 90°C. At 1.05×10^{-2} M and above, ionic strength was adjusted by the addition of gluconic acid (for gluconate) or potassium chloride (for hydrochloride). Regression data for log k against $\sqrt{I}$ is also shown.

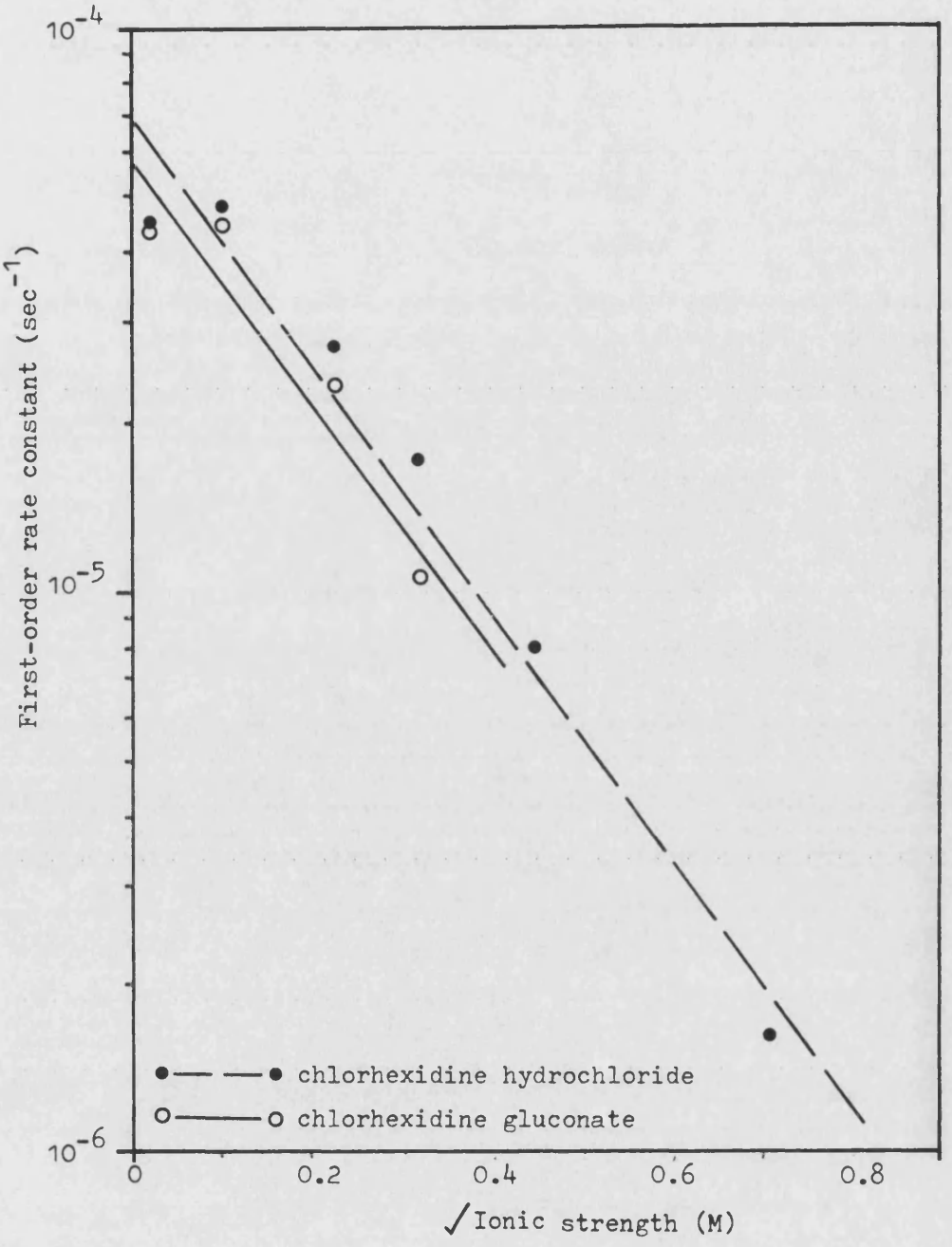

Figure 6.17 Plot of observed first-order degradation rate constant (log scale) against √ionic strength (Brönsted-Bjerrum relationship) for 2.2×10^{-5}M chlorhexidine hydrochloride and gluconate solutions at pH 9.0 and 90°C. Slopes drawn from linear regression analysis

6.6.6 Effect of Degradation Products

Although first-order degradation plots were linear down to approximately 20-30% residual, deviations occurred on more extensive degradation. This is illustrated by Figure 6.18. This observation indicates that the degradation products of the reaction may have some influence on the reaction mechanism and degradation rate constant. Autocatalysis is said to occur when the rate of degradation is accelerated by the presence of degradation products.

Since Figure 6.18 showed that the rate was slowed down at increased levels of degradation products a test was performed to investigate this effect further. A 0.002% w/v chlorhexidine solution was degraded at pH 9.0 (pH-stat) and 90°C. At approximately 30% residual the solution was assayed and chlorhexidine gluconate added to the reactant solution to bring its concentration back to 0.002% w/v (i.e. 100% residual). Degradation was again allowed to proceed to about 50% residual, allowing the theoretical concentration of degradation products to increase before repeating the operation. The degradation profiles produced are shown in Figure 6.19 and rate constant data are listed in Table 6.13.

Reactant solution	Observed first-order degradation rate constant, $sec^{-1} \times 10^{5}$ (SD, $sec^{-1} \times 10^{7}$)
Normal degradation	4.52 (10.0)
Once degraded	3.17 (8.2)
Twice degraded	2.84 (8.1)

Table 6.13 Effect of the presence of degradation products on observed first-order degradation rate constants. Experiments were performed on 0.002% w/v chlorhexidine gluconate degraded at pH 9.0 and 90°C.

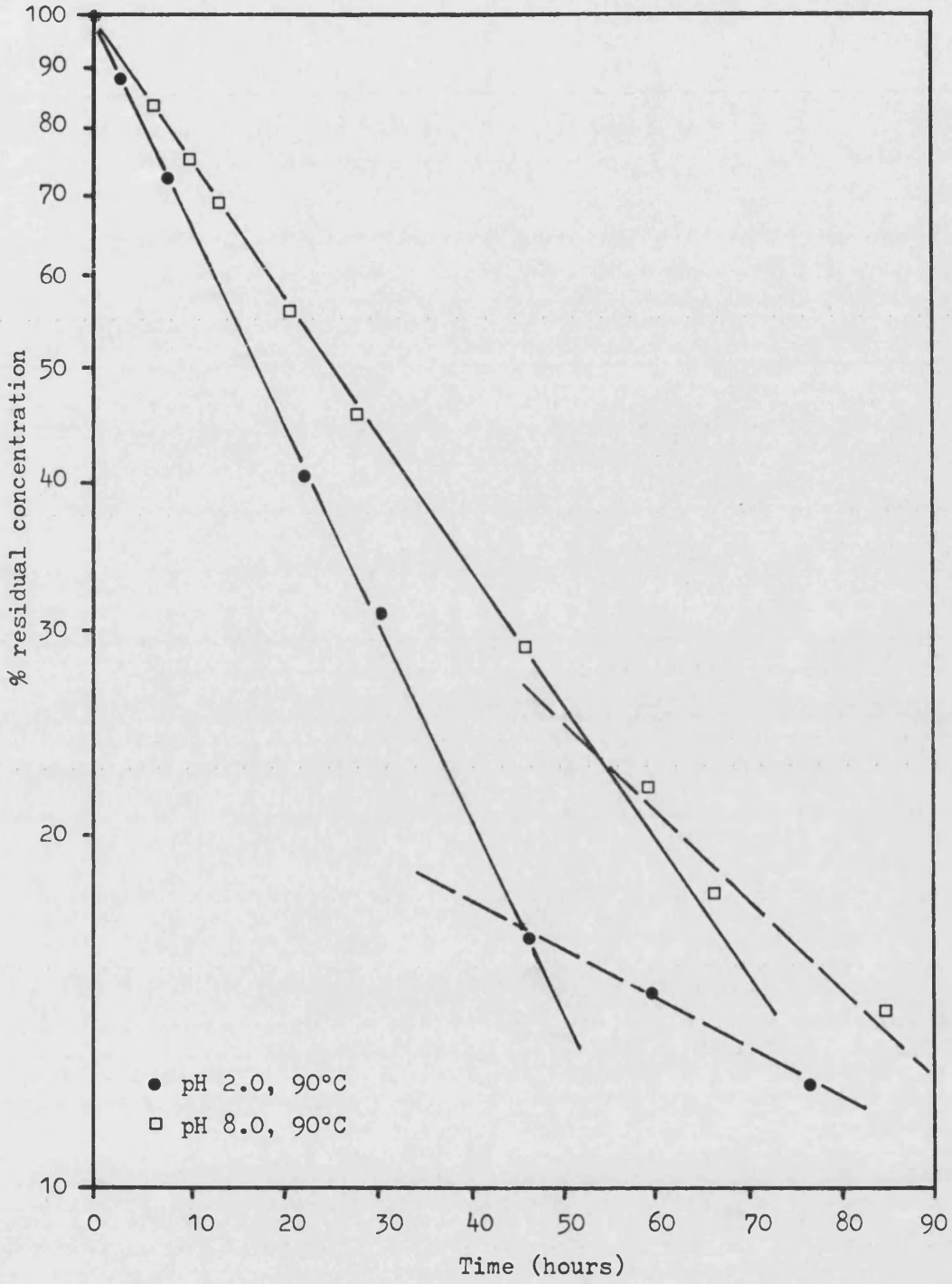

Figure 6.18 Degradation profiles showing non-linearity to first-order kinetics below 20 - 30% residual concentration. Both plots come from experimentation with 0.002% w/v chlorhexidine gluconate

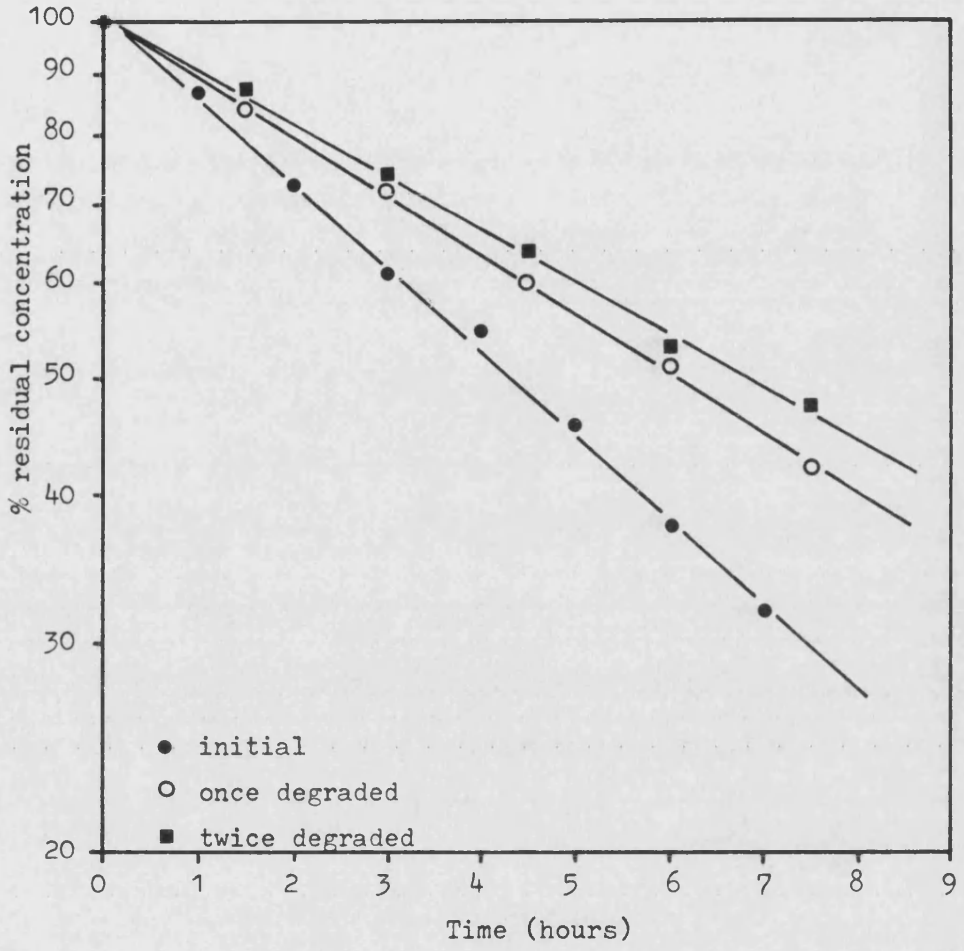

Figure 6.19 Effect of degradation products on first-order degradation plots of 0.002% w/v (initial) chlorhexidine gluconate solutions at pH 9.0 and 90°C. Once and twice degraded solutions were returned to 0.002% w/v initial chlorhexidine gluconate and their new profiles plotted

Although degradation still obeyed first-order kinetics, a decrease in the observed degradation rate constant was noted with increasing degradation product concentration, indicating a reverse-autocatalysis mechanism.

6.6.7 Effect of Buffers

Three buffer systems were chosen, acetate (pH 4.0), phosphate (pH 7.0) and borate (pH 9.0). The reported incompatibility (precipitation) with phosphate and borate salts is dependent on chlorhexidine concentration and generally occurs at >0.05% w/v chlorhexidine gluconate (Martindale, 1982). The following studies were conducted at 0.002% w/v chlorhexidine gluconate and no precipitation was observed at any time during the study period. The buffer salts were chosen due to their acceptability as buffers for ophthalmic preparations. No specific information was available on buffer systems present in chlorhexidine formulations. In order to examine the significance of buffer effects (general acid-base catalysis), observed degradation rate constants were determined at various buffer strengths.

Table 6.14 lists the buffer formulae used in kinetic studies. These compositions were recommended by Perrin and Dempsey (1974) to produce pH values of 4.0, 7.0 and 9.0 at 25°C. However, at the temperature of kinetic experimentation (60 to 90°C), the measured values are obviously different due to the variation of pKa with temperature. Measured pH values of each buffer strength at 25 to 90°C are given in Table 6.15. The ionic strength of each composition at the temperature of kinetic experiments was calculated from equation 40 in order to identify any significant changes. The concentration of each buffer species was calculated from the Henderson-Hasselbalch equation

(69) ignoring activity coefficients, using the experimentally observed pH at each temperature;

$$pH = pKa + \log \frac{[salt]}{[acid]} \quad \ldots\ (69)$$

pKa-temperature relationships for the buffer salts were obtained from Robinson and Stokes (1958). Table 6.15 also lists these calculated ionic strengths. Only slight differences were observed in the acetate and borate systems but a decrease in ionic strength with increasing temperature was apparent in both phosphate systems. However, this variation was not considered significant (see Chapter 8) and no corrective potassium chloride was added.

	Molarity for buffer strength		
	Single strength	Approximately half strength	0.1 strength
pH 4.0 (Acetate) buffer:			
Acetic acid	0.082	-	0.0082
Sodium acetate	0.018	-	0.0018
pH 7.0 (Phosphate) buffer:			
Sodium dihydrogen orthophosphate	0.020	0.0098	0.0022
Disodium hydrogen orthophosphate	0.032	0.0152	0.0034
pH 9.0 (Borate) buffer:			
Disodium tetraborate	0.030	0.0125	0.003
Hydrochloric acid	0.011	0.0046	0.0011

Table 6.14 Buffer compositions for kinetic studies

All tabulated kinetic data include the experimental pH determined at the relevant temperature. The buffer capacity of all solutions was adequate since the measured pH changes (at 25°C) following storage were within the pH-meter sensitivity of ±0.002 pH units (Radiometer PHM64). All studies were performed in amber neutral glass ampoules (chlorhexidine aged).

Buffer systems (strength)		Ionic strength (M) and measured pH at temperature (°C)								
		25	60		70		80		90	
		pH	I	pH	I	pH	I	pH	I	pH
Acetate	(single)	4.011	0.0143	4.033	-	-	0.015	4.126	0.0145	4.151
	(~0.1)	4.016	0.0016	4.090	-	-	0.0017	4.181	0.0016	4.212
Phosphate	(single)	6.996	0.112	6.973	0.109	6.958	0.102	6.920	0.098	6.913
	(~half)	7.003	-		-		-		0.047	6.894
	(~0.1)	7.009	0.0127	7.040	0.0124	7.039	0.0177	6.988	0.010	7.011
Borate	(single)	9.021	0.027	8.960	0.027	8.919	0.027	8.900	0.026	8.883
	(~half)	9.016	-		-		-		0.011	8.861
	(~0.1)	9.024	0.003	9.016	0.003	9.010	0.003	8.983	0.003	8.961

Table 6.15 Variation of buffer pH and ionic strength with temperature

As found previously at high ionic strengths (Chapter 5.1.1.2.4), analytical problems were encountered during the HPLC assay of some buffered solutions. However, prior dilution with distilled water before assay eliminated such problems enabling the accurate quantitation of chlorhexidine.

6.6.7.1 Acetate Buffer pH 4.0

The observed degradation rate constants for 0.002% w/v chlorhexidine gluconate solutions buffered by single strength and 0.1 strength sodium acetate/acetic acid buffer were determined at 60, 80 and 90°C. Table 6.16 lists the degradation rate constants and experimental pH in the presence of these acetate buffers at 60, 80 and 90°C. Rate constants at zero buffer strength derived from the pH-rate profile at 90°C (see section 6.6.1) are also listed in Table 6.16.

Observed rate constants in all single strength buffer systems were significantly higher than those observed for the 0.1 buffer strength systems (t = 9.5, 7.6, 6.3 at 60, 80 and 90°C respectively). Possible explanations for this are discussed in Chapter 8. The experimental pH of each buffer strength was dependent on temperature and the observed downward drift with decreasing temperature obviously introduces error when comparing all data. However reasonable fits to Arrhenius plots (Figure 6.20) were obtained giving activation energies of 57.9 (±8.1) $kJ.mol^{-1}$, (RSD of slope 8.2%) and 66.5 (±7.7) $kJ.mol^{-1}$, (RSD of slope 6.9%) for the single and 0.1 strength buffers respectively.

At 90°C it was noted that the rate constant in single strength buffer was ~5% greater than that obtained from the pH-rate profile, whilst that in 0.1 strength buffer was ~7% lower.

Temperature (°C)	Observed first-order degradation rate constants $sec^{-1} \times 10^7$							
	Single strength buffer			0.1 strength buffer			pH-stat system (calculated)	
	pH	k_{obs}	SD	pH	k_{obs}	SD	pH	k_{obs}
60	4.033	0.57	0.016	4.090	0.38	0.012	-	-
80	4.126	1.67	0.034	4.181	1.35	0.025	-	-
90	4.151	3.30	0.028	4.212	2.88	0.061	4.15 4.20	3.15 3.10
Linear regression analysis of Arrhenius plots:								
Correleation coefficient		0.9966			0.9976			
Slope (SD)		3023.2 (249.4)			3476.9 (239.4)			
RSD slope		8.2%			6.9%			
Intercept (SD)		1.823 (0.715)			3.014 (0.686)			
From slope:								
Apparent Activation energy ($kJ.\ mol^{-1}$ ± 95% confidence limit)		57.9 (±8.1)			66.5 (±7.7)			
From intercept:								
Frequency Factor (sec^{-1})		66.5			1.03×10^3			

Table 6.16 Effect of acetate buffers on the degradation rate constants of 0.002% w/v chlorhexidine gluconate at various temperatures. Arrhenius plot data is also included.

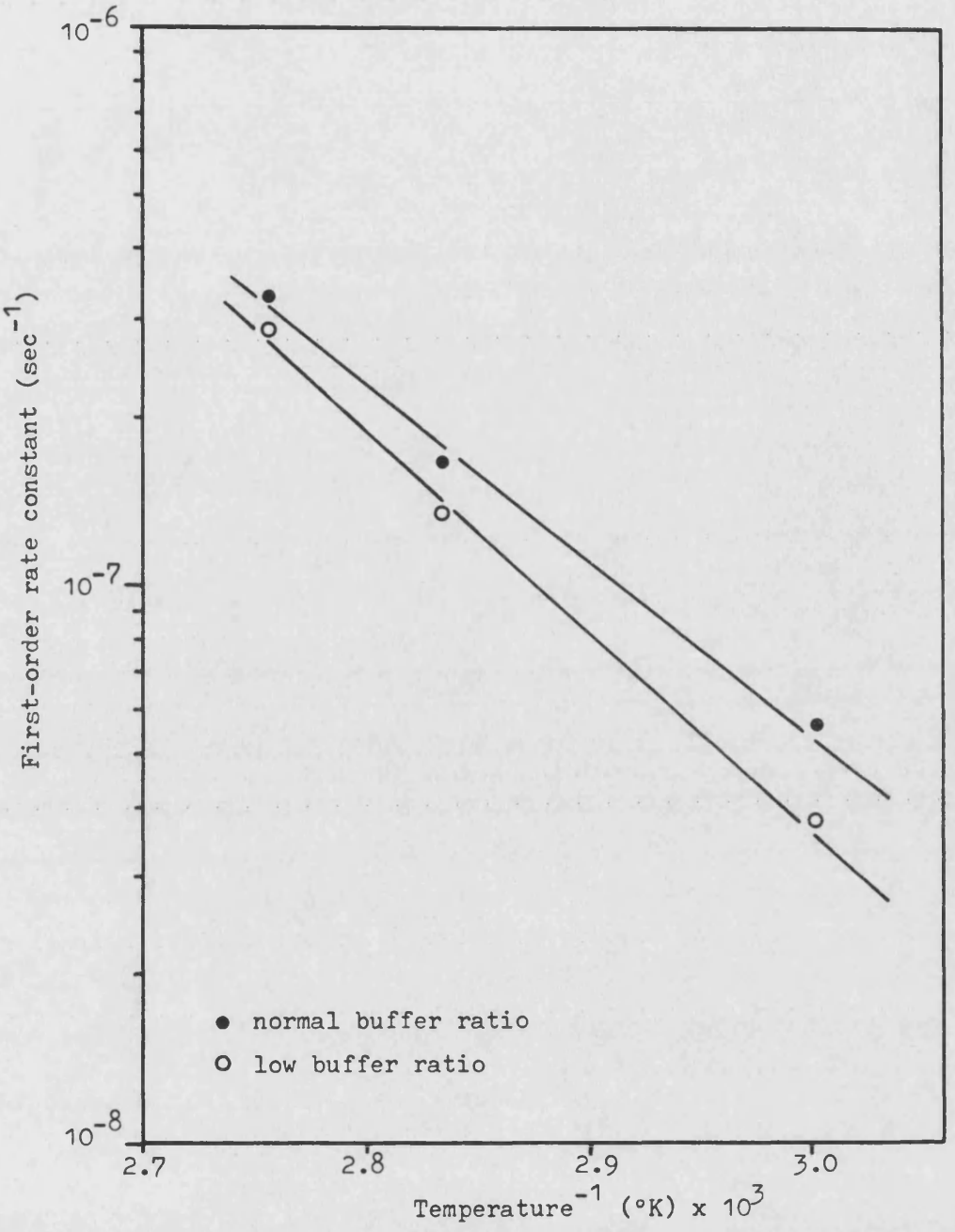

Figure 6.20 Arrhenius plot showing the effect of sodium acetate/acetic acid (~pH 4) buffer ratios on the observed first-order degradation rate constants of 0.002% w/v chlorhexidine gluconate solutions

6.6.7.2 Phosphate Buffer pH 7.0

Degradation rates for 0.002% w/v chlorhexidine gluconate solutions buffered by sodium dihydrogen phosphate/disodium hydrogen phosphate were determined at 90°C with single, half and 0.1 buffer strength systems; ionic strengths at 90°C were 0.098, 0.047 and 0.01 respectively. Table 6.17 lists the observed degradation rate constants, experimental pH and the rate constants at experimental pH derived from the pH-rate profile at 90°C (pH-stat study, see section 6.6.1). All observed rate constants in buffered solution were higher than those obtained from the pH-rate profile with the 0.1 buffer strength system producing a marked three-fold increase in the observed rate constant; this was a greater effect than that seen for the single strength. Data were also generated at 60, 70 and 80°C for single and 0.1 strength buffers systems. Rate constants from these studies are also listed in Table 6.17 and the resultant Arrhenius plots (Figure 6.21) gave activation energies of 85.3 (±4.4) $kJ.mol^{-1}$ and 104.6 (±4.3) $kJ.mol^{-1}$ for the single and 0.1 strength systems respectively. As at 90°C, 0.1 buffer concentration had a greater accelerating effect than full strength buffer. However, extrapolation of Figure 6.21 indicates a possible cross-over at approximately 52°C where the reverse situation should exist. Differences between experimental pH at the different temperatures were not large and good Arrhenius plots (RSD of 4.4 and 3.5%) were produced.

6.6.7.3 Borate Buffer pH 9.0

Observed degradation rate constants for 0.002% w/v chlorhexidine gluconate solutions buffered by sodium tetraborate/hydrochloric acid were determined at 60, 70, 80 and 90°C with single strength, half strength (only at 90°C) and 0.1 strength

Temperature (°C)	Observed first-order degradation rate constants $sec^{-1} \times 10^{6}$ (SD)							
	Single strength buffer			0.1 strength buffer			pH-stat system (calculated)	
	pH	k_{obs}	SD	pH	k_{obs}	SD	pH	k_{obs}
60	6.973	0.0978	0.0026	7.040	0.126	0.0037		
70	6.958	0.282	0.0053	7.039	0.404	0.0074		
80	6.920	0.599	0.0074	6.988	0.980	0.0210		
90	6.913	1.275	0.0153	7.011	2.996	0.0642	6.90	0.90
							7.00	1.00
	(half strength buffer at 90°C only			6.894	1.334	0.035)		
Linear regression analysis of Arrhenius plots:								
Correleation coefficient		0.9980			0.9988			
Slope (SD)		4455.9 (197.5)			5465.4 (192.3)			
RSD slope		4.4%			3.5%			
Intercept (SD)		6.400 (0.568)			9.515 (0.554)			
From slope:								
Apparent Activation energy ($kJ.mol^{-1}$ ±95% confidence limit)		85.3 (±4.4)			104.6 (±4.3)			
From intercept:								
Frequency Factor (sec^{-1})		2.51×10^{6}			3.27×10^{9}			

Table 6.17 Effect of phosphate buffers on the degradation rate constants of 0.002% w/v chlorhexidine gluconate at various temperatures. Arrhenius plot data is also included.

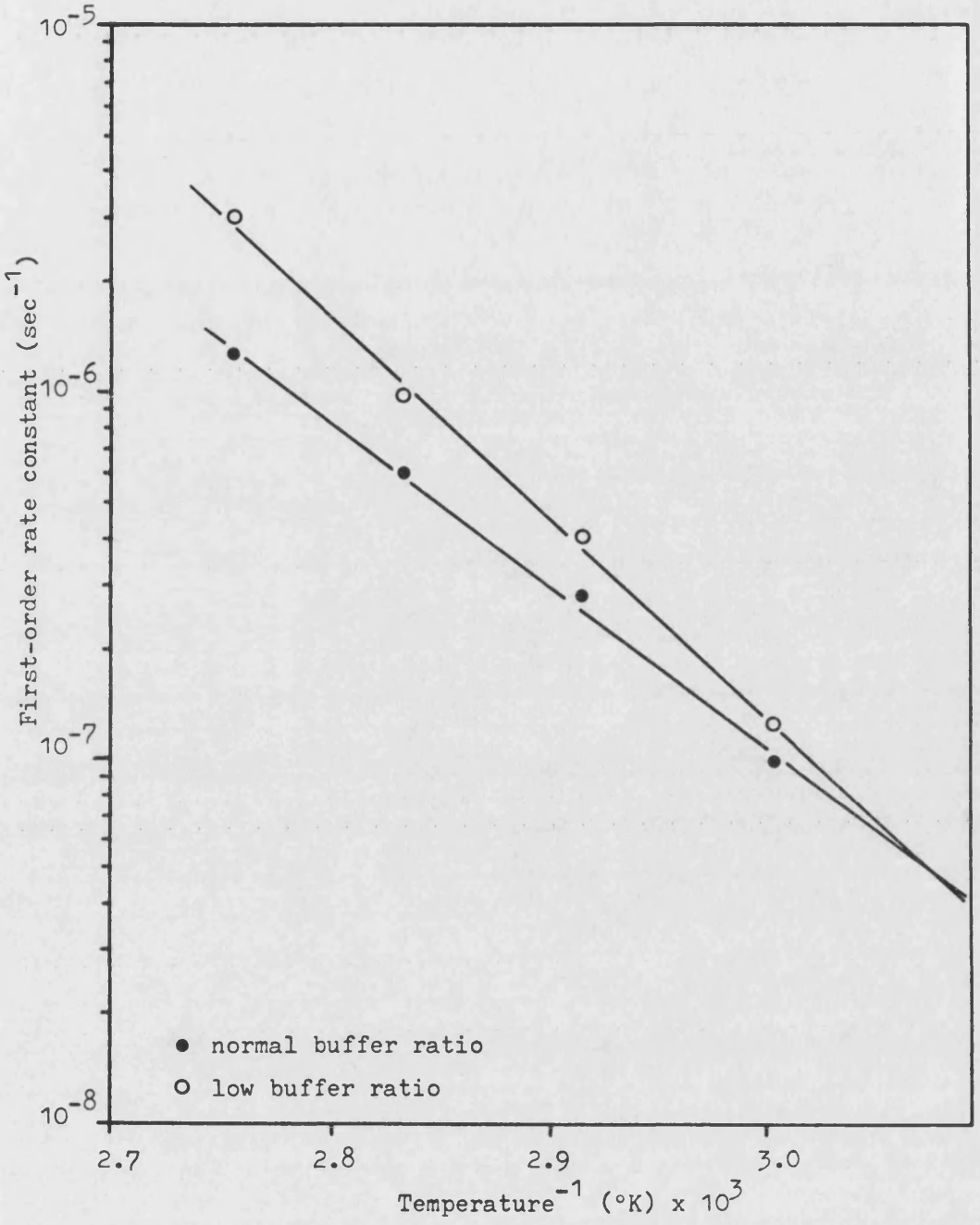

Figure 6.21 Arrhenius plot showing the effect of phosphate buffer ratios (~pH 7) on the observed first-order degradation rate constants of 0.002% w/v chlorhexidine gluconate solutions

buffer systems. Ionic strengths at 90°C were 0.026, 0.011 and 0.003 respectively. The rate constants in buffer, experimental pH and derived rate constants from the pH-rate profile at 90°C are listed in Table 6.18. At 90°C, all strengths of borate buffer decreased the rate relative to that in the absence of buffer by over four fold which is possibly indicative of some complexation between the chlorhexidine dication and the tetraborate anion $(B_4O_7)^{2-}$. It was also noted that the degradation rate constants in the single strength buffer were smaller, at all temperatures, than those in 0.1 strength buffer. However, in comparing these values, the influence of pH variation (up to 0.1 pH unit) between single and 0.1 strength buffer systems must be recognised in a region of specific base catalysis.

Attempts to fit the data for the borate buffer solutions to a linear Arrhenius relationship were unsuccessful (Figure 6.22) with gross curvature being apparent from both sets of data. Such curvature is indicative of complex reaction mechanisms (see Chapter 1.3.3.2). This is discussed further in Chapter 8.

6.6.8 Effect of Surfactants

The effect of surfactants on chlorhexidine gluconate degradation kinetics was investigated since many proprietary products contain non-ionic or cationic surfactants (see Chapter 2.1.5).

6.6.8.1 Choice of Surfactants

Cationic : Many ICI formulations contain various ratios of chlorhexidine and cetrimide BP (a mixture of chiefly tetradecyl trimethylammonium bromide with smaller amounts of dodecyl- and hexadecyl-trimethyl ammonium bromides). However, the cationic surfactant effect study was performed using hexadecyl trimethylammonium bromide (CTAB) and not cetrimide BP because : (i) it was available in a

Temperature (°C)	Observed first-order degradation rate constants $sec^{-1} \times 10^{6}$ (SD)							
	Single strength buffer			0.1 strength buffer			pH-stat system (calculated)	
	pH	k_{obs}	SD	pH	k_{obs}	SD	pH	k_{obs}
60	8.960	0.194	0.0052	9.016	0.47	0.014		
70	8.919	1.84	0.041	9.010	2.65	0.077		
80	8.900	6.12	0.079	8.983	7.76	0.086		
90	8.883	6.56	0.182	8.961	8.99	0.176	8.85	38.0
							8.90	40.0
		(~0.5 strength buffer at 90°C only		8.861	8.48	0.237)	8.95	42.0
							9.00	45.00

Table 6.18 Effect of borate buffers on the degradation rate constants of 0.002% w/v chlorhexidine gluconate at various temperatures

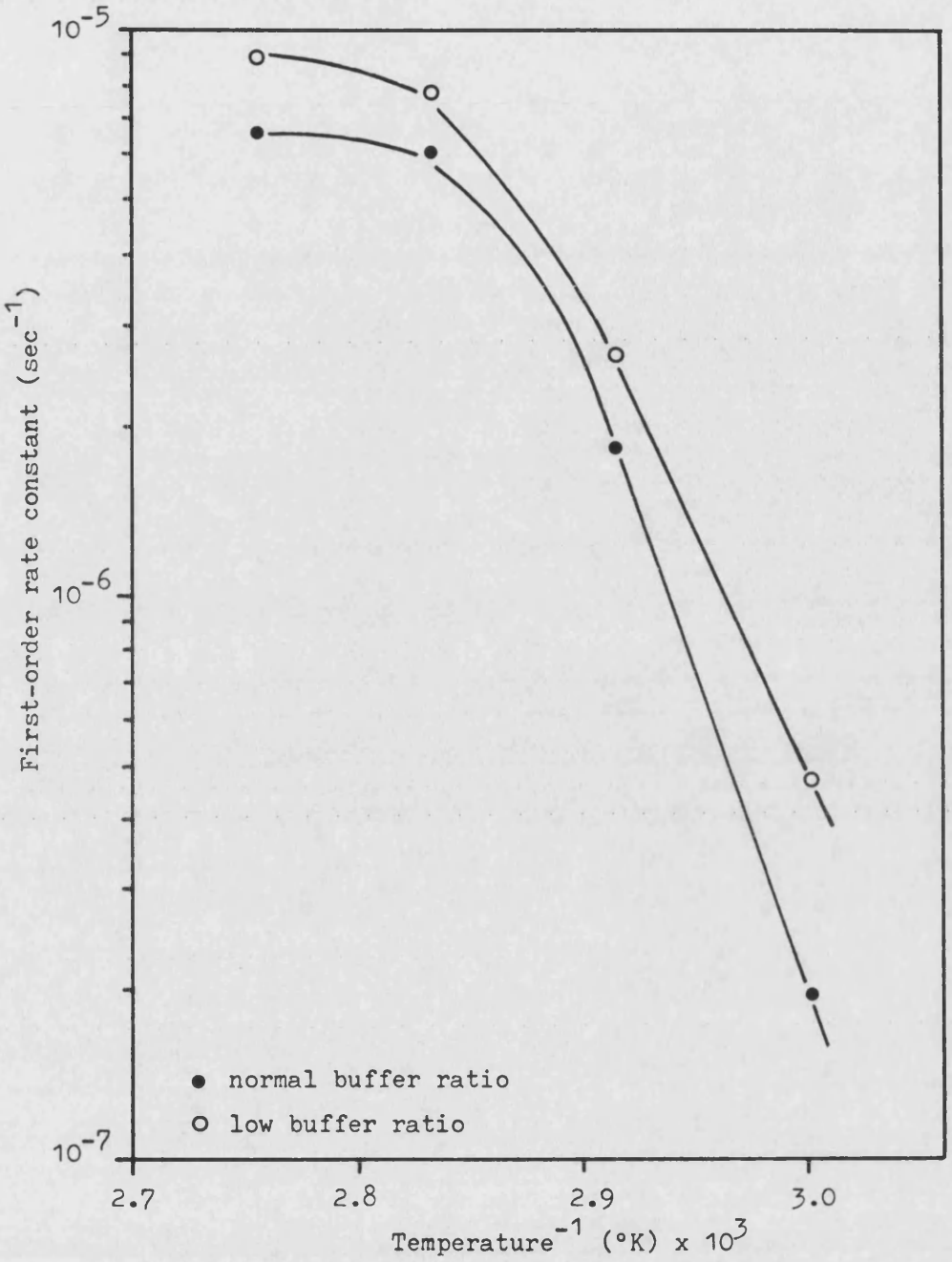

Figure 6.22 Arrhenius plot showing the effect of sodium tetraborate/HCl buffer ratios (~pH 9) on the observed first-order degradation rate constants of 0.002% w/v chlorhexidine gluconate solutions

relatively pure form (>99%, AnalaR, BDH) and not a mixture of several hydrocarbon chain lengths and (ii) its effect on the reactivity of many compounds is well documented in the pharmaceutical literature.

Non-ionic : The surfactant effect of the two standard pharmacopoeial non-ionic surfactants was investigated; cetomacrogol 1000 BP, a polyoxyethylated glycol monoether and polysorbate 80 BP, polyoxyethylene (20) sorbitan mono-oleate. These are both mixtures of various ethylene oxide chain length.

Anionic : Although anionic surfactants are "incompatible" with the cationic chlorhexidine molecule, experimentation was performed with systems containing sodium dodecyl sulphate (NaDS) to investigate whether degradation of complexed systems occurs.

6.6.8.2 Degradation Conditions Used

Surfactant solution properties can be significantly modified by accelerated stress conditions. Temperature can have a pronounced effect inducing coacervation or phase separation above a critical temperature with both cationic and non-ionic surfactants. With the latter the phase separation temperature is referred to as the cloud point. The CMC of surfactants may also be altered by increasing temperature. Therefore literature CMC values, at the nearest temperature to the stability studies, are quoted in the following sections. However, the influence of reactants upon CMC must also be considered (see Chapter 1.6.5.2) and, where possible, experimentation was performed across a wide concentration band in order to identify effects above and below the likely CMC. Also visual inspection of all solutions at the study temperature and after cooling to room temperature confirmed that no system formed a coacervate.

Choice of a stress temperature of 70°C was ultimately made due to the possible auto-oxidation of non-ionic surfactant solutions on storage at elevated temperatures (Donbrow et al, 1978; Hamburger et al, 1975; see also Chapter 1.6.5.5). Donbrow et al (1978) noted a decrease in the cloud point on auto-oxidation of polysorbate 20, however under the conditions used herein (70°C, light shielded) no turbidity was noted on completion of stability studies.

The direct effect of pH on the CMC of surfactants is less well documented. Work in this department has previously shown that, in basic conditions, pH variation had little effect on the CMC of CTAB (Beg, 1977; Shetewi, 1975). In buffered systems effects on CMC are associated with ionic strength changes. In line with the majority of kinetic studies, a pH of 9.0 (pH-stat) was used for degradation studies with surfactant systems.

6.6.8.3 Degradation Kinetics

6.6.8.3.1 Cationic Surfactant

At 70°C, the CMC of CTAB has been reported as ~1.5 x 10^{-3} M (Mukerjee and Mysels, 1971). The influence of CTAB concentrations ranging from 2 x 10^{-5} to 2 x 10^{-2} M on the degradation kinetics of 0.002% w/v chlorhexidine gluconate pH-statted at pH 9.0 and 70°C was investigated. Chlorhexidine could not be quantitatively assayed in CTAB solutions in excess of 2 x 10^{-2} M due to peak interference. As previously the rate data were plotted according to first-order kinetics. Figure 6.23 shows the degradation profiles obtained and Table 6.19 lists the apparent first-order rate constants. The presence of surfactant at 6 x 10^{-5} M and above reduced the degradation rate.

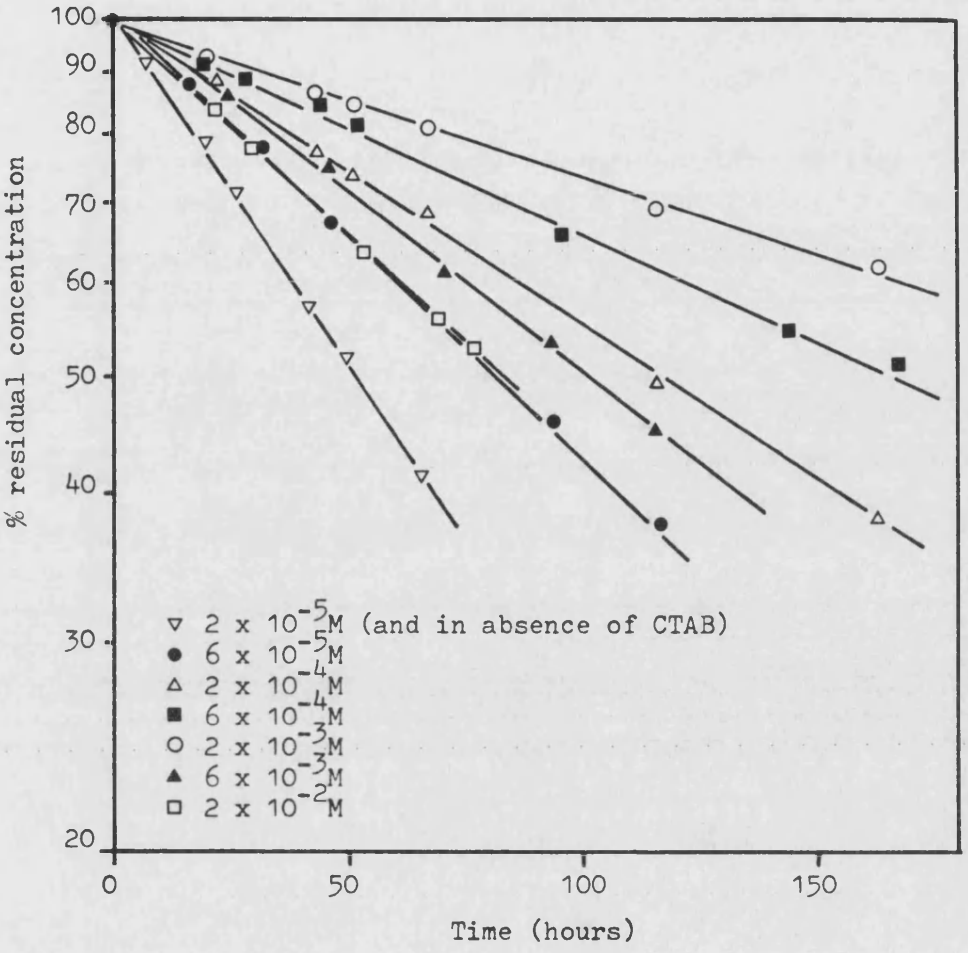

Figure 6.23 Effect of CTAB concentration on the first-order degradation plots of 0.002% w/v chlorhexidine gluconate solutions at pH 9.0 and 70°C. The plot in the absence of CTAB is identical to that in the presence of 2×10^{-5}M CTAB

This protective effect has been expressed in terms of a surfactant effect ratio, i.e. the ratio of k_o : k_{obs} surfactant, where k_o is the rate constant at pH 9.0 (pH-stat) and 70°C of a 0.002% w/v chlorhexidine gluconate solution in the absence of surfactant.

CTAB concentration (molarity)	Observed first-order degradation rate constant		Surfactant effect ratio
	($sec^{-1} \times 10^{6}$)	SD ($sec^{-1} \times 10^{8}$)	(k_o : k_{obs} surfactant)
2×10^{-5}	3.68	6.0	1.00
6×10^{-5}	2.40	7.0	1.53
2×10^{-4}	1.60	4.8	2.29
6×10^{-4}	1.14	3.0	3.22
2×10^{-3}	0.80	2.2	4.59
6×10^{-3}	1.93	5.5	1.90
2×10^{-2}	2.30	2.9	1.60
0	3.67	6.7	

Table 6.19 Effect of CTAB concentration on observed first-order degradation rate constants for 0.002% w/v chlorhexidine gluconate at pH 9.0 and 70°C

Figure 6.26 presents a graphical summary of the generated data as a plot of surfactant effect ratio against CTAB concentration on a log scale. A maximum (smallest degradation rate constant) at 2×10^{-3} M CTAB was noted, this value not being too dissimilar to the literature CMC of CTAB at this temperature (1.5×10^{-3} M). The significance of this surfactant effect is discussed in Chapter 8.

6.6.8.3.2 Non-ionic Surfactants

The effect of cetomacrogol 1000 (CMC at 20°C 6.3 x 10^{-3} M, no estimate available at 70°C, Mukerjee and Mysels, 1971) was determined over the concentration range 1 x 10^{-6} to 2 x 10^{-3} M using 0.002% w/v chlorhexidine gluconate, pH 9.0 (pH-stat) and 70°C. The molecular weight was determined from the nominal formula $CH_3.[CH_2]_{16}.[O.CH_2.CH_2]_{22}.OH$. Cetomacrogol concentrations in excess of 2 x 10^{-3} M interfered with the chlorhexidine peak on HPLC assay, even after prior dilution. Therefore it was not possible to determine the surfactant effect of cetomacrogol at concentrations on and slightly above its literature CMC (at 20°C). Figure 6.24 shows the first-order degradation profiles with degradation rate constants and surfactant effect ratios listed in Table 6.20. Again a stabilising effect is observed.

Surfactant concentration (molarity)	Observed first-order degradation rate constant $(sec^{-1} \times 10^6)$ SD $(sec^{-1} \times 10^8)$	Surfactant effect ratio ($k_o : k_{obs}$ surfactant)
Cetomacrogol 1000:		
1 x 10^{-6}	2.62	6.4	1.40
2 x 10^{-6}	1.84	5.6	1.99
2 x 10^{-5}	1.61	1.4	2.28
2 x 10^{-4}	1.10	2.9	3.34
2 x 10^{-3}	1.07	2.9	3.43
Polysorbate 80:		
2 x 10^{-5}	3.85	10.1	0.95
6 x 10^{-5}	4.00	10.9	0.92
2 x 10^{-4}	4.41	11.0	0.83
6 x 10^{-4}	4.75	12.8	0.77
2 x 10^{-3}	5.25	11.7	0.70
0	3.67	6.7	

Table 6.20. Effect of non-ionic surfactant concentration on observed first-order degradation rate constants for 0.002% w/v chlorhexidine gluconate at pH 9.0 and 70°C

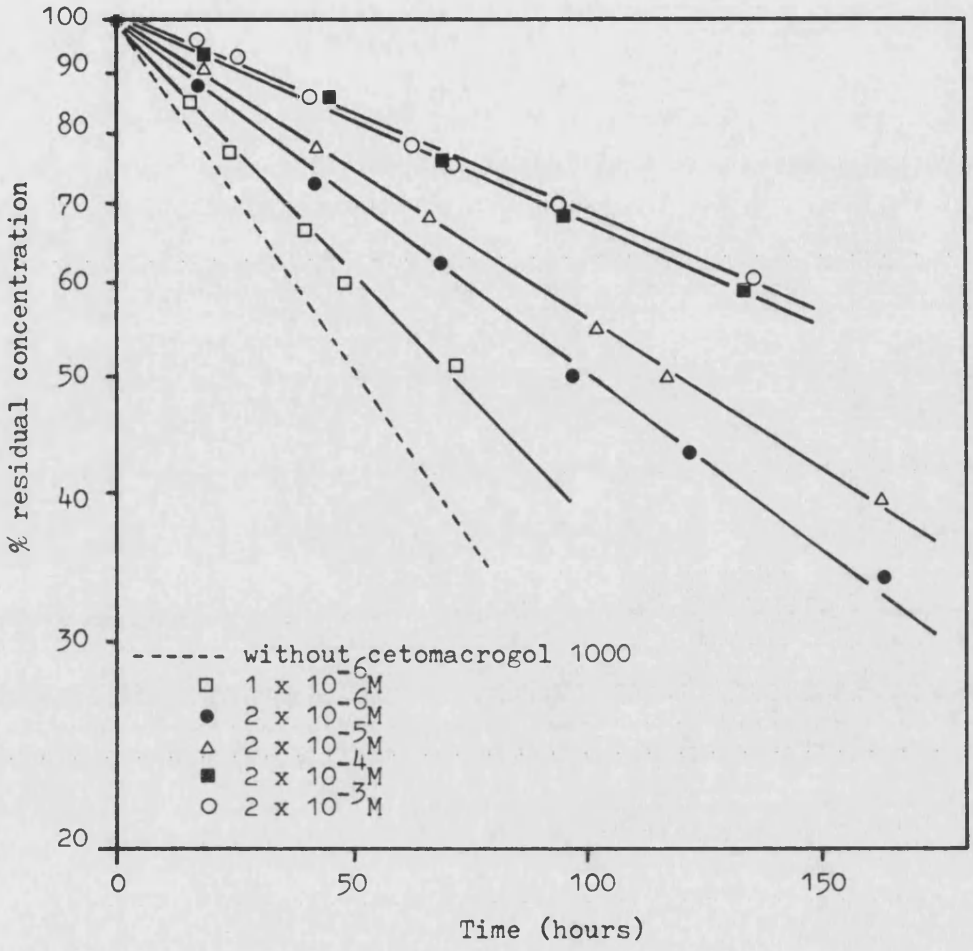

Figure 6.24 Effect of cetomacrogol 1000 on the first-order degradation plots of 0.002% w/v chlorhexidine gluconate solutions at pH 9.0 and 70°C. The plot in the absence of cetomacrogol is shown for reference

Experimentation with polysorbate 80 (CMC at 20°C 1.4×10^{-2} M, no estimate available at 70°C, Mukerjee and Mysels, 1971) was also limited to concentrations below 2×10^{-3} M due to assay interference by the surfactant. The molecular weight was calculated from the nominal formula $C_{64}H_{124}O_{26}$. Figure 6.25 presents the first-order degradation profiles of 0.002% w/v chlorhexidine gluconate solutions, pH 9.0 (pH-stat) and 70°C, in the presence of 2×10^{-5} to 2×10^{-3} M polysorbate 80. Table 6.20 lists the kinetic data and surfactant effect ratios.

Figure 6.26 also summarises the surfactant effect ratio-concentration profiles for the two non-ionic surfactants. Protective effects are shown by cetomacrogol 1000 but chlorhexidine degradation rate is increased by the presence of polysorbate 80.

6.6.8.3.3 Anionic Surfactant

The effect of sodium dodecyl sulphate (NaDS; CMC at 70°C 1.14×10^{-2} M, Mukerjee and Mysels, 1971) on the degradation of 0.002% w/v chlorhexidine gluconate was studied at pH 9.0 (pH-stat) and 70°C. Although hydrolysis of mono-alkyl sulphates has been observed in acidic solution it is reported to be stable under the conditions used for this study (Read and Fredell, 1959). The addition of 2×10^{-4} to 2×10^{-2} M NaDS to 0.002% w/v chlorhexidine gluconate resulted in the expected complex precipitation which was not solubilised at the degradation temperature of 70°. The resultant suspensions were therefore subjected to degradation. The first-order rate plots were still linear, however, as shown in Figure 6.27. The observed first-order degradation rate constants and resulting surfactant effect ratios are listed in Table 6.21.

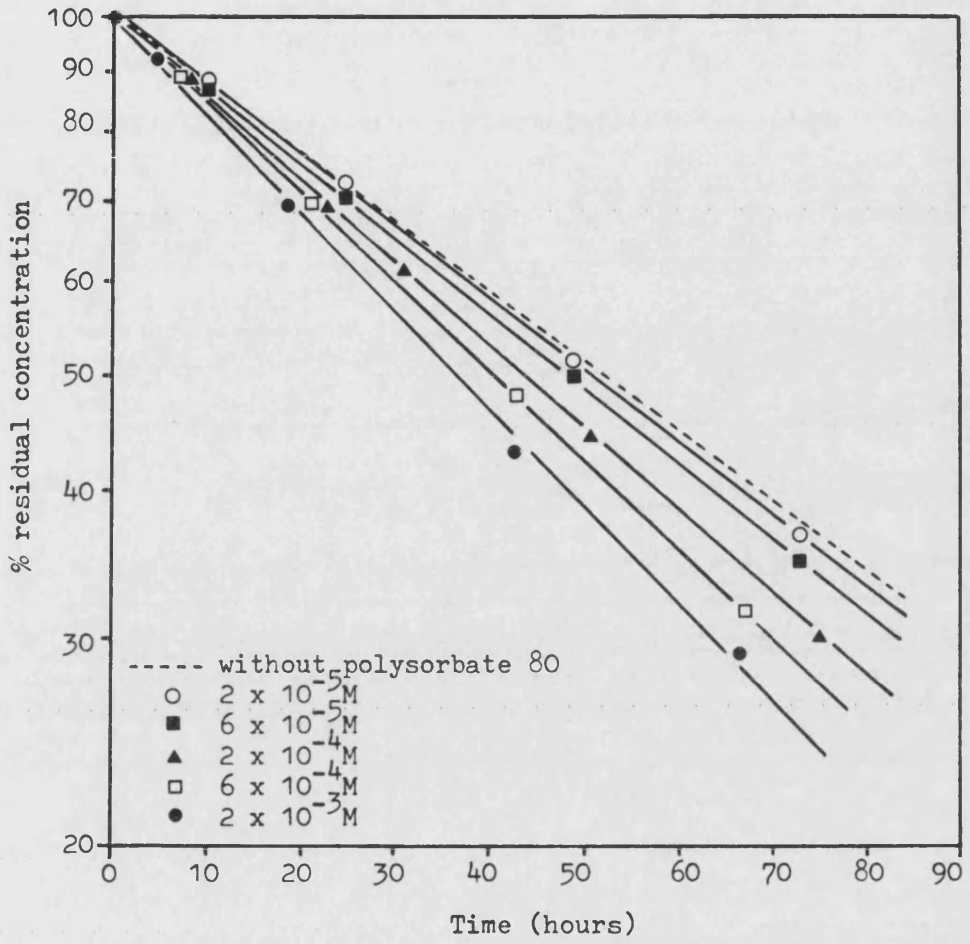

Figure 6.25 Effect of polysorbate 80 concentration on the first-order degradation plots of 0.002% w/v chlorhexidine gluconate solutions at pH 9.0 and 70°C

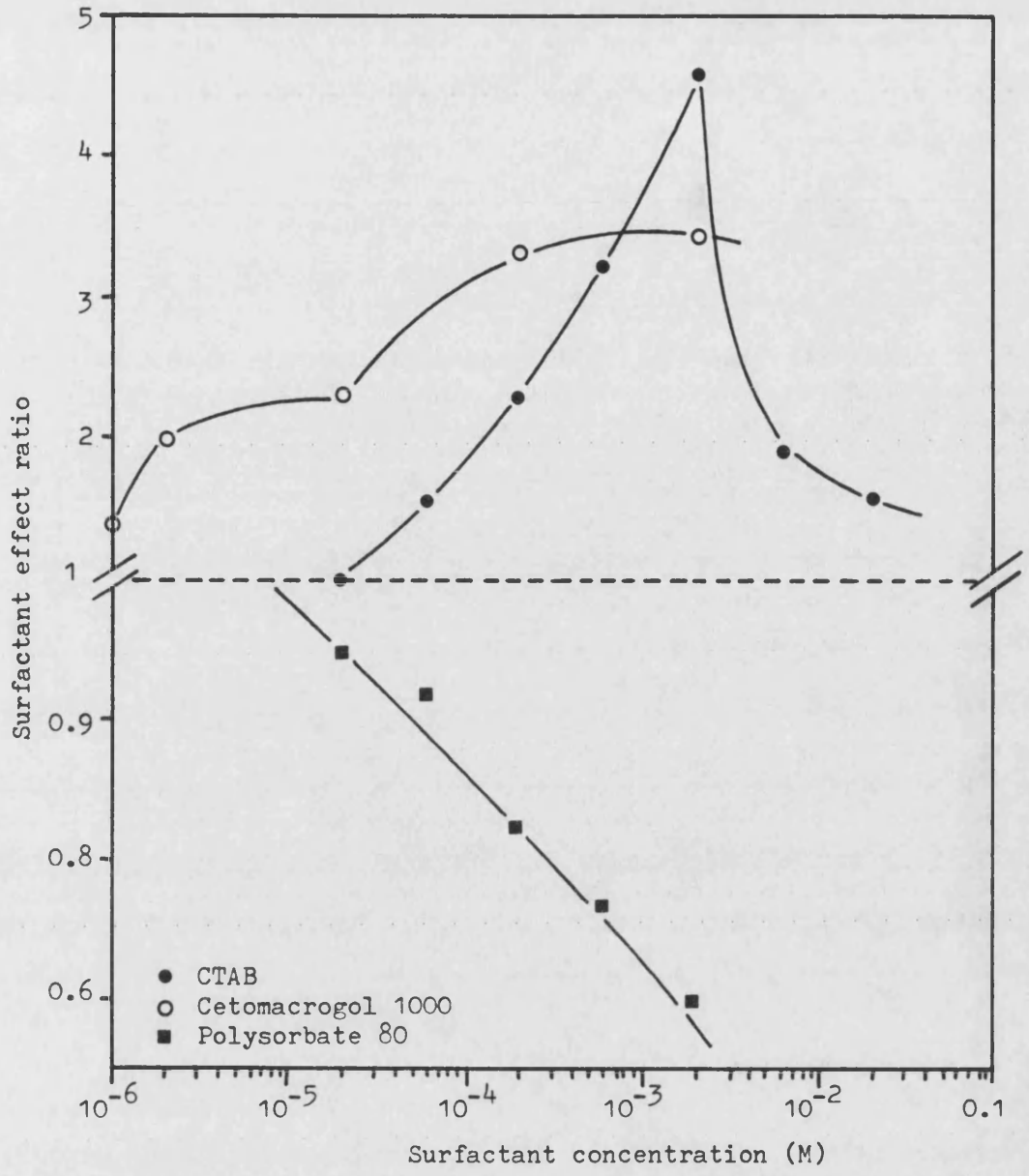

Figure 6.26 Effect of surfactant concentration on the observed first-order degradation rate constant of 0.002% w/v chlorhexidine gluconate solutions at pH 9.0 and 70°C. The surfactant effect ratio (k_o : k_{obs} surfactant) indicates reaction rate inhibition (values > unity) or rate catalysis (< unity)

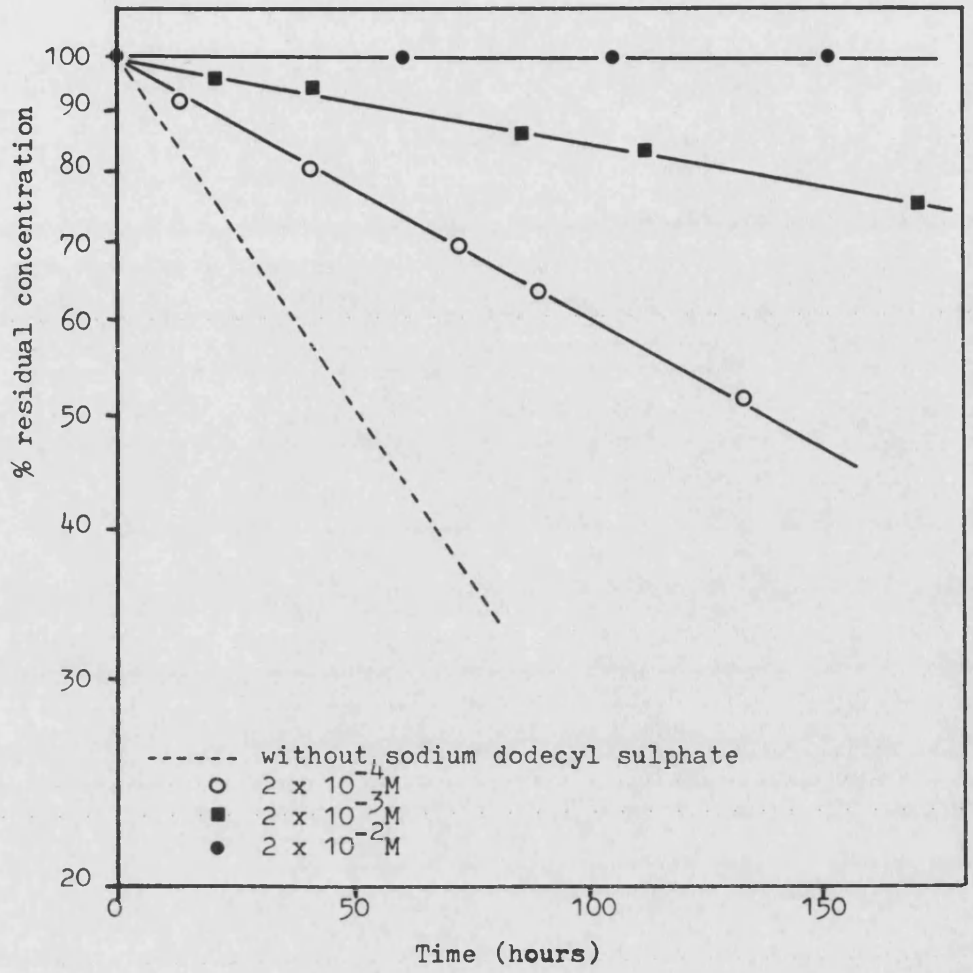

Figure 6.27 Effect of sodium dodecyl sulphate (NaDS) on the first-order degradation plots of 0.002% w/v chlorhexidine gluconate solutions at pH 9.0 and 70°C

NaDS concentration (Molarity)	Observed first-order degradation rate constant ($sec^{-1} \times 10^{6}$)	SD ($sec^{-1} \times 10^{8}$)	Surfactant effect ratio ($k_o : k_{obs}$ surfactant)
2×10^{-4}	1.37	4.1	2.68
2×10^{-3}	0.45	1.2	8.16
2×10^{-2}	no degradation detected		-
0	3.67	6.7	

Table 6.21 Effect of NaDS concentration on the observed first-order degradation rate constants of 0.002% w/v chlorhexidine gluconate at pH 9.0 and 70°C

The generated rate constants are possibly associated with a residual amount of "free" chlorhexidine gluconate in solution at each concentration of NaDS. No observed degradation after 160 hours in 2×10^{-2} M NaDS indicates that chlorhexidine degradation is almost completely inhibited by complexation with NaDS.

6.7 PHOTOCHEMICAL DEGRADATION

6.7.1 Introduction

The BP monograph for chlorhexidine gluconate solution requires that it should be protected from light. Therefore limited experimentation was carried out to investigate the extent of photochemical decomposition of three chlorhexidine gluconate concentrations at their natural pH under accelerated light storage conditions.

6.7.2 Light Source

In pharmaceutical stability studies the use of north facing windows for daylight storage tests is favoured since this avoids any

direct sunlight and associated heating effects. Northlight (Atlas) colour matching fluorescent tubes produce a spectral output very similar to that of north facing daylight (Fowler, 1972) and were therefore used for this study.

The output of fluorescent tubes is known to decrease with time along a "lumen maintenance curve". Output decreases steadily during their first use (100 hours) reaching a practically constant level after ~2000 hours (Fowler, 1972). However, to ensure light intensity remained constant over the period of the experimentation the photo-fading curve for riboflavine was used as control and determined at the start and end of accelerated light storage (see section 6.7.3).

Eight Atlas 18 inch 15W quick-start Northlight colour matching fluorescent tubes were positioned evenly along the two opposite walls of a wooden box (19" x 19" x 16" height). The box interior was painted white to increase light intensity by reflection. A rack to hold the samples was positioned equidistant from the two banks of tubes. Air circulation through the box was aided by a fan but due to fluorescent tube heating effects an air temperature of 28 ± 2°C was constant throughout the experiment.

6.7.3 Light Intensity Measurements

The photo-fading of riboflavine in the presence of non-ionic surfactants has been shown to be a fast process (Kostenbauder et al, 1965); it has previously been used in this department as a control for photostability studies on promethazine (Cox, 1975) and thiomersal (Khammas, 1980). A solution containing 8×10^{-5} M riboflavine with 1% w/v polysorbate (Tween) 80 in Sørensen's phosphate (pH 6.8) buffer was prepared. 5 ml aliquots were filled into 10 ml clear neutral glass ampoules thus leaving a large head space to ensure that oxygen tension

was not a limiting factor. Ampoules were placed in the light cabinet (in the same position as chlorhexidine samples) and on a north facing window sill. At regular intervals over three hours a sample was taken and its absorbance measured spectrophotometrically at 445 nm against a blank buffer at pH 6.8 containing 1% w/v polysorbate 80. The results are shown in Figure 6.28 and provide evidence that the light intensity did not vary during the experimental period.

This experiment also provides an estimation of the accelerative effect due to artificial daylight conditions. Mean 50% absorbance values were 58 and 110 minutes for artificial and natural daylight respectively; this represents a x1.9 acceleration under simulated storage conditions. This value compares well with theoretical light intensities for 8 Northlight fluorescent tubes of 18,000 Foot-candles and 8,000 Foot-candles for daylight (Henderson and Marsden, 1972; Parrott, 1966) or an acceleration factor of x2.25. If a mean of 12 hours natural daylight per day is assumed the acceleration factor of artificial storage conditions are of course doubled.

Accelerations of between 2 and 20 fold have been quoted in the literature (Parrott, 1966; Pope, 1980) but it has been noted by Mendenhall (1984) that a correlation between accelerated light stress and normal conditions often does not exist due to the complexity of photochemical reactions.

6.7.4 Photo-stability of Chlorhexidine

6.7.4.1 Method

The photo-stability of three concentrations of chlorhexidine gluconate in distilled water was tested : 0.002, 0.01 and 0.05% w/v.

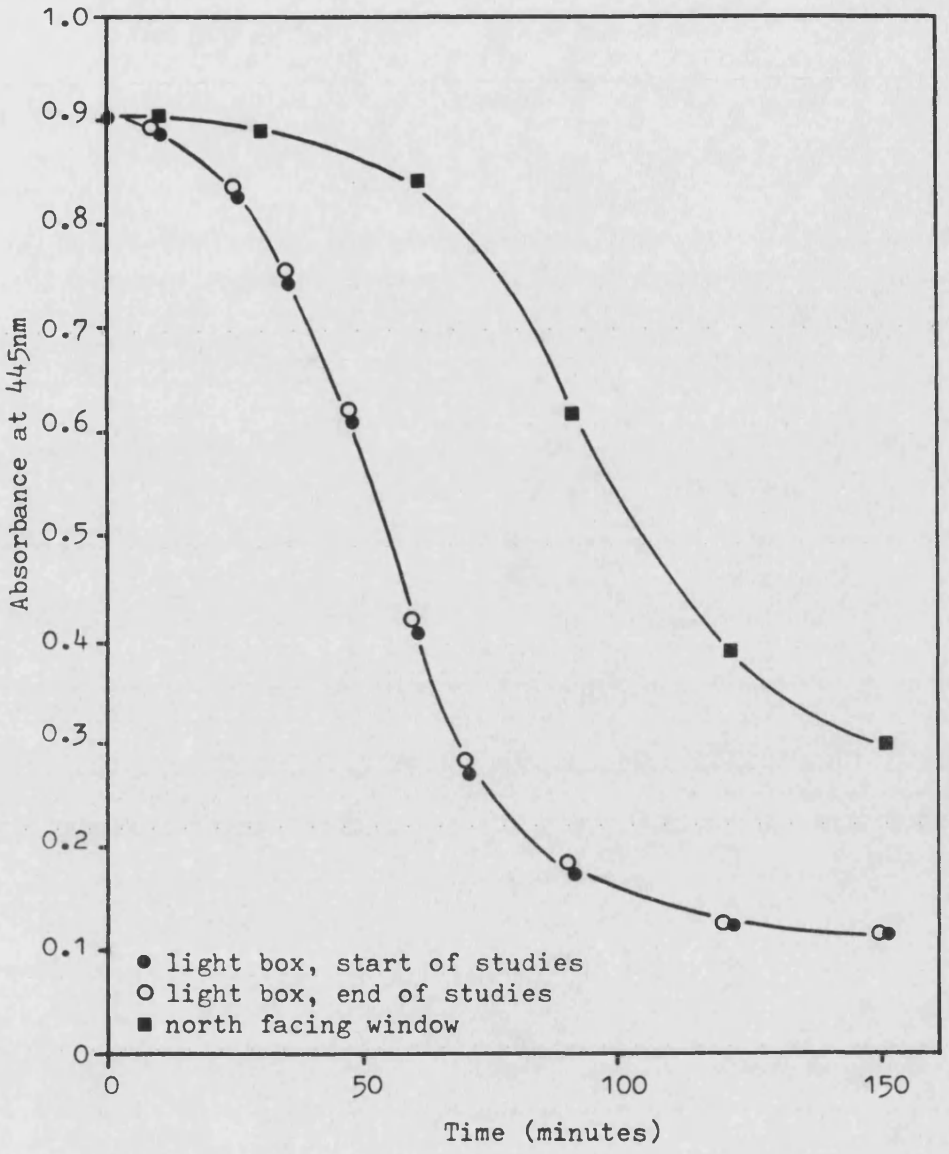

Figure 6.28 Effect of photo-irradiation on the absorbance of an 8.1×10^{-5} M riboflavine solution in pH 6.8 (Sørensen's) buffer containing 1% w/v polysorbate 80. The accelerative effect of light box storage is clearly demonstrated

The solutions (5 ml) were filled into either clear or amber 10 ml neutral glass ampoules (chlorhexidine aged), sealed and placed in the light box.

Two sets of controls were also prepared. As a dark control, clear ampoules containing each concentration were prepared and wrapped in alumunium foil then placed with the other ampoules inside the light box. As a temperature control, sealed clear and amber ampoules containing each concentration were placed in a dark cupboard at ordinary room temperature (~18-20°C).

After intervals of 1, 2, 4, 8 and 16 weeks one ampoule of each test and control was withdrawn and stored in a refrigerator until HPLC assay. Solution pH inside each ampoule was also measured at the start of the experiment and at the end of storage (prior to HPLC assay). No drift greater than ±0.07 pH unit was observed with initial pH being in the range 5.73-5.79.

6.7.4.2 Results

The results of HPLC analysis of the stored samples are shown in Table 6.22 for the concentrations 0.002, 0.01 and 0.05% w/v chlorhexidine gluconate respectively. Percentage residual data shows that no significant degradation was observed in any solution over the test period, all data remaining well within the ±2.6% assay confidence limit discussed earlier (see Chapter 5.1.1.4.3).

Time (weeks)	% Residual chlorhexidine gluconate after storage in:			
	Light box			Dark cupboard
	Clear	Amber	Foil wrapped	
0.002% w/v chlorhexidine gluconate:				
1	99.44	99.07	100.63	100.54
2	99.73	99.95	100.08	100.55
4	99.93	99.84	100.45	99.96
8	99.73	99.87	100.47	100.22
16	98.88	99.03	98.78	99.25
0.01% w/v chlorhexidine gluconate:				
1	100.54	100.01	99.61	100.41
2	99.88	99.78	99.98	99.91
4	100.13	99.60	98.17	100.87
8	99.41	99.60	99.26	99.87
16	99.26	99.50	99.21	98.68
0.05% w/v chlorhexidine gluconate:				
1	100.60	99.67	99.70	99.16
2	100.73	99.16	99.53	99.32
4	100.79	99.54	99.21	99.07
8	100.31	99.45	99.27	99.02
16	100.37	99.63	99.46	98.78

Table 6.22 Effect of accelerated light storage on solutions of chlorhexidine gluconate in distilled water

6.8 STABILITY TO IONISING IRRADIATION

6.8.1 Introduction

γ-irradiation is an alternative method to heat for the sterilisation of pharmaceuticals at a recognised dose of 25 kGy. The general stability of pharmaceuticals towards ionising radiations has been discussed in Chapter 1.6.4. Although sterilisation of water based products by γ-radiation is problematical, it can be successfully applied to dry powders, non-aqueous products and surgical materials. Paraffin gauze dressing (tulle gras) impregnated with chlorhexidine

and sterilised by γ-radiation is used for wound management (Smith and Nephew Pharmaceuticals). Therefore the comparative stability of chlorhexidine in aqueous solution, as a dry solid and dispersed in semisolid water soluble (PEG) and greasy (soft paraffin) ointment bases was investigated over a range of doses to establish the kinetic pattern.

6.8.2 Radiation Source

A 3.5 cm Gravatom ^{60}Cobalt fixed source was used to provide γ-irradation. This source contained four, 15 cm fixed rods of ^{60}Co placed equidistant from a sample cage. Irradiation was carried out in glass sample tubes containing about 2 g of sample and held in a jig accommodating five tubes at a time. Samples were removed at appropriate time intervals and replaced with fresh samples as required. All five positions in the jig held either samples or controls throughout the irradiation period in order to ensure dose uniformity. This system has been fully validated by previous workers at the University of Bath (Fletcher, 1968; Hayes, 1981).

6.8.3 Radiation Dose Rate Measurement

Irradiation dose rate was determined by the standard ferric sulphate "Fricke Dosimeter" system. The dosimetric solution contains ferrous (Fe^{2+}) sulphate which is oxidised through a radiation induced free radical mechanism to ferric ions (Fe^{3+}). The concentration of ferric ions generated is determined spectrophotometrically and the irradiation dose rate calculated from equation 70 (Hayes, 1981)

$$\text{electron-volts min}^{-1} = \frac{\Delta A \cdot N \cdot 100}{t \cdot l \cdot E \cdot G} \quad \ldots\ (70)$$

where ΔA is the difference in absorbance between irradiated and unirradiated control solutions

N is Avogadro's number (6.022×10^{23} molecules $mole^{-1}$)

l is the optical path length (5 mm)

E is the molar extinction coefficient for ferric ions in 0.4 M sulphuric acid at 25°C (2240)

t is time in minutes

G is 15.5 for ferric ions.

However $1Gy = 6.24 \times 10^{15}$ eV g^{-1} and assuming the ferrous ammonium sulphate solution has a density of 1.0, then equation 70 rearranges to equations 71 and 72:

$$Gy\ min^{-1} = \frac{\Delta A \times 6.022 \times 10^{23} \times 100}{t \times 0.5 \times 2440 \times 15.5 \times 1000 \times 6.24 \times 10^{15}} \quad \ldots\ (71)$$

$$= \frac{\Delta A}{t} \times 555.91 \quad \ldots\ (72)$$

Therefore a plot of the absorbance of the dosimetric solution against time will give the dose rate in Gy min^{-1}.

Stock solutions of 4 M sulphuric acid and 1×10^{-2} M sodium chloride were prepared. 25 ml of each were mixed in a 250 ml volumetric flask and 0.0985 g ferrous ammonium sulphate added before making up to volume with double distilled water. This dosimetric solution should always be freshly prepared from the stock solutions to prevent ferrous ion oxidation during storage. Aliquots (3 ml) of the dosimetric solution were irradiated in the irradiation tubes for 5, 10, 15, 20 and 25 minutes in the five tube jig. After the storage period

the absorbance of each irradiated sample was determined in 5 mm cells at 303 nm using the unirradiated solution as blank.

Plots of absorbance against time were constructed for duplicate dose rate determinations. Linear regression data are listed in Table 6.23. The mean slope (1.2304×10^{-2}) was substituted into equation 72 to produce a dose rate of 6.84 $Gy.min^{-1}$ (0.4104 $kGy.hr^{-1}$).

Linear regression analysis	Dose rate determination	
	1	2
Correleation coefficient	0.9999	0.9999
Slope (SD) $x10^2$	1.2297 (0.0097)	1.2311 (0.0101)
Intercept (SD)	0.0114 (0.0029)	0.0087 (0.0031)
RSD slope	0.8%	0.8%

Table 6.23 Experimental data for irradiation dose rate determination by "Fricke Dosimeter"

This dose rate was calculated the day before commencement of irradiation studies. Since experimentation was completed within three weeks and the half-life of ^{60}Co is long (5.23 years), the dose rate was effectively constant during these studies (0.55% change).

6.8.4 Methods

Experimentation was performed using the chlorhexidine acetate reference standard material (known moisture content of 2.6% w/v). A powder sample was irradiated over the dose range 5-75 kGy.

Aqueous chlorhexidine acetate solutions were prepared at 0.002, 0.01 and 0.05% w/v concentrations and irradiated over the dose range 1-20 kGy. Ointment type dilutions of chlorhexidine acetate (0.5% w/w) in either polyethylene glycol (PEG 400: PEG 3400, 80:20 by weight), or white soft paraffin B.P. were prepared by mixing the powder and "ointment base" or a warm glass slate. The effects of irradiation over the range 5-75 kGy were studied for these preparations.

Sample preparation for HPLC assay had to be slightly modified for the "ointment" studies. For the chlorhexidine-PEG mixture approximately one gram, accurately weighed, of the "ointment" was taken and dissolved in about 50 ml warm double distilled water. This solution was transferred to a 100 ml volumetric flask and adjusted to volume with double distilled water rinsings from the beaker. A 2 in 10 dilution with mobile phase gave the HPLC test solution. The presence of PEG did not interfere with the HPLC assay for chlorhexidine.

Since white soft paraffin is insoluble in water approximately one gram, accurately weighed, of the "ointment" was taken and dissolved in the minimum quantity of diethyl ether. Chlorhexidine was then extracted by three 30 ml extractions with double distilled water. Aqueous layers were combined and adjusted to 100 ml with double distilled water. A 2 in 10 dilution with mobile phase gave the HPLC test solution. The extraction technique resulted in a 100% recovery of chlorhexidine acetate as evidenced by the data in Table 6.24.

Nominal chlorhexidine acetate (% w/w)	% recovery after aqueous extraction 1	2	3
0.503	85.62	97.33	99.71
0.513	83.15	96.96	99.45

Table 6.24 Recovery of chlorhexidine acetate from white soft paraffin BP. The ointment was dissolved in diethyl ether and the chlorhexidine recovered with three 30 ml extractions of distilled water.

In all the studies, samples were filled into the glass sample tubes and removed from the ^{60}Co source after appropriate irradiation dose intervals. "Cling film" over the tube tops prevented water evaporation during storage inside the ^{60}Co source. As a control, a sample of each study was kept at ambient temperature during the full time course of the irradiation experiment.

6.8.5 Results

The degradation data for the various systems are shown in Table 6.25.

By HPLC assay no degradation of solid chlorhexidine acetate was observed after an irradiation dose of 75 kGy even though the sample contained 2.6% water. This result is in common with those observed for many other pharmaceuticals in their solid state (Bor, 1981).

	Degradation data for chlorhexidine acetate (solid, in solution and as semi-solid ointment)											
	Solid		Solutions (% w/v)						Ointment (0.5% w/w) in			
	Dose (kGy)	% residual	0.002%		0.01		0.05		PEG mixture		White soft parrafin	
			Dose (kGy)	% residual	Dose (kGy)	% residual	Dose (kGy)	% residual	Dose (kGy)	% residual	Dose (kGy)	% residual
Degradation data	0	100	0	100	0	100	0	100	0	100	0	100
	15.9	97.7	1.74	91.7	1.61	92.2	1.79	94.2	14.4	86.1	13.5	99.2
	28.8	99.4	3.87	82.1	4.43	81.8	3.59	87.3	20.0	79.5	19.6	100.3
	35.5	99.8	6.16	69.1	6.53	72.0	6.10	78.3	25.1	76.6	25.1	100.1
	55.0	100.1	9.79	55.8	10.0	61.8	8.58	70.7	30.1	72.7	30.0	100.2
	65.6	99.9	12.4	47.9	14.1	49.3	12.2	60.3	35.0	70.0	34.8	100.2
	77.3	100.0	16.8	34.5	16.0	44.1	16.3	52.1	40.0	68.6	39.3	100.3
									75.0	50.0	74.5	100.1
Linear regression analysis:												
Rate constant ($kGy^{-1} \times 10^{2}$)	No significant		6.32		5.08		4.09		0.91		No significant	
SD rate constant ($kGy^{-1} \times 10^{4}$)	degradation		13.7		9.2		6.0		3.2		degradation	
RSD slope			2.2%		1.8%		1.5%		3.5%			
Half-life (kGy)			10.96		13.64		16.94		76.46			

Table 6.25 Effect of γ-irradiation of chlorhexidine acetate as a "dry" solid, in aqueous solution and as a semi-solid ointment. Rate constants and half-lives are expressed in radiation dose units (kGy).

The results of irradiation over the range 1 to 20 kGy for chlorhexidine acetate solutions are shown in Figure 6.29. It was noted that the rate of degradation is dependent on the initial concentration of chlorhexidine with the data fitting first-order kinetics. The results show chlorhexidine in aqueous solution to be extremely sensitive to γ-irradiation, degradation rates increasing with decrease in concentration. The degradative mechanism probably involves a free radical mechanism initiated by the splitting of molecular water (see Chapter 1.6.4).

The effects of irradiation over the range 5-75 kGy on the semi-solid ointment type preparations is shown, plotted according to first-order kinetics, in Figure 6.30. Chlorhexidine acetate dispersed in soft paraffin is stable to radiation at doses well above those used for sterilisation. In the PEG mixtures significant degradation occurs with ~20% loss at the standard sterilisation dose of 25 kGy. Degradation in PEG can be fitted better to a first-order rate plot than a zero order plot. The RSD of the rate constant (3.5%) is higher than that seen for the irradiation of the aqueous solutions however (Table 6.25).

Examination of the chromatograms from irradiation induced degraded chlorhexidine samples indicates a different degradation pathway to that arising from thermal degradation.

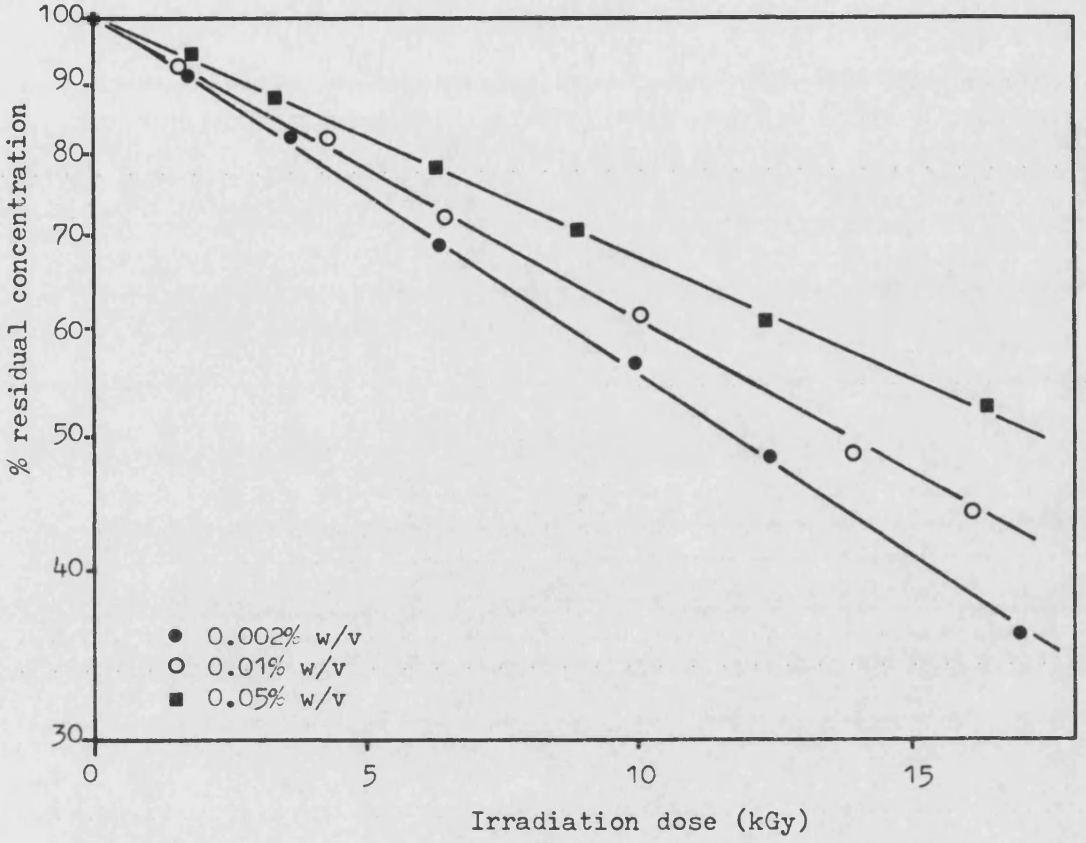

Figure 6.29 Effect of γ-irradiation on the stability of chlorhexidine acetate in aqueous solution

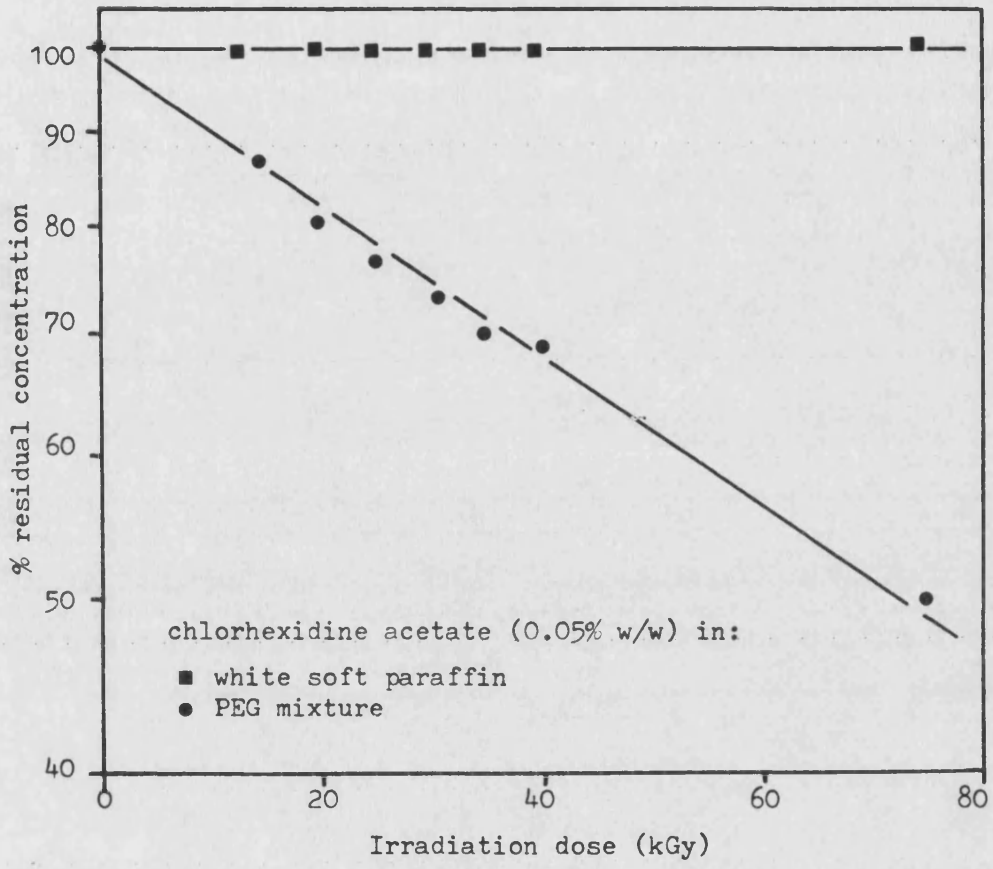

Figure 6.30 Effect of γ-irradiation on the stability of 0.05% w/w chlorhexidine acetate in white soft paraffin or in a PEG 4000 : PEG 3400 mixture (80:20)

CHAPTER 7

DEGRADATION PATHWAY STUDIES

7.1 INTRODUCTION

This chapter describes the experiments performed in an attempt to identify degradation products and construct a reaction pathway for chlorhexidine degradation. Ideally, in order to propose and justify degradation pathways, or reaction mechanisms, several practical criteria must be fulfilled.

(i) Identification

Each degradation product must be identified. This can be achieved either by chemical synthesis or by isolation from degraded samples of the parent molecule. Structure confirmation can then be approached by the use of suitable physico - chemical techniques including NMR and mass spectrometry.

(ii) Quantification

Once identity has been confirmed each degradation product requires quantification under different degradative conditions. Such data then helps to propose : (a) a degradation pathway or cascade from the order and rates of occurrence and loss, (b) reaction mechanisms from combination of kinetic data and apparent degradation pathway (i.e. simultaneous or consecutive reactions).

During the early and throughout the intermediate stages of this work it appeared likely that samples of chlorhexidine degradation

products and/or impurities would be accessible (Fernie, ICI Pharmaceuticals, Personal Communications, 1982-84). Only towards the later stages of the experimental work did it become clear that these compounds would not become available. At this stage of the work it was not practicable to commence a relevant synthetic programme.

Therefore in order to generate some evidence for a proposed degradation scheme, the following kinetic information was assembled.

(i) Quantitative determination of 4-chloroaniline was performed in order to evaluate its significance as a degradation product.

(ii) Chlorhexidine assay values generated by the Holbrook and HPLC methods were compared to identify whether any significant link existed.

(iii) Qualitative information on degradation products, such as rates of appearance/disappearance, was assembled from degradation studies already performed.

Additionally, brief attempts were made to independently identify degradation products by preparative HPLC and HPLC-mass spectrometry.

7.1.1 Significance of 4-chloroaniline as a Degradation Product

Some previous reports have assumed that the loss of chlorhexidine and appearance of 4-chloroaniline are stoichiometrically related. Toxicity considerations have led such workers (Dolby *et al*, 1972; Goodall *et al*, 1968 and Jaminet *et al*, 1970) to express 4-chloroaniline content in units of ppm relative to chlorhexidine. The residual chlorhexidine concentration was then calculated directly from ppm 4-chloroaniline. For example, 3000 ppm 4-chloroaniline was equivalent to 0.3% decomposition according to Goodall *et al*, (1968).

However, two fundamental errors exist in this method of calculation, namely it assumes that 4-chloroaniline is the only degradation product and the use of ppm units ignores molecular weight considerations; 3000 ppm is actually equivalent to 1.6% decomposition of chlorhexidine following the assumption of Goodall et al, (1968) that, stoichiometrically, one mole chlorhexidine gluconate ≡ one mole 4-chloroaniline hydrochloride. It is also clear from previous work that other degradation products are present in degraded chlorhexidine solutions (Chapter 5.1.1.3.2). Therefore, studies were performed to establish the significance of 4-chloroaniline as a degradation product.

7.1.2 Assay of Chlorhexidine by the Holbrook Colorimetric Method

The Holbrook (1958) colorimetric assay for chlorhexidine is in Chapter 5.1.2. It was noted from degradation studies on 0.002% w/v chlorhexidine gluconate at pH 9.0 and 80°C, that the colorimetric method overestimates the residual chlorhexidine content when compared to data generated by the HPLC stability indicating method. At this degradative condition the extent of degradation detected was approximately half that observed by the HPLC method. Further studies were therefore performed in order to identify whether this fraction changes with pH, concentration or salt form.

7.2 SIMULTANEOUS DETERMINATION OF CHLORHEXIDINE GLUCONATE, (HPLC AND HOLBROOK METHOD) AND 4-CHLOROANILINE IN DEGRADED SOLUTIONS

7.2.1 Method

Chlorhexidine gluconate solutions (0.002% w/v) were degraded at pH 2.0 (self-buffering), 6.0 and 9.0 (both pH-stat) and a

temperature of 90°C. These three pH values were used since different degradation mechanisms were observed at acid, alkaline and neutral pH. Samples taken throughout the degradation process, were assayed for 4-chloroaniline content and for residual chlorhexidine (by the stability indicating HPLC and colorimetric methods). The effects of concentration and salt form were studied at pH 9.0 (pH stat) and 90°C using 2.2×10^{-5}M and 5.6×10^{-4}M solutions of chlorhexidine gluconate and acetate (equivalent to 0.002% and 0.05% w/v chlorhexidine gluconate). All samples were again assayed by the three methods.

7.2.2 Treatment of Data

Generated assay data were treated as follows:-

(i) HPLC data were fitted to first-order kinetics as previously performed in Chapter 6.

(ii) The molarity of 4-chloroaniline found in degraded chlorhexidine solutions was related to the original chlorhexidine concentration to calculate an apparent percentage residual chlorhexidine, assuming the chlorhexidine molecule yields one molecule of 4-chloroaniline and that it is the only degradation product. This approach maximises apparent degradation and allows the generated results to be compared with those in the literature where 4-chloroaniline analysis has been used. For example, the generation of 2×10^{-6} moles of 4-chloroaniline from a solution initially containing 2×10^{-5} moles of chlorhexidine was taken as 10% degradation (90% residual). These data were also treated according to first-order kinetics.

(iii) From the difference between (i) and (ii) above, the percentage of total degradation due to 4-chloroaniline was calculated. For example, 50% residual by HPLC assay and 90% apparent residual by

4-chloroaniline content means that 4-chloroaniline contributes 20% of the total degradation products. These data were plotted linearly with time to identify whether the proportion of 4-chloroaniline remains constant or changes as the degradation cascade proceeds.

7.2.3 Results

7.2.3.1 Effect of pH

Table 7.1 shows a typical set of experimental data for 0.002% chlorhexidine gluconate degraded at pH 9.0 and 90°C. The kinetic data are plotted in Figures 7.1 to 7.3 for pH 2, 6 and 9 respectively. The use of the double scaled ordinate allows immediate comparison of the build-up of 4-chloroaniline, within the degradation products, with the first order degradation rate profiles. From linear regression analysis of this plotted data apparent first order degradation rate constants from colorimetric assay of chlorhexidine and 4-chloroaniline were calculated. By comparing these constants (k_{app}) with the "true" rate constants derived from HPLC assay (k_{HPLC}) an underestimation ratio ($R\mu = k_{HPLC}/k_{app}$) for each method was obtained. These ratios, together with linear regression analysis data are listed in Table 7.2.

7.2.3.2 Effects of Concentration and Salt Form

Table 7.3 lists the apparent rate constants generated from 2.2×10^{-5}M and 5.6×10^{-4}M solutions of chlorhexidine gluconate and acetate (equivalent to 0.002 and 0.05% w/v chlorhexidine gluconate). The individual degradation profiles are shown in Figures 7.4 (gluconate and acetate solutions at 2.2×10^{-5}M) and 7.5 (gluconate and acetate solutions at 5.6×10^{-4}M).

Time (hours)	Assay for chlorhexidine (molar concentration x 10^5)				Assay for 4-chloroaniline (molar concentration x 10^6)		
	HPLC		Holbrook				
	Concentration	% residual	Concentration	% residual	Total 4-ca [1] concentration found	Apparent % [2] residual	Percentage of [3] total degradation accountable by 4-ca
0	2.28	100	2.29	100	0.38	100	-
0.5	2.05	89.9	2.21	96.5	0.72	98.5	14.9
1.75	1.74	73.6	2.02	88.2	1.57	94.8	19.7
2.5	1.53	67.1	1.93	84.3	2.04	92.7	22.2
4.0	1.24	54.3	1.71	74.7	3.53	86.2	30.2
5.5	0.95	41.7	1.44	62.9	4.85	80.4	33.6

[1] After subtracting the 4-ca concentration found at zero time, this concentration was assumed to be equivalent to the concentration of chlorhexidine lost (1 mole 4-ca produced by 1 mole degraded chlorhexidine).

[2] $$\% \text{ residual} = \frac{\text{conc. chx at zero time} - (\text{conc. 4-ca found} - \text{conc. initial 4-ca})}{\text{conc. chx at zero time}} \times 100\%$$

[3] $$\frac{\text{apparent \% degraded by 4-ca assay}}{\text{\% degraded by HPLC}} \times 100\%$$

Table 7.1 Typical set of experimental data for the degradation of 0.002% chlorhexidine gluconate at pH 9.0 and 90°C, generated by the three assay methods.

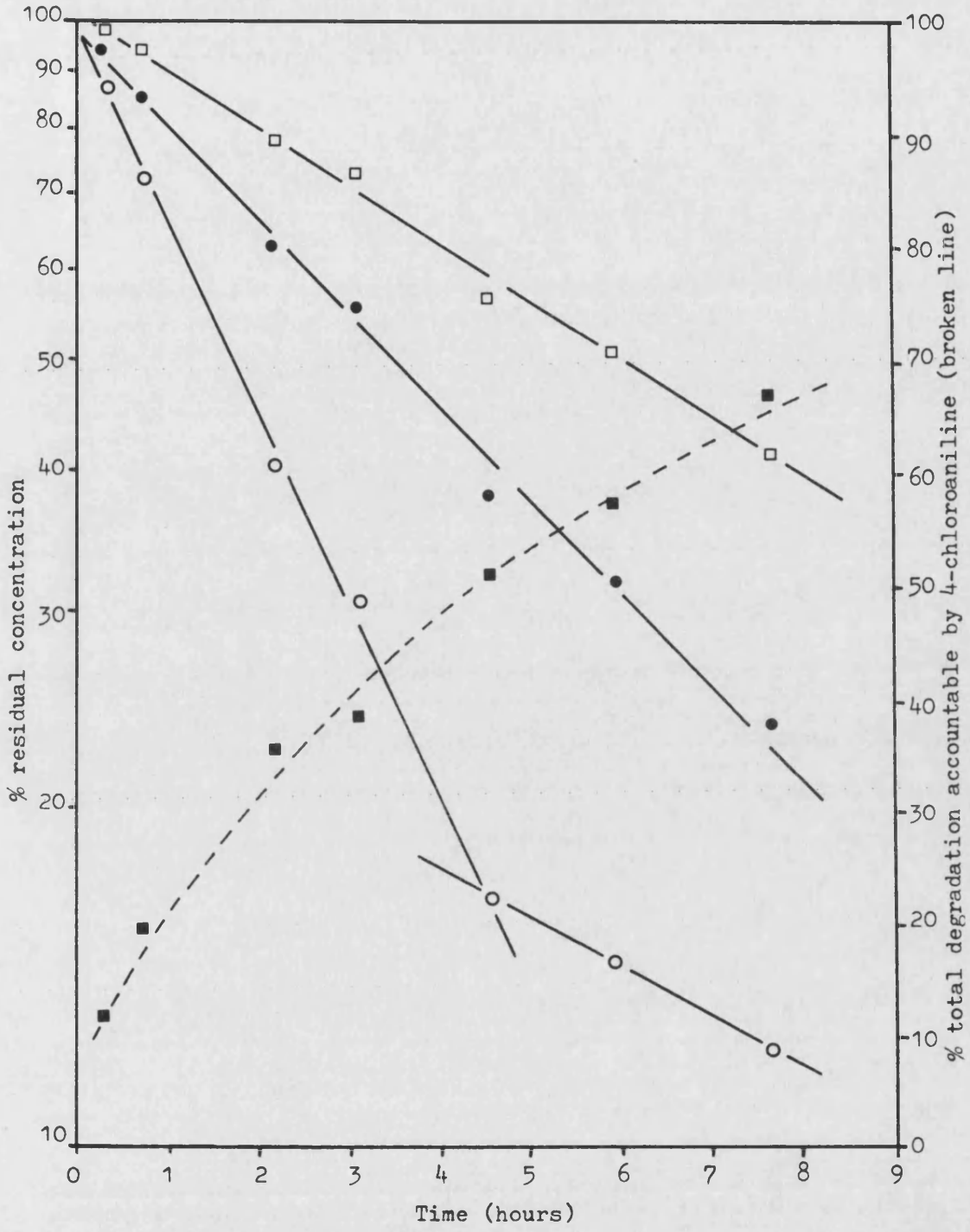

Figure 7.1 Apparent degradation profiles of 0.002% w/v chlorhexidine gluconate at pH 2.0, 90°C, produced from different assay methods:

- ○ HPLC stability indicating
- ● Holbrook colorimetric assay
- □ 4-Chloroaniline assay to predict residual chlorhexidine
- ■ Percentage of total degradation which could be accounted for by 4-chloroaniline content alone

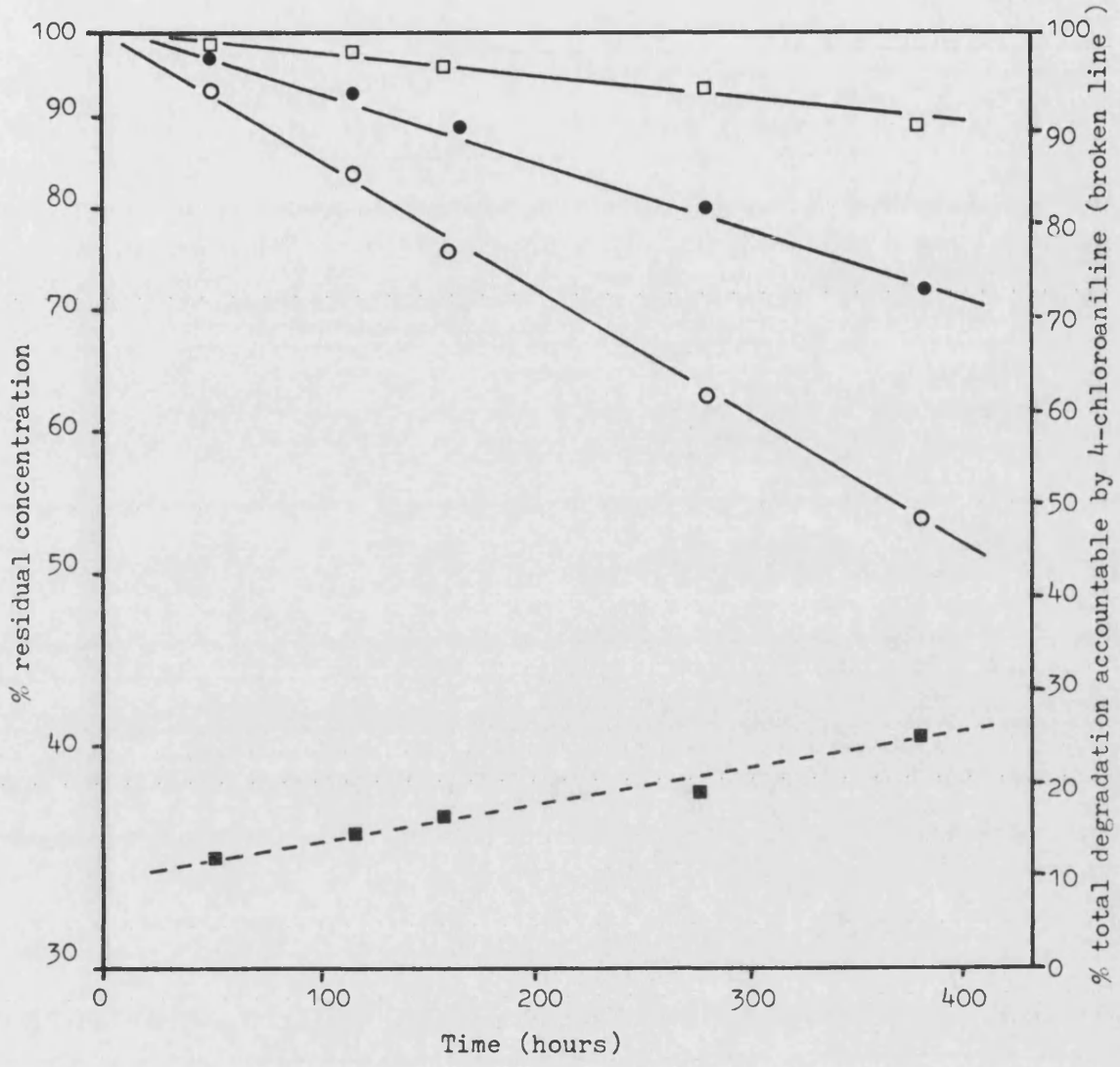

Figure 7.2 Apparent degradation profiles of 0.002% w/v chlorhexidine gluconate at pH 6.0, 90°C, produced from different assay methods:

- ○ HPLC stability indicating
- ● Holbrook colorimetric assay
- □ 4-Chloroaniline assay to predict residual chlorhexidine
- ■ Percentage of total degradation which could be accounted for by 4-chloroaniline content alone

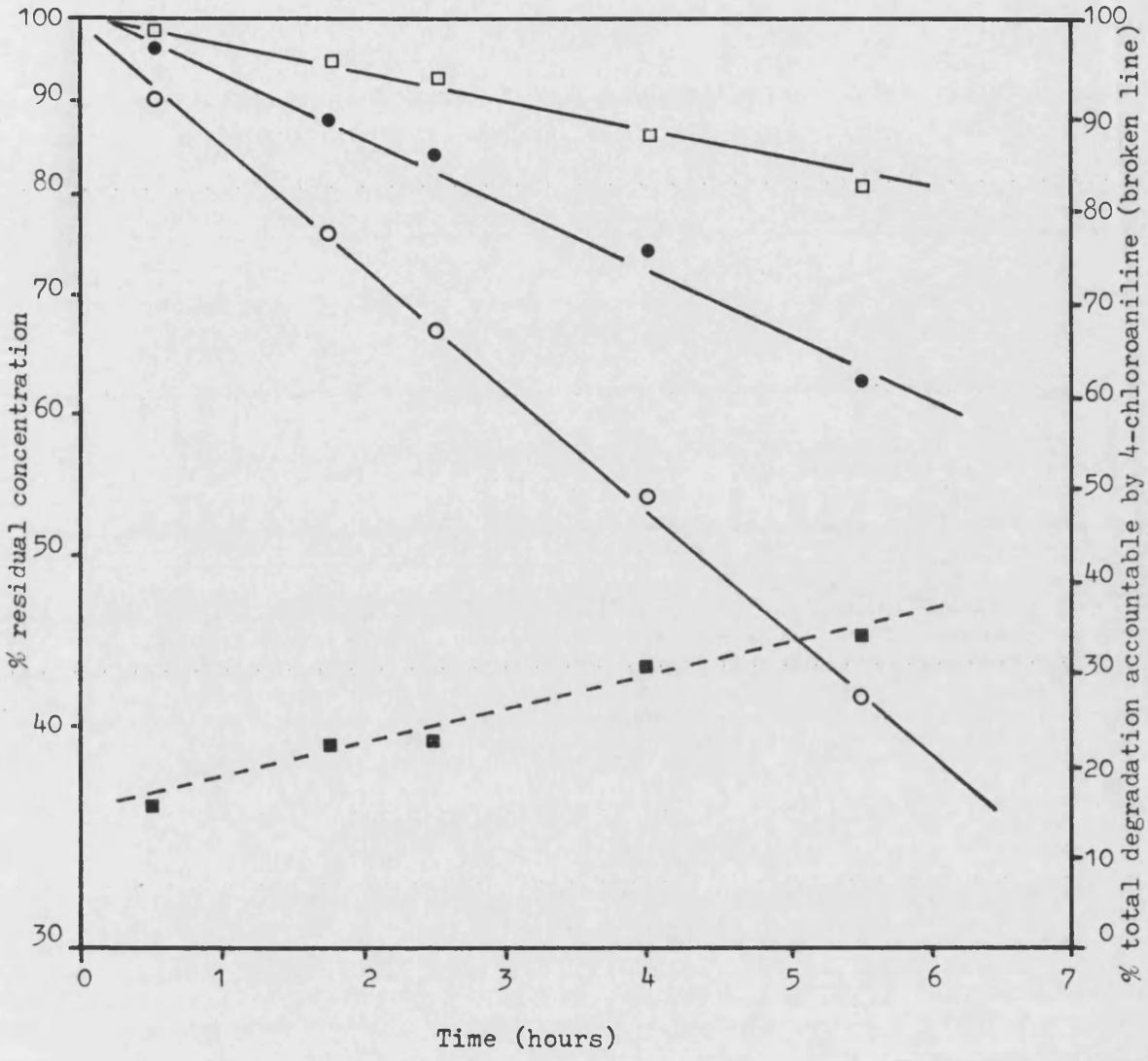

Figure 7.3 Apparent degradation profiles of 0.002% w/v chlorhexidine gluconate at pH 9.0, 90°C, produced from different assay methods:

- ○ HPLC stability indicating
- ● Holbrook colorimetric asaay
- □ 4-Chloroaniline assay to predict residual chlorhexidine
- ■ Percentage of total degradation which could be accounted for by 4-chloroaniline content alone

Quantitative assay method	pH		
	2.0	6.0	9.0
Chlorhexidine : HPLC assay			
Rate constant ($sec^{-1} \times 10^6$)	10.8	0.465	45.0
SD rate constant ($sec^{-1} \times 10^6$)	0.270	0.014	0.543
RSD rate constant	2.5%	3.0%	1.2%
Correlation coefficient	0.9988	0.9953	0.9996
Chlorhexidine : Holbrook assay			
Apparent rate constant ($sec^{-1} \times 10^6$)	5.28	0.244	22.9
SD apparent rate constant ($sec^{-1} \times 10^6$)	0.167	0.016	1.358
RSD apparent rate constant	3.2%	6.5%	5.9%
Correlation coefficient	0.9970	0.9909	0.9930
Underestimation ratio (R_u)	2.05	1.91	1.97
4-chloroaniline : Colorimetric assay			
Apparent rate constant ($sec^{-1} \times 10^6$)	3.29	0.0866	11.0
SD apparent rate constant ($sec^{-1} \times 10^6$)	0.091	0.007	0.637
RSD apparent rate constant	2.8%	8.1%	5.8%
Correlation coefficient	0.9977	0.9872	0.9933
Underestimation ratio (R_u)	3.28	5.37	4.09

Table 7.2 Degradation rate constants (real and apparent) produced by the different assay methods. Underestimation ratio relates k_{obs} (HPLC) to k_{obs} (Holbrook or 4-chloroaniline). These results were obtained from the degradation of 0.002% w/v chlorhexidine gluconate solutions

Quantitative assay method	Chlorhexidine salt form and concentration			
	2.2×10^{-5} M		5.6×10^{-4} M	
	gluconate	acetate	gluconate	acetate
Chlorhexidine : HPLC assay				
Rate constant ($sec^{-1} \times 10^{6}$)	45.0	45.1	5.83	6.03
SD rate constant ($sec^{-1} \times 10^{6}$)	0.543	1.060	0.127	0.119
RSD rate constant	1.2%	2.4%	2.2%	2.0%
Correlation coefficient	0.9996	0.9991	0.9988	0.9990
Chlorhexidine : Holbrook assay				
Apparent rate constant ($sec^{-1} \times 10^{6}$)	22.9	23.6	2.83	2.86
SD apparent rate constant ($sec^{-1} \times 10^{6}$)	1.358	1.266	0.062	0.090
RSD apparent rate constant	5.9%	5.4%	2.2%	3.1%
Correlation coefficient	0.9930	0.9969	0.9988	0.9975
Underestimation ratio	1.97	1.91	2.06	2.11
4-chloroaniline : Colorimetric assay				
Apparent rate constant ($sec^{-1} \times 10^{6}$)	11.0	8.02	1.26	0.97
SD apparent rate constant ($sec^{-1} \times 10^{6}$)	0.637	0.516	0.054	0.065
RSD apparent rate constant	5.8%	6.4%	4.3%	6.7%
Correlation coefficient	0.9933	0.9918	0.9958	0.9892
Underestimation ratio	4.09	5.62	4.63	6.22

Table 7.3 Effect of concentration and salt form on degradation rate constants (real and apparent) produced by different assay methods

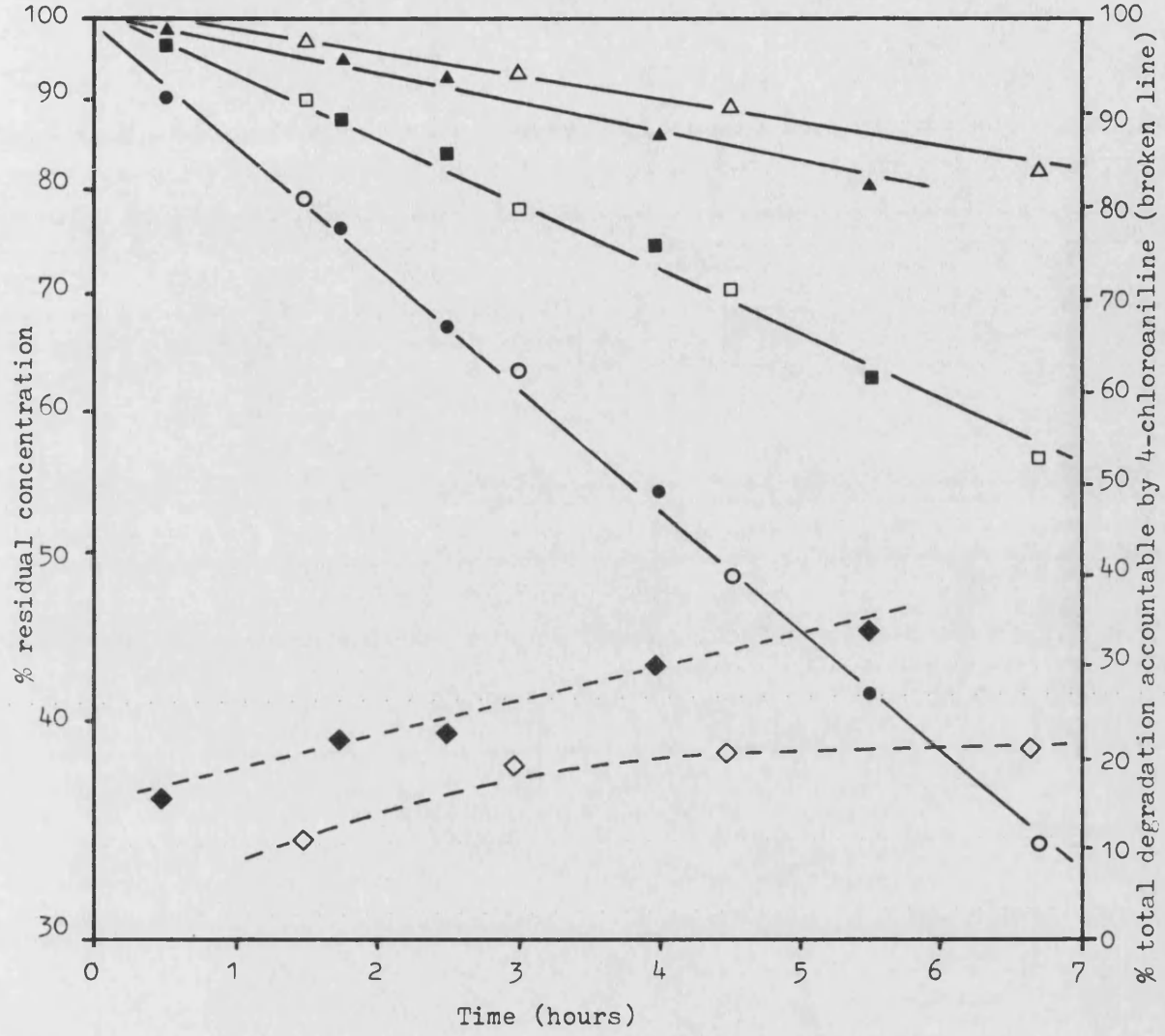

Figure 7.4 Apparent degradation profiles of 2.2×10^{-5}M chlorhexidine gluconate and acetate solutions degraded at pH 9.0, 90°C, produced from different assay methods:

○ ● HPLC stability indicating
□ ■ Holbrook colorimetric assay
△ ▲ 4-Chloroaniline assay to predict residual chlorhexidine
◇ ◆ Percentage of total degradation which could be accounted for by 4-chloroaniline content alone

(closed symbols - gluconate, open symbols - acetate)

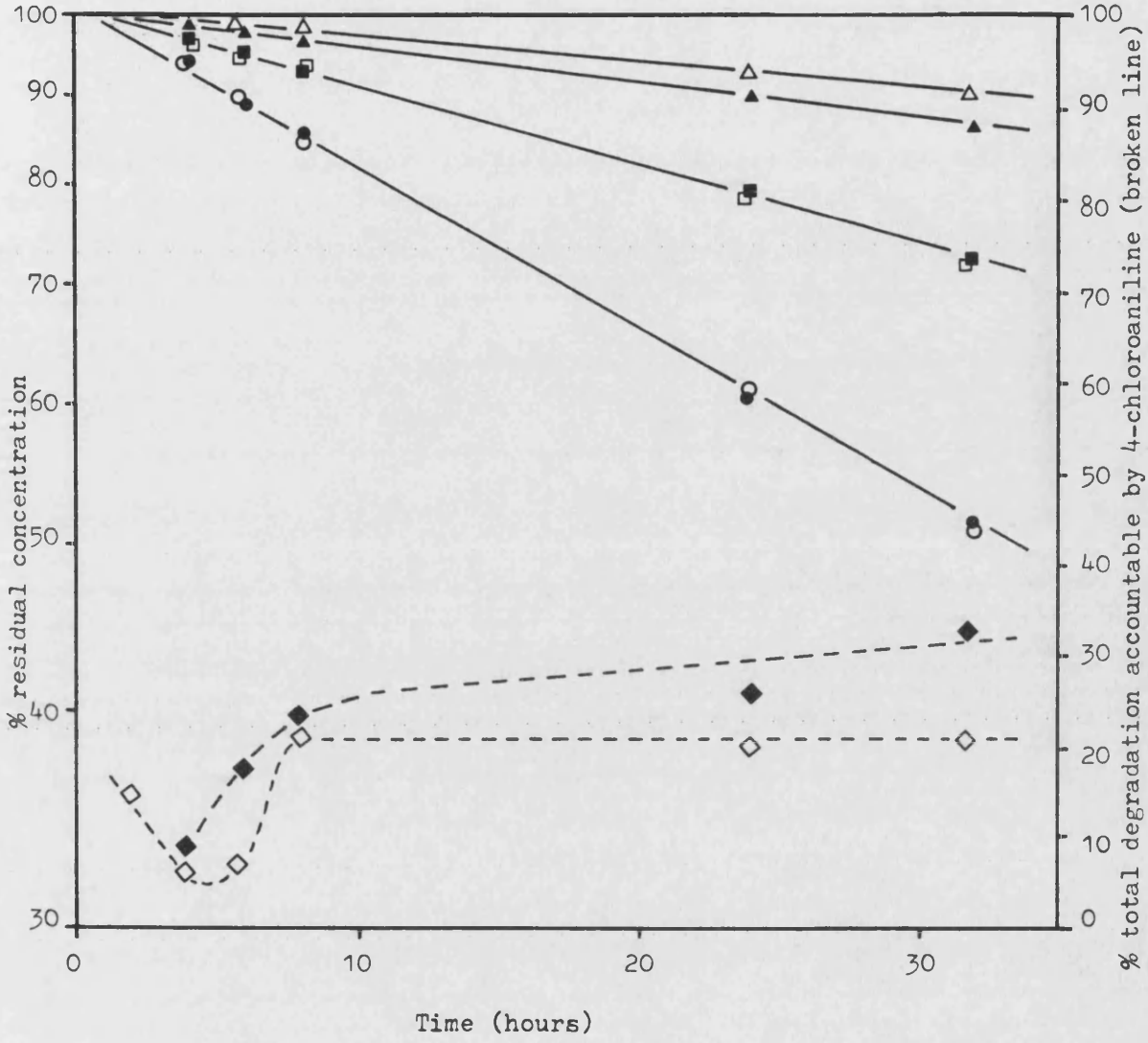

Figure 7.5 Apparent degradation profiles of 5.6×10^{-4}M chlorhexidine gluconate and acetate solutions degraded at pH 9.0, 90°C, produced from different assay methods:

○● HPLC stability indicating
□■ Holbrook colorimetric assay
△▲ 4-Chloroaniline assay to predict residual chlorhexidine
◇◆ Percentage of total degradation which could be accounted for by 4-chloroaniline content alone

(closed symbols - gluconate, open symbols - acetate)

7.2.4 Discussion of Results

Degradation profiles generated from the assay of residual chlorhexidine by the Holbrook assay method, and apparent residual chlorhexidine by the assay of 4-chloroaniline, were linear when plotted according to first-order kinetics (Figures 7.1 to 7.4). However, the RSD of the generated slopes (2.2 to 8.1%) were significantly higher than those obtained from the assay of chlorhexidine by the HPLC stability indicating method (< 3% RSD). This may be associated with the response to a number of degradation products in addition to chlorhexidine (Holbrook assay) or deviations from first-order kinetics (4-chloroaniline production).

Apparent degradation from the Holbrook assay method

The Holbrook colorimetric assay for chlorhexidine underestimates the extent of degradation compared to the stability indicating assay method by a factor of two, which is essentially independent of pH, concentration or salt form (mean 2.00, CV 4.2%).

Since the Holbrook colorimetric assay responds to biguanide containing molecules, whereas the HPLC assay is specific for chlorhexidine, it may be proposed that one half of the chlorhexidine molecule can undergo degradation whilst the other remains intact. This half of the molecule is free to undergo Holbrook colour-complex formation and respond to the assay as half a chlorhexidine molecule, thus underestimating the extent of degradation by a factor of two.

The Holbrook assay results therefore provide evidence that the degradative reaction sequence at one end of the molecule proceeds independently from the other end of the molecule.

Apparent degradation by assay of 4-chloroaniline

The calculation of apparent residual chlorhexidine concentration from 4-chloroaniline assay also underestimates the extent of degradation, all underestimation ratios ($R\mu$ = 3-6) being greater than those observed from the Holbrook assay method. The ratios were also observed to vary with pH, salt form and, to a lesser extent, concentration.

The fact that the underestimation ratio decreased in regions of acid and base catalysis may be explained in terms of parallel reactions; the rate of the hydrolysis reaction responsible for the production of 4-chloroaniline being proportionately greater than other reactions at acidic and alkaline pH. Evidence for this comes from the plots of 4-chloroaniline expressed as a percentage of the total degradation products. For example, from Figures 7.1 to 7.3, at 50% residual chlorhexidine concentration by HPLC, the percentage degradation due to 4-chloroaniline was approximately 29, 25 and 32 at pH 2, 6 and 9 respectively.

The salt form of chlorhexidine also influenced apparent degradation rate constants, the gluconate form producing significantly more 4-chloroaniline than acetate in solutions of equivalent molar concentration (t = 3.64, 3.43 and t_{tab} = 2.02, 1.90 for 0.22 and 5.6×10^{-4}M respectively, p = 0.05). However, previous studies (Chapter 6.6.2) showed no difference between the degradation rate constants when assayed by the stability indicating HPLC method. Therefore, whilst not affecting the overall rate of degradation, it would appear that the gluconate or acetate anions exert some mechanistic influence on the production of 4-chloroaniline. These differences were not due to the

initial concentration of 4-chloroaniline in undegraded solutions since this was always determined and subtracted from the concentration found in degraded solutions.

One common feature of all plots (Figures 7.1 to 7.5) expressing 4-chloroaniline as a percentage of the total degradation products is its increase as degradation proceeds. This suggests that the production of 4-chloroaniline occurs as a result of the second or subsequent stages in a multi-step or consecutive degradation reaction sequence (i.e. 4-chloroaniline is a product of degradation of a previous degradation product). This argument is strengthened by the observation that appreciable levels of 4-chloroaniline were found in extensively degraded chlorhexidine solutions. As degradation proceeded beyond 10 to 20% residual chlorhexidine the degradation product peaks also decrease on HPLC analysis as illustrated by Figure 7.6. It was also noted that the peak due to 4-chloroaniline (as determined in Chapter 5.2.2) becomes more predominant as degradation proceeds. Therefore, 4-chloroaniline appears to be a final product of most degradative reactions.

From the above information it is clear that the application of 4-chloroaniline concentration to predict chlorhexidine degradation is extremely inaccurate since it is not, initially, the major degradation product but results from a complex series of parallel and consecutive reaction processes.

7.3 QUALITATIVE EVALUATION OF DEGRADATION PRODUCTS

It was noted from the HPLC analysis of a wide range of degradation studies that the sequence in which degradation products

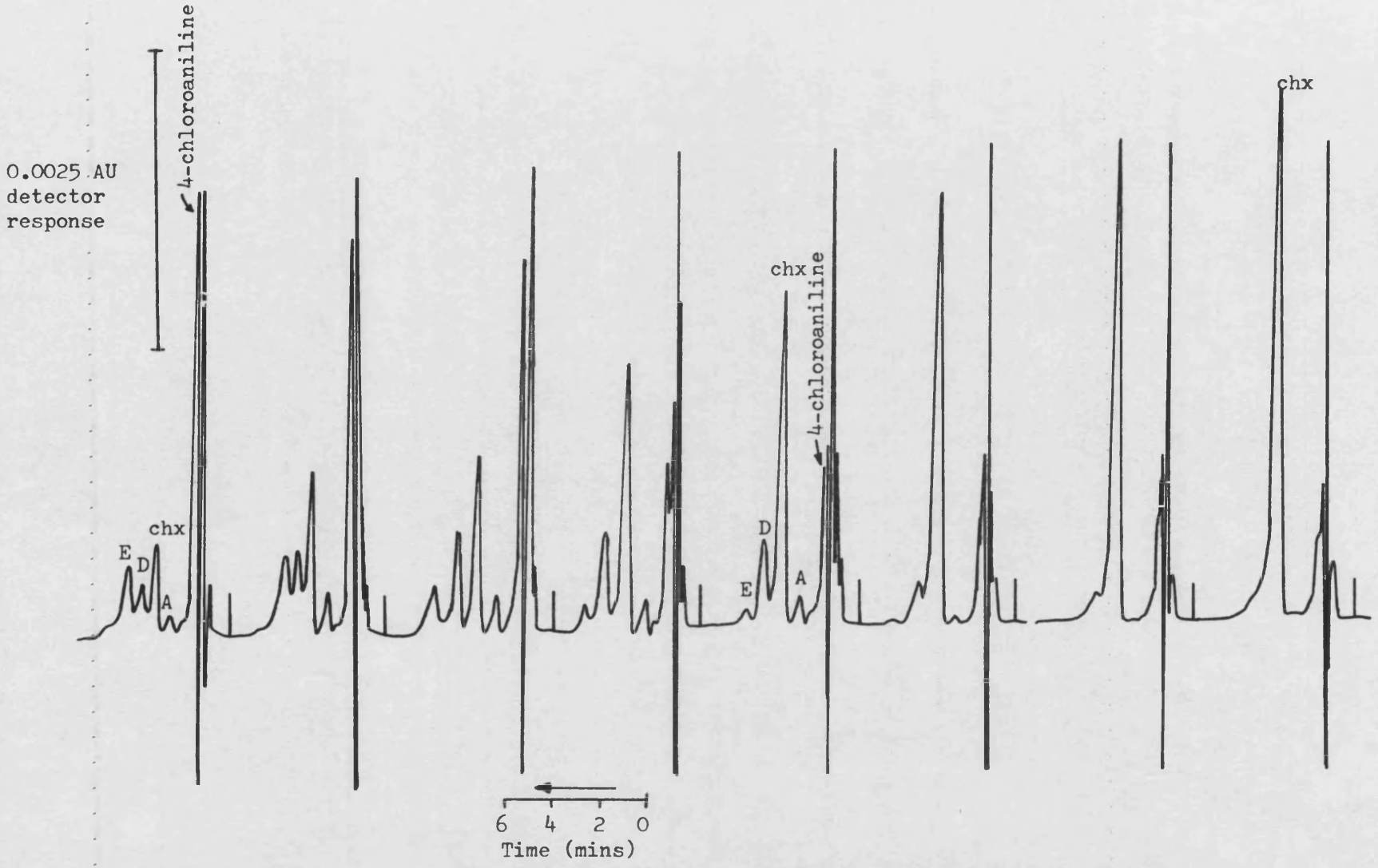

Figure 7.6 Chromatograms showing the sequence of degradation product production (D, A, E with 4-chloroaniline unplaced) and subsequent decrease in peak heights of D and A as chlorhexidine degradation proceeds

appeared remained identical, this being D, A then E as shown by Figure 7.6. Although other degradation products were apparent (α and G), their peaks were too small to positively identify their position within this sequence.

In the absence of pure degradation product samples it is obviously not possible to quantify the kinetic relationship between each step of the degradation cascade since HPLC calibration curves could not be generated. Consequently, qualitative evaluation was performed since this could at least make some contribution towards prediction of the reaction pathway. The following approach was adopted.

Chromatograms resultant from the degradation studies reported in Chapter 6 (Sections 6.6.1 - 6.6.5 and 6.6.7) were used to generate peak height data for degradation products A, D and E. The peak heights of other degradation products (α and G) were too small to be measured meaningfully. Earlier studies (Chapter 5.1.1.3.2) have shown that the degradation products D, A and E also have an apparent λ_{max} at 254 nm, this being similar to chlorhexidine. The peak heights at 254 nm of these degradation products were then expressed as a percentage of the original chlorhexidine peak height (at zero time, 100% residual) and plotted against percent degradation of chlorhexidine. Visual comparison of the various sets of data indicated that there was no obvious specific effect of any degradative condition upon the generation of a degradation product. Therefore all data were pooled together. Since approximately 600 measurements were made for each of the three degradation products, scatter plots were produced

with the data contained between upper and lower boundaries. Smoothed lines representing these boundaries are shown in Figures 7.7 (degradation product D), 7.8 (A) and 7.9 (E).

The following features were noted from these Figures:-

(i) The peak heights (or concentrations) of degradation products D and A show a maximum at approximately 75 and 55% degradation of chlorhexidine respectively. The decrease in peak height as degradation proceeds beyond these values indicates that the degradation products are also degrading. Therefore chlorhexidine and degradation products A and D degrade by a parallel but concentration dependent process.

(ii) Degradation product E did not show a maximum but its "concentration" remained apparently constant beyond 75% degradation of chlorhexidine. In two instances the degradation was continued beyond the time at which all chlorhexidine had degraded. In these solutions the peak of E was seen to decrease. This may indicate that E is a more stable degradation product, or alternatively, that an equilibrium process exists.

(iii) It was noted that the overall loss of D and constant level of E began to occur in a region where the degradation of chlorhexidine ceased to fit first-order kinetics (~ 70 to 80% degradation of chlorhexidine).

(iv) Degradation product D appears to be an important, if not the major, degradation product of chlorhexidine (see also Chapter 8).

7.4 ATTEMPTED IDENTIFICATION OF DEGRADATION PRODUCTS

Attempts were made to isolate and identify degradation products of chlorhexidine by preparative HPLC and HPLC-mass

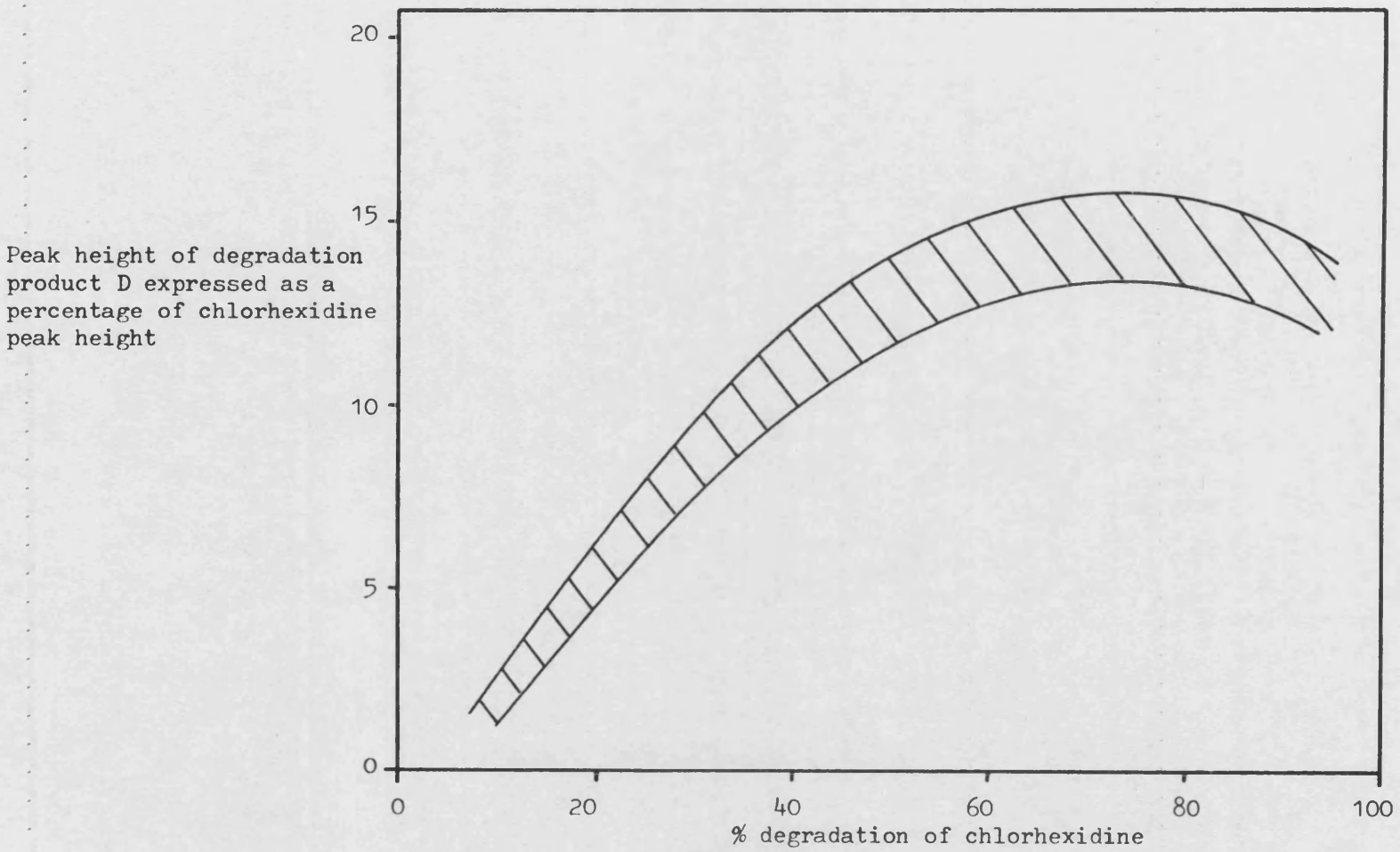

Figure 7.7 Scatter plot showing the change in content of degradation product D with residual chlorhexidine. The curves represent smoothed lines drawn through upper and lower data point boundaries

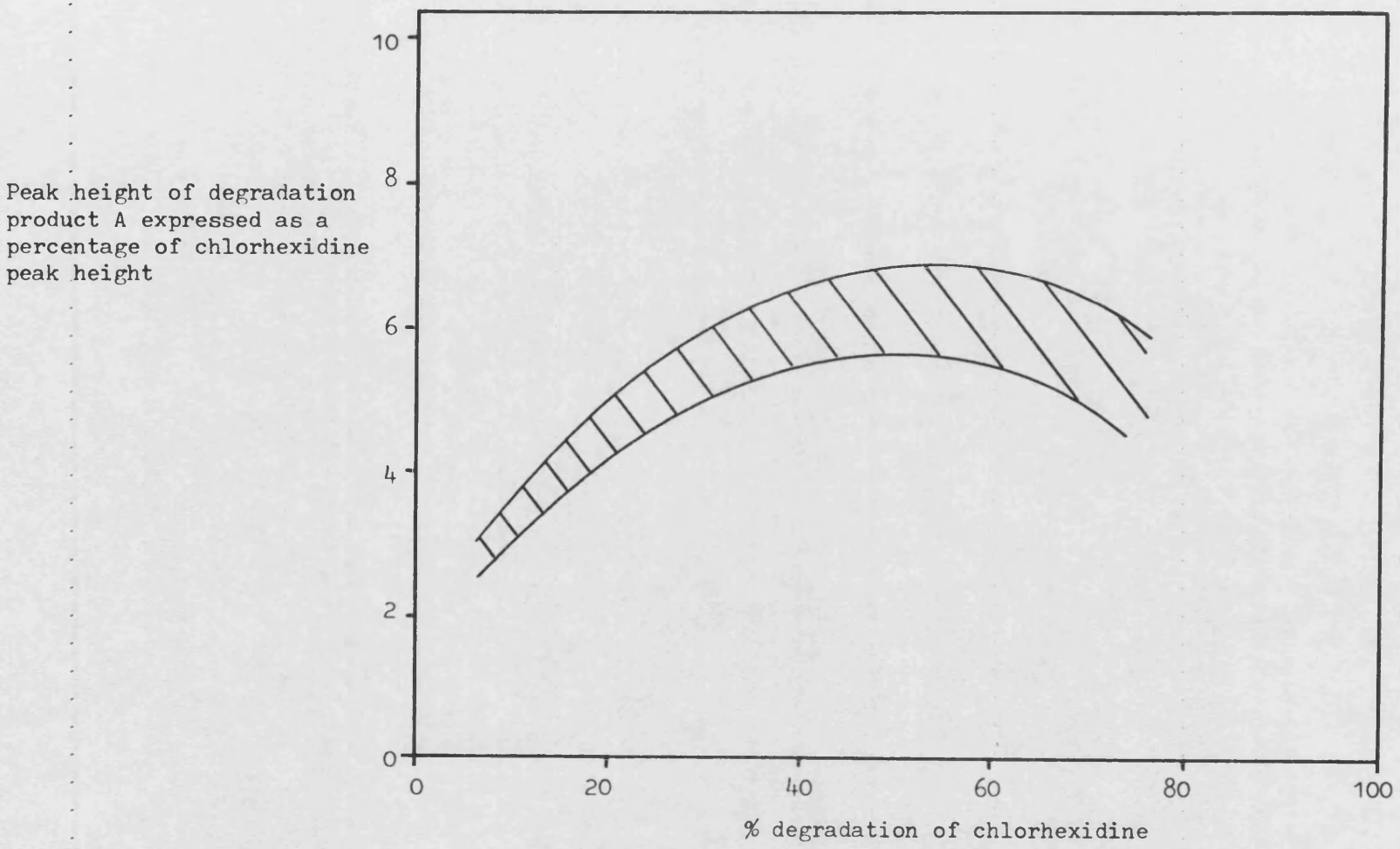

Figure 7.8 Scatter plot showing the change in content of degradation product A with residual chlorhexidine. The curves represent smoothed lines drawn through upper and lower data point boundaries

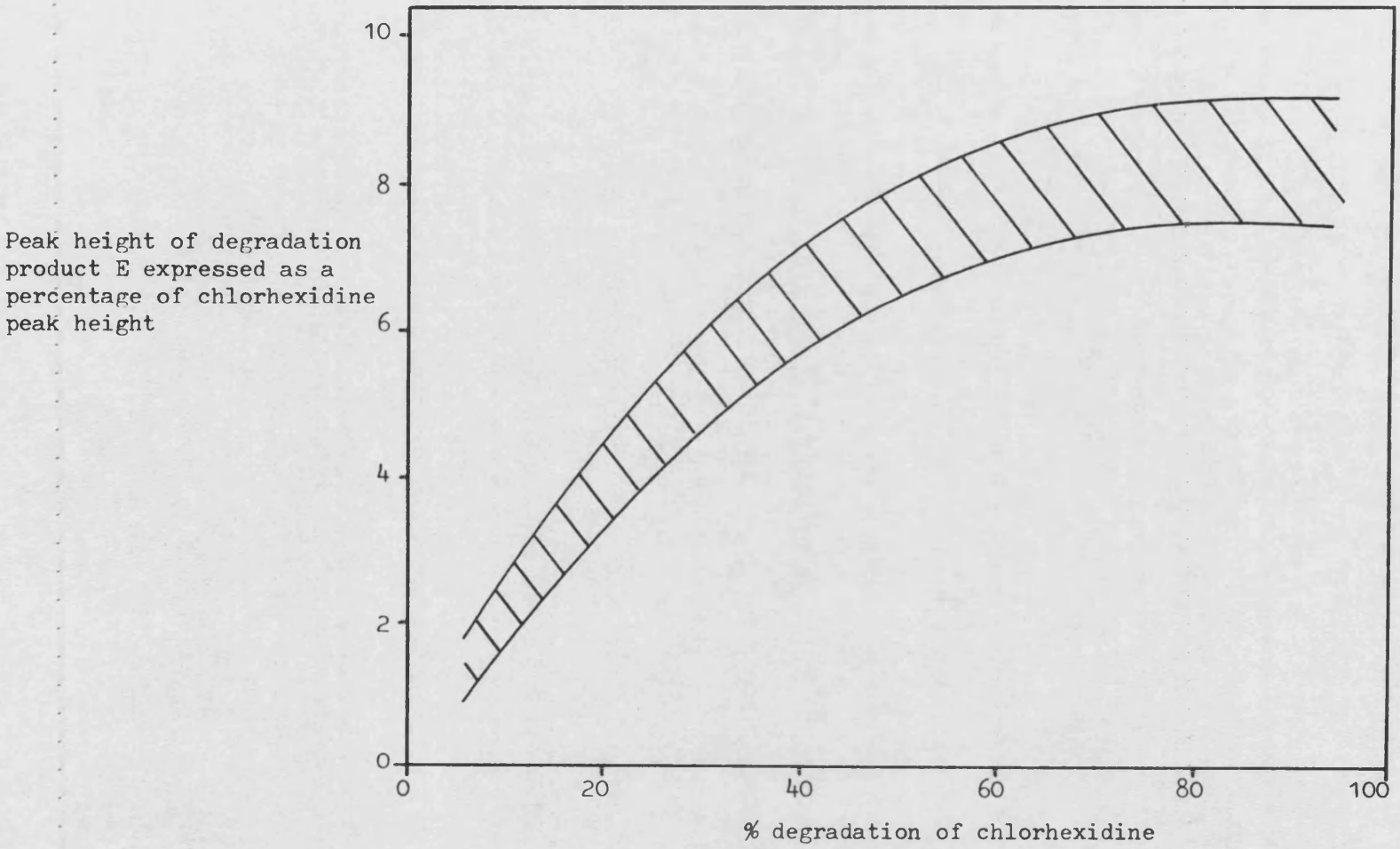

Figure 7.9 Scatter plot showing the change in content of degradation product E with residual chlorhexidine. The curves represent smoothed lines drawn through upper and lower data point boundaries

spectrometry. This work was initiated at a late stage in the project with the results, unfortunately, being inconclusive.

7.4.1 Production of Degraded Solutions

The HPLC stability indicating method has identified five degradation products (plus 4-choroaniline) in heavily degraded solutions (Chapter 5.1.1.3.2). Peak height measurements (Section 7.3) have shown three of these (A, D and E) to be "apparent" major degradation products. Although the HPLC method separates (therefore isolates) these products, the concentrations at which they were present in degraded solutions was insufficient to enable identification. Concentration of degradation products was therefore required. This was performed by degrading a 0.05% w/v chlorhexidine gluconate solution at pH 10 and 90°C (to accelerate decomposition). Approximately 5 ml aliquots of 1.0% w/v chlorhexidine gluconate were frequently added to this degrading solution in order to maximise the rate of production of degradation products, this being monitored by HPLC analysis. The reaction was stopped when an overall loss (decrease in peak height) of degradation products occurred. Figure 7.10(a) shows the chromatogram of a chlorhexidine solution degraded by this method. The degradation products A, D and E are clearly present together with 4-chloroaniline. From the residual chlorhexidine concentration and knowledge of the total chlorhexidine concentration added during degradation it was calculated that the equivalent of 100 mg chlorhexidine gluconate per 250 ml of solution had degraded. This process was repeated several times and the resultant solutions bulked together and concentrated by rotary evaporation to give approximately 1 g of apparent degradation products in 100 ml of aqueous solution. A chromatogram of this

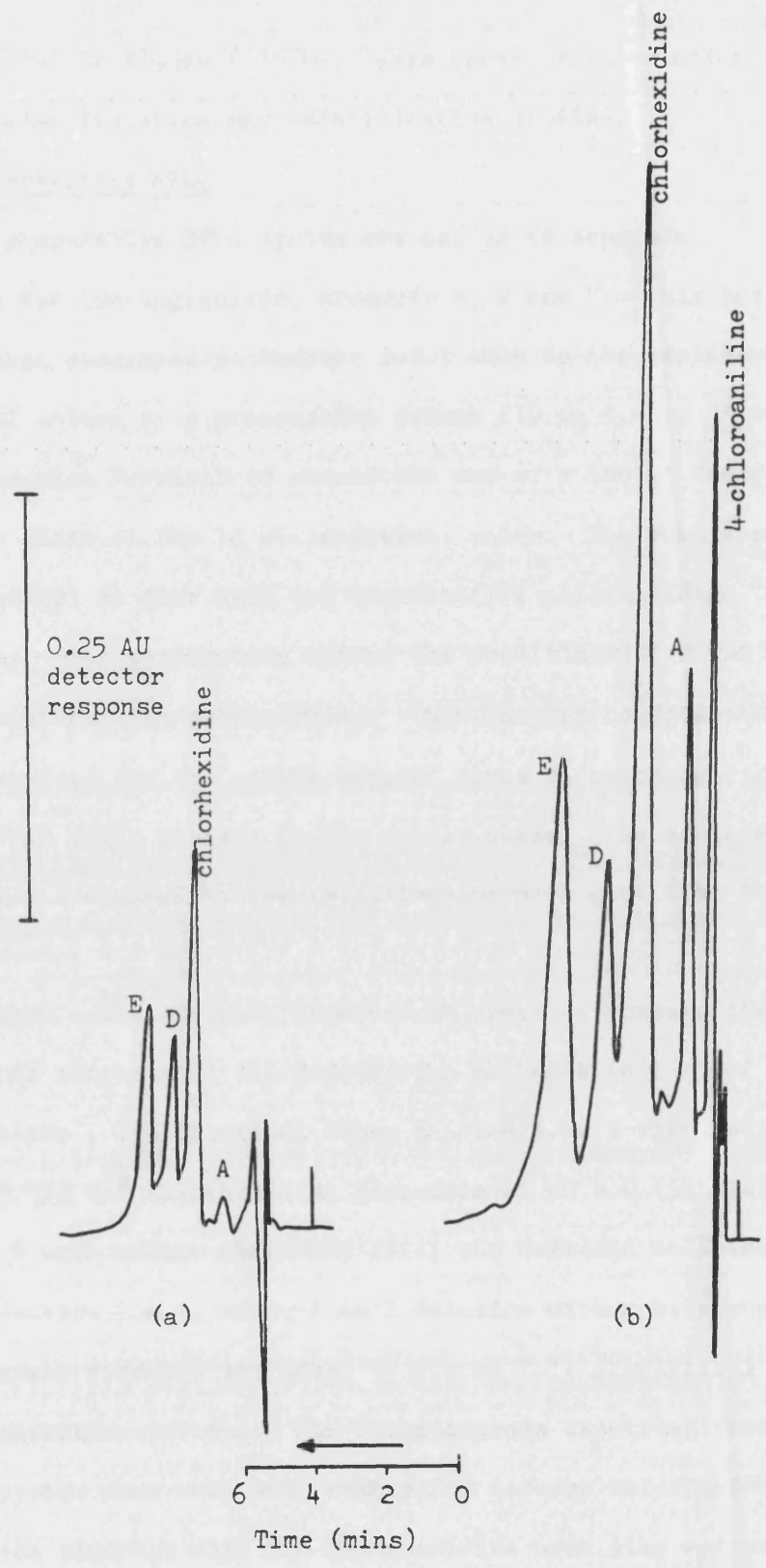

Figure 7.10 Chromatograms of:

(a) Degraded 0.05% w/v chlorhexidine gluconate solution with frequent addition of chlorhexidine gluconate to increase degradation product content

(b) Several solutions, similar to that described above, bulked together and concentrated by rotary evaporation

Both solutions injected as 1 in 5 dilutions in mobile phase

solution is shown in Figure 7.10(b). This concentrate solution was used for the following isolation and identification studies.

7.4.2 Preparative HPLC

A preparative HPLC system was set up to separate chlorhexidine and the degradation products A, D and E. This system differed to that described in Chapter 5.1.1 only in the replacement of the analytical column by a preparative column (10 mm i.d. x 25 cm length) packed with Partisil 10 µm and the use of a 500 µl Rheodyne loop valve in place of the 10 µl analytical valve. The mobile phase remained identical to that used for quantitative chlorhexidine determinations. The preparative column was conditioned for two weeks by constant elution with mobile phase. This lengthy conditioning period was required for the silica support phase to reach an equilibrium with water present in the mobile phase. The achievement of equilibrium was indicated by the establishment of a good flat base line.

Three solutions were injected in order to compare the chromatographic response of the preparative column with that of the analytical column : (i) distilled water diluted 1 in 5 with mobile phase, (ii) 0.05% w/v chlorhexidine gluconate at pH 9.0 (initial), diluted 1 in 5 with mobile phase and (iii) the degraded solution, produced in Section 7.4.1, after 1 in 5 dilution with mobile phase. The chromatograms produced are shown in Figure 7.11 (analytical column) and 7.12 (preparative column). The chromatograms resultant from the preparative system show very poor resolution between chlorhexidine and its degradation products with the chlorhexidine peak also suffering peak splitting and extensive band broadening. It was also noted that

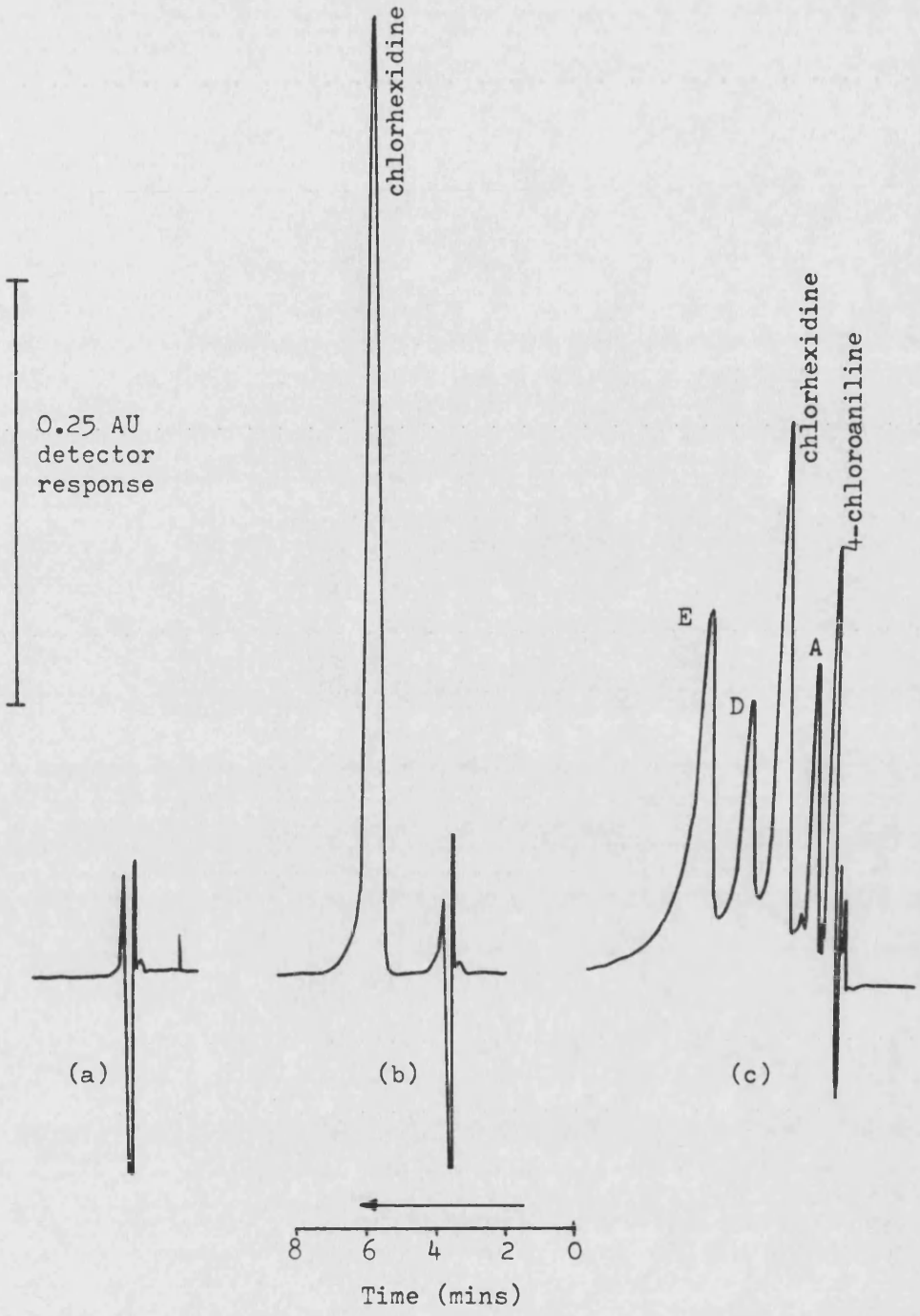

Figure 7.11 Chromatograms produced from the analytical column:

(a) Distilled water

(b) 0.05% w/v chlorhexidine gluconate at pH 9.0 (initial)

(c) Degraded system produced in section 7.4.1

All solutions were injected as 1 in 5 dilutions with mobile phase

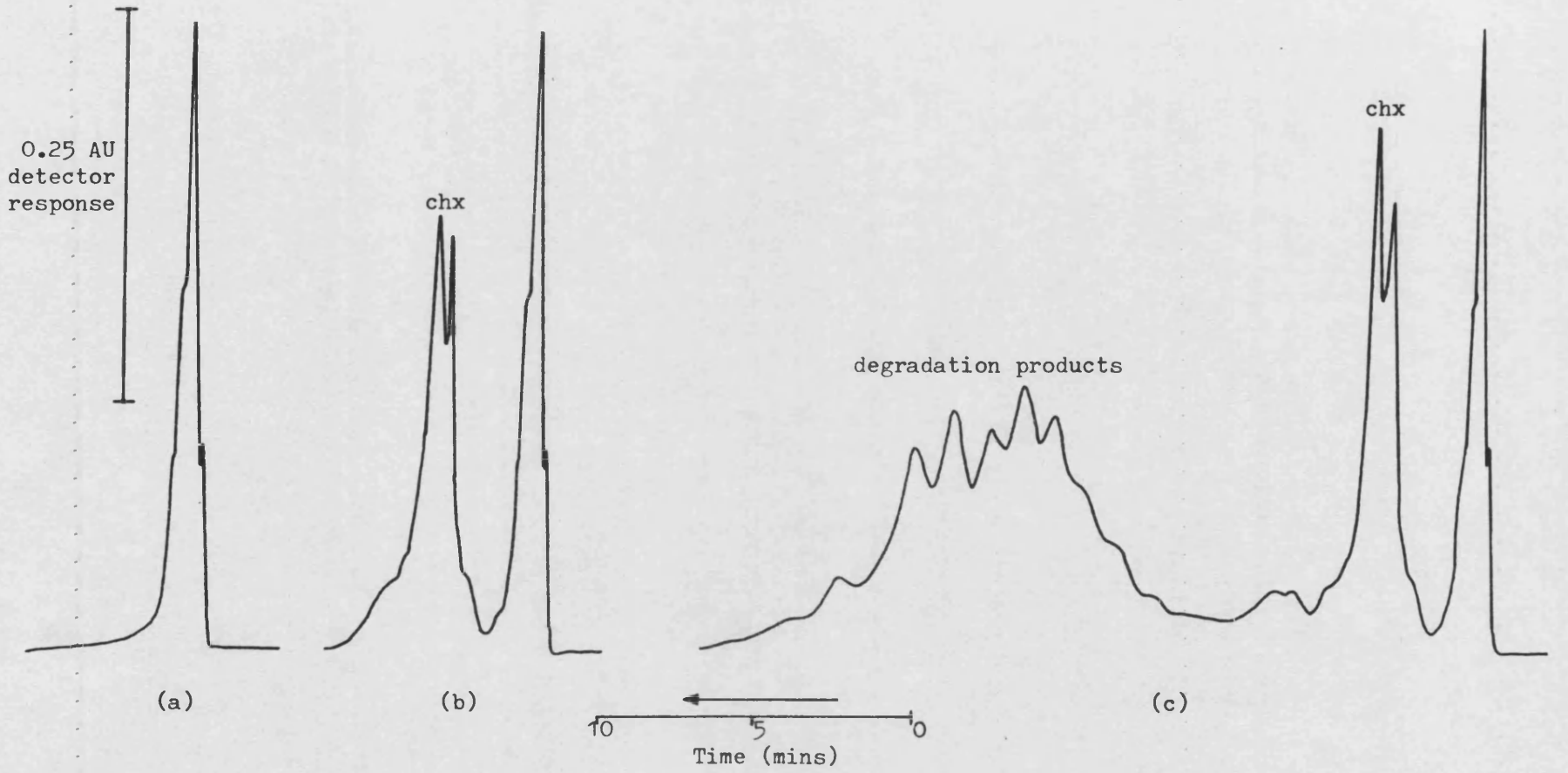

Figure 7.12 Chromatograms produced from the preparative column:

(a) Distilled water

(b) 0.05% w/v chlorhexidine gluconate at pH 9.0 (initial)

(c) Degraded solution produced in section 7.4.1

All solutions were injected as 1 in 5 dilutions with mobile phase

the number of peaks for the degraded solution (iii) had increased from four (plus solvent front) on analytical assay to over ten (possibly also due to peak splitting) on the preparative scale.

No improvements in selectivity or resolution were obtained after alteration of mobile phase flow rate or composition (increasing and decreasing the organic : aqueous ratio; increasing and decreasing phosphoric acid strength). Time dictated that no further attempts could be made to obtain a preparative system with the resolution and selectivity of the analytical method. Recourse was made to HPLC-mass spectrometry (HPLC-MS) techniques.

7.4.3 HPLC - Mass Spectrometry

The technique of combined HPLC-MS couples chromatographic separation with the sensitivity of mass spectrometry. Although this technique is still in its development stage it has been advocated for the identification of drug substances and their degradation products or metabolites (Erni, 1982; Games, 1981).

In order to test whether this method could provide any supportive evidence for the identification of chlorhexidine degradation products, experiments were undertaken at the Department of Chemistry, University College, Cardiff, in the laboratory of Prof. D. E. Games.

A moving belt system (described by Games, 1981) was used to provide the interface between the HPLC and mass spectrometer systems. The HPLC eluant formed a thin film on the moving belt. Solvent was then removed by an infrared lamp and two serial vacuum locks. After removal of solvent the belt passed through a heated chamber adjacent to the ion source where the solutes were flash vaporised into the ionisation chamber. Mass spectra were then collected at various time intervals to identify the pre-resolved degradation products.

The same analytical HPLC column and chromatographic conditions as those detailed in Chapter 5.1 were used (with the replacement of the 10 µl loop valve by a 50 µl loop). The degraded solution produced in Section 7.4.1 was analysed by this technique.

Results : The HPLC moving belt interface provided approximately 100 ng (total) of degradation products to the mass spectrometer. This concentration was considered acceptable for identification purposes. Both electron impact (EI) and chemical ionisation (CI) spectra were produced from the resolved HPLC eluant. However, the spectra produced were very poor and, importantly, showed no evidence of any chlorhexidine peak (contrary to HPLC evidence). A variety of reasons were proposed :

(i) The infrared heater on the moving belt, or flash vaporisation into the ion source, may have caused the pyrolysis of chlorhexidine and its degradation products resulting in artefact peaks and the absence of a chlorhexidine peak.

(ii) The presence of phosphoric acid in the mobile phase produced complicated spectra (from mass spectra of mobile phase alone).

(iii) The EI and CI techniques were possibly too vigorous for chlorhexidine and its degradation products.

Alternative (direct) methods of eluant introduction into the mass spectrometer were either inappropriate or not available at Cardiff. Alternative "softer" ionisation techniques, such as secondary ion mass spectrometry, were also not available at Cardiff. No further work was performed by HPLC-MS. However, this method should not be

totally discounted since, given the appropriate resources, it could still yield valuable information leading to the identity of chlorhexidine degradation products.

DISCUSSION

CHAPTER 8

D I S C U S S I O N

8.1 ANALYTICAL METHODS

At the start of this study no proven stability indicating analytical method for chlorhexidine was available in the literature. However, the method of Bailey et al (1975) provided the basis for the development of a HPLC stability indicating assay by the same workers at ICI Pharmaceuticals. Studies at ICI showed this method to be capable of quantitatively resolving chlorhexidine from its degradation products and impurities, including 4-chloroaniline. Therefore, this unpublished method was used for the quantitative determination of chlorhexidine during the degradation studies reported in this thesis.

Although no further basic development was performed, the experimental methodology required for the assay of chlorhexidine in dilute aqueous solution at ophthalmic concentrations was closely examined. Particular attention was given to validate the quantitative nature of the assay and identification of errors. Quantification was performed by peak height measurement since integration equipment was not routinely available, with reference made to an external standard of chlorhexidine acetate of known purity. Mobile phase composition (pH ~0.8 and presence of excess $H_2PO_4^-$ anions) ensured that solutions of different chlorhexidine

salts were chromatographically equivalent. However, all aqueous solutions required dilution with mobile phase prior to injection by a factor of 5 at least. This was because the equilibrium between the silica stationary phase and water in the eluting mobile phase was easily disturbed upon sample injection. Chromatograms resultant from the injection of purely aqueous samples showed a large solvent response and unresolved chlorhexidine peak (Figure 5.6). The same analytical column was used throughout the whole study without any decrease in measured chromatographic parameters. For example, the column capacity factor (measure of solute retention) and number of theoretical plates (column efficiency) remained practically constant throughout use, being 1.8 to 1.9 and 2200 to 2400 respectively for chlorhexidine.

Linearity of response up to 70 $\mu g.ml^{-1}$ chlorhexidine acetate injected was noted with deviation from Beer-Lambert observed above this concentration (Figure 5.3, Tables 5.3 and 5.4). The detection limit was approximately 0.5 ng chlorhexidine gluconate using a 10 µl loop valve with the limit of accurate quantitative determination being set at 4.5 ng (or 0.45 $\mu g.ml^{-1}$ injected). It is useful to discuss these limits in terms of detector sensitivity and signal to noise (S:N) ratios. The detection limit (or sensitivity) was calculated from the chlorhexidine concentration producing a 10 mm peak height at 0.001 AUFS (S:N ratio 5). Until the advent of the "next generation" of HPLC spectrophotometers, or significant improvements in column efficiency, this limit can only be reduced by the acceptance of lower S:N ratios. The quantitative limit was derived from a S:N ratio of 50 using a 10 µl injection loop.

Greater quantitative sensitivity, but with slight loss of reproducibility, may be achieved by increasing the injection loop volume and reducing the S:N ratio acceptance limit. For example, with a 100 µl loop and S:N ratio of 10, chlorhexidine gluconate solutions as dilute as 10 $ng.ml^{-1}$ injected may be quantitatively determined by this assay method. At this concentration, peak height reproducibility is estimated to be ±5%.

The reproducibility of manual injection was good (CV 1.5% at 1.6 $\mu g.ml^{-1}$ injected), although autosampler injection showed a two fold improvement in coefficient of variation (Tables 5.11 and 5.12). Because peak height-concentration profiles to establish linearity of response occasionally showed an intercept to standard deviation ratio >2 (Table 5.6), calibration plots were prepared daily from injection of standard solutions at the beginning, end and interspersed throughout the day's assays. For greater accuracy of interpolation, three standard solution concentrations were always used in the construction of calibration plots. To identify and reduce errors resultant from variable chromatographic response through the working day, a criterion was established which allowed only ±1.0% change in calibration plot slope during the day. This resulted in a confidence limit ($p = 0.99$) for data generated from the calibration plot of ±2.2% for assays performed on 0.002% w/v chlorhexidine gluconate solutions.

While the presence of surfactants, at the concentrations used for stability studies (Chapter 6.6.8), had little effect on chromatographic response, higher concentrations and the presence of buffers and counter-ions caused the chlorhexidine peak to split

(Figures 5.11(a) and 5.12(a)). This effect was both concentration and species dependent with acetate, phosphate and gluconate anions causing particular problems. In most cases an extra dilution stage prior to dilution with mobile phase was sufficient to "dilute out" this effect. However, chlorhexidine could not be assayed in the presence of acetate concentrations >0.02 M and gluconate >0.1 M, even after pre-dilution. Similarly, the presence of CTAB concentrations $>2 \times 10^{-2}$ M and cetomacrogol 1000 and polysorbate 80 concentrations $>2 \times 10^{-3}$ M prohibited the assay of chlorhexidine due to peak interference.

The selectivity and sensitivity of the method to degradation products was demonstrated by studies at Bath and within ICI Pharmaceuticals Division. The method was capable of resolving chlorhexidine from six unknown degradation products as well as 4-chloroaniline (Figure 5.15), although the latter eluted very close to the solvent front (Figure 5.23). Thin layer and paper chromatographic studies (Chapter 5.1.3) could only identify a maximum of five degradation products including 4-chloroaniline, these at concentrations in vast excess of those required for resolution by HPLC.

Individual sources of error for the HPLC method were identified as the measurement of peak height, glassware (or dilution) errors, reproducibility of injection and calibration plot error (Chapter 5.1.1.4.3). From confidence limits ($p = 0.99$) overall errors of ±2.6% and ±3.0% were calculated for automatic and manual injection respectively (Table 5.14). Whilst these values may appear large in comparison with commonly quoted literature values (0.5 to 2.0%), they represent the statistical overall error from

four individual sources. Close examination of values claimed in the literature often reveals that only one source of error had been quantitatively determined (usually reproducibility of injection).

Since the largest contributant to the overall error was calibration plot error, careful steps were taken to reduce this in the development of a chlorhexidine assay protocol. Measures included the construction of calibration plots from three standard solutions, interpolation and not extrapolation and frequent interspersion of standards with samples. The use of a change in calibration slope criterion also helped to identify any peak height variation which may have occurred due to influences such as temperature or mobile phase composition.

By close examination of the complete method it is possible to identify areas where further improvements and error reduction may be made. For example, the coefficient of variation of injection reproducibility (1.6 $\mu g.ml^{-1}$ chlorhexidine acetate injected) was improved from 1.5% on manual injection to 0.9% using the autoinjector. Current "state of the art" autoinjectors are capable of achieving an injection reproducibility in the order of < 0.5% CV. Improved autoinjector reproducibility also provides scope for the reduction of calibration plot error since injection reproducibility contributes to the accuracy of generated calibration data.

Some degree of error is always present in assay methods using external standardisation. Quantitation by reference to an internal standard is usually more accurate than external standardisation and allows a greater sample throughput. However,

the use of an internal standardisation technique is less appropriate in stability studies due to the potential interference of internal standard and degradation product peaks. Because of slightly greater accuracy and the availability of relatively low cost dedicated data handling systems, quantification by peak area rather than peak height measurement is usually performed. Theoretically, the adoption of peak area measurement may reduce overall error, although the contribution of peak height measurement error towards the overall error was small. However, this improvement is theoretical since the chlorhexidine peak showed a characteristic tail and stability studies indicated that above ~ 95% residual chlorhexidine concentration degradation product D was not resolved from this tail. Thorough validation of the discriminatory power of peak area measurement in regions of modest degradation would therefore be necessary.

The literature carries numerous analytical methods specifically developed for the assay of chlorhexidine in pharmaceutical formulations (particularly ophthalmic products). In these formulations, chlorhexidine is usually present at low concentration (Table 2.1) with the assay further complicated by the presence of other actives and excipients. Consequently, the published methods may only be sensitive and selective to chlorhexidine under a given set of conditions. Since the influence of excipients on the HPLC stability indicating method was not examined during this study it would be unwise to compare this method critically with other analytical techniques. However, in general terms it is pertinent to discuss certain aspects of other methods, particularly those involving HPLC.

Spectroscopic methods derive their specificity towards chlorhexidine from colour-complex formation and extraction procedures. The methods of Andermann et al (1980) and Pinzauti et al (1982) have generated accurate results for the determination of chlorhexidine gluconate in ophthalmic products and cosmetics down to 2.5 $\mu g.ml^{-1}$ (2.5×10^{-4}% w/v). However, their application was limited since many excipients were also observed to co-extract with chlorhexidine forming colour-complexes. The Holbrook colorimetric method has been successfully used by many workers assaying dilute solutions of chlorhexidine gluconate. For example, Richardson et al (1977) recorded a precision of ± 2.8% for the analysis of 0.001% w/v chlorhexidine gluconate solutions. Additionally, this assay procedure was not influenced by commonly used contact lens solution adjuvants and other preservatives. However, previous degradation studies performed within this Department, along with the studies presented in this thesis (Chapter 7.2), have shown that the Holbrook hypobromite colour-complex can also be produced from biguanides such as proguanil and degraded bis-biguanides (chlorhexidine degradation products). This non-selectivity can, therefore, seriously overestimate the chlorhexidine content.

The potentiometric and gravimetric methods of Pinzauti and La Porta (1981) and Pinzauti et al (1976; 1981) are rather complex, non-selective and too insensitive ($\lesssim$ 0.006% w/v chlorhexidine gluconate) for general use.

Due to the combination of selectivity, sensitivity, speed and precision most new analytical methods for chlorhexidine involve the use of HPLC. The first published HPLC method was that of Bailey

et al (1975) who used a silica stationary-phase and acetonitrile : 0.01M sulphuric acid mobile phase. This method was demonstrated to be sensitive, selective and accurate for the determination of chlorhexidine in a wide range of formulations (although certain products required an extraction procedure). This normal-phase adsorption method was the predecessor of the stability indicating method used in this thesis. However, it is surprising to note that all succeeding methods have used reverse-phase ion-pair techniques. This is probably because this technique, rather than that of adsorption chromatography, has become the first-choice when developing a new method.

Bachner et al (1981), Collins et al (1979) and Stuber and Muller (1981) provide methods for the concomitant analysis of chlorhexidine with other active pharmaceuticals in creams, gels and eye drops. In these preparations chlorhexidine gluconate was always present at concentrations > 0.01% w/v. The method of Perez (1980; 1981) was developed to separate and quantify chlorhexidine and 4-chloroaniline in commonly used chlorhexidine solutions which also contained cetrimide and dyes. This method offers an attractive alternative to the colorimetric determination of 4-chloroaniline and separate analysis of chlorhexidine. Quantitative sensitivities to chlorhexidine and 4-chloroaniline were approximately 0.0025 and 0.001% w/v respectively with an accuracy of 3% for chlorhexidine gluconate at 0.015 to 0.05% w/v. However, it should be noted that this method is not stability indicating since it assumes 4-chloroaniline to be the only breakdown product.

A method for the detection of chlorhexidine in blood and urine as well as pharmaceutical preparations has been proposed by Huston et al (1982). This method, admirably supported by experimental validation, has a detection limit of 0.1 $\mu g.ml^{-1}$ and quantitative sensitivity of 1 $\mu g.ml^{-1}$. An extraction stage in the latter method has since been improved by Gaffney et al (1984) with quantitation via one of several internal standards proposed.

Several HPLC methods have also been published since the completion of the experimental studies described in this thesis. Notably, the 1983 Addendum to the British Pharmacopoeia 1980 carries a HPLC method (rather than TLC) for its Related Substances Test in the Chlorhexidine Gluconate Solution monograph. This is again a reverse-phase ion-pair method with the test specification being of the "not greater than" type to limit manufacturing impurities. No mention is made as to the likely position or number of degradation products. In proposing "stability indicating" reverse-phase ion-pair methods, Bauer et al (1983; 1984), Manousaki (1986) and Richard et al (1984) all assumed that 4-chloroaniline is the only breakdown product of chlorhexidine. Studies in this thesis have shown this assumption to be untrue (Figure 5.15). Stevens et al (1986) used a reverse-phase column with mobile phase composition similar to that used in this thesis for the stability indicating normal-phase method. Such a combination produced an accurate method for the determination of chlorhexidine in contact lens solutions although samples had to be pre-diluted in saline before injection. Potential degradation products such as phenylbiguanide and 4-chlorophenylbiguanide in addition to 4-chloroaniline were resolved

by this method. It is significant to note that Stevens et al (1986) make a positive comment that other degradation products are, in certain circumstances, far more predominant than 4-chloroaniline.

Studies have also been performed within this Department using both reverse-phase and the normal-phase stability indicating method to assay degraded chlorhexidine solutions. Whilst the normal-phase method has been fully validated as stability indicating by studies contained within this thesis, its application to the analysis of chlorhexidine in ophthalmic and contact lens solutions has been unsuccessful due to interference from formulation excipients (Purdy et al, 1986). However, assay by a reverse-phase method was found to be much more suitable for these products with normal formulation vehicles and excipients not interfering with the chlorhexidine peak. Comparison of chromatograms produced from injection of the same degraded chlorhexidine solution showed the reverse-phase method to be capable of resolving only two degradation products compared to five resolved by the normal-phase method. However, quantitative comparison of the same degraded samples showed the two methods to give very similar results for the residual chlorhexidine content (Table 8.1). Therefore, although reverse-phase methods are more practically applicable to the analysis of chlorhexidine in ophthalmic products, they should each be fully validated as stability indicating. It would appear that at present this can only be performed by use of the normal-phase adsorption method described in this thesis.

Sample	% residual chlorhexidine gluconate (SD)		
	Normal-phase method (A)	Reverse-phase method (B)	Relative recovery ($\frac{B}{A}$ x 100%)
1	88.0 (2.2)	89.7 (3.2)	101.9
2	72.8 (1.1)	71.7 (0.3)	98.5
3	62.5 (-)*	61.4 (-)*	98.2*
4	35.9 (2.0)	34.8 (2.0)	96.9
5	27.7 (1.5)	26.1 (0.2)	94.2
		Mean relative recovery	97.9(CV 2.9%)

All assays performed in triplicate except * where only one replicate performed.

Table 8.1 Chlorhexidine gluconate content of 0.00184% w/v solutions degraded at pH 9.0 and 90°C. Assays performed by the normal-phase (stability indicating) and reverse-phase HPLC methods (from Purdy et al, 1986).

It should be noted that no other analytical method has demonstated the quantitative sensitivity and detection limit obtained by the normal-phase stability indicating HPLC method. This, combined with speed, accuracy and ease of use, leads to the recommendation that this method should be the method of choice for the assay of chlorhexidine, with reverse-phase methods reserved for application where formulation excipients exert a deleterious influence on the former method.

8.2 DEGRADATION KINETICS

The thermal degradation of chlorhexidine was suspected to occur via a hydrolytic reaction mechanism (Chapter 2.5). The kinetics of such reactions are influenced by many catalytic effects, with most being pH dependent as detailed in Chapter 1.6.2. For example, applying the simple situation of specific acid/base

catalysis, a change of 1.0 pH unit can theoretically alter the observed degradation rate constant by ten-fold. Therefore, in a stability study, the effects of pH need to be clearly defined before investigating other degradative influences. Commonly buffers are used to provide pH control during stability studies. However, their use can hinder the identification of a fundamental kinetic profile since general acid/base catalysis and species dependent effects may be introduced. A pH-stat technique (as described in Chapter 6.3.1) allows the pH to be controlled within very precise limits to investigate the specific effects of hydroxonium and hydroxyl ion concentration.

All studies of the kinetics of chlorhexidine degradation were performed at elevated temperatures to accelerate the rate of reaction and hence generate the maximum amount of stability data. The pH-stat system therefore incorporated a high temperature electrode to maintain a specific pH at each temperature of kinetic experiments. The pH-stat reaction flask system used for the majority of degradation studies is described in detail in Chapter 6.2. Although water vapour leakage at elevated temperature was a potential source of error, the measures taken to prevent this were shown to be effective (Table 6.1).

The repetition of all degradation experiments would have drastically limited the number and extent of degradative influences investigated. However, the validity of data generated was confirmed by examining the reproducibility of representative experiments (Chapter 6.5). Adequacy of pH control was studied in a region of accelerated specific base catalysis (pH 9.0, 90°C) : the apparent first-order

degradation rate constants of six replicate determinations, over a two year period for 0.002% w/v chlorhexidine gluconate, were found to be not significantly different by multiple linear regression (Table 6.3). Moreover, the mean rate constant had a scatter of ~ ± 2.0% which is considerably less than which can be estimated (~ ± 11%) from the limits of pH-stat control (± 0.05 pH unit) assuming specific hydroxyl ion catalysis is occurring. This also suggests that pH-stat control was generally better than ± 0.05 pH unit. To test for a drift in pH-electrode response an experiment was repeated over a long stability study at elevated temperature (pH 7.0, 90°C, duration of experiment = 17 days). Again the generated apparent first-order degradation rate constants were found to be not significantly different at the p = 0.05 level (Table 6.4). Reproducibility was also demonstated for the fastest rate process studied (pH 10.0 at 90°C, half-life ~ 2 hours), where again duplicate rate constants were not significantly different (Table 6.6). Whilst these results indicated that duplication of experimentation was unnecessary, criteria were applied to prevent the acceptance of "rogue" data. These were : tight control of initial chlorhexidine concentration, RSD of observed first-order rate constants < 3% and a check of electrode response/calibration on completion of each stability study (Chapter 6.5.2).

All generated data were calculated according to first-order kinetics to yield the observed degradation rate constant (k_{obs}). Although non-first order dependency of degradation rate was observed at neutral to alkaline pH (Chapter 6.6.3), all degradation data showed a very food fit to first-order rate plots to below 30%

residual chlorhexidine. Quantitative comparison of factors affecting degradation was therefore made by reference to apparent first-order rate constants. This approach is considered valid since all parameters (except concentration) were evaluated at a concentration of 2.2×10^{-5}M (equivalent to 0.002% w/v chlorhexidine gluconate). Good data fit to semi-log plots for non-first order drug degradation processes in aqueous solution are not unusual, for example, thermal degradation of salbutamol (Hakes, 1980), thermal and photochemical degradation of promethazine (Meakin et al, 1978; Cox, 1975) and γ-irradiation degradation of sulphacetamide (Tansey, 1969).

The effect of pH on the degradation rate of 0.002% w/v chlorhexidine gluconate at 90°C is illustrated by Figure 6.4. This pH-rate profile shows both acid and base catalysed regions with a minimum around pH 5. The general shape of the plot is consistent with that of a hydrolytic degradation process. The minimum is lower than would be predicted from the work of Powelczyk and Plotkowiak (1976) who found, using paper chromatographic analysis, that decomposition increased below pH 6. However, the reports of Dolby et al (1972) and Jaminet et al (1970) are both consistent with a pH of maximum stability for chlorhexidine around pH 5 even though their findings were based on the use of the non-specific 4-chloroaniline method of analysis.

In the pH-rate profile, regions of specific acid and specific base catalysis are apparent below pH 3 and between 7.5 - 8.5 respectively, as evidenced by profile slopes of -1.07 and 1.01. Extrapolation from these regions leads to an intersection at

~ pH 5.1 and a rate constant of ~ 6.5×10^{-9} sec^{-1}, compared to an experimental value of ~ 2.9×10^{-7} sec^{-1} (Figure 8.1). It can therefore be concluded that the uncatalysed water reaction makes a significant contribution to the overall rate in the pH region 3.5 to 6.5. The rate constant (k_o) for this uncatalysed reaction can be estimated from equation 31 as follows :

$$k_{obs} = k_o + k_{H^+}[H^+] + k_{OH^-}[OH^-] \quad \ldots\ldots (31)$$

At the point of intersection from extrapolation of the specific acid and base catalysed regions :

$$k_{obs} = k_{H^+}[H^+] = k_{OH^-}[OH^-] = 6.5 \times 10^{-9} \text{ sec}^{-1}$$

$$k_o = 2.9 \times 10^{-7} - (2 \times 6.5 \times 10^{-9}) = 2.8 \times 10^{-7} \text{ sec}^{-1} \text{ at } 90°C$$

An estimate of k_{H^+} and k_{OH^-} at 90°C can be made from the experimental values at pH 3 and pH 8 assuming that specific acid or base catalysis is operative and using equations 32 and 33. At pH 3 and 8 at 90°C it is reasonable to assume activity effects can be ignored in calculating $[H^+]$ from pH and pK_w values; pH 8 has a further advantage in lying in the centre of the linear specifically base catalysed region.

At pH 3 :

$$k_{obs} = k_{H^+}[H^+] = 9.28 \times 10^{-7} \text{ sec}^{-1}$$

$$k_{H^+} = \frac{9.28 \times 10^{-7}}{1 \times 10^{-3}} = \underline{9.28 \times 10^{-4} \text{ sec}^{-1} \text{ l.mol}^{-1}}$$

At pH 8 :

$$k_{obs} = k_{OH^-}[OH^-] = 7.59 \times 10^{-6} \text{ sec}^{-1}$$

$$[OH^-] = \frac{K_w(90°C)}{[H^+]} = \frac{3.55 \times 10^{-13}}{1 \times 10^{-8}} = 3.55 \times 10^{-5}$$

$$k_{OH^-} = \frac{7.59 \times 10^{-6}}{3.55 \times 10^{-5}} = \underline{0.214 \text{ sec}^{-1} \text{ l.mol}^{-1}}$$

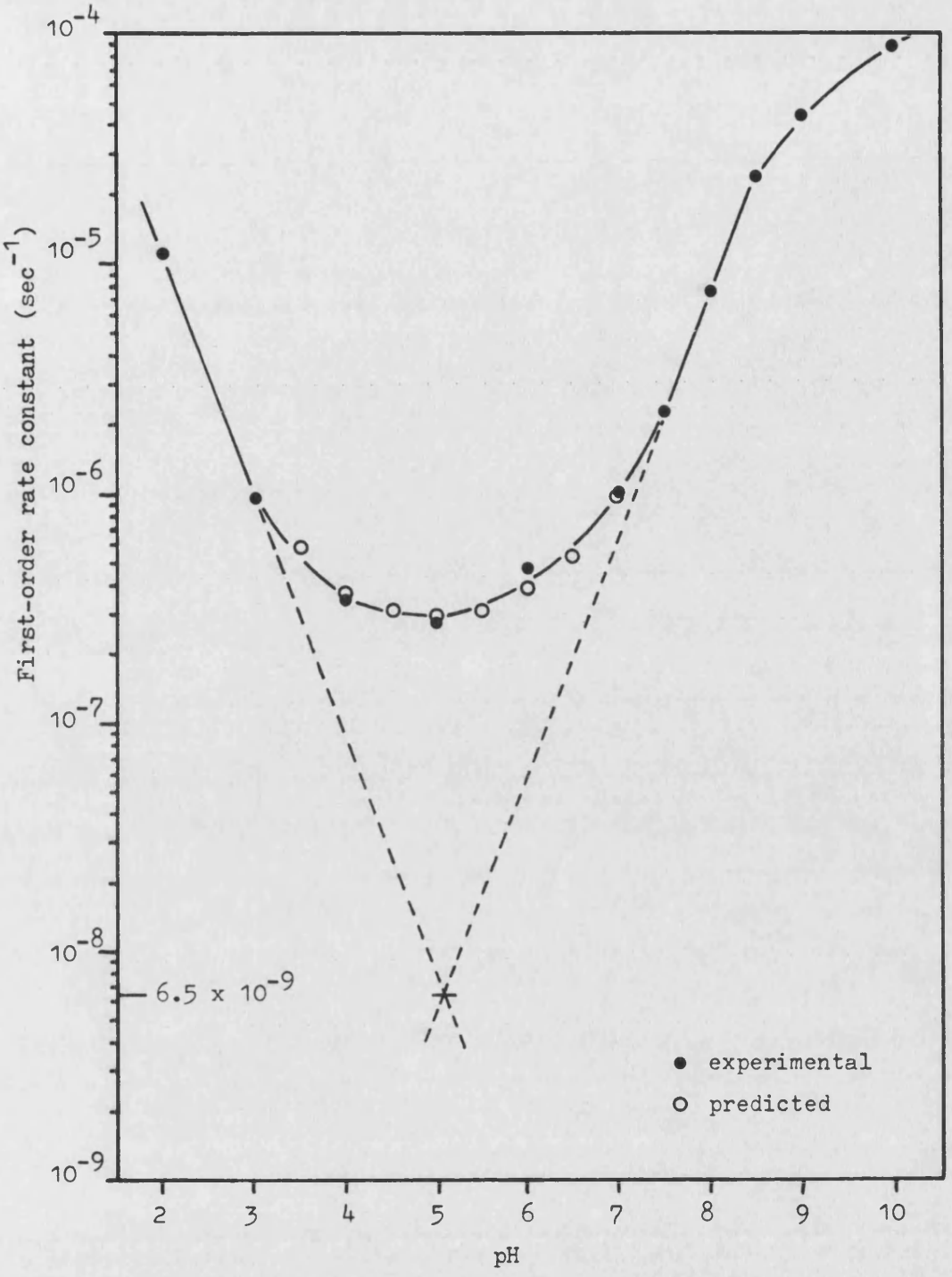

Figure 8.1 pH-rate profile for the degradation of 0.002% w/v chlorhexidine gluconate at 90°C. Regions of acid and base catalysis are extrapolated to yield the rate constant for the uncatalysed (water) reaction. From values of k_o, k_{H^+} and k_{OH^-}, the calculated k_{obs} at various pH was determined

Thus $k_{OH^-} >> k_{H^+}$ which is to be expected since it should be much easier for the hydroxyl ion to attack the chlorhexidine dication than the hydroxonium ion.

From the above estimates of k_{H^+}, k_{OH^-} and k_o it is possible to calculate values for k_{obs} in the water catalysed region using equation 31. These values are shown in Table 8.2 and are also plotted in Figure 8.1. There is reasonably good agreement between calculated and experimental values which serves to confirm the validity of the derived values for k_{H^+}, k_{OH^-} and k_o, and the kinetic mechanism in the pH region 3.5 to 7.0.

pH	k_{obs} ($sec^{-1} \times 10^7$)		
	Experimental	pH profile[1]	Calculated[2]
3.5	-	5.1	5.7
4.0	3.4	-	3.7
4.5	-	2.9	3.1
5.0	2.7	-	2.9
5.5	-	3.5	3.1
6.0	4.7	-	3.6
6.5	-	6.3	5.2
7.0	10.2	-	10.0

[1] values read from Figure 6.4

[2] calculated from equation 31; $k_{H^+} = 9.3 \times 10^{-4}\ sec^{-1}\ l.mol^{-1}$

$k_{OH^-} = 0.21\ sec^{-1}\ l.mol^{-1}$

$k_o = 2.8 \times 10^{-7}\ sec^{-1}$

Table 8.2 Comparison of experimental (actual and derived from pH-rate profile) and calculated degradation rate constants for 0.002% w/v chlorhexidine gluconate at 90°C.

Above pH 8.5 the pH-rate profile deviates from that of the specific base catalysed reaction, the experimental apparent

first-order rate constants being smaller than would be predicted. Such deviations are often due to a change in the drug species. The predicted pK_a at 90°C for the ionisation of the chlorhexidine dication to the unprotonated base is 8.92 (Appendix 5, Table A5.4). A discontinuity in the profile might be expected to occur around pH 9 therefore, if the specific base catalysed rate constants differ for the two chlorhexidine species. At high pH, water catalysed reactions are not expected to be of significance. The rate process above pH 8.5 could therefore be described by equation 72 :

$$k_{obs} = k^{2+}_{OH^-} f(Chx^{2+})[OH^-] + k^{00}_{OH^-} f(Chx)[OH^-] \quad .....(72)$$

where $f(Chx^{2+})$ and $f(Chx)$ represent the fractions of chlorhexidine present as the dication and unprotonated base respectively and $k^{2+}_{OH^-}$ and $k^{00}_{OH^-}$ represent the respective second-order rate constants. Ignoring activity effects, the fraction of each species can be calculated from the Henderson-Hasselbalch equation (69) using the estimated pK_a value of 8.92 at the experimental pH values of 9 and 10. Using the experimental rate constants (k_{obs}) in equation 72 gives a pair of simultaneous equations from which values of 0.28 sec^{-1} $l.mol^{-1}$ for $k^{2+}_{OH^-}$ and 4.8×10^{-3} sec^{-1} $l.mol^{-1}$ for $k^{00}_{OH^-}$ are obtained. 0.28 sec^{-1} $l.mol^{-1}$ for $k^{2+}_{OH^-}$ compares with 0.21 sec^{-1} $l.mol^{-1}$ for this value derived at pH 8 (Chapter 6.5.1). Given the various assumptions made in the derivation and uncertainty over the pK_a value, these values are in reasonable agreement. It should also not be forgotten that there is the possibility of three "ionic" types (dication, monocation and base) in this region since theory predicts overlapping pK_a values (Chapter 2.4.5), although these could not be demonstrated experimentally (Appendix 5). A further complicating

factor could be the existence of tautomers for the dication and base species (see Chapter 2.3 and below). The higher value for $k_{OH^-}^{2+}$ compared to $k_{OH^-}^{00}$ is again consistent with electrostatic interaction enhancing attack by the hydroxyl ion on the protonated species.

Although the overall shape of the predicted pH-rate profile at 25°C should be similar to that shown in Figures 6.4 and 8.1 (unless specific temperature influences are present), the pH of maximum stability and discontinuity due to the presence of chlorhexidine base will be different. A pK_w for water of 14.004 at 25°C should shift the pH of optimum stability nearer to pH 6 and an inflection due to the presence of chlorhexidine base would not be seen until ~ pH 10.

Since ophthalmic products containing chlorhexidine are generally formulated on the alkaline side of neutral, most subsequent studies were performed at pH 9.0 (90°C) where hydroxyl ion catalysis was rapid, thus allowing numerous effects to be studied.

The effect of concentration was studied over the range 0.001 to 0.05% w/v chlorhexidine gluconate, at pH 2.0 (80°C), ~ 6 (90°C) and 9.0 (80°C) (Chapter 6.6.3). At pH 2.0, the rate constants of 0.002 to 0.05% w/v chlorhexidine gluconate solutions degraded at 80°C were found to be not significantly different. The order of reaction, produced from a plot of log initial concentration (C_o) against log half-life ($t_{\frac{1}{2}}$), was 0.99 (Figure 6.11, Table 6.10); this agrees with that predicted for a first-order specific acid catalysed reaction.

At pH ~ 6, the experimentation was performed in ampoules due to the low degradation rate constant in this region. Although it was not possible to control the pH inside each ampoule (buffers were not considered due to potential catalytic effects), measurement of pH at the start and end of storage at 90°C showed a total scatter of < 0.2 pH unit (measured at 25°C, Table 6.9). The experimental pH at which degradation was performed was 6.1 ± 0.1. The rate constants were found to decrease with concentration. To establish this effect was real and not due to pH fluctuation, the rate constants produced at each concentration were fitted to the pH-rate profile shown in Figure 6.10 to determine the pH-range which would be required to account for such a range of rate constants. The range produced (pH 5.6 to 6.7) confirmed that the observed effects were due to concentration and not pH variation. The plot of log C_o against log $t_{\frac{1}{2}}$ at pH 6.1 was reasonably linear (Figure 6.11). The apparent order of reaction produced was ~ 0.7.

At pH 9.0 (80°C), a decrease in the observed rate constant was noted with increasing concentration in the region 0.001 to 0.055% w/v chlorhexidine gluconate. However, a non-linear relationship was observed when the data were plotted as log C_o against log $t_{\frac{1}{2}}$ (Figure 6.11). Tangents drawn to the curve give an apparent order of reaction ranging from 0.4 to 0.8.

Fractional orders, as produced here at pH 6.1 and 9.0, are often associated with complex reaction pathways (Chapter 1.2.3). In order to propose simultaneous reactions it is pertinent to re-examine the structure of chlorhexidine in its

various ionic states. Since no formal structural information is available for chlorhexidine its structure has been inferred from that of biguanide (Chapter 2.3). Unprotonated biguanide has conventionally been given the structure X but spectroscopic evidence favours the existence of a conjugated tautomer (Xa). Monoprotonation results in resonance hybridisation for which four equivalent canonical forms may be written. Diprotonation of biguanide occurs on to the bridging nitrogen (XIV) but the literature contains slightly conflicting evidence favouring partial (Fanshawe et al, 1964) or total (Wellman et al, 1967) delocalisation of charge. These structural theories are in fact very similar to those detailed in part of an ICI Pharmaceuticals internal memorandum which was recently made available (Leahy, 1987, Personal Communication). Therefore the various structures of chlorhexidine base, dication and tetracation may be written from structural analogy to biguanide as shown in Figure 8.2.

The presence of various forms for each chlorhexidine species offers a possible explanation for the calculated fractional order of reaction obtained at pH 6.1 and 9.0. At pH 6.1 (90°C), four simultaneous reactions are predicted with each of the canonical forms of the chlorhexidine dication possibly having a different site of hydrolytic attack. The calculated reaction order of ~ 0.7 may therefore reflect the composite of all individual orders. At pH 9.0 (80°C), the situation is further complicated by the presence of tautomeric forms of the unprotonated species (pK_a^1 at 80°C is 9.12, Table 5.4). Additionally, Figure 6.11 showed a non-linear relationship to exist between log C_o and log $t_{½}$ at this pH.

Chlorhexidine base:

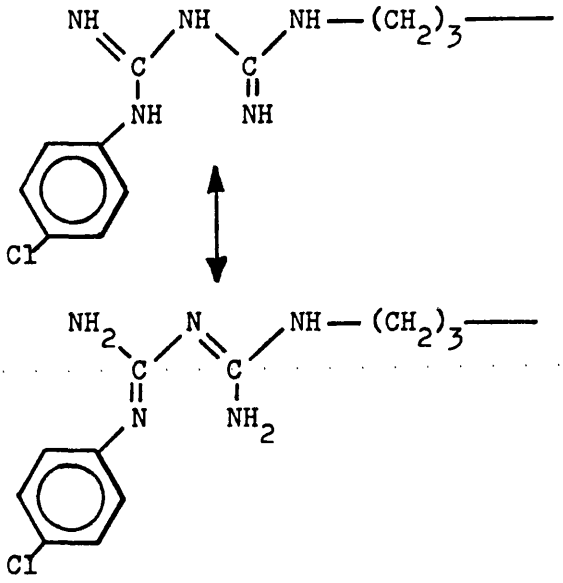

"normal structure"

tautomer

Chlorhexidine dication:

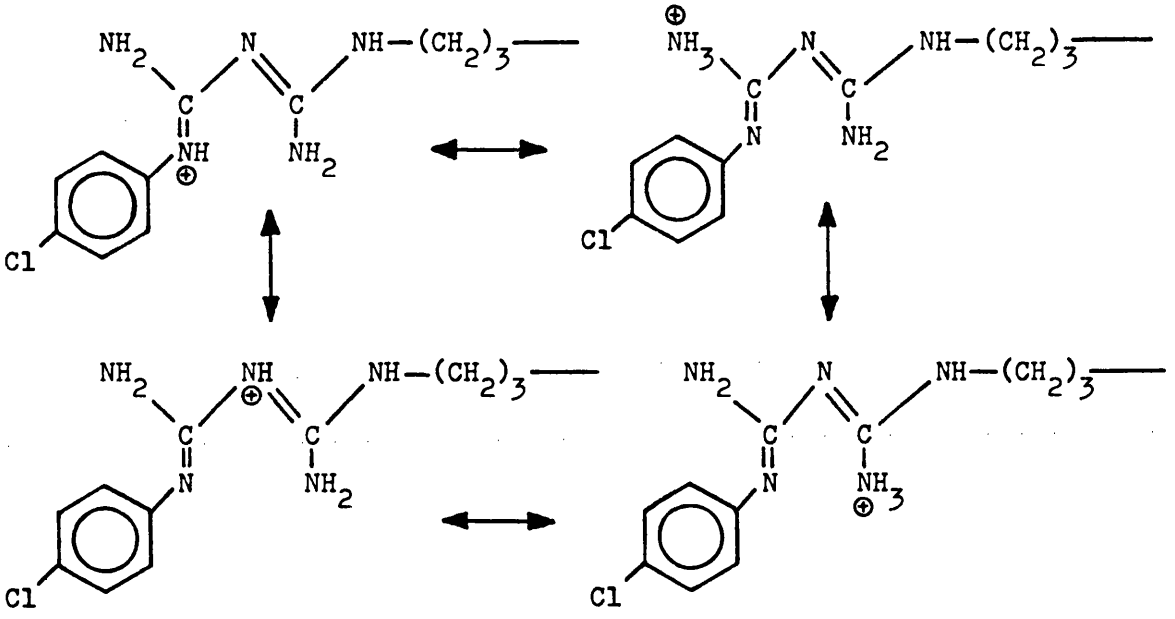

Chlorhexidine tetracation:

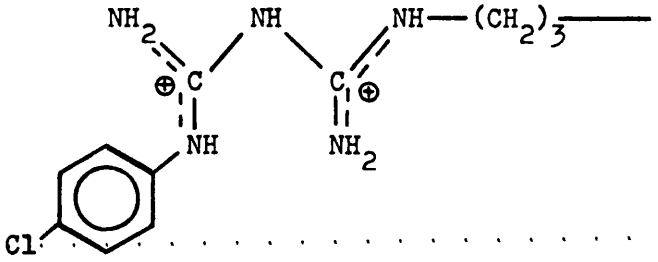

Figure 8.2 The various structures of chlorhexidine base, dication and tetracation written from structural analogy to biguanide. Each structure represents the chlorhexidine "half molecule"

However, studies on the effect of degradation product concentration showed rate retardation to occur rather than autocatalysis as the apparent concentration of degradation products increased (Chapter 6.6.6, Figure 6.19). Therefore, the change in apparent reaction order with initial chlorhexidine concentration at pH 9.0 may be due to the combined influences of chlorhexidine structure (dication and base forms) and mechanistic effects due to the presence of degradation products.

The more marked effect of concentration at pH 9.0 meant that slight variations in concentration around 0.002% w/v chlorhexidine gluconate (i.e. 0.0018 to 0.0023% w/v) were found to significantly affect the observed degradation rate constant (Table 6.8). This was an important finding since, in addition to pH and temperature, initial chlorhexidine concentration had to be precisely controlled when investigating other degradative effects. A rejection of data criterion was thus implemented into the experimental procedure (Chapter 6.5.2).

Linear Arrhenius plots were produced over the temperature range 60 to 90°C at pH 2.0, ~ 6 and 9.0 for 0.002% w/v chlorhexidine gluconate solutions (Figure 6.15). Table 6.11 lists the data generated from plots of log k against 1/T. Calculation of the data in the form of the Absolute rate equation (equation 30) rather than the conventional form of $\log_e k$ against 1/T did not alter the calculated activation energies. This served to illustrate that the observed activation energies did not vary with temperature over the range studied (Chapter 1.3.3.1). However, since simultaneous reactions are predicted which involve a variety of attacking species

and chlorhexidine in several 'ionic' and structural forms, the activation energies produced represent the composite of individual processes. Therefore the experimental values obtained are more correctly termed "apparent" activation energies.

At pH 2.0, degradative reactions may involve hydroxonium ion attack on both dicationic and tetracationic chlorhexidine since the "macro"-acidic pK_a is 2.8 (at 25°C). Therefore the apparent activation energy of 69.5 ± 2.8 $kJ.mol^{-1}$ may be a composite of two reactions, although without knowledge of the temperature dependency of the "macro"-acidic ionisation constant this assumption is theoretical.

At pH ~ 6, the apparent activation energy (96.1 ± 4.1 $kJ.mol^{-1}$) is a composite of both the hydroxyl ion and water catalysed reactions. Although attack is exclusively on the chlorhexidine dication at this pH, the individual process may be further complicated by structural influences discussed earlier. The fact that the apparent activation energy at this pH is larger than those at pH 2.0 and 9.0 confirms that the water catalysed reaction exerts a significant influence on the overall rate of degradation at pH ~ 6. This is supported by the value for k_o of 2.8×10^{-7} sec^{-1} compared to a k_{obs} of 6.5×10^{-7} sec^{-1} at 90°C.

At pH 9.0, the apparent activation energy is the sum of the activation energies of the composite specific hydroxyl ion catalysed reactions for the two species present (chlorhexidine base and dication) and the standard enthalpy for the ionisation of water (55.71 $kJ.mol^{-1}$, Chapter 1.6.2.3). Subtraction of the latter value from the experimental apparent activation energy gives an Ea_{OH^-}

(apparent) value of 73.4 ± 3.5 $kJ.mol^{-1}$. However, since the second-order rate constant for hydroxyl ion attack on the chlorhexidine dication has been shown to be ~ 50 times larger than that for attack on chlorhexidine base ($k^{2+}_{OH^-} >> k^{00}_{OH^-}$, discussed earlier), the apparent activation energy probably approximates to Ea_{OH^-}.

From degradation studies using the 4-chloroaniline method of analysis, ICI have found an apparent activation energy at pH 6.5 of 95 $kJ.mol^{-1}$ (Leahy, 1987, Personal Communication). This is in very close agreement to the value of 96.1 ± 4.1 $kJ.mol^{-1}$ obtained in this study at pH ~ 6. The only other literature citation is 77.6 $kJ.mol^{-1}$ at pH 3.3 by Powelczyk and Plotkowiak (1976) using paper chromatographic analysis. Given the slight deviation away from specific acid catalysis at this pH, as evidenced by the pH-rate profile (Figure 6.4), this value is comparable to the apparent activation energy of 69.5 ± 2.8 $kJ.mol^{-1}$ produced in this study at pH 2.0.

The calculated frequency factors at pH 2.0, ~ 6 and 9.0 were 1.06×10^5, 4.20×10^7 and 1.73×10^{14} sec^{-1} respectively (Table 6.11). Again these values are a result of composite processes and are therefore "apparent". Additionally, to obtain a "true" value at pH 9.0 the apparent frequency factor (A^1) requires correction for the $[H^+]$ term present in equation 56. This correction gives a "true" frequency factor of 1.73×10^5 sec^{-1} for the composite reactions at pH 9.0.

At a concentration of 2.2×10^{-5}M (equivalent to 0.002% w/v chlorhexidine gluconate) the original salt form of

chlorhexidine did not have any significant influence on the rate of degradation (Figures 6.5 and 6.6). In common with most of the degradation studies this effect was obtained from experimentation at pH 9.0 and 90°C. Therefore other data generated at this pH using the gluconate salt should be equally applicable to equimolar solutions of acetate, hydrochloride or base form.

Significant stabilising effects were noted when chlorhexidine gluconate and hydrochloride solutions of increasing ionic strength were subjected to degradation (Table 6.12). To eliminate the possibility of combined counter-ion effects, ionic strength was adjusted by potassium chloride for chlorhexidine hydrochloride and gluconic acid for chlorhexidine gluconate. Due to HPLC assay difficulties experimentation with chlorhexidine acetate/acetic acid systems could not be performed.

The data generated (at pH 9.0 and 90°C) up to 0.1M (gluconate) and 0.5M (chloride) are presented according to the Brönsted-Bjerrum relationship in Figure 6.17 (log k_{obs} against $\sqrt{I}$, equation 41). The decrease in observed rate constant with increasing ionic strength illustrates the presence of a negative salt effect. Such an effect fits that theoretically predicted for reactions between ions of opposite charge (dicationic chlorhexidine and OH^-, Chapter 1.5.2). According to equation 41 the slope produced is equal to $2Q.Z_AZ_B$, where 2Q is a constant related to temperature and Z_AZ_B is the product of the respective charges of the two reacting species. At 90°C, 2Q has a value of 1.174 (Harned and Owen, 1958). The slopes obtained from linear regression analysis were -2.20 and -2.17 for the chloride and gluconate solutions

respectively (Table 6.12); these values are not significantly different (t_{calc} 0.055, t_{tab} 1.94, p = 0.05). Division of the slopes by 2Q yields Z_AZ_B values of -1.87 and -1.85 for the chloride and gluconate solutions respectively. These values are very close to the value of -2 theoretically predicted (Z_AZ_B = Chx^{2+} x OH^- = -2).

Although linear regression of the data fits well with the Brönsted-Bjerrum relationship, the individual data points for 4.64×10^{-4}M and 1.05×10^{-2}M ionic strength did not show any great variation in k_{obs}. Data generated at 4.64×10^{-4}M ionic strength were taken from experimentation on the effect of salt form (Chapter 6.6.2) whilst those at 1.05×10^{-2}M ionic strength represent the first data points of added counter-ion. It would therefore appear that the negative salt effect only occurs above an ionic strength of ~ 0.01M. This deviation from the Brönsted-Bjerrum relationship may possibly be explained in terms of a secondary salt effect becoming important at ionic strengths < 0.01M. Such an effect would influence the dissociation of the chlorhexidine salt producing a greater proportion of the chlorhexidine dication at lower counter-ion concentrations; since this species is more susceptible to hydrolysis the overall degradation rate should increase. However, since the negative salt effect is protective, no significant increase in observed rate constant occurs. Above ~ 0.01M the negative primary salt effect predominates and fits the Brönsted-Bjerrum relationship. The other possibility is that complex reaction mechanisms of different ionic character occur, each influenced individually by ionic strength. This conclusion has been

drawn to explain many fractional kinetic salt effects observed in the degradation of other pharmaceuticals (Chapter 1.5.2).

Catalysis by buffer salts is well documented in the pharmaceutical literature (Chapter 1.4.2). However, their direct catalytic effect can easily be confused by the influence buffers have on ionic strength, this resulting in the various primary salt effects noted in Chapter 1.5.2.

Therefore, experimentation into the effect of buffers on chlorhexidine degradation was structured to identify both ionic strength (primary salt) effects and general acid/base (buffer) catalytic effects. The effect of standard (single) and low (~ 0.1) buffer strengths were noted at 60 to 90°C for acetate, phosphate and borate buffer systems listed in Table 6.14. Analytical problems prevented the effect of more concentrated buffer systems being investigated. Whilst the calculated ionic strength for acetate and borate systems did not vary significantly with temperature (Table 6.15) the phosphate systems showed drifts of 0.112M (60°C) to 0.098M (90°C) and 0.0127M (60°C) to 0.010M (90°C) for single and 0.1 strength systems respectively.

The presence of either strength of acetate buffer (pH 4.0) did not significantly influence the observed degradation rate constants at 90°C when compared to those calculated from the pH-rate profile (Table 6.16); the values being 5% greater and 7% lower for single and 0.1 strength systems respectively indicating the absence of acetate buffer catalysis. Observed rate constants at all temperatures (60, 80 and 90°C) were always greater in the single strength system than in the 0.1 strength system. This may be

accountable by a simple primary salt (ionic strength) effect. Theoretically, in this region of acid catalysed hydrolysis a positive salt effect is predicted (rate constant increases with increasing ionic strength for reactants of the same charge). Calculation of the rate data (Table 6.16) according to the Brönsted-Bjerrum relationship (log k against $\sqrt{I}$) yields slopes of +2.21, +1.14 and +0.74 at 60, 80 and 90°C respectively. Division of these values by the appropriate value of 2Q at each temperature (Harned and Owen, 1958) gives $Z_A Z_B$ values of +2.02, +1.00 and +0.63 at 60, 80 and 90°C respectively. The decrease in $Z_A Z_B$ with increasing temperature agrees with the theory that the uncatalysed water reaction (predicted $Z_A Z_B = 0$) becomes more significant as pH 4.0 becomes nearer to neutral pH at elevated temperatures.

The acetate data also fits the Arrhenius relationship reasonably well (Table 6.16). Although slight curvature is present on examination of the plots (Figure 6.20) calculated activation energies and frequency factors were virtually unaltered by plotting according to the Absolute rate equation (30). The lower observed activation energy at higher ionic strength (single strength buffer system) fits with that expected for a positive salt effect.

The effects due to phosphate buffers are more difficult to explain. At 90°C the observed rate constants for buffered systems were larger than those calculated from the pH-rate profile (Table 6.17). However, the rate constant at 0.1 buffer strength was three-fold larger whilst those at single and half-strength were only ~30% larger. Rate constants generated at 60, 70 and 80°C also show larger values at 0.1 strength than in single strength systems. At pH 7, both hydroxyl ion and water

catalysed reactions occur (from pH-rate profile, Figure 6.4) and a negative salt effect is therefore predicted. The data generated were plotted according to log k_{obs} against $\sqrt{I}$ and produced negative slopes of 0.49, 0.71, 1.01 and 1.79 and $Z_A Z_B$ values of -0.45, -0.64, -0.88 and -1.52 at 60, 70, 80 and 90°C respectively. These values are consistent with a negative salt effect. The effects of temperature on the predominance of water catalysed and specific base catalysed reactions may explain the observed increased in $Z_A Z_B$ with increasing temperature. As temperature increases neutrality pH decreases (pH 6.2 at 90°C) and at pH 7 there are effectively more hydroxyl ions at 90°C than at 60°C. Therefore the magnitude of the rate constant for specific base catalysis ($k_{OH^-}[OH^-]$) increases in relation to that for the water catalysed reaction and the slope increases with increasing temperature. However, some form of general base catalysis by phosphate anions ($H_2PO_4^-$ and HPO_4^{2-}) is suspected since the observed rate constant at 0.1 buffer strength is three-fold greater than in the absence of buffer at 90°C. Since the pKa for $H_2PO_4^{2-}$ to HPO_4^- is temperature dependent (7.197 at 60°C, 7.301 at 90°C, Robinson and Stokes, 1959) the observed effects may also be a function of a variation in the ratio of the buffer species. Further evidence of the existence of general base catalysis by the phosphate anions comes from the Arrhenius plots (Figure 6.21), which produce a lower activation energy for the single strength system (85.3 $kJ.mol^{-1}$) than the 0.1 strength system (104.6 $kJ.mol^{-1}$).

Experimentation with borate buffer systems again produced smaller rate constants for single strength systems than 0.1 buffer strength at all temperatures studied (Table 6.18). Whilst

this is again consistent with a negative salt effect, at 90°C the four-fold reduction in rate constant at 0.1 buffer strength (0.003 M ionic strength) is double that predicted from ionic strength considerations alone; Figure 6.17 predicts a two-fold reduction at 0.003 M ionic strength. It is therefore suspected that complexation between the chlorhexidine dication and tetraborate anion occurs. The potential molecular size of such a complex probably reduces the degradation rate by steric hinderance with an overall ionic charge reduction also occurring on complexation. Attempts to fit the data to a linear Arrhenius relationship were unsuccessful (Figure 6.22) and the gross curvature produced provides further evidence of the likelihood of complex reaction mechanisms in borate buffered systems.

The effects of surfactants, particularly at concentrations in excess of the CMC, on rates of reaction have been briefly considered in Chapter 1.6.5. Whilst a comprehensive study of surfactant effects on the stability of chlorhexidine was not possible within the time-frame of this thesis, limited studies were performed since surfactants are present in many chlorhexidine formulations (particularly antiseptic/disinfectant solutions for hospital use, Table 2.1). The effect of hexadecyl trimethyl ammonium bromide, CTAB (cationic), polysorbate 80 and cetomacrogol 1000 (non-ionic) and sodium dodecyl sulphate, NaDS (anionic) surfactants on the degradation of 0.002% w/v chlorhexidine gluconate at pH 9.0 and 70°C was investigated over a range of surfactant : chlorhexidine ratios typical of those found in formulated products. The investigated molar ratio for CTAB : chlorhexidine was 1:1 to

910:1 which adequately covered that found in formulated products containing cetrimide/chlorhexidine combinations (~27;1). In ophthalmic/contact lens product formulations, non-ionic surfactant concentrations range from 0.1 to 1.0%; however, assay problems limited the maximum investigated non-ionic concentration to ~0.2%. The rate constant data generated in the presence of surfactants were related to the rate constant in their absence by a surfactant effect ratio (k_o:k_{obs} surfactant). Thus, values in excess of unity indicated surfactant (or micellar) inhibition whilst those less than unity indicated a catalytic effect. The degradation pattern of chlorhexidine in the presence of the surfactants studied still fitted first-order kinetics as illustrated by Figures 6.23 to 6.25 and 6.27. The data for CTAB and the two non-ionic surfactants were conveniently summarised by a plot of surfactant effect ratio against surfactant concentration as shown in Figure 6.26.

With CTAB, degradation rate inhibition (surfactant effect ratio >1) was noted at concentrations of 6×10^{-5} M and above. Figure 6.26 clearly shows a maximum surfactant effect ratio of 4.6 at 2×10^{-3} M CTAB, this value being close to the experimentally obtained CMC of ~1.5×10^{-3} M for CTAB at 70°C (Mukerjee and Mysels, 1971). The theories behind micellar catalysis and inhibition have been widely reviewed and explained according to the electrostatic and pseudophase models (Chapter 1.6.5); these would predict little effect below the CMC but an increase in the base catalysed rate of degradation once micelles had formed. The generally observed decrease in chlorhexidine degradation rate constant with increasing CTAB concentration, particularly at concentrations well below the proposed CMC, is therefore unexpected.

The decrease in rate constant is much too large to be accounted for by a simple ionic strength effect of CTA^+Br^- addition. However, the large bromide anion may, by counter ion binding, result in the steric hinderance of hydroxyl ion catalysis. It has already been noted that the presence of the borate anion results in a decrease in the expected degradation rate constant. Another possibility is the presence of sub-micellar associations of chlorhexidine and CTAB. Energetically, the association between cationic CTAB and chlorhexidine base is favoured more than an association of CTAB and chlorhexidine dication. This association would also result in much more of the base form being bound since the latter would be "partitioned" resulting in a greater binding than that predicted from the fraction present as chlorhexidine base at pH 9.0. This partitioning may also be further influenced by the presence of an increased hydroxyl ion concentration at the surface of the aggregate compared to the bulk aqueous solution. In this environment a larger fraction of chlorhexidine will be in the base form than predicted from bulk aqueous studies. However, the above arguments assume that the pH and presence of chlorhexidine have no effect on the CMC of CTAB (Chapter 1.6.5.2).

It would be difficult to explain the maximum surfactant effect ratio, followed by its rapid decline, other than due to the effect of micellisation at $\sim 2 \times 10^{-3}$ M CTAB. Upon micellisation, chlorhexidine must become sited in an environment where the rate of hydrolysis is greater than at sub-micellar concentrations, although it should be noted that a surfactant effect ratio greater than unity is still observed. This decrease in rate

inhibition due to micellisation could be accounted for by the electrostatic attraction of hydroxyl ions to the cationic micelle. The fact that micellar catalysis is not observed may be due to a protective effect, similar to that occurring at sub-micellar concentrations, being residual at concentrations greater than the CMC.

The two non-ionic surfactants used for kinetic investigation had opposite effects on the degradation of chlorhexidine. Cetomacrogol 1000, a polyoxyethylated glycol monoether, had a stabilising effect at all concentrations studied (Figure 6.24), although HPLC assay problems prohibited experimentation near its literature CMC at 20°C. Stabilisation by non-ionic surfactants is typically predicted by micellar reaction models. Figure 6.26 shows a slight discontinuity in the surfactant effect profile with no significant increase in the stabilising effect occurring above 2×10^{-4} M cetomacrogol. This overall effect may again be proposed to be due to sub-micellar associations. Although such associations are likely to be hydrated, chlorhexidine may be positioned in an environment which affords some protection from hydrolysis. However the effect of temperature on the CMC of cetomacrogol is unknown, therefore the argument for sub-micellar associations is theoretical.

Increasing concentrations of polysorbate 80 (polyoxyethylene [20] sorbitan mono-oleate) caused acceleration of the rate of chlorhexidine degradation (Figure 6.25). Again experimentation was limited to concentrations below the literature CMC of polysorbate 80 at 20°C. The resultant surfactant effect

ratio-concentration profile (Figure 6.26) could be a result of the direct effect of polysorbate - chlorhexidine sub-micellar associations being more susceptible to hydrolysis or more likely due to the catalytic effect of peroxide impurities present in polysorbate (Chapter 1.6.5.5). Significant auto-oxidation of polysorbate 80 at the degradation conditions used for these stability studies was not suspected since no turbidity (lowered cloud point) was noted on completion of the degradation experiments. To prove the absence of an auto-oxidative effect the experimentation with polysorbate 80 should be repeated in the presence of an anti-oxidant.

For completeness, degradation experiments were also performed in the presence of the anionic surfactant sodium dodecyl sulphate (NaDS). Chlorhexidine and NaDS are incompatible and precipitation was observed at all NaDS concentrations studied. The degradation profiles produced were still linear when plotted according to first-order kinetics. This is somewhat surprising since zero-order kinetics are to be expected for a suspension system. However, below the literature CMC of NaDS at 20°C (1.1×10^{-2} M, Mukerjee and Mysels, 1971) the observed rate constants may be associated with a residual amount of "free" chlorhexidine gluconate or chlorhexidine base (which would not ionically complex with NaDS) in solution. Above the CMC no degradation was detected with 100% of the nominal chlorhexidine concentration still being present after 160 hours at pH 9.0 and 70°C. This suggests that both chlorhexidine base and chlorhexidine dication partition into the micelle and are therefore protected from hydrolysis by electrostatic repulsion of the hydroxyl ion, although

the kinetic study showed that the complex precipitate was not simply solubilised into micelles (Chapter 6.6.8.3.3).

Brief studies were performed on the photostability of chlorhexidine gluconate solutions (Chapter 6.7). Solutions of 0.002, 0.01 and 0.05% w/v chlorhexidine gluconate in distilled water (pH 5.7 to 5.8) were subjected to simulated daylight storage for 16 weeks. This period was calculated to be equivalent to ~60 weeks storage in normal (north-facing) daylight. No significant difference in chlorhexidine content was noted between samples subjected to simulated daylight storage and control samples after storage intervals of up to 16 weeks. These results are in agreement with Dolby et al (1972) who observed no degradation after storage in natural daylight for one year (assay of chlorhexidine by 4-chloroaniline content). The 12 to 17% loss of chlorhexidine observed by Madsen (1967) over the same storage period may be due to the sorption of chlorhexidine on to glass or thermal degradation since similar results were attained for dark controls (see section 8.4).

The investigation of the stability of chlorhexidine to ionising irradiation produced results which are consistent with data obtained for other pharmaceuticals (Chapter 1.6.4). As a dry powder chlorhexidine acetate (containing 2.6% w/w moisture) was stable to a γ-irradiation of 75 kGy (Table 6.25). However, in aqueous solution (0.002, 0.01 and 0.05% w/v), chlorhexidine acetate exhibited concentration dependent apparent first-order degradation with extensive degradation occurring at irradiation doses well within that recommended for sterilisation (Figure 6.29). This result agrees with that of McCarthy (1978) who concluded that

chlorhexidine in aqueous solution was unstable to the effects of γ-irradiation at standard sterilisation doses.

Since a paraffin gauze dressing product containing chlorhexidine is sterilised by γ-irradiation (Bactigras, Smith and Nephew Pharmaceuticals) the stability of chlorhexidine acetate (0.5% w/w) in soft paraffin was compared to that in a semi-solid water soluble (polyethylene glycol) base. Figure 6.30 shows the degradation profile produced for the PEG system over the irradiation range 5 to 75 kGy which indicates it is not amenable to sterilisation by γ-irradiation. Chlorhexidine acetate dispersed in soft paraffin is clearly stable to γ-irradiation over the same dose range however.

Examination of the chromatograms produced from γ-irradiation induced degradation showed the presence of different degradation products to those resultant from aqueous hydrolysis. A degradation pathway involving free radical mechanisms is however usually implicated in radiation induced pharmaceutical degradation (Chapter 1.6.4).

8.3 DEGRADATION PATHWAY AND PROPOSED DEGRADATION PRODUCTS

Degraded chlorhexidine solutions were assayed by three methods (HPLC stability indicating, Holbrook and 4-chloroaniline content) to establish a link between true and apparent degradation rate constants (Chapter 7.2). Qualitative studies were also performed on the rate of occurrence/loss of the major degradation products identified by the HPLC stability indicating method (Chapter 7.3). From these studies, the information relevant to the proposal of a degradative pathway for chlorhexidine may be summarised as follows.

Relative to other degradation products, the proportion of 4-chloroaniline increased as the percentage residual chlorhexidine decreased (Figures 7.1 to 7.5). The production of 4-chloroaniline may therefore be associated with the second or successive stages of a multi-step reaction (i.e. degraded chlorhexidine molecules are more sensitive to hydrolytic cleavage to 4-chloroaniline). From the chromatographic studies, the sequence in which degradation products occur follows a definite order : D, A then E (Figure 7.6). Since 4-chloroaniline is produced throughout the degradation process it is difficult to ascribe its position within this order. The sequential order supports the proposal of a degradation cascade (consecutive reactions) although without quantitative evidence the existence of parallel reactions cannot be discounted. Analysis of degraded samples by the Holbrook assay method confirmed that for practical purposes only one end of the symmetrical chlorhexidine molecule needs to be considered in terms of the degradation sequence (Chapter 7.2.4). Qualitative studies (Figures 7.7 and 7.8) provided some evidence that the degradation products A and D also degrade as the residual chlorhexidine content drops below 20 to 40%. The deviation from first-order kinetics shown by degradation profiles in the region 20 to 30% residual chlorhexidine (Figure 6.18) also appears to be coincident with a net loss of degradation product D. The degradation of chlorhexidine and D may be postulated to occur in parallel since quantitative degradation studies (Chapter 6.6.6) showed the overall rate of chlorhexidine degradation to be decreased in the presence of relatively large concentrations of its degradation products. Both

quantitative and qualitative studies presented in Chapter 7 indicate that 4-chloroaniline and degradation product E appear to be the final degradation products.

By consideration of the above evidence a schematic degradation cascade may be proposed, as illustrated in Figure 8.3 (tentative pathways are indicated by broken arrows).

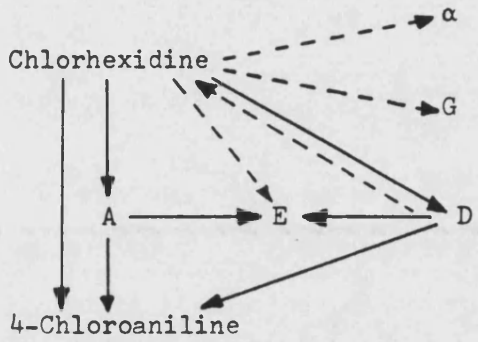

Figure 8.3 Schematic degradation mechanism for chlorhexidine. The pathways indicated by broken arrows are only tentative. Degradation products are given an alphabetic nomenclature as in Chapter 5.1.1.3

It is apparent from Figure 8.3 that the proposed degradation pathway is a complex combination of parallel, consecutive and possibly reversible processes. However, before this pathway is accepted, it must be supported by quantitative studies on all degradation products. This, of course, requires the identification of each degradation product. Experimentation with this aim, detailed in Chapter 7.4 was unsuccessful. Therefore the following discussions are only valid in a theoretical context.

It has been proposed that chlorhexidine degrades by a hydrolysis mechanism (Chapter 2.5). The production of the only identified degradation product, 4-chloroaniline, may be written as in Figure 8.4. It should be noted that hydrolytic cleavage also produces another degradation product.

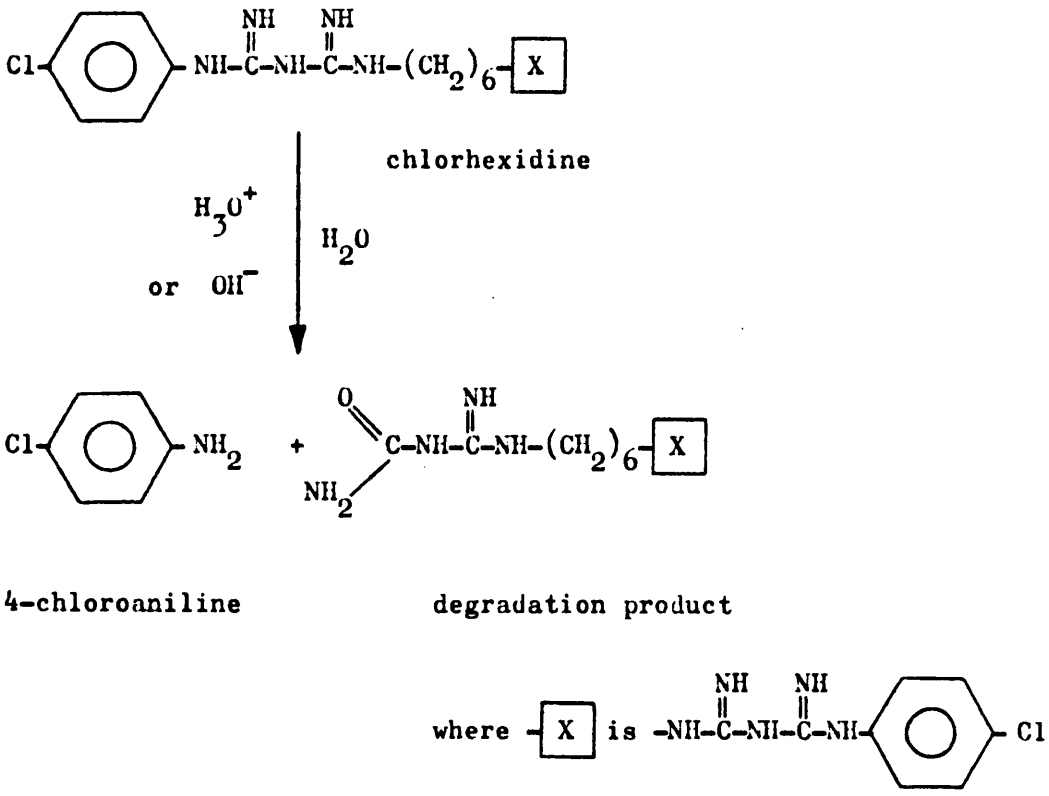

Figure 8.4 Hydrolytic cleavage of chlorhexidine yielding 4-chloroaniline and another degradation product

Without any supportive experimental evidence being made available the degradation product structures shown in Figure 8.5 have been proposed (Fernie, 1982, ICI Pharmaceuticals, Personal Communication). It is immediately noticeable from the proposed structures of α, A, D and E that cleavage of the biguanide chain has already taken place. Consequently significant amounts of 4-chloroaniline should also be present in degraded solutions containing the above degradation products. Further, it would also be expected that the assay of 4-chloroaniline should be stability indicating for chlorhexidine assuming that all degradative pathways yield 4-chloroaniline. However, the data presented in Chapter 7.2 illustrated that 4-chloroaniline was not initially a significant degradation product and that assay of the latter to predict chlorhexidine degradation underestimated the rate constant by a factor of 3 to 6.

Degradation Product | Structure

α

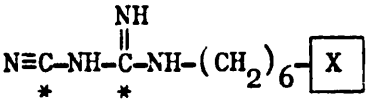

A

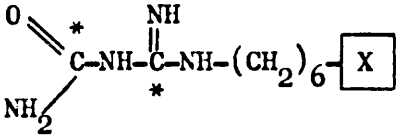

D

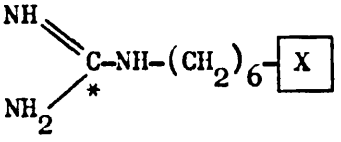

or

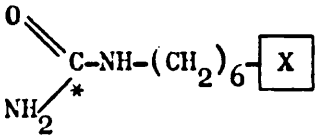

E

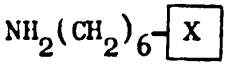

F

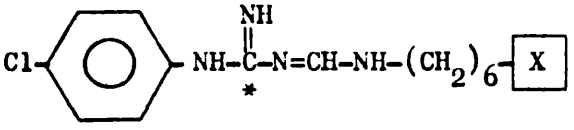

where  is

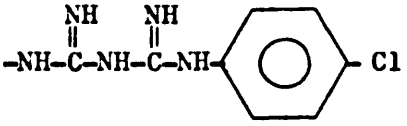

Figure 8.5 Proposed structures of the degradation products of chlorhexidine. The structures are shown in their unionised, non-conjugated form.

*Potential site of interaction with 4-chloroaniline

The validity of the proposed degradation product structures may be further investigated by insertion of these structures into the proposed degradation pathway (Figure 8.3) to produce Figure 8.6. Whilst most of the degradation paths are theoretically valid, those from degradation products A and D to 4-chloroaniline cannot occur without the involvement of the other, previously undegraded, end of the chlorhexidine molecule.

The other degradation product yielded from the direct cleavage of chlorhexidine to 4-chloroaniline (Figure 8.4) has the same structure as that proposed for degradation product A. Qualitative studies (Chapter 7.3 and Figure 7.8) have shown that this degradation product increases steadily as degradation proceeds up to about 55% and is then followed by an apparent decrease which may be associated with its degradation. Therefore, one of the degradative pathways may be written as follows:

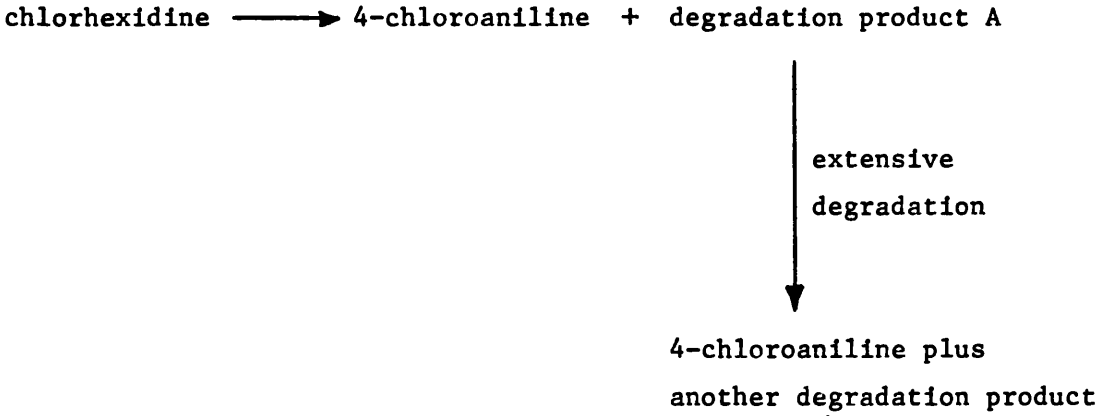

The major degradation product has been proposed to be D (Chapter 7.3). However, its proposed alternative structures do not fit with those expected from kinetic considerations as the

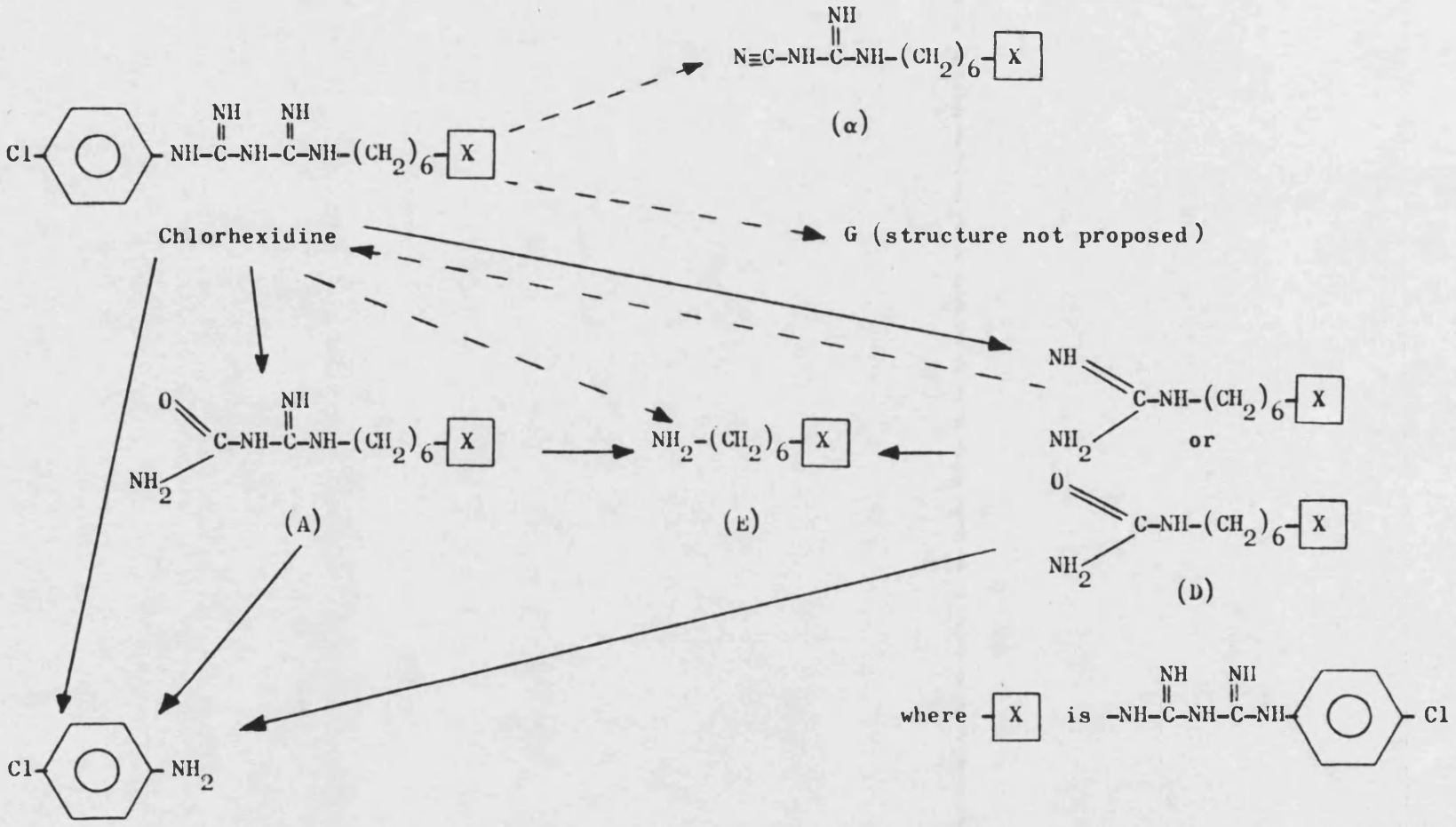

Figure 8.6 Combination of proposed structures of degradation products with the proposed degradation mechanism. Pathways are drawn from qualitative chromatographic studies (broken lines indicate tentative pathways).

structures demand 4-chloroaniline to be cleaved. The quantity of 4-chloroaniline expected from such a reaction is not, however, apparent from the analysis of 4-chloroaniline content of degraded solutions.

The proposed structure of degradation product E agrees well with qualitative studies noted in Chapter 7.3 as follows. Cleavage of the biguanide chain opens up a series of hydrolytic deamination or chain hydrolytic reactions. The sequential removal of ammonia or carbon dioxide eventually yields degradation product E. Figure 7.9 suggested that this product was the final, or most stable, degradation product. The two instances where its apparent content decreased may be accounted for by the degradation of the undegraded end of the molecule.

There are two possible explanations of the lower than expected 4-chloroaniline content of degraded solutions assuming that the proposed degradation product structures are correct. Firstly, 4-chloroaniline may take place in an addition reaction with chlorhexidine degradation products; the potential site of interaction for each degradation product is marked with an asterisk in Figure 8.5. Secondly, cleavage of the biguanide chain may occur at sites other than adjacent to the 4-chlorophenyl group. For example, 4-chlorophenylguanidine (Figure 2.8) may be produced. Stevens et al (1986) have in fact shown similar compounds to be present in degraded chlorhexidine solutions, although degradative conditions were much more severe than those performed herein.

From a review of the degradative reactions of amidines and biguanides (Chapter 2.5.2 and 2.5.3) it was noted that hydrolysis generally produced the corresponding amidinourea compound as shown in Figure 2.5. Biguanide chain cleavage was only noted after extended alkaline hydrolysis (Figure 2.6). Therefore an obvious, but as yet unproposed, degradation product is the corresponding amidinourea of chlorhexidine as shown in Figure 8.7. This structure retains the terminal 4-chlorophenyl group.

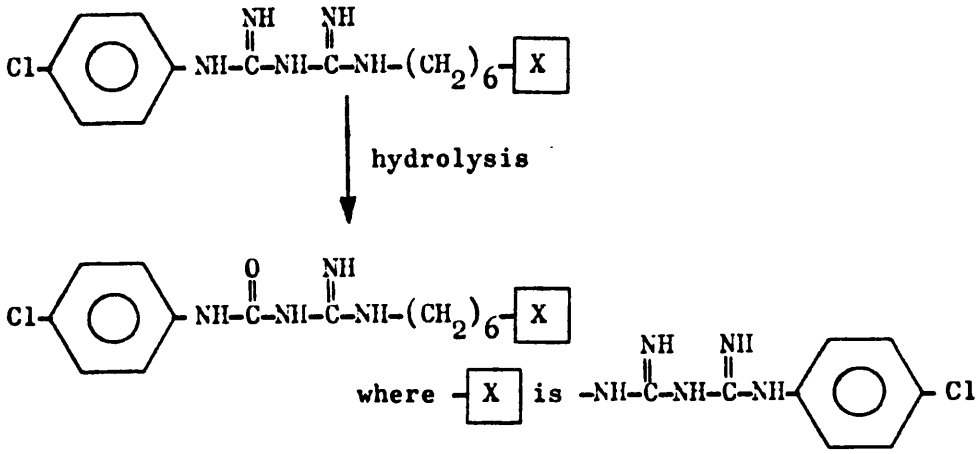

Figure 8.7 Hydrolysis of chlorhexidine to yield the corresponding amidinourea compound

Another degradative sequence may be the reversal of the pathway for chlorhexidine synthesis. Figure 2.1 outlines the synthetic reaction sequence with compounds I (hexamethylene diamine) and III (hexamethylene bisdicyandiamide - HMBDA) being similar to those of proposed degradation products E and α respectively. However, if this were a major degradative pathway significant amounts of 4-chloroaniline would also be detected.

However, it must again be emphasised that much of the above discussion is theoretical or "moulded" to fit chromatographic observations. It has been assumed throughout that the reaction sequence only occurs at one end of the chlorhexidine molecule. This assumption was made from the Holbrook method assay data which underestimated chlorhexidine degradation by a factor of two (Chapter 7.2). Since no direct evidence is available to validate this assumption, the possibility must remain that similar degradative reactions occur at the other end of the chlorhexidine molecule.

In summary, the degradative reaction pathway for chlorhexidine is potentially extremely complex with a whole series of consecutive and parallel processes implicated. The exact nature of particular degradation reactions cannot be identified until each degradation product is known and quantitatively analysed.

8.4 PHARMACEUTICAL IMPLICATIONS

Accelerated stability studies are performed to predict the effect of storage at ambient conditions and propose a shelf-life. Some of the kinetic studies performed within this thesis allow the direct calculation of degradation rate constants at room temperature and, for sterile products, typical autoclaving temperatures. The pharmaceutical implications of other studies are also discussed.

Table 8.3 lists the calculated shelf-life at 25°C (allowing ⅓5% decomposition) for 0.002% w/v chlorhexidine gluconate solutions at pH 2.0, ~6 and 9.0. Also presented are the predicted

percentage residual values after autoclaving at 100°C for 30 minutes or 121°C for 20 minutes (representing the sterilisation methods of Heating with a Bactericide and Moist Heat respectively). These predictions were made using equation 20 with activation energies and frequency factors taken from Table 6.11. The 95% confidence limit of each calculated activation energy (Table 6.11) has been used to generate 95% confidence limits for all values listed in Table 8.3.

pH	Shelf-life at 25°C (≯5% decomposition)	Predicted percentage residual after autoclaving	
		100°C x 30 min	121°C x 20 min
2.0	8.5 (±0.8) days	95.6 (±0.1)	92.2 (±0.6)
~6	2.70 (±0.40) years	99.7 (±0.1)	99.1 (±0.1)
9.0	0.40 (±0.06) years	77.2 (±0.1)	none (total decomposition)

Table 8.3 Effect of pH on predicted shelf-life at 25°C, and percentage residual after autoclaving, of 0.002% w/v chlorhexidine gluconate (±95% confidence limits for all values given in brackets)

It is noted that chlorhexidine has excellent stability at around pH 6 whilst the acidic and alkaline solutions have limited stability (especially alkaline solutions subjected to autoclaving). Concentration effects have been noted at pH ~6 and 9.0 which will potentially improve the stability of more concentrated chlorhexidine solutions. The type of chlorhexidine salt present is however unlikely to be an important influence.

From experimentation on buffered systems, similar predictions can be made for acetate (pH 4.0) and phosphate (pH 7.0) buffer systems of single and 0.1 strength (Table 8.4); data obtained

with borate buffers (pH 9.0) did not fit a linear Arrhenius relationship. The shelf-life at 25°C of 0.002% w/v chlorhexidine gluconate in both single strength buffers and autoclaving of 0.1 strength phosphate buffer systems may be a potential problem.

Buffer system (pH at 25°C)	Shelf-life at 25°C (±5% decomposition)	Predicted percentage residual after autoclaving	
		100°C x 30 min	121°C x 20 min
Acetate (pH 4.0):			
Single strength	0.34 (±0.13) years	99.9 (±0.02)	99.8 (±0.03)
0.1 strength	0.72 (±0.25) years	99.9 (±0.02)	99.8 (±0.04)
Phosphate (pH 7.0):			
Single strength	0.58 (±0.17) years	99.5 (±0.02)	98.5 (±0.05)
0.1 strength	1.08 (±0.23) years	98.7 (±0.10)	94.7 (±0.70)

Table 8.4 Effect of buffers on predicted shelf-life at 25°C, and percentage residual after autoclaving, of 0.002% w/v chlorhexidine gluconate (±95% confidence limits for all values given in brackets)

At 90°C the pH of maximum stability was identified as pH 5.0 for 0.002% w/v chlorhexidine gluconate. Compensating for the pK_w of water, at 25°C the pH of maximum stability is predicted to be approximately pH 6.

No direct comparison can be made between the results presented in this thesis and stability data generated by previous workers since they have all estimated chlorhexidine degradation from 4-chloroaniline content. This method has been shown to be extremely inaccurate since it underestimates chlorhexidine degradation by between three- and six-fold (Chapter 7.2). Additionally, previous

workers have quantified 4-chloroaniline content according to toxicity limitations and ignored molecular weight considerations in their calculation of percentage decomposition. Table 8.5 presents published stability study data and corrects these to give the true decomposition due to 4-chloroaniline content and predicted "total" decomposition using a rather charitable underestimation ratio of three.

The corrected values cast a serious doubt on the stability of chlorhexidine to the autoclaving process in slightly alkaline conditions (i.e. pH >7.5); this is in marked contrast to the opposite conclusions of Goodall et al (1968) and Jaminet et al (1970). However, since specific-base catalysed hydrolysis has been shown to be responsible for the degradation of chlorhexidine between ~pH 6 and 10, careful control of pH will limit the extent of degradation during autoclaving. The validity of this argument is supported by the fact that many chlorhexidine containing products are sterilised by autoclaving. In formulated products a compromise situation often exists since chlorhexidine is more active as an antimicrobial at slightly alkaline pH with many ophthalmic products buffered to pH 7.4. The presence of salts as tonicity adjusters may stabilise chlorhexidine by a negative primary salt effect.

The stability study performed by Pawelczyk and Plotkowiak (1976) using paper chromatographic analysis agrees well with the data generated herein : At pH 3.27 (formate buffer) the rate of reaction was dependent on buffer and ionic strength (a positive salt effect was noted, consistent with acid catalysed hydrolysis of the chlorhexidine dication). A pH of maximum stability at pH 6 was

Reference	Chlorhexidine concentration (% w/v) and salt	Sterilisation conditions		Resultant 4-chloroaniline content	"True"[1] 4-chloroaniline content (% w/v)	Total[2] decomposition (%)
Goodall et al (1968)	0.01 gluconate and acetate	98°C x 135 min		640[a]	0.33	1.0
		116°C x 30 min 126°C x 10 min		2370-2820	1.26-1.5	3.8-4.5
Polack (1967)	0.3 acetate	99°C x 8 hrs 120°C x 3 hrs	pH 5.3	1.4[b]	1.4	4.2
				4.0	5.4	16.2
		99°C x 5 hrs 120°C x 3 hrs	pH 6.8	1.3	1.75	5.3
				5.2	7.2	21.6
Jaminet et al (1970)	0.02 gluconate	120°C x 30 min	pH 4.7	0.13[c]	0.92	2.8
			pH 6.3	0.27	1.91	5.7
			pH 7.3	0.37	2.62	7.9
			pH 8.4	0.75	5.3	15.9
			pH 9.0	1.56	11.0	33.0
Dolby et al (1972)	0.05 acetate	116°C x 20 min		5000[a]	2.5	7.5
		121°C x 20 min		10500	5.2	15.6

Reference	Chlorhexidine concentration (% w/v) and salt	Sterilisation conditions	Resultant 4-chloroaniline content	"True"[1] 4-chloroaniline content (% w/v)	Total[2] decomposition (%)
Dolby et al (1972)	0.05 acetate	115°C x 30 min pH 5	2100	1.1	3.3
		6	2200	1.1	3.3
		6.5	3000	1.5	4.5
		7	4500	2.3	6.9
		7.5	8200	4.1	12.3
		8	11000	5.5	16.5

[1] "True" content from molecular weight considerations

[2] Total % decomposition of chlorhexidine assuming an underestimation ratio of 3

[a] Units of ppm relative to chlorhexidine

[b] Units of mg 4-chloroaniline per litre of solution

[c] Units of mg 4-chloroaniline per 100 mg chlorhexidine gluconate

Table 8.5 Published data for the stability of chlorhexidine to autoclaving. Data are corrected to give the "true" percentage concentration of 4-chloroaniline and calculated percentage decomposition of chlorhexidine.

noted at 80°C with an apparent activation energy of 77.6 $kJ.mol^{-1}$ at pH 3.27. All studies were performed on 0.018 to 0.045% w/v chlorhexidine gluconate.

The effect of surfactants on the degradation of 0.002% w/v chlorhexidine gluconate was investigated at pH 9.0 and 70°C. Whilst protective effects were observed in the presence of CTAB and cetomacrogol 1000, rate enhancement was observed with polysorbate 80. Surfactant effects are very prone to temperature influences, therefore it would be unwise to predict the effects of surfactants at room temperature other than to expect effects to be present.

A recent study (Pinzauti et al, 1984) has attempted to clarify the problems associated with the sorption of chlorhexidine on to glass. Chlorhexidine, present in buffered simulated contact lens solutions, was rapidly adsorbed on to all types of glass, except Type I (borosilicate) glass, under normal storage conditions. The residual chlorhexidine concentration of unbuffered solutions (initial pH 6.0) was also noted to decrease. However, the time dependency of loss and final alkaline pH (8.0 to 9.5) noted in Type III(soda-lime) glass suggests a chemical instability due to alkali shedding rather than a sorption process. The above study highlights the need to control all glassware used in performing experimentation on chlorhexidine. For example, during analytical procedures borosilicate glass should always be used and as an additional precaution it is recommended that this glass should also be chlorhexidine "aged" by soaking in the appropriate concentration of chlorhexidine before use.

8.5 SUGGESTIONS FOR FUTURE WORK

Since no formal stability study is complete without the identification of degradation products, future work is required with this aim. Although attempts to use preparative HPLC proved to be unsuccessful in this study for the separation of chlorhexidine degradation products, more detailed work may prove this method advantageous. Alternatively, paper/thin layer chromatography may be of use. Once isolated the traditional analytical methods of NMR, mass spectra, IR and UV spectroscopy should yield useful structural information. The identification of degradation products should enable the degradation mechanism to be accurately determined and provide further explanation for the observed kinetic effects.

Another area of useful research would be to investigate the specific effects of excipients and adjuvants present in chlorhexidine formulations now that a basic kinetic pattern has been established.

As yet, non-isothermal stability testing (Chapter 1.7.2) has only been applied to relatively simple compounds exhibiting comparatively uncomplicated degradative reactions (i.e. ester hydrolysis). With an accurate and sensitive temperature programmer and computer data handling it may be possible to use the degradation of chlorhexidine to assess the applicability of the non-isothermal method to complicated degradation processes.

APPENDIX 1

LEAST SQUARES REGRESSION ANALYSIS

When a linear relationship is assumed to exist between variables it is usual to fit a straight line by a least squares regression analysis. The simplest statistical model for this assumes that the independent variable X is known without error of measurement, and that the corresponding measured values of the dependent variable, Y are scattered normally from their true values. Hence each value Yi of the dependent is normally distributed with a mean $\alpha + \beta$ Xi.

The method of least squares obtains estimates of a and b in the equation Y = a + bX such that the sum of the squares of the deviations of the observations Yi from their mean of $\alpha + \beta$ Xi is a minimum.

These values are:-

$$a = \frac{\Sigma Yi - b\Sigma Xi}{n} = \bar{Y} - b\bar{X}$$

$$b = \frac{n\Sigma XiYi - \Sigma Xi \Sigma Yi}{n\Sigma Xi^2 - (\Sigma Xi)^2}$$

$$= \frac{\Sigma(Xi - \bar{X})(Yi - \bar{Y})}{\Sigma(Xi - \bar{X})^2}$$

where n = the number of points on the line.

Variance of the Slope (b)

This is termed S_b^2 and is given by the equation:-

$$S_b^2 = \frac{\sigma e^2}{\Sigma(Xi - \bar{X})^2}$$

where σe^2 is the residual variance of the dependent variable Y and is obtained from:-

$$\sigma e^2 = \frac{\Sigma D^2}{n-2}$$

where ΣD^2 is the residual sum of squares. ΣD^2 is obtained from the equation:-

$$\Sigma D^2 = \Sigma(Yi - \bar{Y})^2 - b^2 \Sigma(Xi - \bar{X})^2$$

The standard deviation of the slope is given by the square root of the variance.

Variance of the intercept (a)

This is termed $S_a^2 = \frac{\Sigma Xi^2 \quad \sigma e^2}{n \Sigma(Xi - \bar{X})^2}$

where $\sigma e^2 = \frac{\Sigma D^2}{(n-2)}$

The standard deviation of the intercept is given by the square root of the variance.

Correlation Coefficient

The correlation coefficient r is defined as:-

$$r = \frac{\Sigma(Xi - \bar{X})(Yi - \bar{X})}{\sqrt{\{[\Sigma(Xi-\bar{X})^2][\Sigma(Yi-\bar{Y})^2]\}}}$$

To represent a linear relationship between two variables, X and Y, r must be ± unity. The calculated value of r is compared with the tabulated value at the 5% probability level for n-2 degrees of freedom, and if found to be greater than the tabulated value, the observations are considered to be linearily related.

These calculations were converted to a BASIC computer program which ran on an Apple II europlus (Silentype printer). The program listing is given overleaf:-

```
10  DIM X(100),Y(100)
20  HOME : INVERSE : SPEED= 100: PRINT "           LINEAR REGRE
    SSION            ": NORMAL : SPEED= 255: PRINT : PRINT "BY
    G.BIRD & K.PURDY JULY 1985": PRINT "----------------------
    -----"
30  PRINT : PRINT "WITH CALCULATION FOR THE STANDARD": PRINT "D
    EVIATION IN SLOPE & INTERCEPT": PRINT : PRINT "PRESS RETURN
    ": PRINT "             ";: INPUT RT$
40  GOSUB 100: GOSUB 1000: GOSUB 1200: GOSUB 1400: GOSUB 1500: GOSUB
    1600: GOSUB 1700
100  HOME : PRINT "NAME FOR X-VALUES": PRINT : INPUT XN$
110  HOME : PRINT "NAME FOR Y-VALUES": PRINT : INPUT YN$
120  HOME : INVERSE : PRINT "ENTER THE VALUES IN THE TABLE BELO
    W": NORMAL : PRINT
130  PRINT "USE 99999 TO TERMINATE INPUT"
140  PRINT "---------------------------"
150  POKE 36,5: INVERSE : PRINT XN$;: POKE 36,20: PRINT YN$: NORMAL

160 Z = 1
170  POKE 36,5: GOSUB 900:X(Z) = XYZ
180  IF X(Z) > 99998 GOTO 220
190  POKE 36,20: GOSUB 900:Y(Z) = XYZ
210  PRINT :Z = Z + 1: GOTO 170
220  FOR Q = 1 TO 1000: NEXT Q
230  HOME :N = Z - 1
240  POKE 36,3: INVERSE : PRINT "£";: POKE 36,8: PRINT XN$;: POKE
    36,23: PRINT YN$: NORMAL
250  PRINT
260  FOR Z = 1 TO N
270  POKE 36,3: PRINT Z;: POKE 36,8: PRINT X(Z);: POKE 36,23: PRINT
    Y(Z)
280  NEXT Z
290  PRINT : PRINT "ARE THEY CORRECT (Y/N) ";: INPUT Z$
300  IF Z$ <  > "Y" AND Z$ <  > "N" THEN 290
310  IF Z$ = "Y" THEN 430
320  PRINT : PRINT "ENTER £ TO BE CORRECTED";: INPUT R
330  PRINT : PRINT "ENTER VALUE TO BE CORRECTED"
340  PRINT : PRINT XN$" TYPE X"
350  PRINT : PRINT YN$" TYPE Y"
360  PRINT "             ";: INPUT Z$
370  IF Z$ = "X" THEN 390
380  IF Z$ = "Y" THEN 410
390  PRINT : PRINT "THE INCORRECT OF "XN$" IS "X(R)
400  PRINT : PRINT "ENTER THE CORRECT VALUE ";: INPUT X(R): GOTO
    230
410  PRINT : PRINT "THE INCORRECT OF "YN$" IS "Y(R)
420  PRINT : PRINT "ENTER THE CORRECT VALUE ";: INPUT Y(R): GOTO
    230
430  RETURN
900 Z$ = "  "
910  GET A$: IF A$ =  CHR$ (13) THEN 940
920  IF A$ =  CHR$ (8) THEN  POKE 36, PEEK (36) - 1: PRINT " ";
    : POKE 36, PEEK (36) - 1:Z$ =  LEFT$ (Z$, LEN (Z$) - 1): GOTO
    910
930  PRINT A$;:Z$ = Z$ + A$: GOTO 910
940 Z$ =  RIGHT$ (Z$, LEN (Z$) - 2):XYZ =  VAL (Z$)
950  RETURN
1000  REM  CALCULATION OF A & B
1010  REM  SUM OF X AND Y =J
1020  FOR Z = 1 TO N
1030 J = J + (X(Z) * Y(Z))
```

```
1050  REM  SUM OF X = SX SUM OF Y = SY
1060 SX = SX + (X(Z))
1070 SY = SY + (Y(Z))
1075 MX = SX / N:MY = SY / N
1080  REM  SUMX * SUMY=K
1090 K = SX * SY
1100  NEXT Z
1110  REM SUMX^2=L
1120  FOR Z = 1 TO N
1130 L = L + (X(Z) ^ 2)
1140  NEXT Z
1150  REM  SUM X ALL SQUARED=M
1160 M = (SX) ^ 2
1170 B = ((N * J) - (SX * SY)) / ((N * L) - (M))
1180 A = MY - (B * MX)
1190  RETURN
1200  REM  VARIANCE OF SLOPE (SB) MEAN Y = MY AND MEAN X = MX
1210 MY = SY / N:MX = SX / N
1220  REM  CALCULATION OF D^2
1230  REM  A1= SUM(Y(Z)-MY)^2                          B1=B^2
                                   C1= SUM(X(Z)-MX)^2
1240  FOR Z = 1 TO N
1250 A1 = A1 + ((Y(Z) - MY) ^ 2):B1 = B ^ 2:C1 = C1 + ((X(Z) -
    MX) ^ 2)
1260 D = ( ABS (A1 - (B1 * C1)))
1270 E =  ABS (D / (N - 2))
1280 SB = E / C1
1285 SB =  SQR (SB)
1300  RETURN
1400  REM  VARIANCE OF INTERCEPT(SA)
1410 SA = (L * E) / (N * C1):SA =  SQR (SA)
1420  RETURN
1500  REM   CORRELATION COEFFICIENT
1510  FOR Z = 1 TO N
1520 R = R + ((X(Z) - MX) * (Y(Z) - MY))
1525  NEXT Z
1527 R = R / ( SQR (C1 * A1))
1530  RETURN
1600  REM  RESULTS
1610  PRINT : PRINT "SLOPE = "B
1620  PRINT : PRINT "INTERCEPT = "A
1630  PRINT : PRINT "CORRELATION = "R
1640  PRINT : PRINT "SLOPE STD DEV = "SB
1650  PRINT : PRINT "INTERCEPT STD DEV = "SA
1700  REM  PRINTOUT
1710  PRINT : PRINT "PRINTOUT Y/N ";: INPUT Z$
1720  IF Z$ <  > "Y" AND Z$ <  > "N" THEN 1710
1730  IF Z$ = "N" THEN 1810
1735  PR£ 1
1740  POKE 36,5: PRINT XN$;: POKE 36,30: PRINT YN$
1750  FOR Z = 1 TO N
1760  POKE 36,5: PRINT X(Z);: POKE 36,30: PRINT Y(Z)
1770  NEXT Z
1780  PRINT : PRINT "SLOPE = "B: PRINT : PRINT "INTERCEPT = "A
1790  PRINT : PRINT "CORRELATION COEFFICIENT = "R: PRINT : PRINT
    "SLOPE STD DEV = "SB
1800  PRINT : PRINT "INTERCEPT STD DEV = "SA
1810  PR£ 0: END
```

APPENDIX 2

TO DETERMINE THE EQUALITY OF TWO ESTIMATES OF A PARAMETER

The test is generally known as Student's t test.

(i) Comparison of Two Means

The comparison of means of two small samples uses the "student t test" in the form:-

$$t = \frac{\bar{X}_1 - \bar{X}_2}{S\sqrt{\frac{1}{n_1} + \frac{1}{n_2}}}$$

where $\bar{X}_1$ and $\bar{X}_2$ are the means and n_1 and n_2 are the number of observations. S is the estimate of standard deviation based on both samples jointly and is given by:-

$$S^2 = \frac{\Sigma(X_1 - \bar{X}_1)^2 + \Sigma(X_2 - \bar{X}_2)^2}{n_1 + n_2 - 2}$$

The calculated value of t is compared with the tabulated values for $n_1 + n_2 - 2$ degrees of freedom.

(ii) Comparison of Two Slopes

The equality of estimates P_1 and P_2, with variances S_1^2 and S_2^2 respectively, of a parameter P is assessed by means of the following statistic:-

$$t = \frac{P_1 - P_2}{\sqrt{S_1^2 + S_2^2}}$$

The value of t is compared with tabulated values with $n_1 + n_2 - 4$ degrees of freedom, where n_1 and n_2 are the number of observations used in the estimation of P_1 and P_2 respectively. If the calculated value of t exceeds the tabulated value at the 5% probability level, the parameters are considered to be significantly different at that level.

APPENDIX 3

MULTIPLE LINEAR REGRESSION ANALYSIS

Linear regression analysis can be extended to situations where the value of one variable is affected by changes in the values of other variables. From computations performed on all data and individual sets of data, multiple linear regression analysis determines the equality of regression lines across groups (F_{ratio}). The significance of the F_{ratio} was then tested at the 5% level of probability using the appropriate degrees of freedom.

Multiple linear regression analyses were run on an IBM main frame computer using the BMDP-1R program from the BMDP Statistical Software Package (1964 Westwood Boulevard, Suite 202, Los Angeles, California). F_{ratio} and degrees of freedom were printed out to allow analysis at various levels of probability.

APPENDIX 4

CONFIDENCE LIMITS

The confidence limit of an estimate of a parameter is given by the statistic:-

$$\frac{S}{\sqrt{n}} .t$$

where S is the standard deviation of the estimate and n is the number of observations. The value of t is the tabulated value at the required degree of confidence with n-1 degrees of freedom.

APPENDIX 5

ESTIMATION OF APPARENT BASIC IONISATION CONSTANT (K^1)

A5.1 INTRODUCTION

Literature citations of pKa values for chlorhexidine generally quote those given by Hugo and Longworth (1964) although these authors refer to a personal communication from ICI for the values of 2.2 and 10.3. It has proved difficult to ascertain the methodology or temperature of determination for this data. Recently, part of an internal memorandum has been made available (Leahy, 1987, ICI Pharmaceuticals, Personal Communication) which cites thermodynamic pK_a values of 2.8 and 10.2 for chlorhexidine at 25°C. It is understood that these were determined by UV spectroscopy.

Since the kinetic studies showed there to be a discontinuity in the pH-degradation rate profile in alkaline conditions (at 90°C), determination of the basic pK_a value over the temperature range 25-60°C was attempted, with a view to predicting the value at 90°C from the Van't Hoff equation (A1)

$$pK_a = \frac{\Delta H^\circ}{2.303RT} + \text{constant} \quad .... \quad (A1)$$

where ΔH° is the standard ionisation enthalpy, R is the gas constant and T the absolute temperature.

Methods routinely applied to the determination of ionisation constants include UV spectroscopy and potentiometric titration. Preliminary investigation indicated there was little difference between the UV spectra for 1.53×10^{-5}M chlorhexidine base in 1.0M

hydrochloric acid, 10^{-4}M hydrochloric acid (pH 4.2) or 0.1M sodium hydroxide (Figure A5.1). Additionally, the presence of buffer to control pH for spectroscopic analysis may be problematical due to anion binding associated with the high buffer to chlorhexidine concentration ratio in such solutions. Consequently the potentiometric titration method described by Albert and Serjeant (1984) was applied. Although chlorhexidine base has a reported solubility of ~ 1.6×10^{-4}M (Senior, 1973), initial experimentation showed that a 3.29×10^{-4}M solution of chlorhexidine acetate could be titrated with 0.5M potassium hydroxide up to ~ 75% theoretical stoichiometric equivalence before precipitation occurred.

A5.2 EXPERIMENTAL

A5.2.1 Standardisation of pH Equipment

A Pye-Ingold 465-90 high temperature pH electrode was used in conjunction with a Radiometer PHM64 pH-meter (sensitivity ± 0.002 pH units). Standardisation was made with 0.01 molal sodium tetraborate and 0.025 molal sodium hydrogen carbonate - 0.025 molal sodium carbonate (Perrin and Dempsey, 1974) at the appropriate temperature. Electrode response to the standard buffers was also checked at the end of each potentiometric titration to ensure it remained within specification (± 0.002 pH unit).

A5.2.2 Preparation of Solutions

All solutions were prepared from freshly boiled and cooled double distilled water held in well closed containers until cool. 0.5M carbonate free potassium hydroxide, standardised against AR potassium hydrogen phthalate, was prepared according to Albert and Serjeant

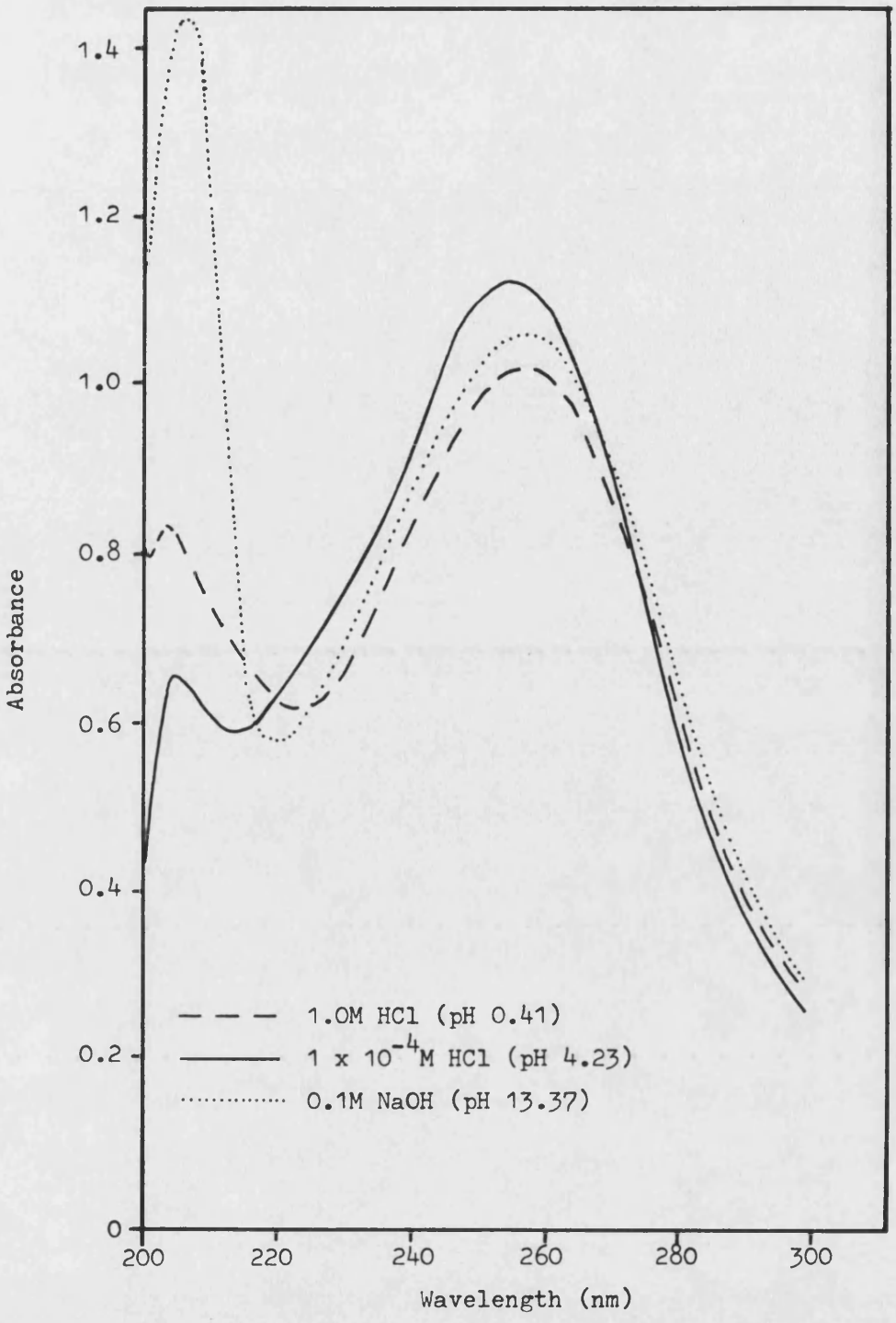

Figure A5.1 UV spectra for 1.53×10^{-5}M chlorhexidine base in 1.0M HCl, 1×10^{-4}M HCl and 0.1M NaOH

(1984). 3.29×10^{-4}M chlorhexidine acetate solutions were prepared from the standard reference material supplied by ICI and the theoretical concentration verified by HPLC analysis.

A5.2.3 Titration

The reaction vessel and stirrer system used for the kinetic experiments (Chapter 6.2.1) was fitted with the pH electrode and a fine capillary plastic tube delivering oxygen-free nitrogen (white spot, BOC) to prevent access of carbon dioxide. Nitrogen flow was limited to ensure no loss of solution as spray. Titrant was delivered in 0.025 ml increments from an "Agla" micrometer syringe (total volume 0.25 ml) fitted with a fine straight glass needle. After electrode standardisation the experiment was set-up by pipetting 250 ml of 3.29×10^{-4}M chlorhexidine acetate solution into the vessel, starting the gas supply and allowing the system to equilibrate to temperature (± 0.1°C). After recording the initial pH, titrant was added, allowing ~ 10 minutes between increments to allow the pH meter reading to stabilise. Variation in the third place was within instrument sensitivity (± 0.002 pH units) and several readings were averaged to give the recorded data (Table A5.1). Each determination was performed in duplicate together with a "blank" to act as control. Determinations were carried out at 25°, 40°, 50° and 60°C.

A5.3 TREATMENT OF POTENTIOMETRIC TITRATION DATA

It is generally assumed that the ionisation of chlorhexidine involves the simultaneous loss of two protons, one from each biguanide

Titrant volume (ml)	Measured pH											
	25°C			40°C			50°C			60°C		
	1	2	blank	1	2	blank	1	2	blank	1	2	blank
Initial	6.331	6.349	6.918	6.504	6.441	6.877	6.569	6.555	6.818	6.480	6.512	6.773
0.050	9.758	9.790	10.102	9.388	9.346	9.889	9.108	9.113	9.880	8.919	8.929	9.771
0.075	9.981	10.007	10.197	9.610	9.586	9.961	9.323	9.299	9.947	9.124	9.131	9.836
0.100	10.133	10.161	10.316	9.757	9.744	10.011	9.472	9.499	9.998	9.268	9.278	9.886
0.125	10.253	10.281	10.410	9.881	9.864	10.180	9.588	9.589	10.157	9.379	9.369	10.060
0.150	10.351	10.379	10.506	9.958	9.962	10.301	9.682	9.691	10.276	9.473	9.471	10.181
0.175	10.433	10.460	10.577	10.079	10.041	10.360	9.761	9.777	10.333	9.556	9.560	10.229
0.200	10.509	10.531	10.626	10.124	10.112	10.413	9.831	9.847	10.410	9.627	9.630	10.322
0.225	10.569	10.592	10.677	10.190	10.174	10.461	9.892	9.925	10.455	9.690	9.711	10.349

TABLE A5.1 Data for the determination of basic apparent pK_a^1 values by potentiometric titration of 3.29×10^{-4}M chlorhexidine acetate (250 ml) with 0.5M potassium hydroxide.

group at the acid and basic ionisation steps, i.e.

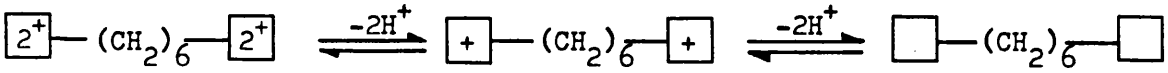

tetracation dication base

where □ represents the 4-chlorophenyl-biguanide group. Quoted pK_a values therefore derive from "macro" - ionisation constants. For the chemically related compound hexamethylenebisbiguanide, the two proton loss under either acid or basic conditions has been shown to occur sequentially rather than simultaneously (Dutta and Gupta, 1961) leading to the possibility of overlapping pK_a^1 values for chlorhexidine, with values of ~ 1.7, 2.9, 10.3 and 10.8 being predicted from structural analogy (Chapter 2.4.5 iii).

Methods for examining potentiometric titration data for overlapping pK_a values have been described by Albert and Serjeant, (1984) and Benet and Goyan, (1965; 1967). However this approach proved inapplicable to the chlorhexidine acetate titration results and apparent "macro" - pK_a^1 values were therefore estimated using the simple form of the Henderson - Hasselbalch equation (A2) :

$$pH = pK_a^1 + \log \frac{[CX]}{[CXH+]} \quad .... \quad (A2a)$$

or

$$pK_a^1 = pH + \log R \quad .... \quad (A2b)$$

where R is $[CXH+]/[CX]$

If the assumption of simultaneous loss of two protons from each of the two biguanidine residues is made, then effectively, a

3.29×10^{-4}M solution of chlorhexidine acetate which forms the dication species, behaves as if it were a 6.58×10^{-4}M solution of monoprotonated species, whose concentration is represented by [CXH+] in equation A2; [CX] is thus the concentration of the equivalent unprotonated free base species.

A5.4 RESULTS

Potentiometric titration data are given in Table A5.1 and a specimen calculation shown in Table A5.2. Mean pK_a^1 values were obtained by converting individual values to ionisation constants, calculating the mean K_a and reconverting this to give the mean pK_a^1. Estimates for the four temperatures are shown in Table A5.3. Standard deviations (σ) were calculated from equation A3 (Albert and Serjeant, 1984) :

$$\sigma = \sqrt{\frac{(pK_a(expt) - pK_a(mean))^2}{n}} \quad .... \quad (A3)$$

0.5M KOH (ml)	pH	[CXH+] ($Mx10^4$)	[CX] ($Mx10^4$)	log R	pK_a^1
0.050	9.758	5.580	1.000	0.747	10.50
0.075	9.981	5.080	1.500	0.530	10.51
0.100	10.133	4.581	1.999	0.360	10.49
0.125	10.253	4.081	2.499	0.213	10.56
0.150	10.351	3.582	2.998	0.077	10.51
0.175	10.433	3.082	3.498	-0.055	10.45
0.200	10.509	2.583	3.997	-0.190	10.32
0.225	10.635	2.084	4.496	-0.334	10.30
Mean					10.45
Standard deviation					0.09
Range					±0.15

Table A5.2 Calculation of basic pK_a^1 values from determination 1 at 25°C (using data from Table A5.1).

Temperature (°C)	Apparent pK_a^1						
	Determination 1			Determination 2			Mean
	pK_a^1	S.D.	range	pK_a^1	S.D.	range	
25	10.45	0.09	±0.15	10.45	0.10	±0.20	10.45
40	10.03	0.09	±0.19	10.05	0.10	±0.20	10.04
50	9.76	0.10	±0.21	9.77	0.09	±0.18	9.77
60	9.56	0.10	±0.20	9.56	0.10	±0.19	9.56

Table A5.3 Effect of temperature on apparent basic pK_a^1 values for chlorhexidine.

A5.5 DISCUSSION

The experimental data in Table A5.1 shows the pH values from the "blank" titrations were all greater than those for solutions containing chlorhexidine acetate although differences become less as the temperature decreased, thus reducing the confidence in the derived values. Consideration of the standard deviation and ranges given in Table A5.3 suggests 95% confidence limits of ~ ± 0.1 pH unit.

Figure A5.2 shows a good linear fit to the Van't Hoff equation (A1). Regression analysis data and derived apparent pK_a^1 values at 70°, 80° and 90°C are given in Table A5.4.

Regression Analysis Data for plot of pK_a^1 vs 1/T			
Slope (x 10^{-3})	2.545		
SD slope (x 10^{-3})	0.040		
RSD slope	1.6%		
Correlation coefficient	0.9996		
Temperature (°C)	70°	80°	90°
Predicted pK_a^1	9.33	9.12	8.92

Table A5.4 Van't Hoff plot regression analysis data and predicted pK_a^1 values for chlorhexidine ionisation in basic conditions.

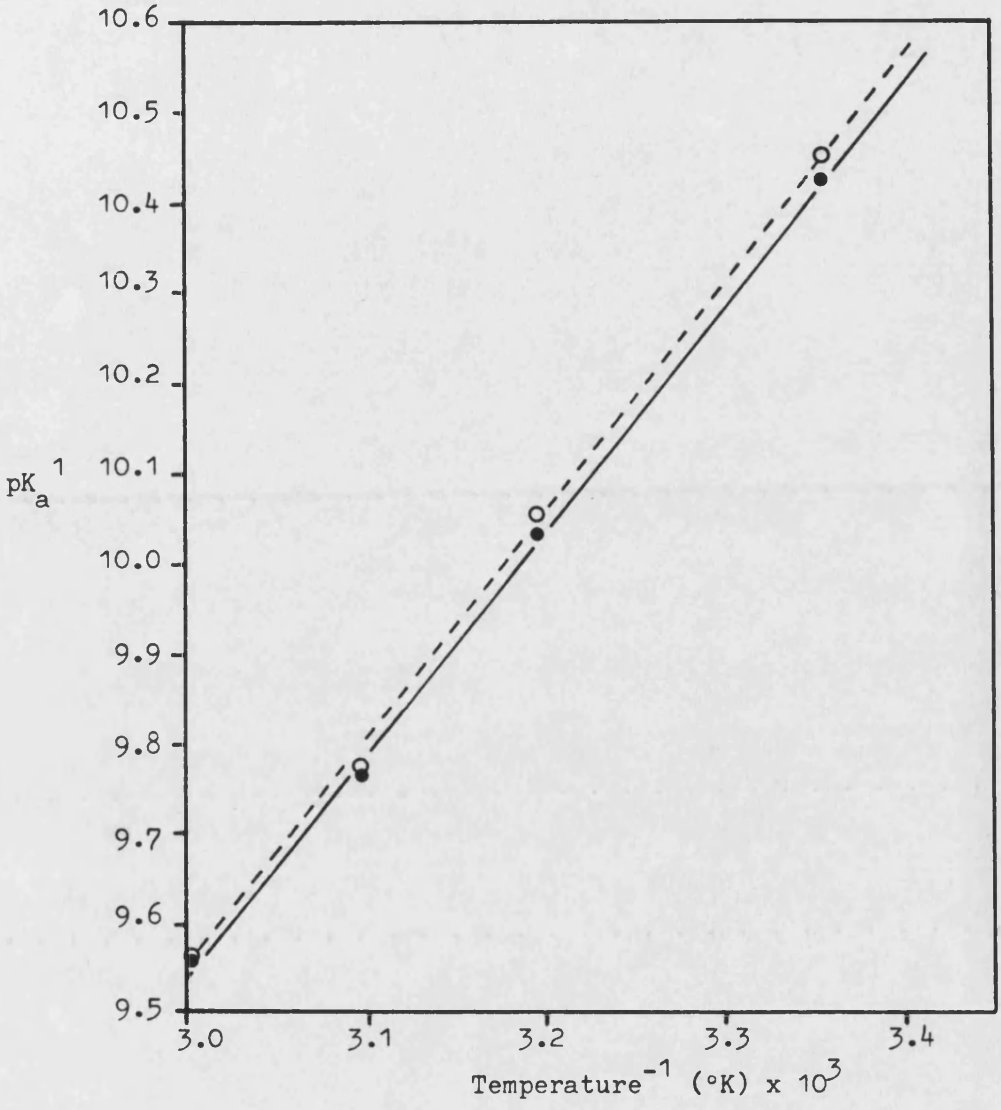

Figure A5.2 Van't Hoff plot of pK_a^1 against temperature for the "macro" basic ionisation constant of chlorhexidine

REFERENCES

Albert, A. and Serjeant, E. P. (1984)
The Determination of Ionisation Constants, London : Chapman and Hall.

Allen, A. E. and Gupta, V. D. (1974)
J. Pharm. Sci., 63, 107.

Andermann, G., Buhler, M. O. and Erhart, M. (1980)
J. Pharm. Sci., 69, 215.

Ansel, H. C. (1967)
J. Pharm. Sci., 56, 616.

Attwood, D. (1968)
J. Phys. Chem., 72, 339.

Attwood, D. and Florence, A. T. (1983)
Surfactant Systems, London : Chapman and Hall.

Attwood, D. and Natarajan, R. (1980)
J.Pharm. Pharmacol., 32, 460.

Azaz, E., Donbrow, M. and Hamburger, R. (1973)
Pharm. J., 211, 15.

Bachner, J., Heinisch, G. and Matous, H. (1981)
J. High Resolut. Chromatogr. Chromatogr. Commun., 4, 132.

Bailey, F., Brittain, P. N. and Williamson, B. F. (1975)
J. Chromatogr., 109, 305.

Bauer, M., Mailhe, L., Menard, D. and Rouanet, J. P. (1983)
J. Chromatogr., 259, 360.

Bauer, M., Degude, C. and Mailhe, L. (1984)
J. Chromatogr., 315, 457.

Beg, A. E. (1977)
Ph.D. Thesis, University of Bath.

Bell, N. A., Hutley, B. G., Shelton, J. and Turner, J. B. (1977)
Thermochimica Acta, 21, 255.

Benet, L. Z. and Goyan, J. E. (1965)
J. Pharm. Sci., 54, 1179.

Benet, L. Z. and Goyan, J. E. (1967)
J. Pharm. Sci., 56, 665.

Benson, S. W. (1960)
The Foundations of Chemical Kinetics, New York : McGraw Hill.

Bentley, D. L. (1970)
J. Pharm. Sci., 59, 464.

Berge, S. M., Henderson, N. L. and Frank, M. J. (1983)
J. Pharm. Sci., 72, 59.

Blaha, J. M., Knevel, A. M., Kessler, D. P., Mincy, J. W. and Hem, S. L. (1976)
J. Pharm. Sci., 65, 1165.

Bor, C. (1981)
Zfi. Mitt., 43B, 445.

Bratton, A. C. and Marshall, E. K. (1939)
J. Biol. Chem., 128, 537.

British Pharmacopoeia, 1980 and Addendum, 1983
London : H.M.S.O.

British Pharmaceutical Codex 1959
London : Pharmaceutical Press.

Brown, C. J. (1967)
J. Chem. Soc., 1967(A), 60.

Browne, R. K., Anderson, A. N., Charvez, B. W. and Azzarello, R. J. (1975)
Toxicol. Appl. Pharmacol., 32, 621.

Bunton, C. A. (1973)
in : Cordes, E. H. (ed.), Reaction Kinetics in Micelles, p72, New York : Plenum Press.

Bunton, C. A. (1979a)
in : Mittal, K. L. (ed.), Solution Chemistry of Surfactants, Vol. 2, p519, New York : Plenum.

Bunton, C. A. (1979b)
Catal. Rev. - Sci. Eng., 20, 1.

Bunton, C. A. and Romsted, L. R. (1982)
in : Mittal, K. L. and Fendler, E. J. (eds.), Solution Behaviour of Surfactants, Vol. 2, p975.

Butler, W. H. and Iswaran, T. J. (1979)
in : Problems in the Control of Hospital Infection, Royal Society of Medicine International Congress and Symposium Series No. 23, London : Academic Press.

Calman, R. M. and Murray, J. (1956)
Brit. Med. J., 2, 200.

Carstensen, J. T. (1970)
J. Pharm. Sci., 59, 1140.

Carstensen, J. T. and Su, K. S. E. (1971)
Bull. Parent. Drug Assoc., 25, 287.

Chaimovich, H., Aleixo, R. M. V., Cuccovia, I. M., Zanette, D. and Quina, F. H. (1982)
in : Mittal, K. L. and Fendler, E. J. (eds.), Solution Behaviour of Surfactants, Vol. 2, p949.

Chung, P. H., Chin, T. F. and Lach, J. L. (1970)
J. Pharm. Sci., 59, 1300.

Ciarlone, A. E., Gangarosa, L. P. and Fong, B. C. (1976)
J. Dent. Res., 55, 918.

Clark, C. J. and Hudson, H. E. (1968).
Manufact. Chem., 39, Jan. 25.

Clarke, E. G. C. (1975)
Isolation and Identification of Drugs in Pharmaceuticals, Body Fluids and Post-mortem Material, Vol. 2, London : Pharmaceutical Press.

Colin, H., Krstulovic A. M., Excoffier, J. L. and Guiochon, G. (1985)
A Guide to the HPLC Literature, Vol. 1-3, New York : John Wiley and Sons.

Collins, A. J., Campbell, A. T. and Bain, A. (1979)
J. Clin. Pharm., 4, 205.

Connors, K. A. (1981)
J. Parent. Sci. Tech., 35, 186.

Connors, K. A., Amidon, G. L. and Kennon, L. (1979)
Chemical Stability of Pharmaceuticals, New York : John Wiley & Sons.

Cox, N. I. (1975)
M.Sc. Thesis, University of Bath.

Cropper, E., Platt, P. and Puttnam, N. A. (1975)
J. Soc. Cosmet. Chem., 26, 355.

Crounse, N. N. (1951)
J. Org. Chem., 16, 492.

Curd, F. H. S. and Rose, F. L. (1946)
J. Chem. Soc., 1946, 729.

Curd, F. H. S., Davey, D. G. and Richardson, D. N. (1949)
J. Chem. Soc., 1949, 1732.

Cutler, R. A., Diana, G. D. and Schalit, S. (1966)
Soap Chem. Spec., 1966, 45.

Davies, A. (1973)
J. Periodont. Res., 8; Suppl. 12 : 68.

Davies, A. and Field, B. S. (1969)
J. Appl. Bact., 32, 233.

Davies, G. E., Francis, J., Martin, A. R., Rose, F. L. and Swain, G. (1954)
Brit. J. Pharmacol., 9, 192.

Davies, O. L. and Budgett, D. A. (1980)
J. Pharm. Pharmacol., 32, 155.

DeWolfe, R. H. (1975)
in : Patai, S. (ed.), The Chemistry of Amidines and Imidates,
London : John Wiley and Sons.

Dolby, J., Gunnarsson, B., Kronberg, L. and Wikner, H. (1972)
J. Hosp. Pharm., 30, 223-226 and 244-251.

Donbrow, M., Azaz, E. and Pillersdorf, A. (1978)
J. Pharm. Sci., 67, 1676.

Dutta, R. L. and Gupta, N. R. S. (1961)
J. Indian Chem. Soc., 38, 741.

Dziegielewski, J. O. (1975)
Int. J. Radiat. Phys. Chem., 7, 507.

Edwards, L. J. (1950)
Trans. Faraday Soc., 46, 723.

Edwards, L. J. (1952)
Trans. Faraday Soc., 48, 696.

Elpbern, B. (1968)
Ann. N. Y. Acad. Sci., 148, 577.

Eriksen, S. P. and Stelmach, H. (1965)
J. Pharm. Sci., 54, 1029.

Erni, F. (1982)
J. Chromatogr., 251, 141.

Fabbrizzi, L., Micheloni, M., Paoletti, P. and Schwarzenbach, G. (1977)
J. Am. Chem. Soc., 99, 5574.

Fanshawe, W. J., Bauer, V. J., Ullman, E. F. and Safir, S. R. (1964)
J. Org. Chem., 29, 308.

Felmeister, A. and Discher, C. A. (1964)
J. Pharm. Sci., 53, 756.

Felmeister, A., Schaubman, R. and Howe, H. (1965)
J. Pharm. Sci., 54, 1589.

Fendler, J. H. and Fendler, E. J. (1975)
Catalysis in Micellar and Macromolecular Systems, New York : Academic Press.

Fendler, E. J. and Fendler, J. H. (1980)
in : Gold, V. (ed.), Advances in Physical Organic Chemistry, Vol. 8, p271, London : Academic Press.

Finholt, P. and Higuchi, T. (1962)
J. Pharm. Sci., 51, 655.

Finholt, P., Jurgensen, G. and Kristiansen, H. (1965)
J. Pharm. Sci., 54, 387.

Finholt, P., Kristiansen, H., Krowczynski, L. and Higuchi, T. (1966)
J. Pharm. Sci., 55, 1435.

Fiomaro, R., Rossi, G. and Pinzauti, S. (1983)
Bull. Soc. Ital. Farm. Osp., 29, 287.

Fisher, R. G., Quintana, R. P. and Boulware, M. A. (1975a)
J. Dent. Res., 54, 20.

Fisher, R. G. and Quintana, R. P. (1975b)
J. Dent. Res., 54, 25.

Fletcher, G. (1968)
M.Sc. Thesis, University of Bath.

Foster, J. H. S. (1965)
Manufact. Chem., 36, May 45 and June 43.

Fowler, K. E. (1972)
in : Henderson, S. T. and Marsden, A. M. (eds.), Lamps and Lighting, 2nd edn., London : Edward Arnold.

Frost, A. A. and Pearson, R. G. (1961)
Kinetics and Mechanism, 2nd edn., New York : Wiley.

Funusaki, N. and Murata, A. (1980)
Chem. Pharm. Bull., 28, 803.

Gaffney, M. H., Cooke, M. and Simpson, R. (1984)
J. Chromatogr., 306, 303.

Gage, J. C. (1949)
J. Chem. Soc., 1949, 221.

Games, D. E. (1981)
Biomed. Mass Spectrom., 8, 454.

Gardner, L. A. and Goyan, J. E. (1973)
J. Pharm. Sci., 62, 1026.

Garrett, E. R. (1957)
J. Am. Chem. Soc., 79, 340.

Garrett, E. R. (1962)
J. Pharm. Sci., 51, 811.

Garrett, E. R., Bojarski, J. T. and Yakatan, G. J. (1971)
J. Pharm. Sci., 60, 1145.

Goodall, R. R., Goldman, J. and Woods, J. (1968)
Pharm. J., 200, 33.

Goyan, J. E., Shaikh, Z. I. and Autian, J. (1960)
J. Am. Pharm. Assoc. Sci. Ed., 49, 627.

Grimm, W. (1973)
Pharm. Ind., 35, 733.

Guttman, D. E. and Meister, P. D. (1958)
J. Am. Pharm. Assoc. Sci. Ed., 47, 773.

Haas, D. J., Harris, D. R. and Mills, H. H. (1965)
Acta Crystallogr., 19, 676.

Hafelinger, G. (1975)
in : Patai, S. (ed.), The Chemistry of Amidines and Imidates,
London : John Wiley and Sons.

Hajratwala, B. R. and Dawson, J. E. (1977)
J. Pharm. Sci., 66, 27 and 1259.

Hakes, L. B. (1980)
Ph.D. Thesis, University of Bath.

Hall, R. (1967)
Proc. Biochem., 1967, Nov. 24.

Hamburger, R., Azaz, E. and Donbrow, M. (1975)
Pharm. Acta Helv., 50, 10.

Hansen, J., Kreilgard, B., Nielsen, O. and Veje, J. (1983)
Int. J. Pharm., 16, 141.

Harned, H. S. and Owen, B. B. (1958)
Physical Chemistry of Electrolytic Solutions, 3rd edn., New York : Reinhold.

Hartley, G. S. (1934)
Trans. Faraday Soc., 30, 444.

Hartley, G. S. (1948)
Quart. Rev. (London), 2, 152.

Hashimoto, N., Tasaki, T. and Tanaka, H. (1984)
J. Pharm. Sci., 73, 369.

Hayes, R. (1981)
M.Sc. Thesis, University of Bath.

Heard, D. D. and Ashworth, R. W. (1968)
J. Pharm. Pharmacol., 20, 505.

Heimlich, K. R. and Martin, A. N. (1960)
J. Am. Pharm. Assoc. Sci. Ed., 49, 592.

Henderson, S. T. and Marsden, A. M. (1972)
Lamps and Lighting, 2nd edn., London : Edward Arnold.

Higuchi, T. and Bias, C. D. (1953)
J. Am. Pharm. Assoc. Sci. Ed., 42, 707.

Higuchi, T., Marcus, A. D. and Bias, C. D. (1954)
J. Am. Pharm. Assoc. Sci. Ed., 43, 129.

Holbrook, A. (1958)
J. Pharm. Pharmacol., 10, 370.

Hou, J. P. and Poole, J. W. (1969)
J. Pharm. Sci., 58, 447.

Hou, J. P. and Poole, J. W. (1971)
J. Pharm. Sci., 60, 503.

Hugo, W. B. and Longworth, A. R. (1964)
J. Pharm. Pharmacol., 16, 655.

Hugo, W. B. and Longworth, A. R. (1965)
J. Pharm. Pharmacol., 17, 28.

Hugo, W. B. and Longworth, A. R. (1966)
J. Pharm. Pharmacol., 18, 569.

Hussain, A., Schurman, P., Peter, V. and Milosovich, G. (1968)
J. Pharm. Sci., 57, 411.

Huston, C. E., Wainwright, P., Cooke, M. and Simpson, R. (1982)
J. Chromatogr., 237, 457.

Jacobs, G. P. and Melumad, D. (1976)
Pharm. Acta Helv., 51, 313.

Jacobsen, E. and Glyseth, B. (1975)
Talanta, 22, 1001.

Jaminet, Fr., Delattre, L., Delporte, J. P. and Moes, A. (1970)
Pharm. Acta Helv., 45, 60.

Jensen, J. E. and Christensen, F. (1971)
J. Periodont. Res., 6, 306.

Johnson, J. R., Woodward, R. B. and Robinson, R. (1949)
in : Clarke, H. T., Johnson, J. R. and Robinson, R. (eds.),
The Chemistry of Penicillin, Princeton : Princeton University Press

Kalyanasundaram, K. and Thomas, J. K. (1977)
J. Phys. Chem., 81, 2176.

Kelly, C. A. (1970)
J. Pharm. Sci., 59, 1053.

Khammas, Z. N. (1980)
M.Sc. Thesis, University of Bath.

Khan, M. N. and Khan, A. A. (1976)
J. Chem. Soc. Perkin II, 1976, 1009.

Kiro, Z. B., Teterin, Yu. A., Nikolenki, L. N. and Stepanov, B. I. (1972)
Org. Khim., 8, 2573.

Koshy, K. T. (1969)
J. Pharm. Sci., 58, 560.

Kostenbauder, H. B. and Bogardus, J. B. (1985)
in : Gennaro, A. R. (gen.ed.) Remington's Pharmaceutical Sciences,
Easton : Mack.

Kostenbauder, H. B., DeLuca, P. P. and Kowarski, C. R. (1965)
J. Pharm. Sci., 54, 1243.

Kotera, A., Morita, T., Aoyagi, S., Kakiuchi, Y., Nagakura, S. and Kume, K.
(1961)
Nippon Kagaku Zassi, 82, 302.

Kundu, N. (1953)
J. Indian Chem. Soc., 30, 627.

Kundu, N. and Ray, P. (1952)
J. Indian Chem. Soc., 29, 811.

Kurz, J. L. (1962)
J. Phys. Chem., 66, 2239.

Kurzer, F. and Pitchfork, E. D. (1968)
Topics in Current Chemistry, 10, 375.

Laidler, K. J. (1965)
Chemical Kinetics, 2nd edn., New York : McGraw Hill.

Lawrence, C. A. (1960)
J. Am. Pharm. Assoc. Sci., Ed., 49, 731.

Leach, S. A. (1977)
Borderl. Caries Periodontal. Dis. Proc. Conf., 1977, 105.

Lin, S. (1969)
Bull. Parent. Drug Assoc., 23, 269.

Lin, S. and Lachman, L. (1969)
Bull. Parent. Drug Assoc., 23, 149.

Lippold, B. C. and Garrett, E. R. (1971)
J. Pharm. Sci., 60, 1019.

Lippold, B. C., Thoma, K. and Ullman, E. (1972)
Arch. Pharm., 11, 803.

Longworth, A. R. (1971)
in : Hugo, W. B. (ed.), Inhibition and Destruction of the Microbial Cell, London : Academic Press.

Lowbury, E. J. L. (1977)
Acta Pharm. Chemi., 84, 787.

Lowry, J. B. (1979)
J. Pharm. Sci., 68, 110.

Lund, W. and Waaler, T. (1968)
Acta Chem. Scand., 22, 3085.

MacKeen, D. L. and Green, K. (1978)
J. Pharm. Pharmacol., 30, 678.

Madsen, W. S. (1967)
Farm. Tidende, 77, 1185.

Manousaki, A. (1986)
Proc. 1st. Int. Meet. Am. Assoc. Pharm. Sci., PPD 211.

Marcus, A. D. and Taraszka, A. J. (1959)
J. Am. Pharm. Assoc. Sci. Ed., 48, 77.

Martinek, K., Yatsimirski, A. K., Levashov, A. V. and Berezin, I. V. (1977)
in : Mittal, K. L. (ed.), Micellization, Solubilization and Microemulsions, Vol. 2, p489, New York : Plenum.

Martindale The Extra Pharmacopoeia (1982)
Reynolds, E. F. (ed.), 28th edn., London : Pharmaceutical Press.

Matter-Muller, C. and Strumm, W. (1984)
in : Grayson, M. (ed.) Kirk-Othmer Encyclopaedia of Chemical Technology, 3rd edn., Vol. 25, New York : John Wiley and Sons.

Mauger, J. W., Paruta, A. N. and Gerraughty, R. J. (1969)
J. Pharm. Sci., 58, 574.

Maulding, H. V., Nazareno, J. P., Pearson, J. E. and Michaelis, A. F. (1975)
J. Pharm. Sci., 64, 278.

Maulding, H. V. and Zoglio, M. A. (1970)
J. Pharm. Sci., 59, 333.

Mayer, W., Erbe, S., Wolf, G. and Voigt, R. (1974)
Pharmazie, 29, 700.

McCarthy, T. J. (1970)
Pharm. Weekblad, 105, 557.

McCarthy, T. J. (1978)
Pharm. Weekblad, 113, 698.

McCormick, J. R. D., Fox, S. M., Smith, L. L., Bitler, B. A., Reichenthal, J., Origoni, V. E., Muller, V. H., Witerbottom, R. and Doerschuk, A. P. (1957)
J. Am. Chem. Soc., 79, 2849.

McLeod, H. A., Pelletier, O. and Campbell, J. A. (1958)
Can. Pharm. J. 1958, 173.

McTaggart, C. M., Ganley, J., Eaves, T., Walker, S. E. and Fell, M. J. (1979)
J. Pharm. Pharmacol., 31, 60P.

Meakin, B. J., Stevens, J. and Davies, D. J. G. (1978)
J. Pharm. Pharmacol., 30, 75.

Meakin, B. J., Tansey, I. P. and Davies, D. J. G. (1971a)
J. Pharm. Pharmacol., 23, 252.

Meakin, B. J., Winterborn, I. K. and Davies, D. J. G. (1971b)
J. Pharm. Pharmacol., 23, Suppl., 255.

Mendenhall, D. W. (1984)
Drug Dev. Ind. Pharm., 10, 1297.

Miribel, L., Brazier, J. L., Comet, F. and Lecompte, D. (1983)
J. Chromatogr., 268, 321.

Mollica, J. A., Rehm., C. R., Smith, J. B. and Govan, H. K. (1971)
J. Pharm. Sci., 60, 1380.

Mollica, J. A., Ahuja, S. and Cohen, J. (1978)
J. Pharm. Sci., 67, 443.

Mukerjee, P. and Mysels, K. J. (1971)
Critical Micelle Concentrations of Aqueous Surfactant Systems,
NSRDS-NBS 36, Washington DC : US Gov. Printing Office.

Nandi, S. D. (1972)
Tetrahedron, 28, 845.

Oesterling, T. O. (1970)
J. Pharm. Sci., 59, 63.

Oesterling, T. O. and Guttman, D. E. (1964)
J. Pharm. Sci., 53, 1189.

Parris, N. A. (1976)
Instrumental Liquid Chromatography, Amsterdam : Elsevier.

Parrott, E. L. (1966)
J. Am. Pharm. Assoc., NS6, 73.

Pearson, R. M. (1985)
Pharm. J., 234, 686.

Perez, R. L. (1980)
J. Liq. Chromatogr., 3, 1227.

Perez, R. L. (1981)
J. Chromatog. Sci., 19, 570.

Perrin, D. D. and Dempsey, B. (1974)
Buffers for pH and Metal Ion Control, London : Chapman and Hall.

Perrin, D. D., Dempsey, B. and Serjeant, E. P. (1981)
pKa Prediction for Organic Acids and Bases, London :
Chapman and Hall.

Perrin, J. H. and Witzke, E. (1971)
J. Pharm. Pharmacol., 23, 76.

Pinzauti, S., Dal Piaz, V. and La Porta, E. (1976)
J. Pharm. Sci., 65, 1251.

Pinzauti, S. and La Porta, E. (1981a)
Pharm. Acta Helv., 56, 155.

Pinzauti, S., La Porta, E. and Papeschi, G. (1981b)
Pharm. Acta Helv., 56, 337.

Pinzauti, S., La Porta, E., Casini, M. and Petti, C. (1982)
Pharm. Acta Helv., 57, 334.

Pinzauti, S., La Porta, E. and Papeschi, G. (1984)
J. Pharm. Biomed. Anal., 2, 101.

Plaut, B. S., Meakin, B. J. and Davies, D. J. G. (1980)
J. Pharm. Pharmacol., 32, 453.

Polack, A. E. (1967)
Aust. J. Pharm., 48, S64.

Pope, D. G. (1980)
Drug Cosmet. Ind., 1980, Nov. 54 and Dec. 48.

Powelczyk, E. and Plotkowiak, Z. (1976)
Farm. Pol., 32, 467.

Pride, A. and Gilbert, M. T. (1979)
Applications of High Performance Liquid Chromatography,
London : Chapman and Hall.

Purdy, K. R., Khammas, Z. N. and Meakin, B. J. (1986)
Proc. 4th Int. Conf. Pharm. Tech., III, 322.

Quintana, R. P. (1973)
in : Lasslo, A. and Quintana, R. P. (eds.), Surface Chemistry
and Dental Integuments, Springfield : Charles C. Thomas.

Quintana, R. P., Fisher, R. G. and Lasslo, A. (1972)
J. Dent. Res., 51, 1687.

Ravin, L. J., Rattie, E. S., Peterson, A. and Guttman, D. E. (1978)
J. Pharm. Sci., 67, 1523.

Ray, P. (1955)
J. Indian Chem. Soc., 32, 141.

Ray, P. (1961)
Chem. Rev., 61, 313.

Read, R. R. and Fredell, W. G. (1959)
Drug Cosmet. Ind., 84, 178.

Rehm, C. R. and Smith, J. B. (1960)
J. Am. Pharm. Assoc. Sci. Ed., 49, 386.

Richard, A., Elbaz, M. and Andermann, G. (1984)
J. Chromatogr., 298, 356.

Richardson, N. E., Davies, D. J. G., Meakin, B. J. and Norton, D. A.
(1977)
J. Pharm. Pharmacol., 29, 717.

Richardson, N. E., Davies, D. J. G., Meakin, B. J. and Norton, D. A. (1979)
Pharm. J., 223, 462.

Richardson, N. E., Plaut, B. S., Davies, D. J. G., Norton, D. A. and Meakin, B. J. (1980)
Plastics and Rubber : Materials and Applications, 1980, 173.

Robinson, R. A. and Stokes, R. H. (1959)
Electrolyte Solutions, 2nd edn., London : Butterworths.

Rogers, A. R. (1963)
J. Pharm. Pharmacol., 15, 101T.

Rogers, A. R. (1970)
Pestic. Sci., 1, 266.

Romsted, L. R. (1977)
in : Mittal, K. L. (ed.), Micellization, Solubilization and Microemulsions, Vol. 2, p509, New York : Plenum Press.

Rose, F. L. and Swain, G. (1956)
J. Chem. Soc., 1956, 4422.

Ruben, M. (1980)
Contact Lens J., 9, 3.

Rye, R. M. and Wiseman, D. (1964)
J. Pharm. Pharmacol., 16, 516.

Rye, R. M. and Wiseman, D. (1965)
J. Pharm. Pharmacol., 17, 295.

Sarma, B. D. (1952)
J. Indian Chem. Soc., 29, 217.

Saunders, L. and Fleming, R. (1971)
Mathematics and Statistics, 2nd edn., London : Pharmaceutical Press.

Schram, S. B. (1980)
The LDC Basic Book of Liquid Chromatography, St. Petersburg : Milton Roy.

Schwartz, M. A. (1964)
J. Pharm. Sci., 53, 1433.

Scott, A. I. and Eccleston, E. (1966)
Proc. European Soc. for Study of Drug Toxicity, 8, 195.

Senior, N. (1973)
J. Soc. Cosmet. Chem., 24, 259.

Shapiro, S. L., Parrino, V. A. and Freedman, L. (1959a)
J. Am. Chem. Soc., 81, 2220.

Shapiro, S. L., Parrino, V. A. and Freedman, L. (1959b)
J. Am. Chem. Soc., 81, 3728.

Shetewi, B. B. (1975)
Ph.D. Thesis, University of Bath.

Shih, I. K. (1971)
J. Pharm. Sci., 60, 786.

Siefert, K., Casagrande, D. and Silberman, H. (1975)
J. Chromatogr., 109, 193.

Snyder, L. R. and Kirkland, J. J. (1979)
Introduction to Modern Liquid Chromatography, 2nd edn., New York : Wiley.

Stevens, L. E., Durrwachter, J. R. and Helton, D. O. (1986)
J. Pharm. Sci., 75, 83.

Stigter, D. (1974)
J. Phys. Chem., 78, 2480.

Stuber, V. B. and Muller, K. H. (1981)
Pharm. Acta Helv., 56, 344.

Tansey, I. P. (1969)
M.Sc. Thesis, University of Bath.

Tanzer, J. M., Reid, Y. and Reid, W. (1972)
Antimicrob. Agents Chemother., 1, 376.

Tanzer, J. M., Slee, A. M. and Kamay, B. A. (1977)
Antimicrob. Agents Chemother., 12, 721.

Trigger, D. J. and Caldwell, A. D. S. (1968)
J. Hosp. Pharm., 25, 259.

Tucker, I. G. (1981)
Drug Dev. Ind. Pharm., 7, 231.

Tucker, I. G. and Owen, W. R. (1982)
J. Pharm. Sci., 71, 969.

Van Ketel, W. G. and Melzer-van Riemsdijk, F. A. (1980)
Contact Dermatitis, 6, 321.

Walters, W. A. (1950)
Physical Aspects of Organic Chemistry, 4th edn., New York : E. Van Nostrand.

Waltersson, J. O. and Lundgren, P. (1983)
Acta Pharm. Suec., 20, 145.

Warner, V. D., Lynch, D. M. and Ajemian, R. S. (1976)
J. Pharm. Sci., 65, 1070.

Warner, V. D., Lynch, D. M., Ki Hwan Kim and Grunewald, G. L. (1979)
J. Med. Chem., 22, 359.

Weinburg, E. D. (1968)
Ann. N. Y. Acad. Sci., 148, 587.

Wellman, K. M. and Harris, D. L. (1967)
Chem. Comm., 1967, 568.

Wesolowski, J. W., Blaug, S. M., Chin, T. F. and Lach, J. L. (1968)
J. Pharm. Sci., 57, 811.

Wesoluch, F., Florence, A. T., Puisieux, F. and Carstensen, J. T. (1979)
Int. J. Pharm., 2, 343.

Windheuser, J. J. and Higuchi, T. (1962)
J. Pharm. Sci., 51, 354.

Yamana, T. and Tsuji, A. (1976)
J. Pharm. Sci., 65, 1563.

Yang, W. (1982)
Drug Dev. Ind. Pharm., 8, 189.

Yang, W. and Banker, G. B. (1981)
Drug Dev. Ind. Pharm., 7, 113.

Zoglio, M. A., Maulding, H. V., Streng, W. H. and Vincek, W. C. (1975)
J. Pharm. Sci., 64, 1381.

Zoglio, M. A., Windheuser, J. J., Vatti, R., Maulding, H. V.,
Kornblum, S. S., Jacobs, A. and Hamot, H. (1968)
J. Pharm.Sci., 57, 2080.

Zvirblis, P., Socholitsky, I. and Kondritzer, A. A. (1956)
J. Am. Pharm. Assoc. Sci. Ed., 45, 450.